Human Intestinal Organoids as a Model to Study Intestinal Infection by the Foodborne Pathogen *Salmonella enterica*

by

Anna-Lisa E. Lawrence

A dissertation submitted in partial fulfillment
of the requirements of the degree of
Doctor of Philosophy
(Microbiology and Immunology)
in the University of Michigan
2022

Doctoral Committee:

Professor Mary X.D. O'Riordan, Chair
Associate Professor Michael A. Bachman
Professor Vernon B. Carruthers
Professor Asma Nusrat
Professor Vincent B. Young

“It’s hard to explain what I did so we might as well move on”

– Sarah Lawrence, age 8

Anna-Lisa E. Lawrence

aelawren@umich.edu

ORCID iD 0000-0002-2865-0238

DEDICATION

To my mom and dad

For instilling a love of science in me from a young age

ACKNOWLEDGMENTS

Science doesn't happen in a bubble and so there are many people who I would like to thank for making this PhD possible. I would like to start first by thanking my mentor, Dr. Mary O'Riordan. You have been such a kind and supportive mentor throughout a challenging thesis project. This was a new field to both of us and although it came with more than a few challenges, I thoroughly enjoyed going through the learning process with you. I also feel so fortunate that you have allowed me to have 'some fun' toward the end of my PhD and pursue a side project to appreciate how cool both *Listeria* and macrophages are. You have pushed me to become a more independent scientist and created an environment that both challenged me to be a better scientist, but also made me feel that it was ok to vent about whatever was on my mind when I needed to. I'm so happy you accepted me into your lab 5 years ago- I'm still not sure how the time went by so quickly. You have been such a great role model in both your mentorship style, scientific thinking, and your ability to assemble a great team of scientists and one day I hope to be as awesome of a scientist and person as you!

When I joined the O'Riordan lab back in 2017, I joined knowing there was a possibility that there would be a huge turnover of personnel since the lab consisted of senior postdocs and research scientists. Luckily, everyone ended up staying a few years after that, so I had the chance to soak up all the scientific knowledge from them. I am thankful to Dr. Basel Abuaita for being a partner in the HIO project. Basel, you have been

both an incredible mentor and partner in the lab. My thesis would be nowhere near this stage without you- this has been a true partner project. I really enjoyed our never-ending science chats and I am so happy that you have finally gotten the position you deserve. I'm really excited to see what you do with your own lab in the following years.

I would also like to thank the rest of the O'Riordan lab. From the members who were there when I joined, Basel Abuaita, Karla Passalacqua, Marie-Eve Charbonneau, and Ryan Berger who allowed a young graduate student to join them and pushed me to become a better scientist, to the members who joined later on; Mack Reynolds, Mike McFadden, and Zach Powers. It took some adjusting going from majority girls in the lab to being the only girl, but you guys create a fun environment to come in and work every day. I would also like to thank my undergraduate student, Naethan Kanneganti. It's been a lot of fun mentoring a young scientist! Thank you for plating bacteria for so many enteroid experiments that unfortunately didn't make it into this dissertation and helping me to move our new *Listeria* project forward while I've been stuck writing!

Next, I would like to acknowledge my committee members: Drs. Vernon Carruthers, Vince Young, Michael Bachman, and Asma Nusrat. Thank you for your scientific input and support throughout my PhD. You all provided a very helpful advice and perspective on a project that was new to us. I always looked forward to meeting with you and receiving your feedback during my committee meetings. I truly value the mentorship I received from you all.

I would also like to thank members of the organoid team: PIs Drs. Mary O'Riordan Vince Young, Jason Spence, and Christiane Wobus, as well as the lab members who generated the HIOs for our experiments, particularly Sha Huang, Veda Yadagiri, and Brooke Bons. This thesis would not be possible without all your hard work. Generating HIOs is an art form and not everyone has that skill, so thank you for making this work possible.

Thank you to all the friends I've made along this journey. My micro cohort Austin Campbell, Edmond Atindaana, Matt Schnizlein, Stephanie Thiede, Yolanda Rivera-Cuevas, and adoptive member Zack Mendel. From studying together for checkpoint 1, to my first camping trip, and blind taste-testing chocolate, you all made this journey so much fun! I'm so lucky to have been surrounded by so many wonderful friends and great scientists. I would also like to thank my two closest friends Sumin Kim and Samantha Neagle. Sumin, you were the first person I met at orientation and I'm so happy we've remained friends through all these years and have supported each other through the highs and lows of graduate school. Samantha, you've been one of my closest friends since middle school and I'm so happy to have that one non-science friend to keep everything in perspective.

Lastly, I would like to thank my family starting with my parents Maria Sandkvist and Dan Lawrence. You have shown me how to be an amazing scientist from an early age. I feel so lucky that I'm able to talk science with you from troubleshooting experiments, to having a critical eye looking over my grant applications. I'm so thankful to have parents who understand how stressful graduate school can be sometimes- you guys have given me

never ending support. I'm so happy I decided to stay in Ann Arbor for my PhD and have remained close to you- it will be weird not being in the same building and department anymore after this! I also want to thank my sister Sarah. Thank you for continuously reminding me that there's more to talk about than just science. We've had lots of fun adventures over the last few years, and I look forward to many more in the years to come!

And finally, I can't forget, thanks to Sniff for providing all the cuddles after long days in the lab.

TABLE OF CONTENTS

LIST OF FIGURES

ABSTRACT

Salmonella enterica is a prominent human pathogen causing over 100 million infections every year. Serovars of *S. enterica* are very closely related, but due to differences in infection progression in animal models, host responses that drive human infection outcomes are not well understood. Nontyphoidal serovars, like *S. enterica* serovar Typhimurium (STM) and Enteritidis (SE), cause an inflammatory infection in the gut and recruit neutrophils to clear the infection. In contrast, typhoidal serovars, including serovar Typhi (ST), infect via the same route yet clinically go largely undetected prior to spreading systemically to cause severe disease. Both groups utilize Type-three secretion systems (T3SSs) to infect. T3SS-1 secretes proteins to promote invasion into non-phagocytic cells. T3SS-2 in contrast, is active once bacteria are intracellular and modulate host cell dynamics to create a niche that is favorable for bacterial replication.

In this dissertation, I summarize work using a human intestinal organoid (HIO) model, a 3-dimensional tissue culture model consisting of primary human intestinal epithelial cells and mesenchyme, to study host responses to three major serovars relevant to human health, STM, SE, and ST.

First, we used a transcriptomics approach to define which epithelial responses to infection were dependent on either T3SS-1 or T3SS-2. Surprisingly, we found that T3SS-1 mutant

(T3SS-1^{mut}) bacteria, previously reported not to induce a robust inflammatory response in cell lines,

elicited a similar response to WT bacteria when cultured in the luminal space of the HIO. Additionally, we found that WT STM suppressed cell cycle progression, which was dependent on T3SS-1 and T3SS-2.

Next, we infected HIOs with STM, SE, and ST and measured serovar-specific HIO transcriptional responses and evaluated differences in bacterial invasion, replication and host cellular functions. We found that HIOs responded uniquely to all three serovars including distinct responses between the two non-typhoidal serovars. Each serovar varied in its ability to invade and replicate within HIOs and to trigger HIO stress pathways, leading to different outcomes in host cell death, replication, and reactive oxygen species formation.

Although the HIOs allow us to study human intestinal epithelial responses to *Salmonella*, there are critical host components absent from HIOs that influence infection outcome. Neutrophils are dominant early responders to non-typhoidal serovar infections, which are characterized by gastroenteritis. To investigate the contribution of neutrophils in host defense against non-typhoidal serovars, we co-cultured neutrophils with HIOs and characterized the infection. We found that instead of killing bacteria, neutrophils enhanced epithelial intrinsic defenses. This included increased production of pro-inflammatory markers and enhanced extrusion of epithelial cells into the HIO lumen. Enhanced cell shedding decreased intracellular bacterial burden in the epithelial

monolayer, suggesting that neutrophils can protect against *Salmonella* infection by promoting expulsion of infected cells from the intestine.

Overall, this dissertation provides insights into human epithelial responses specific to individual *Salmonella enterica* serovars and emphasizes intriguing differences between closely related serovars that deserve further study. We also found a new and unexpected role of luminal bacteria in inducing host inflammatory responses, an aspect of intestinal infection biology that has been challenging to study using standard cell culture models. Lastly, by co-culturing HIOs with neutrophils we revealed an underappreciated contribution of innate immune cells in controlling epithelial defense mechanisms during infection by *Salmonella.*

Chapter 1

Introduction

1.1 Abstract

Physiological modeling of the human gut is essential to better understand infections caused by intestinal pathogens. While several model systems are commonly used to study aspects of enteric infection, each has limitations in the representation of the human gut. Small animal models are one of the most complex models, and while they recapitulate most major components of the human gut, key differences in host genetics and microbiome cause bacterial pathogens to present with differing diseases compared to human infections. In contrast, human cell lines reflect the appropriate host genetic background, but lack some of the complexity of the mature human gut. Recently, human intestinal organoids (HIOs) and enteroids (HIEs), have been developed. These in vitro models are more complex as they are comprised of differentiated polarized primary human epithelial cells or epithelial cells differentiated from human stem cells and thus allow for more physiological modeling of human gut characteristics. Here I review current uses of HIOs and HIEs, and some of the benefits and limitations of these models for studying host-bacterial interactions.

1.2 Introduction

The intestines serve as a primary interface between the outside world and our bodies. Intestinal tissue must balance water and nutrient absorption following digestion of food with serving as a protective barrier to invading pathogens from the external environment. The intestine is a complex and heterogenous environment comprised of multiple cell types that serve specific roles in these processes. The intestinal epithelium alone has several subtypes, each having a specialized function. Goblet cells produce and secrete mucus to create a protective barrier separating the resident microbiota and invading pathogens from the epithelial lining, enteroendocrine cells secrete hormones and participate in cell signaling, Microfold (M) cells sample the luminal environment by taking up and processing material for presentation to resident immune cells, while Paneth cells produce and secrete antimicrobial molecules to kill invading pathogens (*1*). The most abundant cell type in the epithelium is the enterocyte which participates in nutrient absorption (*1*). The cells lining the epithelium are joined by junctions to create a tight and selective barrier to protect the underlying tissue (*2*). Underneath the epithelial barrier is the lamina propria, home to resident immune cells which serve as the next line of defense if the barrier is breached, and together these cells can quickly recruit additional immune cells such as neutrophils and macrophages to respond to infection (*1*, *3*).

1.3 Common model systems of the gut

Due to the complexity of the human gut, it has been difficult to faithfully model this organ in the lab to study intestinal pathogens. Mouse models are commonly used to study intestinal biology. There are several benefits to using mice to study the intestine such as

the representation of all major cell types as well as the ability to genetically modify the mouse to determine the contribution of specific genes in gut physiology. Also, due to their small size, it is easy to house rodents in a laboratory setting.

Unfortunately, there are some key differences between mouse and human gut physiology that create some restrictions in using the mouse model to study gut pathogens. First, due to differences in diet and microbiome composition, the luminal environment is distinct from the human intestine (*4*). This limits the types of pathogens that can be studied to gain insight into human disease, requiring mouse-adapted strains or pretreatment of mice with antibiotics to allow gastrointestinal colonization of species such as *Salmonella enterica* serovar Typhimurium (*5*). In some cases, entirely different pathogens are used; for example, the mouse-specific pathogen *Citrobacter rodentium* is commonly used as a model to understand *in vivo* infection kinetics of the human-specific enteropathogenic *E. coli* (EPEC and EHEC) as they share certain virulence factors (*6*). Additionally, key differences in genetics between mice and humans means that some pathogens are unable to infect the mouse intestine. This is the case for *Listeria monocytogenes* that requires the human E-cadherin protein as a receptor to invade via the intestine (*7*). Lastly, disease presentation and progression between mice and humans can also be quite different depending on the infecting pathogen (*8*, *9*). For example, diarrhea does not effectively develop in mouse models of diarrheal diseases (*10*). These species-specific differences highlight the limitation of using mouse models to study gastrointestinal infection.

Another animal model that can be used to study enteric infection is the bovine ileal loop model. Since these animals are significantly bigger than mice, housing them is expensive and fewer animals are used per experiment. However, due to their larger size, intestinal loops can be ligated in multiple segments, allowing several experimental conditions to be tested per animal. One advantage of the bovine ileal loop model compared to mice is that the fluid flux associated with diarrhea can be observed and measured with diarrhea-inducing bacterial pathogens (*11*). Most commonly, the loop models are used to study *Salmonella enterica* and *E. coli* and important insights into pro-inflammatory mediators of these pathogens as well as host components that respond to infection have been uncovered (*11–14*). The rabbit ileal loop model is similar to the bovine model and has been used to determine the activity of toxins from pathogens such as EHEC and *Vibrio cholerae* although species-specific reagents can be more difficult to find (*15*, *16*).

Human transformed cell lines, such as Caco-2, HCT116, HeLa, and HT29 cells, are among the most commonly used tools to study intestinal epithelial cell biology. Derived from human tissue, they should more closely reflect human-specific epithelial responses to various stimuli. Single cell-based assays using these cell lines can reveal valuable insight into specific mechanisms of how different pathogens interact with the host cell. Since these cells are transformed, they are fast growing and can be easily used in high-throughput assays allowing for several conditions to be analyzed simultaneously. Some of these cell lines can be easily transfected allowing for genetic manipulation. However, limitations to using transformed cells lines include their clonal nature and limited genetic diversity. Additionally, they do not accurately reflect the different specialized cell types

found in the intestine such as Goblet and Paneth cells. Importantly, these transformed cell lines are isolated from cancerous human tissue, suggesting they have accumulated genetic mutations that alter physiological functions like metabolism and cell cycle checkpoints, to name a few. With few exceptions, like Caco-2 colonic epithelial cells which can be plated under specific conditions to induce polarization, these cell lines are often used for infection experiments in their unpolarized state (*17*). Polarization is a characteristic behavior of the intestinal epithelium that enables its barrier function. Intestinal epithelial cells distribute proteins and other cellular components to apical or basolateral regions of the polarized cell, which can impact how pathogens interact with these cells (*18*). Non-intestinal epithelial cell lines, such as the HeLa cervical epithelial cell line, are easily used to study intestinal pathogens, but may lead to conclusions that do not accurately reflect interactions that occur in the human gut.

1.4 Human intestinal organoids and enteroids

Over the last ten years, due to advances in our understanding of developmental biology, improved *in vitro* models have been developed to study human intestinal biology. Human intestinal organoids (HIOs) and enteroids (HIEs), differentiated from stem cells and intestinal crypt cells respectively, feature aspects of the human intestine that are not replicated in the previously discussed model systems.

Human intestinal organoids

Human intestinal organoids (HIOs) are differentiated from pluripotent stem cells, either derived from embryonic stem cells or induced pluripotent stem cells **(Fig 1.1)**. These stem cells are cultured with defined growth factors to induce endoderm formation prior to hind-

or mid-gut differentiation (*19*, *20*). These cells self-organize to form spheroids which differentiate when cultured in an extracellular matrix like Matrigel in the presence of EGF, Noggin, and Rspondin1 growth factors into the mature organoid comprised of epithelial cells and mesenchymal cells (*19*, *20*).

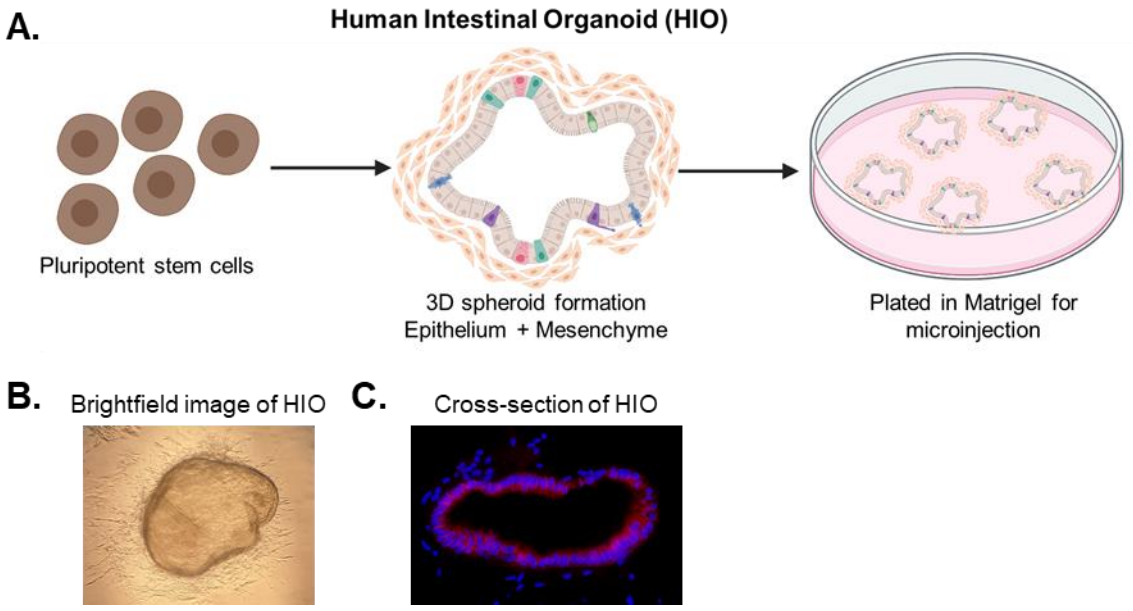

Figure 1.1 Human intestinal organoids (A) Cartoon diagram of HIO development and experimental set-up. (B) Brightfield image of HIO taken at 4x magnification. (C) Cross-section of HIO sectioned at 12µm thickness. Stained with DAPI (blue) to mark nuclei and E-cadherin antibodies (red) to label epithelial cells.

In studies of host-pathogen interactions, HIOs can be microinjected with the organism of interest. While more technically challenging than infecting a monolayer of cells, this protocol both preserves the 3D architecture and polarity of the HIO and maintains a luminal microenvironment. Previous studies have measured formation of a mucus layer during bacterial colonization, reduced luminal oxygen concentrations following colonization with aerobic bacteria, and have reported using dye microinjection that a tight barrier is formed, preventing contents from passing through in an unregulated manner

(*21*, *22*). Fluid flux can also be measured following microinjection with cholera toxin, showing that diarrheal-like phenotypes can be measured (*23*).

The HIOs differentiate over the course of a month and require substantial manual work to trim spheroids but provide notable experimental advantages. These cells are derived from primary human stem cell lines which avoid the use of transformed cells. HIOs form a polarized epithelial layer and contain most of the epithelial cell subtypes found in the intestine including Goblet, Paneth, enteroendocrine, and enterocyte cells, although they still lack M cells (*19*, *20*). Since HIO differentiation also generates supporting mesenchymal cells, the contribution of the mesenchyme in determining infection outcome can be probed using this model (*19*, *20*).

Human intestinal enteroids (HIEs)

While HIEs share some similarities to HIOs, they are derived from a different tissue source. Intestinal biopsies from healthy or diseased individuals are obtained and crypt epithelial cells are enriched through scraping away villus cells prior to centrifugation to collect crypts (*24–26*). These cells are then grown in the presence of Wnt-3a, Noggin, EGF, and R-spondin growth factors to maintain their crypt-like programming (*24–26*). During this culturing process, HIEs, which are composed of exclusively epithelium and no mesenchyme, self-organize to form 3-dimensional spheroids **(Fig 1.2)**.

Although HIEs can be microinjected, they are typically smaller and more fragile than HIOs, making this technique even more challenging for infection studies. HIEs can instead be separated into a single cell suspension using mechanical disruption and

trypsin digestion and plated as a single epithelial layer on Transwell membranes (*27*). After a few days, the epithelial cells will polarize and form a tight barrier on the membranes. Barrier integrity of the enteroid monolayers can be measured by transepithelial electrical resistance (TEER) or

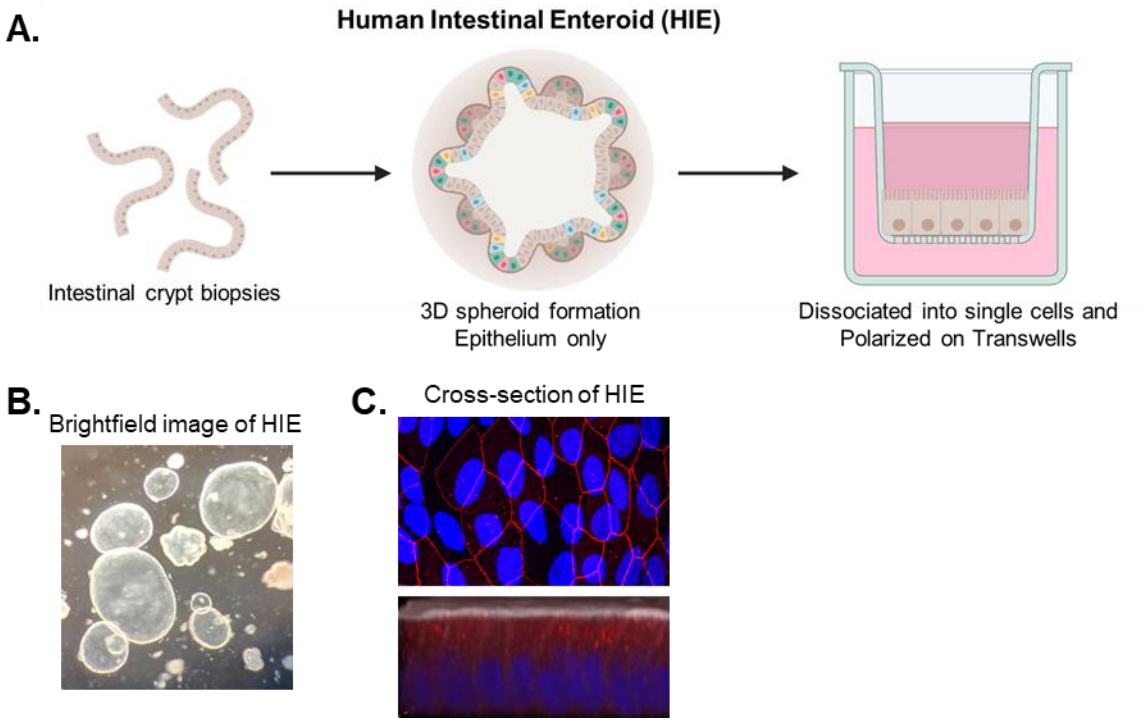

Figure 1.2 Human intestinal enteroids (A) Cartoon diagram of HIE development and experimental set-up. (B) Brightfield image of HIEs taken at 4x magnification prior to dissociation into single cell suspension for experiments. (C) Cross-sectional view of HIEs dissociated into single cell suspension and plated on transwells. HIEs were stained with DAPI (blue) to show nuclei, ZO-1 antibody (red, top) to show tight junctions, E-cadherin antibody (red, bottom) to mark epithelial cells, and Phalloidin (white) to stain actin to show apical surface.

by adding fluorescent dyes of different molecular weights to the apical compartment and monitoring the rate at which they flow to the basal side (*28*). Once the cells are confluent, growth factors can be removed to induce differentiation into mature villus-like cells. This procedure has been well characterized and all major cell types are present (*24–26*); in some culture conditions, it has been reported that even M cells can be found in the

enteroid cultures (*29*). As further validation, in a similar mouse enteroid culturing model, transcriptomics analyses were performed on enteroid cultures passaged for 12 weeks and they maintained transcriptional signatures of the intestinal segments from which they were originally derived (*30*). Retention of segment specific identity over time also allows researchers to probe segment-specific interactions and responses to various pathogens which is not possible using transformed cell lines.

1.5 Current uses of HIOs and HIEs

Over the past 10 years use of HIOs and HIEs to study host-pathogen interactions has rapidly increased. HIOs and HIEs are now utilized to study bacteria, viruses, and parasites including, but not limited to *Clostridioides difficile, Salmonella enterica, Escherichia coli,* SARS-CoV-2, and Norovirus (*31–43*). Here we will highlight some of the current uses of these models and what has been learned so far in the field of intestinal bacteria.

Escherichia coli

E. coli is among one of the most commonly used species to study host-bacterial interactions using the HIO/HIE models since conventional mice are not as amenable to colonization with pathogenic *E. coli* strains (*44*). HIOs and HIEs have been used to examine colonization responses to both commensal strains of *E. coli* (*21*, *45*) as well as pathogenic strains such as enteroaggregative (EAEC) and enterohemorrhagic (EHEC) *E. coli* (*46–49*).

Using a human commensal strain of *E. coli,* Hill et al. found that HIOs were able to support colonization of *E. coli* for more than 7 days without causing much damage to the HIO (*21*). In response to colonization, luminal oxygen concentrations were reduced, mucus production increased and there were signs of epithelial cell maturation (*21*). *E. coli* is one of the first species to colonize the human gut after birth and so these findings strongly support the use of the HIO model to further study initial stages of colonization (*50*). Additionally, since there was very little damage to the HIO by this commensal *E. coli* strain, it is also feasible that a more complex microbiota could be microinjected into the lumen to further study development.

Conversely, in a study that compared infection with pathogenic *E. coli* in different intestinal segments of HIEs, Rajan et al. found that HIEs colonized with a commensal strain of *E. coli* exhibited distinct clustering patterns from EPEC and EHEC-infected duodenum HIEs as measured by principal component analysis (PCA) of host transcriptional responses to colonization (*46*). Further analysis went on to show that the EAEC isolate also induced mucus secretion to enhance a protective response in the HIEs (*46*). While they did not report any disruption of barrier integrity, this latter study only went out to 6h post infection (hpi) and so it is possible that additional differences between the commensal and pathogenic strains would be further emphasized at later time points. In another study using HIOs reported loss of barrier integrity and activation of HIO stress responses by shiga toxin producing EHEC (*51*). Additional studies from Rajan et al. showed different adherence patterns of EAEC to individual intestinal segments

emphasizing the need to study segment-specific interactions between pathogens and the host (*48*).

Salmonella enterica

S. enterica is another intestinal pathogen that has been studied in the HIOs and HIEs. Once again, since small animal models do not faithfully replicate the infection progression that is observed in humans researchers have jumped at the opportunity to better understand how different serovars of *S. enterica* interact with the human epithelium (*52*). A few transcriptomics studies, including the results from Chapters 2 and 3 of this dissertation, have now been published using the HIO model to probe the host response to various serovars and mutants of *S. enterica* (*34–36*). These studies have also led to the appreciation that individual serovars of *S. enterica* interact uniquely with the host by infecting at different rates and inducing different host stress responses (*34*).

In addition to global characterization of host responses to infection, more mechanistic studies of *S. enterica* infection have also been performed in HIEs. Using quantitative microscopy techniques, Geiser et al. studied infection kinetics of *S. enterica* serovar Typhimurium (STM) and the contribution of specific virulence factors in driving invasion into epithelial cells (*38*). Forbester et al. revealed an important contribution of IL-22 signaling in the epithelial antimicrobial response to STM (*37*). And finally, Holly et al. revealed differences in epithelial intrinsic inflammasomes between mice and humans in controlling infection by STM further highlighting the need to study species specific host responses to bacterial infections (*53*).

Shigella flexneri

S. flexneri also fits into the category of intestinal pathogens that are difficult to model with other systems and therefore researchers have decided to utilize HIEs and HIOs to better understand its interaction with intestinal epithelial cells (*54–56*). Like *S. enterica, S. flexneri* actively invades intestinal cells and replicates within them inducing a robust inflammatory response (*57*). Using HIEs, Koestler et al. (2019) and Ranganathan et al. (2019) demonstrated a basolateral preference for epithelial invasion of *S. flexneri* and showed successful bacterial replication in HIEs derived from all intestinal segments (*54*, *55*). Both groups also found that a robust inflammatory response was induced during infection (*54*, *55*). Additionally, HIOs have been useful in testing feasibility of bacteriophage therapy in antibiotic resistant strains of *S. flexneri* (*56*). Together these findings provide evidence that HIOs and HIEs faithfully replicate known aspects of *S. flexneri* infection and characterize different uses for these models.

Clostridioides difficile

All bacterial species highlighted so far in this review are facultative anaerobes. Prior to colonization with bacteria however, HIOs and traditional Transwell culture of HIEs have measurable oxygen levels, including a HIO luminal oxygen concentration of ~7.5%. Whether HIOs and HIEs would be supportive of infection with anaerobic bacteria was initially unclear (*21*). More recently, several reports on the viability of *C. difficile* in HIOs have been published suggesting that interactions between HIOs and anaerobic bacteria are experimentally feasible (*39–42*).

Leslie et al. showed that *C. difficile* remained viable in HIOs up to 12h post microinjection and that toxin secretion caused destruction of barrier integrity (*39*). *C. difficile* toxin also induces responses in HIEs, exhibiting less sensitivity and delayed cell rounding compared to transformed cell lines (*40*). Additional characterization measured differences in toxin receptor expression in transformed cell lines compared to HIEs. More work from this group showed that HIOs microinjected with *C. difficile* exhibited altered mucus secretion compared to mock-infected controls, a phenotype consistent with biopsies from infected patients (*41*). Together these findings establish that HIOs and HIEs can support infection with *C. difficile* and opens the possibility of studying other anaerobic bacteria with these models.

1.6 Challenges

Acquisition of materials

While the popularity of HIOs and HIEs in pathogenesis research continues to increase (*58*), use of the HIO/HIE models do not come without challenges. Primary cells are more sensitive to culture conditions than transformed cell lines and thus strict adherence to culture protocols and use of fresh reagents is essential. Additionally, some commercially available growth factors are insufficient to maintain cell type identity in these models, and specialized reagents are required, such as cell lines that secrete specific growth factors like Wnt3a, to make conditioned media (*59*). Generation of HIO and HIE culture media is time-intensive. Carefully following protocols and generating frozen stocks speeds up this process, but reliance on some commercial materials such as Matrigel and Transwell

plates make HIO/HIE culture susceptible to supply chain shortages. Thus, strategic planning is more important for the use of these 3D/2D cultures than for standard tissue culture models of infection.

Experimental and culture variability

In addition to the challenges associated with acquiring materials to generate and maintain the HIOs/HIEs, there can also be variation associated with culture. Batch to batch variation associated with growth factors in the complex culture medium is common, often leading to changes in differentiation and growth of these cells. While this variation can sometimes be controlled by activity assays, some variation in the culture protocols cannot be avoided, and different lines of HIEs grow at different rates and in different patterns. Lastly, differentiation can be difficult to control. Depending on how efficient the differentiation process is, there can be variation in the distribution of the intestinal cell types present in the mature HIO or HIE, which can alter how they respond to various pathogens since some pathogens prefer one cell type over another.

Genetic manipulation

One advantage of using mice or transformed cell lines to investigate host-pathogen interactions is the genetic tractability of these models that allows for determining the contribution of specific genes in regulating infection outcome. Genetic manipulation can be difficult in the HIO and HIE models due to the nature of working with primary cells and the long period of time required for differentiation. Achieving sufficient transfection efficiency in stem cells can be challenging which is required for genetically modifying the

cell line to generate HIOs. In fact, extensive characterization to identify the most efficient way to transfect adult stem cells is an area of active research (*60*). After optimization of transfection efficiency, CRISPR-Cas9-mediated knockouts can be generated (*61*). Alternatively, lentiviral knockdowns have successfully been demonstrated. Unfortunately, since differentiation occurs after genetic manipulation, if the gene of interest is important for intestinal development, HIO differentiation may not be possible, or in the case of shRNA-mediated knockdown, differentiation may select for lower knockdown efficiency.

Since HIOs are differentiated from a cell line, genetic manipulation is somewhat more tractable than with HIEs. HIEs are grown 3D in culture from crypt cells and so they typically do not survive well in single cell suspension, making it difficult to generate a clonal knockout population. However, researchers have found a way around this problem by using spin-inoculation retroviral-mediated knockdown using shRNA constructs (*62*). By adding the lentiviral construct during the normal passaging step of HIE culturing, the HIEs are already broken into smaller pieces which allows for a more effective selection process. By maintaining selection on the cultures over multiple passages effective knockdown can be established **(Fig 1.3)**, although it is important to note that there will be cell-to-cell variation in the effectiveness of knockdown since clonal populations were not established

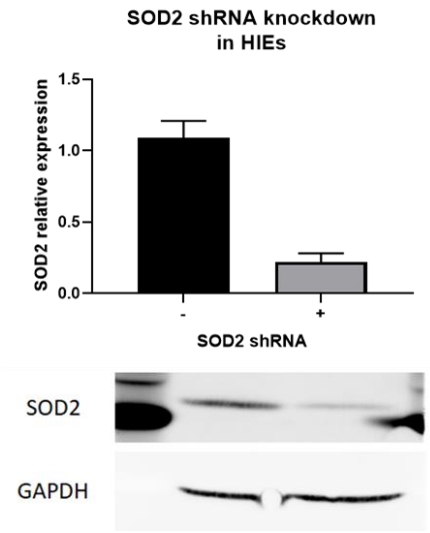

Figure 1.3 shRNA-mediated knockdown in HIEs shRNA-mediated knockdown of SOD2 expression in adult HIEs. Knockdown efficacy was tested after 4 passages with 1µg/ml puromycin selection. Lentiviral transduction was performed during passaging by spinning down dissociated HIEs with the lentiviral construct for 30min at 4°C. HIEs were then incubated for another 2h at 37°C prior to washing the HIEs and re-embedding them in Matrigel. Western blot of SOD2 expression in untreated or SOD2 shRNA knockdown cells. Expression was normalized to GAPDH.

Infection protocols

One last challenge that is important to note prior to implementing HIO research is that infection/inoculation protocols can be more technically demanding than standard tissue culture infections. For HIOs, microinjection is typically used to inoculate pathogens into the luminal compartment which requires specifically calibrated micro-injection equipment (*22*).

HIEs in contrast, are easier to infect after dissociating them into a monolayer on Transwell inserts and infection protocols are largely similar to standard tissue culture techniques. Additionally, one group found that removing certain growth factors from the HIE culture medium can induce polarity flipping of the epithelial monolayer thus exposing the apical surface to the surrounding media (*63*). Although one needs to consider the cost of losing

the controlled luminal microenvironment outlined above, infections are much easier to perform in these cultures.

One last technical consideration for using HIOs in bacterial infection models is that Matrigel, which is used as the HIO supportive matrix, contains the antibiotic gentamicin. Depending on the degree of sensitivity of the bacterial species of interest, this antibiotic can kill the bacterial inoculum after microinjection into the HIO. After optimization of HIO infection protocols with *S. enterica* and *L. monocytogenes*, allowing HIOs to grow in Matrigel for 5-7 days prior to infection was usually sufficient to reduce the levels of gentamicin and allow for a productive infection (*34*, *35*). Since each bacterial species can differ in the degree of sensitivity to gentamicin, this is an important aspect of infection protocols that needs to be optimized when exploring the use of HIOs for bacterial colonization or pathogenesis.

1.7 Future directions

So far, many HIO and HIE studies have focused on validating the model; either studying the cell types present within these different models or testing whether known phenotypes of colonization or infection with different bacteria are recapitulated. These studies have shown that HIOs and HIEs are a good alternative *in vitro* model of the human intestinal epithelium and therefore the field is likely to expand in the coming years. Based on the studies performed so far and what components are currently missing from the HIOs/HIEs the following directions may be a focus of interest:

One of the limitations thus far of the HIO/HIE models is that some hallmarks of the mature gut are missing. Two of these components are the microbiota and immune cells. Both factors are known to strongly affect infection outcome, and some preliminary work has been done to show that both colonization with individual species found in the microbiota as well as co-culture with immune cells are possible with the HIOs/HIEs. Hill et al. found that HIO co-culture with a commensal strain of *E. coli* was possible for more than one week (*21*). Numerous pre-prints are emerging along with some published studies showing co-culture of HIEs/HIOs with innate immune cells is feasible, and previously underappreciated interactions between the epithelium and immune cells leading to differences in infection outcome are being revealed (*51*, *64–67*) (and Chapter 5 of this dissertation).

In addition to adding microbiome and immune cell components, further refinement of culture protocols will also help move the field forward. Although anaerobic bacteria like *C. difficile* can be maintained in the HIO model, commonly used protocols do not allow for long-term culture. Development of more sophisticated anaerobic co-culture set-ups will help to establish the HIOs/HIEs as a more faithful model of the complex redox environment of the gut. Sasaki et al. used colonic epithelial cells in a Transwell support and showed that a cap blocking oxygen influx into the apical side supported growth of anaerobic bacteria (*68*). In a preprint describing a similar set-up, HIEs cultured in an anaerobic chamber and supplied with oxygen on the basolateral side allowed for replication of *Bacteroides thetaiotaomicron* (*69*). Other components that could be enhanced to better reflect the human intestine could include changing plating conditions

of the cultures consistent with organ on a chip technology to add mechanical force which simulates movement in the intestine (*70*), or culturing HIOs using air-liquid interface technology (ALI) allowing for longer-term culturing to permit further tissue maturation (*71*).

Overall, tremendous strides have been made in the HIO and HIE field over the last 10 years to better replicate the human intestinal environment. Although these models are more challenging to work with than standard cell lines, there is a huge opportunity to learn about aspects of the human gut that would not be possible otherwise.

1.8 In this dissertation

In this dissertation, I describe how I have optimized and used the HIO model to study *Salmonella enterica* infection. *S. enterica* is a Gram-negative foodborne pathogen that infects over 115 million people every year and is comprised of over 2500 serovars (*72*, *73*). These serovars are extremely closely related at the genome level with only a few hundred genes that are unique to each serovar (*74*), but these serovars cause a range of diseases in humans. Serovars are classified into two major groups based on the most common disease presentation in humans. Non-typhoidal serovars cause a highly inflammatory infection restricted to the gut that is dominated by a robust neutrophil-mediated immune response (*75*). These infections are typically self-resolving and do not require antibiotic treatment. In contrast, typhoidal serovars remain relatively silent during initial stages of intestinal infection before spreading systemically to cause more severe infections; infection with typhoidal serovars are responsible for an estimated 200,000 deaths annually (*75*). In some immunocompromised or malnourished individuals non-

typhoidal serovars can also cause systemic infections leading to higher mortality rates (*76*). This variability in infection outcome suggests that initial host responses in the gut are likely a contributing factor to these differences in disease progression.

Host responses to infection with different *S. enterica* serovars are not fully understood due to reliance on non-physiological model systems to study infection as well as most published studies focusing on only a few serovars of *S. enterica* to represent the entire species. While *S. enterica* is comprised of over 2500 serovars, *S. enterica* serovar Typhimurium (STM) has been selected as the model organism to study *Salmonella* pathogenesis. There are a few issues with this; first, STM has been used in mice to study typhoidal *Salmonella* infections since conventional mice develop systemic infections with STM unless pretreated with antibiotics to disrupt the microbiota (*76*). Since STM does not cause typhoid fever in humans and since the typhoidal serovar *S. enterica* serovar Typhi (ST) does not infect mice, mechanisms of disease progression are likely very different between the two models. Additionally, STM has been selected as the representative serovar for nontyphoidal serovars. While STM is one of the most prevalent serovars causing human disease, other serovars including *S. enterica* serovar Enteritidis (SE) cause just as many, if not more infections world-wide each year (*77*). Genomic comparisons between STM and SE have identified notable differences between these two serovars suggesting that they may have unique ways of interacting with their human host (*78*). As highlighted above, many *Salmonella* infection studies have been performed in mouse models or transformed epithelial cell lines, and therefore some of the key

limitations to these models may result in scientific conclusions that are not representative of infection in the human gut.

In the following chapters I describe my work using human intestinal organoids and enteroids to better understand human primary intestinal epithelial responses to three serovars of *S. enterica*; *S. enterica* serovar Typhimurium (STM), Enteritidis (SE), and Typhi (ST). STM and SE cause the majority of NTS infections world-wide and studying the two in combination have revealed some interesting differences in interaction with the host. In combination with studying ST, a typhoidal serovar, we can better understand how nontyphoidal serovars and typhoidal serovars interact uniquely with the human intestinal epithelium. Beginning in Chapter 2 of this dissertation, we performed initial characterization of the HIO model to study *Salmonella* pathogenesis. We elected to use the well-studied serovar, STM, to validate the HIO infection model as well as including existing STM mutants to characterize how host responses are dependent on different *Salmonella* virulence factors. In Chapter 3, after validating the utility of the HIO model to study *Salmonella,* we employed transcriptomics approaches to directly compare host responses to three prevalent *S. enterica* serovars. And finally, in Chapter 4, we developed a co-culture model of HIOs and human primary neutrophils to understand how the immune system contributes to intestinal host defense against STM. The findings described in the following chapters emphasize the need to study individual serovars to better understand mechanisms of interaction with the host and lay the groundwork for future studies using the HIO model to investigate the role of immune cells in regulating host defense during intestinal infections.

References

1. L. W. Peterson, D. Artis, Intestinal epithelial cells: regulators of barrier function and immune homeostasis. *Nat. Rev. Immunol.* **14**, 141–153 (2014).

2. C. Chelakkot, J. Ghim, S. H. Ryu, Mechanisms regulating intestinal barrier integrity and its pathological implications. *Exp. Mol. Med.* **50**, 103 (2018).

3. A. M. Mowat, W. W. Agace, Regional specialization within the intestinal immune system. *Nat. Rev. Immunol.* **14**, 667–685 (2014).

4. F. Hugenholtz, W. M. de Vos, Mouse models for human intestinal microbiota research: a critical evaluation. *Cell. Mol. Life Sci.* **75**, 149–160 (2018).

5. M. Barthel, S. Hapfelmeier, L. Quintanilla-Martínez, M. Kremer, M. Rohde, M. Hogardt, K. Pfeffer, H. Rüssmann, W.-D. Hardt, Pretreatment of mice with streptomycin provides a Salmonella enterica serovar Typhimurium colitis model that allows analysis of both pathogen and host. *Infect. Immun.* **71**, 2839–2858 (2003).

6. J. W. Collins, K. M. Keeney, V. F. Crepin, V. A. K. Rathinam, K. A. Fitzgerald, B. B. Finlay, G. Frankel, Citrobacter rodentium: infection, inflammation and the microbiota. *Nat. Rev. Microbiol.* **12**, 612–623 (2014).

7. M. Lecuit, S. Dramsi, C. Gottardi, M. Fedor-Chaiken, B. Gumbiner, P. Cossart, A single amino acid in E-cadherin responsible for host specificity towards the human pathogen Listeria monocytogenes. *EMBO J.* **18**, 3956–3963 (1999).

8. Y. Valdez, G. A. Grassl, J. A. Guttman, B. Coburn, P. Gros, B. A. Vallance, B. B. Finlay, Nramp1 drives an accelerated inflammatory response during Salmonella-induced colitis in mice. *Cell. Microbiol.* **11**, 351–362 (2009).

9. D. M. Monack, D. M. Bouley, S. Falkow, Salmonella typhimurium persists within macrophages in the mesenteric lymph nodes of chronically infected Nramp1+/+ mice and can be reactivated by IFNgamma neutralization. *J. Exp. Med.* **199**, 231–241 (2004).

10. S. Hapfelmeier, W.-D. Hardt, A mouse model for S. typhimurium-induced enterocolitis. *Trends Microbiol.* **13**, 497–503 (2005).

11. R. L. Santos, R. M. Tsolis, S. Zhang, T. A. Ficht, A. J. Bäumler, L. G. Adams, Salmonella-induced cell death is not required for enteritis in calves. *Infect. Immun.* **69**, 4610–4617 (2001).

12. Elfenbein Johanna R., Endicott-Yazdani Tiana, Porwollik Steffen, Bogomolnaya Lydia M., Cheng Pui, Guo Jinbai, Zheng Yi, Yang Hee-Jeong, Talamantes Marissa, Shields Christine, Maple Aimee, Ragoza Yury, DeAtley Kimberly, Tatsch Tyler, Cui

Ping, Andrews Katharine D., McClelland Michael, Lawhon Sara D., Andrews-Polymenis Helene, Fang F. C., Novel Determinants of Intestinal Colonization of Salmonella enterica Serotype Typhimurium Identified in Bovine Enteric Infection. *Infect. Immun.* **81**, 4311–4320 (2013).

13. I. Vlisidou, M. Lyte, P. M. van Diemen, P. Hawes, P. Monaghan, T. S. Wallis, M. P. Stevens, The neuroendocrine stress hormone norepinephrine augments Escherichia coli O157:H7-induced enteritis and adherence in a bovine ligated ileal loop model of infection. *Infect. Immun.* **72**, 5446–5451 (2004).

14. C. Menge, I. Stamm, P. M. van Diemen, P. Sopp, G. Baljer, T. S. Wallis, M. P. Stevens, Phenotypic and functional characterization of intraepithelial lymphocytes in a bovine ligated intestinal loop model of enterohaemorrhagic Escherichia coli infection. *J. Med. Microbiol.* **53**, 573–579 (2004).

15. K. P. Keenan, D. D. Sharpnack, H. Collins, S. B. Formal, A. D. O'Brien, Morphologic evaluation of the effects of Shiga toxin and E coli Shiga-like toxin on the rabbit intestine. *Am. J. Pathol.* **125**, 69–80 (1986).

16. G. J. Leitch, M. E. Iwert, W. Burrows, Experimental cholera in the rabbit ligated ileal loop: toxin-induced water and ion movement. *J. Infect. Dis.* **116**, 303–312 (1966).

17. T. Lea, in *The Impact of Food Bioactives on Health: in vitro and ex vivo models*, K. Verhoeckx, P. Cotter, I. López-Expósito, C. Kleiveland, T. Lea, A. Mackie, T. Requena, D. Swiatecka, H. Wichers, Eds. (Springer International Publishing, Cham, 2015), pp. 103–111.

18. N. V. Guseva, S. Dessus-Babus, C. G. Moore, J. D. Whittimore, P. B. Wyrick, Differences in Chlamydia trachomatis serovar E growth rate in polarized endometrial and endocervical epithelial cells grown in three-dimensional culture. *Infect. Immun.* **75**, 553–564 (2007).

19. J. R. Spence, C. N. Mayhew, S. A. Rankin, M. F. Kuhar, J. E. Vallance, K. Tolle, E. E. Hoskins, V. V. Kalinichenko, S. I. Wells, A. M. Zorn, N. F. Shroyer, J. M. Wells, Directed differentiation of human pluripotent stem cells into intestinal tissue in vitro. *Nature*. **470**, 105–109 (2011).

20. K. W. McCracken, J. C. Howell, J. M. Wells, J. R. Spence, Generating human intestinal tissue from pluripotent stem cells in vitro. *Nat. Protoc.* **6**, 1920–1928 (2011).

21. D. R. Hill, S. Huang, M. S. Nagy, V. K. Yadagiri, C. Fields, D. Mukherjee, B. Bons, P. H. Dedhia, A. M. Chin, Y.-H. Tsai, S. Thodla, T. M. Schmidt, S. Walk, V. B. Young, J. R. Spence, Bacterial colonization stimulates a complex physiological response in the immature human intestinal epithelium. *Elife*. **6** (2017), doi:10.7554/eLife.29132.

22. D. R. Hill, S. Huang, Y.-H. Tsai, J. R. Spence, V. B. Young, Real-time Measurement of Epithelial Barrier Permeability in Human Intestinal Organoids. *J. Vis. Exp.* (2017), doi:10.3791/56960.

23. D. D. Zomer-van Ommen, A. V. Pukin, O. Fu, L. H. C. Quarles van Ufford, H. M. Janssens, J. M. Beekman, R. J. Pieters, Functional Characterization of Cholera Toxin Inhibitors Using Human Intestinal Organoids. *J. Med. Chem.* **59**, 6968–6972 (2016).

24. T. Sato, D. E. Stange, M. Ferrante, R. G. J. Vries, J. H. Van Es, S. Van den Brink, W. J. Van Houdt, A. Pronk, J. Van Gorp, P. D. Siersema, H. Clevers, Long-term expansion of epithelial organoids from human colon, adenoma, adenocarcinoma, and Barrett's epithelium. *Gastroenterology*. **141**, 1762–1772 (2011).

25. M. M. Mahe, N. Sundaram, C. L. Watson, N. F. Shroyer, M. A. Helmrath, Establishment of human epithelial enteroids and colonoids from whole tissue and biopsy. *J. Vis. Exp.* (2015), doi:10.3791/52483.

26. P. Jung, T. Sato, A. Merlos-Suárez, F. M. Barriga, M. Iglesias, D. Rossell, H. Auer, M. Gallardo, M. A. Blasco, E. Sancho, H. Clevers, E. Batlle, Isolation and in vitro expansion of human colonic stem cells. *Nat. Med.* **17**, 1225–1227 (2011).

27. W. Y. Zou, S. E. Blutt, S. E. Crawford, K. Ettayebi, X.-L. Zeng, K. Saxena, S. Ramani, U. C. Karandikar, N. C. Zachos, M. K. Estes, (Humana Press, 2017), pp. 1–19.

28. I. Schoultz, Å. V. Keita, The Intestinal Barrier and Current Techniques for the Assessment of Gut Permeability. *Cells*. **9** (2020), doi:10.3390/cells9081909.

29. J. D. Rouch, A. Scott, N. Y. Lei, R. S. Solorzano-Vargas, J. Wang, E. M. Hanson, M. Kobayashi, M. Lewis, M. G. Stelzner, J. C. Y. Dunn, L. Eckmann, M. G. Martín, Development of Functional Microfold (M) Cells from Intestinal Stem Cells in Primary Human Enteroids. *PLoS One*. **11**, e0148216 (2016).

30. S. Middendorp, K. Schneeberger, C. L. Wiegerinck, M. Mokry, R. D. L. Akkerman, S. van Wijngaarden, H. Clevers, E. E. S. Nieuwenhuis, Adult stem cells in the small intestine are intrinsically programmed with their location-specific function. *Stem Cells*. **32**, 1083–1091 (2014).

31. M. M. Lamers, J. Beumer, J. van der Vaart, K. Knoops, J. Puschhof, T. I. Breugem, R. B. G. Ravelli, J. Paul van Schayck, A. Z. Mykytyn, H. Q. Duimel, E. van Donselaar, S. Riesebosch, H. J. H. Kuijpers, D. Schipper, W. J. van de Wetering, M. de Graaf, M. Koopmans, E. Cuppen, P. J. Peters, B. L. Haagmans, H. Clevers, SARS-CoV-2 productively infects human gut enterocytes. *Science*. **369**, 50–54 (2020).

32. S.-C. Lin, L. Qu, K. Ettayebi, S. E. Crawford, S. E. Blutt, M. J. Robertson, X.-L. Zeng, V. R. Tenge, B. V. Ayyar, U. C. Karandikar, X. Yu, C. Coarfa, R. L. Atmar, S. Ramani, M. K. Estes, Human norovirus exhibits strain-specific sensitivity to host interferon pathways in human intestinal enteroids. *Proc. Natl. Acad. Sci. U. S. A.* **117**, 23782–23793 (2020).

33. K. Ettayebi, S. E. Crawford, K. Murakami, J. R. Broughman, U. Karandikar, V. R. Tenge, F. H. Neill, S. E. Blutt, X.-L. Zeng, L. Qu, B. Kou, A. R. Opekun, D. Burrin, D.

Y. Graham, S. Ramani, R. L. Atmar, M. K. Estes, Replication of human noroviruses in stem cell-derived human enteroids. *Science*. **353**, 1387–1393 (2016).

34. B. H. Abuaita, A.-L. E. Lawrence, R. P. Berger, D. R. Hill, S. Huang, V. K. Yadagiri, B. Bons, C. Fields, C. E. Wobus, J. R. Spence, V. B. Young, M. X. O'Riordan, Comparative transcriptional profiling of the early host response to infection by typhoidal and non-typhoidal Salmonella serovars in human intestinal organoids. *PLoS Pathog.* **17**, e1009987 (2021).

35. A.-L. E. Lawrence, B. H. Abuaita, R. P. Berger, D. R. Hill, S. Huang, V. K. Yadagiri, B. Bons, C. Fields, C. E. Wobus, J. R. Spence, V. B. Young, M. X. O'Riordan, Salmonella enterica Serovar Typhimurium SPI-1 and SPI-2 Shape the Global Transcriptional Landscape in a Human Intestinal Organoid Model System. *MBio*. **12** (2021), doi:10.1128/mBio.00399-21.

36. J. L. Forbester, D. Goulding, L. Vallier, N. Hannan, C. Hale, D. Pickard, S. Mukhopadhyay, G. Dougan, Interaction of salmonella enterica serovar Typhimurium with intestinal organoids derived from human induced pluripotent stem cells. *Infect. Immun.* **83**, 2926–2934 (2015).

37. J. L. Forbester, E. A. Lees, D. Goulding, S. Forrest, A. Yeung, A. Speak, S. Clare, E. L. Coomber, S. Mukhopadhyay, J. Kraiczy, F. Schreiber, T. D. Lawley, R. E. W. Hancock, H. H. Uhlig, M. Zilbauer, F. Powrie, G. Dougan, Interleukin-22 promotes phagolysosomal fusion to induce protection against Salmonella enterica Typhimurium in human epithelial cells. *Proc. Natl. Acad. Sci. U. S. A.* **115**, 10118–10123 (2018).

38. P. Geiser, M. L. Di Martino, P. Samperio Ventayol, J. Eriksson, E. Sima, A. K. Al-Saffar, D. Ahl, M. Phillipson, D.-L. Webb, M. Sundbom, P. M. Hellström, M. E. Sellin, Salmonella enterica Serovar Typhimurium Exploits Cycling through Epithelial Cells To Colonize Human and Murine Enteroids. *MBio*. **12** (2021), doi:10.1128/mBio.02684-20.

39. J. L. Leslie, S. Huang, J. S. Opp, M. S. Nagy, M. Kobayashi, V. B. Young, J. R. Spence, Persistence and toxin production by Clostridium difficile within human intestinal organoids result in disruption of epithelial paracellular barrier function. *Infect. Immun.* **83**, 138–145 (2015).

40. M. A. Engevik, H. A. Danhof, A. L. Chang-Graham, J. K. Spinler, K. A. Engevik, B. Herrmann, B. T. Endres, K. W. Garey, J. M. Hyser, R. A. Britton, J. Versalovic, Human intestinal enteroids as a model of Clostridioides difficile-induced enteritis. *Am. J. Physiol. Gastrointest. Liver Physiol.* **318**, G870–G888 (2020).

41. M. A. Engevik, M. B. Yacyshyn, K. A. Engevik, J. Wang, B. Darien, D. J. Hassett, B. R. Yacyshyn, R. T. Worrell, Human Clostridium difficile infection: altered mucus production and composition. *Am. J. Physiol. Gastrointest. Liver Physiol.* **308**, G510-24 (2015).

42. M. A. Engevik, K. A. Engevik, M. B. Yacyshyn, J. Wang, D. J. Hassett, B. Darien, B. R. Yacyshyn, R. T. Worrell, Human Clostridium difficile infection: inhibition of NHE3 and microbiota profile. *Am. J. Physiol. Gastrointest. Liver Physiol.* **308**, G497-509 (2015).

43. K. L. Mohawk, A. D. O'Brien, Mouse models of Escherichia coli O157:H7 infection and shiga toxin injection. *J. Biomed. Biotechnol.* **2011**, 258185 (2011).

44. M. R. Barron, R. J. Cieza, D. R. Hill, S. Huang, V. K. Yadagiri, J. R. Spence, V. B. Young, The lumen of human intestinal organoids poses greater stress to bacteria compared to the germ-free mouse intestine: Escherichia coli deficient in RpoS as a colonization probe. *mSphere*. **5** (2020), doi:10.1128/mSphere.00777-20.

45. A. Rajan, M. J. Robertson, H. E. Carter, N. M. Poole, J. R. Clark, S. I. Green, Z. K. Criss, B. Zhao, U. Karandikar, Y. Xing, M. Margalef-Català, N. Jain, R. L. Wilson, F. Bai, J. M. Hyser, J. Petrosino, N. F. Shroyer, S. E. Blutt, C. Coarfa, X. Song, B. V. Prasad, M. R. Amieva, J. Grande-Allen, M. K. Estes, P. C. Okhuysen, A. W. Maresso, Enteroaggregative E. coli Adherence to Human Heparan Sulfate Proteoglycans Drives Segment and Host Specific Responses to Infection. *PLoS Pathog.* **16**, e1008851 (2020).

46. G. Swaminathan, N. Kamyabi, H. E. Carter, A. Rajan, U. Karandikar, Z. K. Criss, N. F. Shroyer, M. J. Robertson, C. Coarfa, C. Huang, T. E. Shannon, M. Tadros, M. K. Estes, A. W. Maresso, K. J. Grande-Allen, Effect of substrate stiffness on human intestinal enteroids' infectivity by enteroaggregative Escherichia coli. *Acta Biomater.* **132**, 245–259 (2021).

47. A. Rajan, L. Vela, X.-L. Zeng, X. Yu, N. Shroyer, S. E. Blutt, N. M. Poole, L. G. Carlin, J. P. Nataro, M. K. Estes, P. C. Okhuysen, A. W. Maresso, Novel Segment- and Host-Specific Patterns of Enteroaggregative Escherichia coli Adherence to Human Intestinal Enteroids. *MBio*. **9** (2018), doi:10.1128/mBio.02419-17.

48. J. In, J. Foulke-Abel, N. C. Zachos, A.-M. Hansen, J. B. Kaper, H. D. Bernstein, M. Halushka, S. Blutt, M. K. Estes, M. Donowitz, O. Kovbasnjuk, Enterohemorrhagic Escherichia coli reduce mucus and intermicrovillar bridges in human stem cell-derived colonoids. *Cell Mol Gastroenterol Hepatol*. **2**, 48-62.e3 (2016).

49. T. Secher, C. Brehin, E. Oswald, Early settlers: which E. coli strains do you not want at birth? *Am. J. Physiol. Gastrointest. Liver Physiol.* **311**, G123-9 (2016).

50. S. S. Karve, S. Pradhan, D. V. Ward, A. A. Weiss, Intestinal organoids model human responses to infection by commensal and Shiga toxin producing Escherichia coli, 1–20 (2017).

51. Y. Yin, D. Zhou, Organoid and Enteroid Modeling of Salmonella Infection. *Front. Cell. Infect. Microbiol.* **8**, 102 (2018).

52. M. K. Holly, X. Han, E. J. Zhao, S. M. Crowley, J. M. Allaire, L. A. Knodler, B. A. Vallance, J. G. Smith, Salmonella enterica Infection of Murine and Human Enteroid-Derived Monolayers Elicits Differential Activation of Epithelium-Intrinsic Inflammasomes. *Infect. Immun.* **88** (2020), doi:10.1128/IAI.00017-20.

53. B. J. Koestler, C. M. Ward, C. R. Fisher, A. Rajan, A. W. Maresso, S. M. Payne, Human Intestinal Enteroids as a Model System of Shigella Pathogenesis. *Infect. Immun.* **87** (2019), doi:10.1128/IAI.00733-18.

54. S. Ranganathan, M. Doucet, C. L. Grassel, B. Delaine-Elias, N. C. Zachos, E. M. Barry, Evaluating Shigella flexneri Pathogenesis in the Human Enteroid Model. *Infect. Immun.* **87** (2019), doi:10.1128/IAI.00740-18.

55. A. Llanos-Chea, R. J. Citorik, K. P. Nickerson, L. Ingano, G. Serena, S. Senger, T. K. Lu, A. Fasano, C. S. Faherty, Bacteriophage Therapy Testing Against Shigella flexneri in a Novel Human Intestinal Organoid-Derived Infection Model. *J. Pediatr. Gastroenterol. Nutr.* **68**, 509–516 (2019).

56. T. L. Hale, G. T. Keusch, in *Medical Microbiology*, S. Baron, Ed. (University of Texas Medical Branch at Galveston, Galveston (TX), 2011).

57. A. Haage, What's it all about? Organoids (2017), (available at https://www.ascb.org/science-news/whats-it-all-about-organoids/).

58. S. S. Wilson, M. Mayo, T. Melim, H. Knight, L. Patnaude, X. Wu, L. Phillips, S. Westmoreland, R. Dunstan, E. Fiebiger, S. Terrillon, Optimized Culture Conditions for Improved Growth and Functional Differentiation of Mouse and Human Colon Organoids. *Front. Immunol.* **11**, 547102 (2020).

59. U. Lakshmipathy, B. Pelacho, K. Sudo, J. L. Linehan, E. Coucouvanis, D. S. Kaufman, C. M. Verfaillie, Efficient transfection of embryonic and adult stem cells. *Stem Cells*. **22**, 531–543 (2004).

60. C. Rajendra, T. Wald, K. Barber, J. R. Spence, F. Fattahi, O. D. Klein, Generation of Knockout Gene-Edited Human Intestinal Organoids. *Methods Mol. Biol.* **2171**, 215–230 (2020).

61. B.-K. Koo, D. E. Stange, T. Sato, W. Karthaus, H. F. Farin, M. Huch, J. H. van Es, H. Clevers, Controlled gene expression in primary Lgr5 organoid cultures. *Nat. Methods*. **9**, 81–83 (2011).

62. J. Y. Co, M. Margalef-Català, X. Li, A. T. Mah, C. J. Kuo, D. M. Monack, M. R. Amieva, Controlling Epithelial Polarity: A Human Enteroid Model for Host-Pathogen Interactions. *Cell Rep.* **26**, 2509-2520.e4 (2019).

63. L. Dolat, R. H. Valdivia, An endometrial organoid model of interactions between Chlamydia and epithelial and immune cells. *J. Cell Sci.* **134** (2021), doi:10.1242/jcs.252403.

64. J. M. Lemme-Dumit, M. Doucet, N. C. Zachos, M. F. Pasetti, Epithelial and neutrophil interactions and coordinated response to Shigella in a human intestinal enteroid-neutrophil co-culture model. *bioRxiv* (2021), p. 2020.09.03.281535, , doi:10.1101/2020.09.03.281535.

65. G. Noel, N. W. Baetz, J. F. Staab, M. Donowitz, O. Kovbasnjuk, M. F. Pasetti, N. C. Zachos, A primary human macrophage-enteroid co-culture model to investigate mucosal gut physiology and host-pathogen interactions. *Sci. Rep.* **7**, 45270 (2017).

66. J. F. Staab, J. M. Lemme-Dumit, R. Latanich, M. F. Pasetti, N. C. Zachos, Co-culture system of human enteroids/colonoids with innate immune cells. *Curr. Protoc. Immunol.* **131**, e113 (2020).

67. N. Sasaki, K. Miyamoto, K. M. Maslowski, H. Ohno, T. Kanai, T. Sato, Development of a Scalable Coculture System for Gut Anaerobes and Human Colon Epithelium. *Gastroenterology*. **159**, 388-390.e5 (2020).

68. T. Y. Fofanova, C. J. Stewart, J. M. Auchtung, R. L. Wilson, R. A. Britton, K. J. Grande-Allen, M. K. Estes, J. F. Petrosino, A novel human enteroid-anaerobe co-culture system to study microbial-host interaction under physiological hypoxia. *bioRxiv* (2019), p. 555755.

69. L. Sunuwar, J. Yin, M. Kasendra, K. Karalis, J. Kaper, J. Fleckenstein, M. Donowitz, Mechanical Stimuli Affect Escherichia coli Heat-Stable Enterotoxin-Cyclic GMP Signaling in a Human Enteroid Intestine-Chip Model. *Infect. Immun.* **88** (2020), doi:10.1128/IAI.00866-19.

70. X. Li, A. Ootani, C. Kuo, in *Gastrointestinal Physiology and Diseases: Methods and Protocols*, A. I. Ivanov, Ed. (Springer New York, New York, NY, 2016), pp. 33–40.

71. J. A. Crump, S. P. Luby, E. D. Mintz, The global burden of typhoid fever. *Bull. World Health Organ.* **82**, 346–353 (2004).

72. S. E. Majowicz, J. Musto, E. Scallan, F. J. Angulo, M. Kirk, S. J. O'Brien, T. F. Jones, A. Fazil, R. M. Hoekstra, The Global Burden of Nontyphoidal *Salmonella* Gastroenteritis. *Clin. Infect. Dis.* **50**, 882–889 (2010).

73. V. Singh, Salmonella serovars and their host specificity. *J. Vet. Sci. Anim. Husb.* **1** (2013), doi:10.15744/2348-9790.1.301.

74. C. Tükel, M. Raffatellu, D. Chessa, R. P. Wilson, M. Akçelik, A. J. Bäumler, Neutrophil influx during non-typhoidal salmonellosis: who is in the driver's seat? *FEMS Immunol. Med. Microbiol.* **46**, 320–329 (2006).

75. N. A. Feasey, G. Dougan, R. A. Kingsley, R. S. Heyderman, M. A. Gordon, Invasive non-typhoidal salmonella disease: an emerging and neglected tropical disease in Africa. *Lancet*. **379**, 2489–2499 (2012).

76. G. Arya, R. Holtslander, J. Robertson, C. Yoshida, J. Harris, J. Parmley, A. Nichani, R. Johnson, C. Poppe, Epidemiology, Pathogenesis, Genoserotyping, Antimicrobial Resistance, and Prevention and Control of Non-Typhoidal Salmonella Serovars. *Current Clinical Microbiology Reports*. **4**, 43–53 (2017).

77. N. R. Thomson, D. J. Clayton, D. Windhorst, G. Vernikos, S. Davidson, C. Churcher, M. A. Quail, M. Stevens, M. A. Jones, M. Watson, A. Barron, A. Layton, D. Pickard, R. A. Kingsley, A. Bignell, L. Clark, B. Harris, D. Ormond, Z. Abdellah, K. Brooks, I. Cherevach, T. Chillingworth, J. Woodward, H. Norberczak, A. Lord, C. Arrowsmith, K. Jagels, S. Moule, K. Mungall, M. Sanders, S. Whitehead, J. A. Chabalgoity, D. Maskell, T. Humphrey, M. Roberts, P. A. Barrow, G. Dougan, J. Parkhill, Comparative genome analysis of Salmonella Enteritidis PT4 and Salmonella Gallinarum 287/91 provides insights into evolutionary and host adaptation pathways. *Genome Res.* **18**, 1624–1637 (2008).

Chapter 2

Salmonella enterica Serovar Typhimurium SPI-1 and SPI-2 Shape the Global Transcriptional Landscape in a Human Intestinal Organoid Model System

2.1 Abstract

The intestinal epithelium is a primary interface for engagement of the host response by foodborne pathogens, like Salmonella enterica Typhimurium (STM). While the interaction of STM with the mammalian host has been well studied in transformed epithelial cell lines or in the complex intestinal environment in vivo, few tractable models recapitulate key features of the intestine. Human intestinal organoids (HIOs) contain a polarized epithelium with functionally differentiated cell subtypes, including enterocytes and goblet cells and a supporting mesenchymal cell layer. HIOs contain luminal space that supports bacterial replication, are more amenable to experimental manipulation than animals and are more reflective of physiological host responses. Here, we use the HIO model to define host transcriptional responses to STM infection, also determining host pathways dependent on Salmonella pathogenicity island-1 (SPI-1)- and

This chapter represents a published article: Lawrence A-LE*, Abuaita BH*, Berger RP, Hill DR, Huang S, Yadagiri VK, Bons B, Fields C, Wobus CE, Spence JR, Young VB, O'Riordan MX. 2021. Salmonella enterica serovar Typhimurium SPI-1 and SPI-2 shape the global transcriptional landscape in a human intestinal organoid model system. mBio 12:e00399-21. https://doi.org/10.1128/mBio.00399-21.
*Anna-Lisa E. Lawrence and Basel H. Abuaita contributed equally to this work. Order was determined alphabetically by first name.

-2 (SPI-2)-encoded type 3 secretion systems (T3SS). Consistent with prior findings, we find that STM strongly stimulates proinflammatory gene expression. Infection-induced cytokine gene expression was rapid, transient, and largely independent of SPI-1 T3SS-mediated invasion, likely due to continued luminal stimulation. Notably, STM infection led to significant downregulation of host genes associated with cell cycle and DNA repair, leading to a reduction in cellular proliferation, dependent on SPI-1 and SPI-2 T3SS. The transcriptional profile of cell cycle-associated target genes implicates multiple miRNAs as mediators of STM-dependent cell cycle suppression. These findings from Salmonella-infected HIOs delineate common and distinct contributions of SPI-1 and SPI-2 T3SSs in inducing early host responses during enteric infection and reinforce host cell proliferation as a process targeted by Salmonella.

2.2 Importance

Salmonella enterica serovar Typhimurium (STM) causes a significant health burden worldwide yet host responses to initial stages of intestinal infection remain poorly understood. Due to differences in infection outcome between mice and humans, physiological human host responses driven by major virulence determinants of Salmonella have been more challenging to evaluate. Here, we use the three-dimensional human intestinal organoid model to define early responses to infection with wild-type STM and mutants defective in the SPI-1 or SPI-2 type-3 secretion systems. While both secretion system mutants show defects in mouse models of oral Salmonella infection, the specific contributions of each secretion system are less well understood. We show that STM upregulates proinflammatory pathways independently of either secretion system, while the downregulation of the host cell cycle pathways relies on both SPI-1 and SPI-2.

These findings lay the groundwork for future studies investigating how SPI-1- and SPI-2-driven host responses affect infection outcome and show the potential of this model to study host-pathogen interactions with other serovars to understand how initial interactions with the intestinal epithelium may affect pathogenesis.

2.3 Introduction

Enteric bacterial infections constitute a major human disease burden worldwide, with *Salmonella* species accounting for the most hospitalizations in outbreaks with a confirmed cause. In total, *Salmonella* causes an estimated 1.35 million infections in the US alone (1). Enteric infections occur in a complex and highly dynamic environment that traverses the distinct landscapes of the gastrointestinal tract. Relevant to understanding infection are the host processes that shape physicochemical properties of the intestine, including regulation of pH and nutrient absorption, the epithelial layer, which establishes a barrier using epithelial tight junctions, mucus and antimicrobial peptides, the microbiome and the pathogen itself. While animal models are valuable *in vivo* approaches to understand enteric infections, these models suffer from two major limitations. First, the complexity of the mammalian intestine makes finely controlled experimental manipulation and observation challenging. Second, the physiology of the intestine in different organisms can differ sharply, i.e., mice rarely exhibit diarrhea upon infection by pathogens that would cause diarrhea in humans.

Salmonella enterica serovar Typhimurium (STM) infection is a prime example of this disease difference between humans and mice. While STM infection is most commonly associated with self-limiting gastroenteritis in otherwise healthy humans, it causes

systemic acute disease in C57Bl/6 mice (naturally Nramp-deficient) or chronic disease in Nramp-sufficient mouse strains (2, 3). To interrogate molecular mechanisms of host:pathogen interactions during intracellular STM infection, many previous studies have relied on transformed human epithelial cell lines, such as HeLa cervical adenocarcinoma cells or Caco-2 colorectal adenocarcinoma cells, or primary mouse cells like embryonic fibroblasts or macrophages. These cell culture models have revealed much about STM infection, yet do not recapitulate several key features likely to be important during STM enteric infection. These include the continued presence of STM in the lumen, known to be an environment that supports robust replication, and interaction with non-transformed intestinal epithelial cells (IEC) which have specific properties, like mucus secretion or controlled cell cycle regulation. Thus, elucidating the cellular and molecular basis of STM:epithelial interactions in non-transformed human epithelial cells will advance our understanding of aspects of infection that may be relevant to human disease.

In the last decade, human intestinal organoid (HIO) systems have been developed to enable study of more complex IEC characteristics. These organoids are differentiated from non-transformed human pluripotent stem cell lines such as embryonic or induced pluripotent stem cells (ESC/iPSC), and form 3D cyst-like structures delineated by polarized epithelium with a mesenchymal layer surrounding a luminal space (4). HIOs contain multiple epithelial cell subsets, including enterocytes and goblet cells (4). A previous study characterized the global transcriptional profile of WT STM-infected HIOs using human induced pluripotent stem cells (hiPSC) and demonstrated that this IEC model could support STM infection (5). Their results established that the IEC

transcriptional response to WT STM infection from the apical or basolateral route was dominated by pro-inflammatory innate immune signaling pathways. Additional studies have shown that HIOs can support survival and or replication of both pathogenic and commensal bacteria, and that commensal organisms, like *Escherichia coli* (ECOR2), stimulate cell proliferation, epithelial maturation and barrier function (6, 7).

Here we use HIOs derived from the H9 human embryonic stem cell line to define the host transcriptional response to infection by the commonly used laboratory strain STM SL1344 compared to isogenic mutants lacking functional SPI-1 or SPI-2 Type 3 secretion systems (T3SS), major virulence determinants of STM that inject effector proteins into the host for cellular invasion and remodeling of host processes (8, 9). We find that STM-infected HIOs recapitulate some known aspects of intracellular infection, and also report new infection-induced host response profiles that are revealed by the unique features of the HIO model, notably sustained stimulation of the pro-inflammatory by luminal bacteria and crosstalk between the host epithelium and mesenchyme.

2.4 Results

2.4.1 Luminal Salmonella enterica serovar Typhimurium replicates within HIOs and invades HIO epithelial cells

To better recapitulate the *in vivo* human intestinal epithelial response to Salmonella infection, we used the 3-dimensional HIO model that allows longer-term bacterium-host interactions compared to traditional cell lines by maintaining the bacteria in the luminal space throughout the course of infection. STM was inoculated into the HIO lumen by microinjecting each HIO with ~10^3 CFU (low inoculum used for experiments with 24-h

duration) or phosphate-buffered saline (PBS) as a control **(Fig 2.1A)**. HIOs were allowed to recover for 2 h prior to a 15-min treatment with medium containing 100 μg/ml gentamicin to kill bacteria that were introduced into the culture medium during microinjection. Subsequently, HIOs were cultured in medium containing 10 μg/ml gentamicin for the remainder of the experiment to prevent replication of STM outside the HIOs. To confirm that STM replication could take place within HIOs, HIOs were injected with STM harboring the pGEN plasmid encoding the fluorescent protein DsRed (10), and bacterial burden was monitored by live fluorescence microscopy **(Fig 2.1B and C)**. Fluorescence intensity substantially increased by 24 h postinfection (pi), indicating that STM replicated within the HIOs. Replication appeared to occur predominantly in the lumen. Histological analysis of HIO sections suggested that luminal STM invaded intestinal epithelial cells and migrated to the basolateral side **(Fig 2.1D)**. Invasion did not occur uniformly across the HIO, as not all epithelial cells became infected. Additionally, infection was accompanied by increased mucus production on the luminal surface of the epithelial barrier and did not appear to cause major structural damage to the HIO that could be observed by hematoxylin and eosin (H&E) staining **(Fig 2.2)**. To further quantify bacterial burden and to maximize invasion for subsequent experiments, we microinjected HIOs with $\sim 10^5$ CFU (higher inoculum used for experiments with 8-h duration) and enumerated total bacterial CFU per HIO at indicated times postinfection. Comparing results at 2.5 h to those at 8 hpi, we observed an approximately 1-log increase in the number of CFU **(Fig 2.1E)**, confirming that bacteria were replicating within the HIO. To test the contribution of the major virulence determinants, STM type III secretion system 1

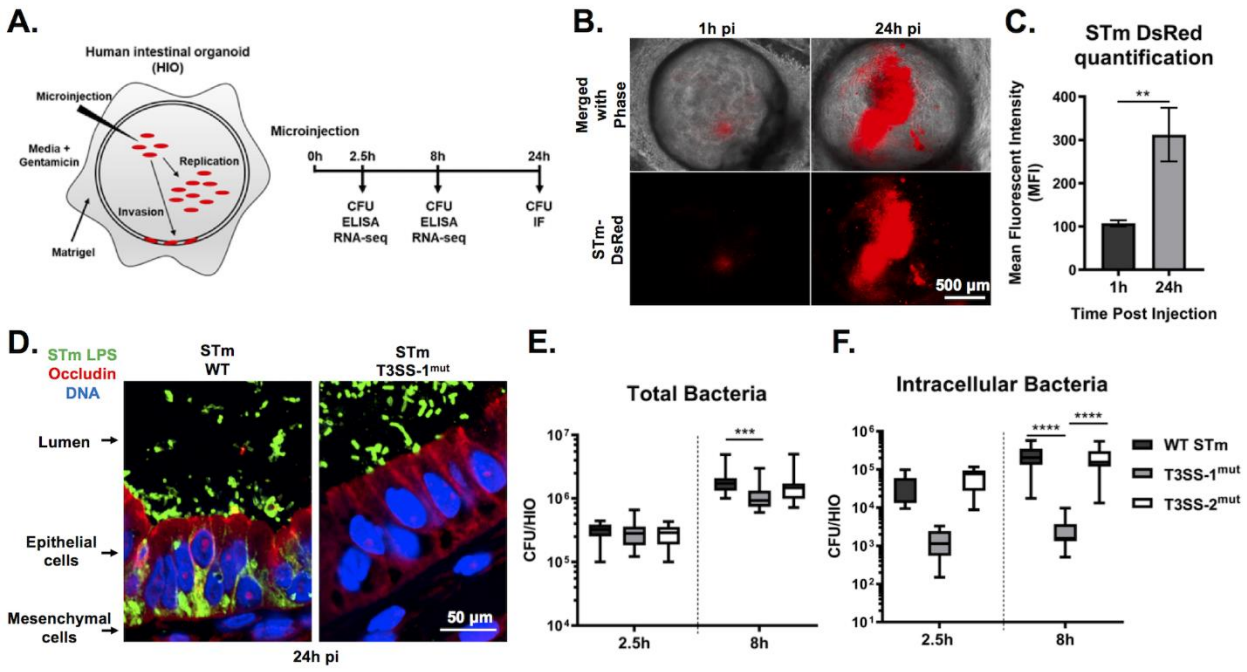

Figure 2.1. WT STM (STM) replicates within the lumen of HIOs and invades IECs dependent on T3SS-1. (A) Diagram of experimental protocol. (B) Fluorescence microscopy of HIOs injected with STM-DsRed, a strain that harbors the pGEN plasmid encoding red fluorescence protein (DsRed) (10). (C) Quantification of panel B. n = 3 biological replicates. Error bars represent SD. P = 0.0047 by unpaired t test. (D) Immunofluorescence of HIO sections infected with STM WT (left) and STM T3SS-1^{mut} (right). LPS, lipopolysaccharide. (E) Total bacteria in HIOs at 2.5 and 24 h postinjection. n = 16 biological replicates. Whiskers represent minimum and maximum values. Significance was calculated by two-way analysis of variance (ANOVA). (F) Intracellular bacteria in HIOs at 24 h postinjection. n > 31 biological replicates. Whiskers represent minimum and maximum values. Significance was calculated by Mann-Whitney test.

(T3SS-1) and 2 (T3SS-2), to bacterial replication within the HIO, we microinjected HIOs with ΔorgA (T3SS-1^{mut}) and ΔssaV (T3SS-2^{mut}) isogenic mutants. We found that both mutants could replicate within HIOs, since we also observed an approximately 1-log increase in total bacteria from 2.5 h to 8 hpi, although T3SS-1^{mut} did not reach levels as high as those of either the WT or T3SS-2^{mut} **(Fig 2.1E)**. Consistent with previous reports, invasion was largely dependent on the STM type III secretion system (T3SS) on pathogenicity island 1 (SPI-1) (11), as an in-frame deletion in a structural gene of the T3SS apparatus (ΔorgA) drastically reduced intracellular CFU numbers **(Fig 2.1F)**. Together, these results demonstrate that the HIO model supports robust luminal and

intracellular replication of STM and that invasion of HIO epithelial cells is dependent on T3SS-1.

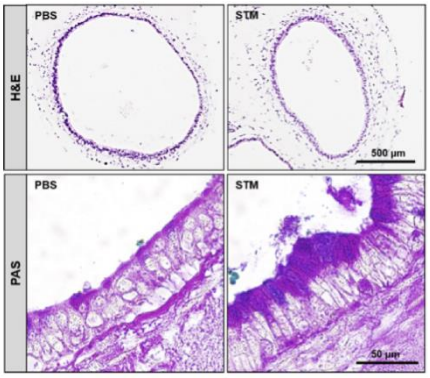

Figure 2.2. Histology of HIO sections fixed 24 hpi with PBS (left) or STM (right). Sections were stained with hematoxylin and eosin (top) and periodic acid-Schiff (bottom) to detect mucus.

2.4.2 Kinetic analysis of HIO transcriptional profiles defines the acute response to Salmonella infection

To gain insight into global HIO transcriptional responses stimulated by STM infection and to define the relative contributions of the major virulence determinants, T3SS-1 and -2, we performed global RNA sequencing (RNA-seq) with HIOs microinjected with PBS, WT STM, T3SS-1^{mut}, and T3SS-2^{mut}. RNA was isolated at 2.5 and 8 hpi to characterize early and intermediate transcriptional responses to infection, including any initial responses that occurred upon immediate recognition of the bacteria. Principal-component analysis (PCA) showed that all infected HIOs displayed markedly different transcriptional profiles than those injected with PBS **(Fig 2.3A)**. Notably, sample clustering occurred primarily by time postinfection, because HIOs infected for 2.5 h and 8 h segregated from each other along the first principal component (x-axis). This difference accounted for 40% of the total variance and suggested that time postinfection is a greater determinant of transcriptional

variance than the contributions of the SPI-1 or SPI-2 T3SS. Similar patterns were observed by Pearson's correlation clustering, which showed clustering of 2.5-h and 8-h samples **(Fig 2.3B)**. In addition, the Pearson's correlation heat map showed that HIOs infected with the invasion-defective T3SS-1^{mut} segregated away from samples infected with WT STM and T3SS-2^{mut} at 2.5 hpi, while at 8 hpi, HIOs infected with WT STM separated from both mutants. These data suggest that T3SS-2^{mut} is attenuated later in

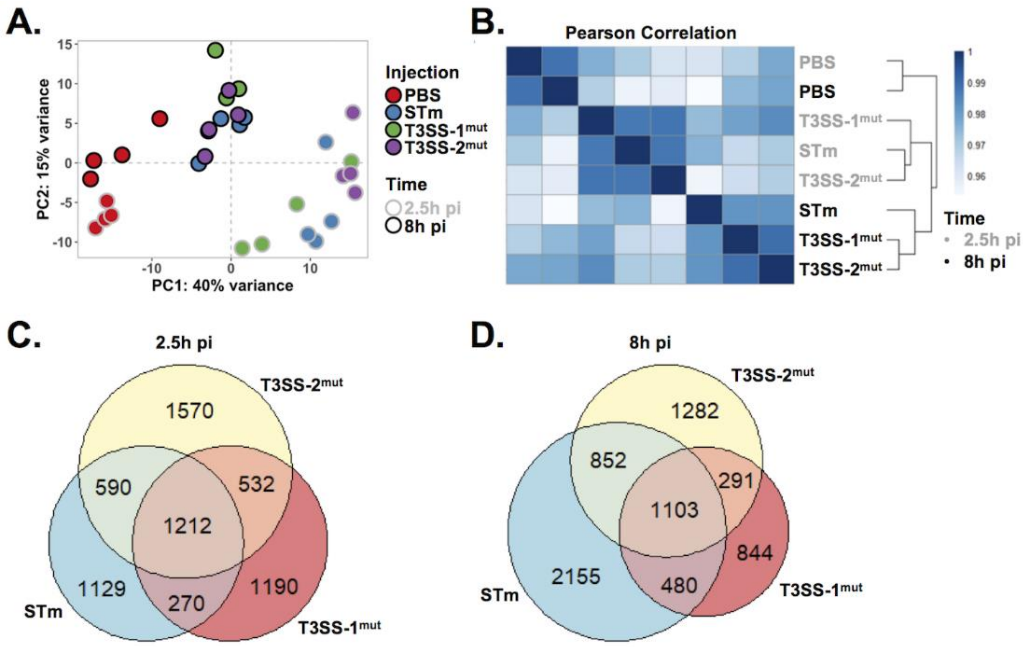

Figure 2.3. HIOs mount an acute transcriptional response to Salmonella infection. (A) Principal-component analysis of HIOs injected with STM T3SS mutants. Each circle represents a biological replicate. (B) Sample distance plot of each HIO condition at 2.5 h (gray) and 8 h (black) postinjection. Sample distance was calculated from normalized gene counts across 4 biological replicates. (C and D) Euler diagram comparison of gene changes in each HIO condition relative to PBS-injected HIOs at 2.5 h (C) and 8 h (D) postinjection. Genes were filtered by a P value of <0.05.

infection than the wild type, a time point at which bacteria have invaded the epithelium, and T3SS-2 is thought to be active in maintaining intracellular infection (9, 12, 13). Using differential gene expression (DEG) analysis, we found that HIOs injected with any of the 3 strains of STM resulted in similar numbers of significant gene changes ($P < 0.05$) at 2.5

hpi compared to PBS controls, suggesting that the early HIO response is driven primarily by luminal bacteria **(Fig 2.3C)**. In contrast, at 8 h both T3SS mutant strains induced fewer significant gene changes than the WT, suggesting that T3SS-1 and -2 effectors are required for STM-induced responses later during infection **(Fig 2.3D)**.

2.4.3 Immune pathways and cell cycle pathways are inversely regulated during *Salmonella* infection

To determine which pathways drive the HIO response to STM infection, we performed pathway enrichment analysis using the Reactome database. Clustering of subpathways into major cellular processes in the Reactome database indicated that the majority of upregulated pathways under all three infection conditions clustered into immune response and signal transduction processes **(Fig 2.4A)**. We examined individual pathway enrichment by gene ratio (fraction of genes in a pathway that were significantly changed) and the $-\log_{10}$(P value) to identify pathways modulated by STM infection and dependence on T3SS-1 or T3SS-2. To our surprise, we observed similar gene ratios between infection with WT STM and the two T3SS mutants in several cytokine signaling pathways, including interleukin-4 (IL-4), IL-17, and IL-10 signaling pathways **(Fig 2.4B, top)**. These results are in contrast to previous reports that T3SS-1-dependent invasion strongly contributes to the inflammatory response, including upregulation of chemokines such as IL-8 (14–16). However, distinct from most tissue culture infection models, the HIO model system features sustained epithelial interaction with both luminal and intracellular Salmonella, pointing to a strong contribution of luminal bacteria in triggering early inflammation. Importantly, not all inflammatory pathways were equally enriched under all 3 infection

conditions; innate immune signaling pathways, including Toll-like receptor (TLR) signaling cascades, were less enriched in T3SS-1^{mut}-infected HIOs at 2.5 hpi and in both T3SS-1^{mut}- and T3SS-2^{mut}-infected HIOs compared to the WT at 8 hpi, suggesting that modulation of these pathways is enhanced by intracellular infection **(Fig 2.4B, middle)**.

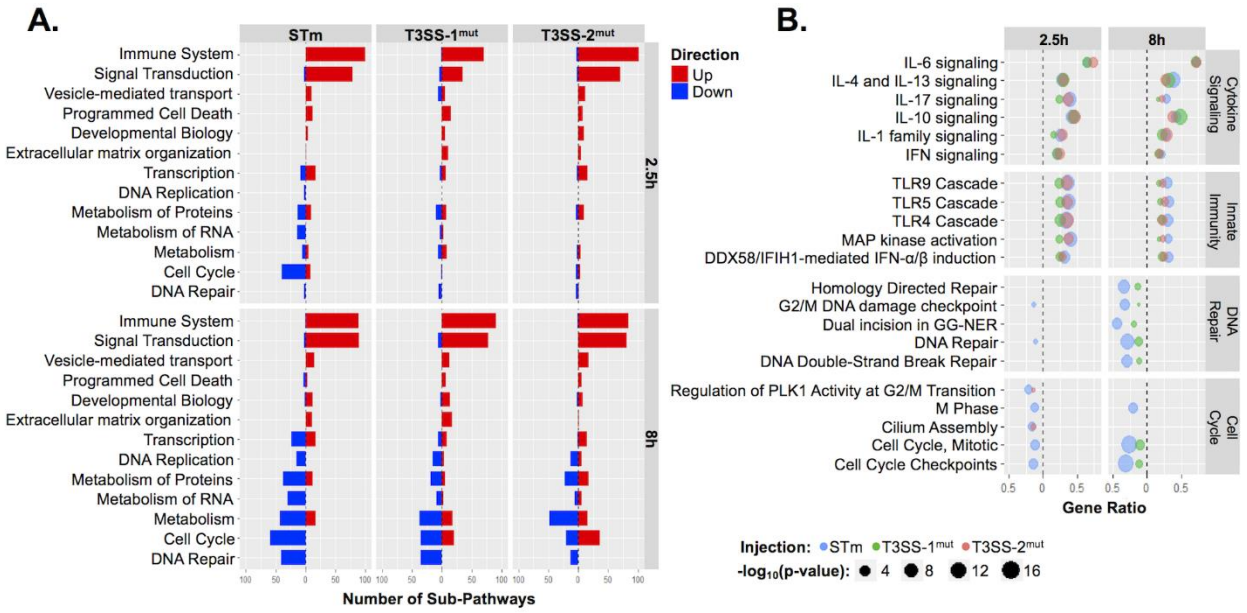

Figure 2.4. Reactome pathway enrichment reveals upregulation of immune system pathways and downregulation of cell cycle and DNA repair pathways. (A) Number of subpathways clustering into major Reactome pathways. Significantly upregulated (red) or downregulated (blue) genes were analyzed using ReactomePA (41), and pathways were clustered into the major pathways from the Reactome database. Major pathways were filtered so that at least 12 subpathways were significantly enriched under at least one condition. (B) Dot plot showing top pathways enriched from Reactome database. Pathway coverage is shown as a gene ratio. –Log10(P value) is presented as the dot size, with WT STM in blue, T3SS-1^{mut} in green, and T3SS-2^{mut} in red. Upregulated pathways are shown on the right of the dotted line and downregulated pathways on the left.

Few downregulated pathways were observed at 2.5 hpi, with more evident by 8 hpi, largely related to cell cycle and DNA repair. Genes involved in cell cycle processes, including checkpoints and mitotic (M) phase pathways, were more highly suppressed in WT-infected HIOs than in T3SS-1^{mut}- and T3SS-2^{mut}-infected HIOs **(Fig 2.4B, bottom)**. Taken together, our findings show that upregulated pathways primarily consisted of

immune-related pathways that were only partially dependent on the two T3SS, while downregulated pathways dominated by cell cycle processes required both T3SS-1 and T3SS-2.

2.4.4 Luminal STM contributes to rapid induction of inflammatory gene expression

We also analyzed the expression of individual genes, selecting proinflammatory gene sets from the Reactome database (cytokines, chemokines, and antimicrobial peptides [AMPs]), to examine fold change relative to PBS-injected control HIOs **(Fig 2.5A to C and Fig 2.6)**. Induction of genes in all three categories occurred rapidly, characterized by markedly increased levels of cytokine, chemokine, and AMP transcripts at 2.5 hpi that were reduced by 8 hpi. Global patterns revealed that infection with T3SS-1^{mut} induced weaker stimulation of these proinflammatory mediators than the other infection conditions, although many transcripts were still upregulated compared to PBS-injected HIOs. The strongest responders to infection were cytokines CSF3, also called granulocyte colony-stimulating factor (G-CSF), and IL17C, and the antimicrobial peptide beta defensin-2 (DEFB4). Strong upregulation of IL17C and DEFB4, genes involved in epithelial intrinsic defenses (17–19), suggests that upon sensing infection, epithelial cells mount a direct antimicrobial response in addition to producing chemokines to recruit other immune cells. Notably, chemokine genes were not induced as strongly at these time points as cytokine and AMP genes **(Fig 2.5B)**. Some other responses occurred independently of either T3SS-1 and T3SS-2, including tumor necrosis factor (TNF), IL-8, and CXCL5 genes, as fold change was comparable between the three conditions while IL-6 expression was dependent on T3SS-1.

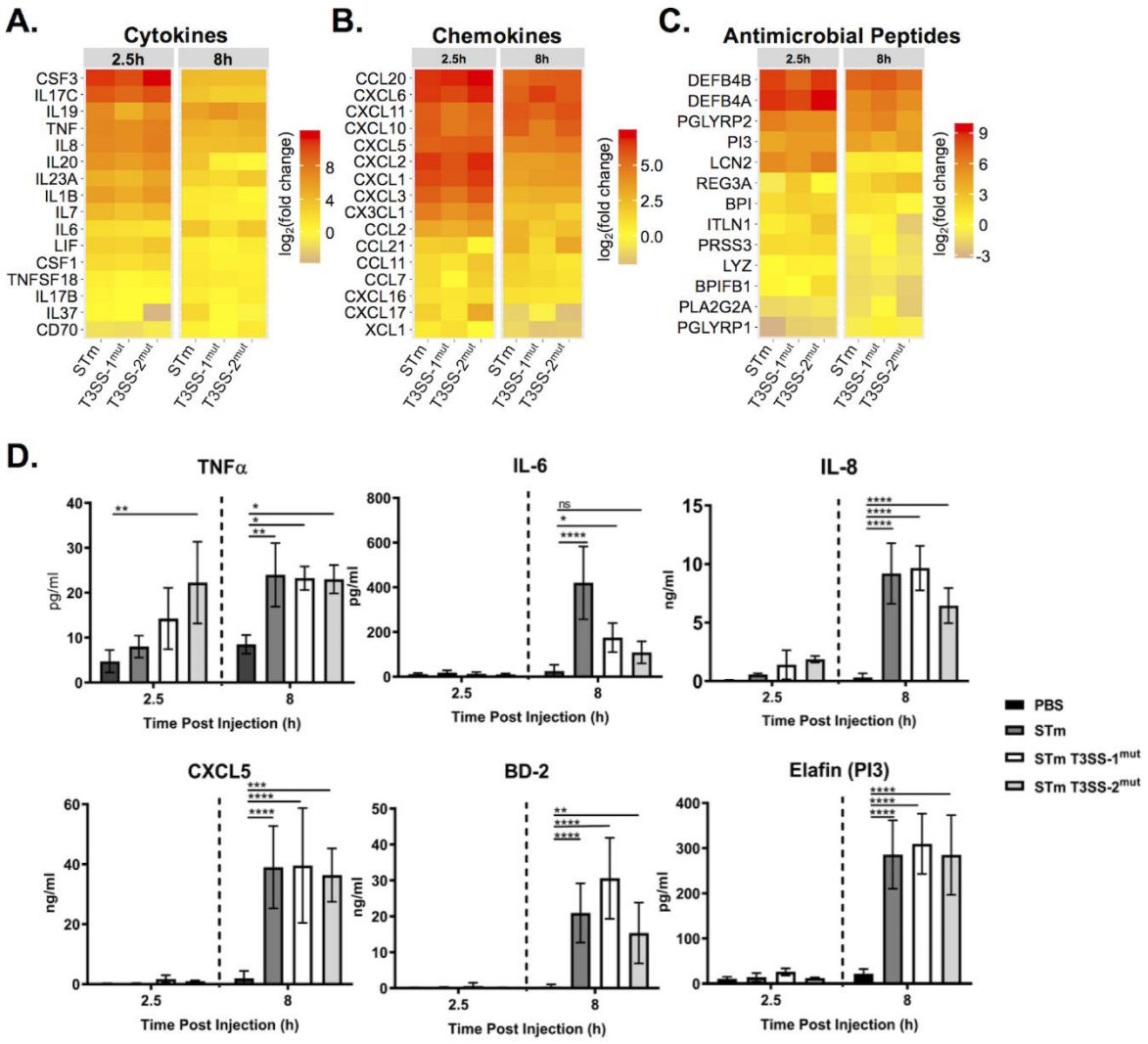

Figure 2.5. Cytokine, chemokine, and antimicrobial peptide induction is not dependent on T3SS-1 or T3SS-2. (A to C) Gene expression presented as log2(fold change) relative to PBS injected HIOs at 2.5 h and 8 h postinjection. (A) Cytokine expression; (B) chemokine expression; (C) antimicrobial peptide expression. (D) Cytokine, chemokine, and antimicrobial peptide levels measured from HIO supernatant at 2.5 and 8 h postinjection via ELISA. n = 4 biological replicates. Error bars represent SD. Significance was calculated by two-way ANOVA.

To test whether gene expression level differences were reflected at the protein level, we collected supernatants from infected HIOs at 2.5 h and 8 hpi and measured cytokines by enzyme-linked immunosorbent assay (ELISA). In concordance with the transcript data, release of TNF, IL-8, and CXCL5 was consistent across all three infection conditions **(Fig**

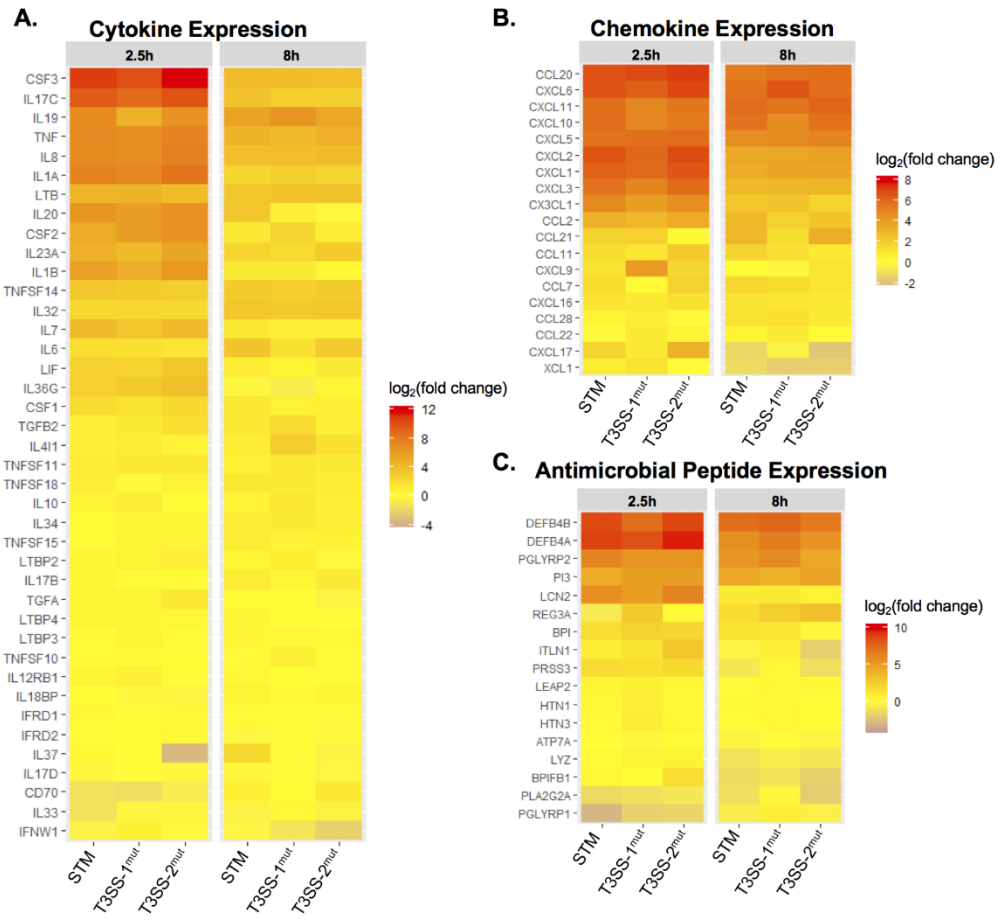

Figure 2.6. Complete cytokine, chemokine, and antimicrobial peptide gene lists from Reactome. Gene expression presented as log2(fold change) relative to PBS-injected HIOs at 2.5 h and 8 h postinjection. (A) Cytokine expression. (B) Chemokine expression. (C) Antimicrobial peptide expression

2.5D and Fig 2.7). While the degree of transcript upregulation for AMPs varied between time points across the three infections, release of these mediators (Beta Defensin-2 and ELAFIN) into the medium did not significantly differ between WT and mutant infections. In contrast, IL-6 was present at significantly lower levels in supernatants from HIOs infected with either mutant, even though transcripts were increased in STM- and T3SS-2^{mut}-infected HIOs by 8 hpi. Reduced levels of IL-6 in the supernatant in T3SS-2^{mut}-infected HIOs, even though IL-6 transcript was induced to WT levels, suggest additional posttranscriptional regulation affecting IL-6 production in infected HIOs. Collectively,

these results show that the HIOs mount a rapid proinflammatory, antimicrobial transcriptional response to STM infection and that invasion-defective T3SS-1^{mut} bacteria, previously reported to have a large defect in inducing an inflammatory response, can signal through the luminal compartment to induce robust inflammation following prolonged interactions with the epithelium.

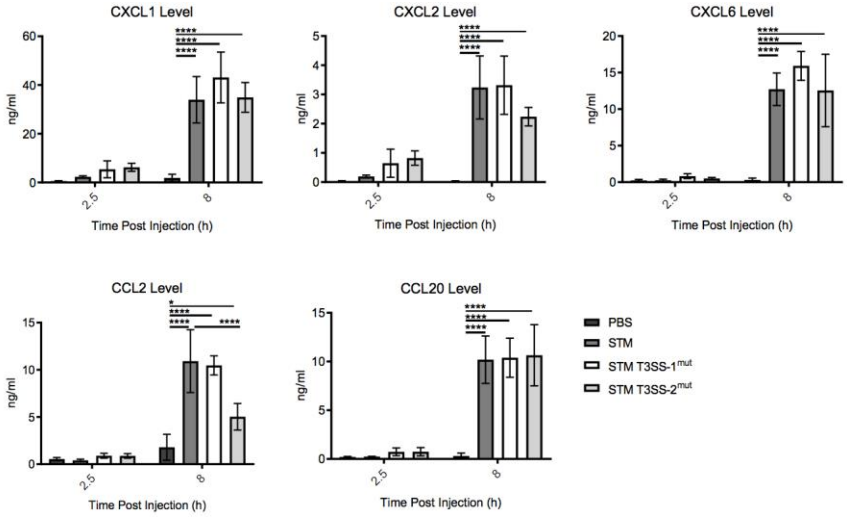

Figure 2.7. Chemokine levels measured from HIO supernatant at 2.5 h and 8 h postinjection via ELISA. n = 4 biological replicates. Error bars represent SD. Significance was calculated by two-way ANOVA.

2.4.5 Downregulation of cell cycle pathways during STM infection is dependent on T3SS-1 and T3SS-2

We next evaluated genes that were downregulated during STM infection. Our pathway enrichment analysis identified cell cycle as the category containing the most significantly downregulated pathways. To assess whether downregulation of cell cycle-related pathways was dependent on T3SS-1 and/or -2, we directly compared genes in the cell cycle pathway that were significantly changed under the three infection conditions. In agreement with our pathway-level analysis **(Fig 2.4A)**, we found relatively few genes in

the cell cycle pathway significantly downregulated compared to PBS-injected HIOs at 2.5 hpi **(Fig 2.8A)**. However, by 8 hpi the number of significantly downregulated genes substantially increased from 76 genes to 161 genes in the WT-infected HIOs **(Fig 2.8B)**. Downregulation of gene expression was partially dependent on both T3SS-1 and -2, as only 68 genes and 58 genes, respectively, were significantly downregulated at 8 hpi. To validate these findings, reverse transcription-quantitative PCR (RT-qPCR) was performed on RNA isolated at 8 hpi. While there was some variation across biological replicates, we consistently observed the downregulation of cell cycle genes CDK1, CDC23, and CDC25a in 3 out of our 4 biological replicates infected with WT STM but not in HIOs infected with either T3SS-1 or T3SS-2 mutants **(Fig 2.8C)**. These observations are consistent with a role for the T3SS in establishing an intracellular niche for STM replication.

Decreases in transcript levels can occur through several mechanisms, including halting synthesis of new transcripts or through degradation of existing transcripts by microRNA (miRNA). Evidence for miRNA expression manipulation by pathogens, including Salmonella, continues to emerge (20–24), so we used gprofiler2 (25) as the basis for an informatics approach to identify potential regulatory miRNAs associated with our downregulated gene sets. Analysis of infected HIOs with gprofiler2 yielded several miRNAs predicted to be associated with the WT STM-downregulated gene sets, while no miRNA was strongly associated with downregulated gene sets from T3SS-1^{mut}- or T3SS-2^{mut}-infected HIOs **(Fig 2.8D)**. Several of these miRNA species, including miR-192-5p and miR-215-5p, which were significantly associated with the WT STM-infected HIO gene

set, regulate cell proliferation (26, 27), and miR-16-5p overexpression during Salmonella infection (20) alters cell cycle progression. To validate whether specific miRNA species were altered during infection in the HIOs, we tested expression of miR-192-5p, miR-215-5p, and miR-16-5p by RT-qPCR. Consistent with our bioinformatics prediction, we observed significant upregulation of the top predicted miRNA species miR-192-5p and miR-215-5p in STM-infected HIOs compared to PBS-injected control HIOs but did not observe a significant difference in miR-16-5p levels **(Fig 2.8E)**. To evaluate if decreased cell cycle-associated transcripts functionally impacted cell cycle progression, we treated HIOs with EdU for 24 h to monitor cellular proliferation in HIOs that were injected with PBS or WT STM. STM significantly reduced the number of EdU-positive cells in the HIOs **(Fig 2.8F and G)**. Strikingly, we did not observe EdU-positive staining in cells actively infected by STM; instead, EdU was primarily associated with the surrounding mesenchymal cells **(Fig 2.8H)**. Taken together, these data suggest that downregulation of cell cycle genes during WT STM infection, likely driven in part by miRNA-mediated silencing, leads to a decrease in cellular proliferation in supporting mesenchymal cells.

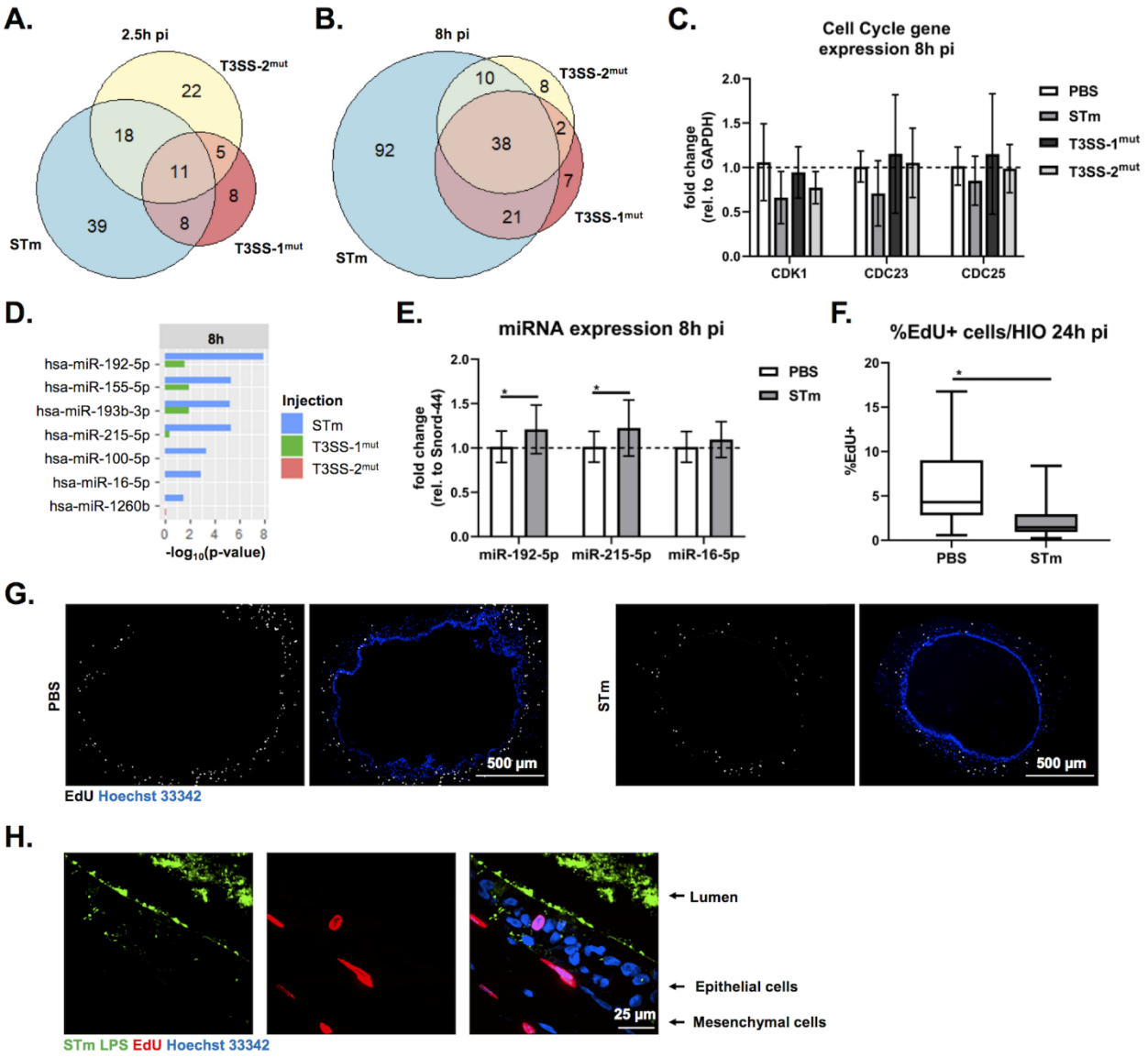

Figure 2.8. STM infection suppresses cell cycle dependent on T3SS-1 and T3SS-2. (A and B) Euler diagram comparison of cell cycle genes downregulated compared to PBS injected HIOs at 2.5 h (A) and 8 h (B) postinjection. Genes were filtered by a P value of <0.05. (C) RT-qPCR validation of RNA-seq data testing expression of select cell cycle genes at 8 hpi. (D) miRNA enrichment profiles were calculated using Gprofiler package in R (25) based on significantly downregulated genes compared to PBS injected HIOs. –Log10(P value) is plotted for each miRNA that is significantly enriched under at least one infection condition. (E) RT-qPCR testing miRNA expression in infected HIOs at 8 hpi. Significance was determined by one-tailed t test (*, $P < 0.05$). (F) Quantitation of EdU-positive cells per HIO at 24 hpi. Outliers were removed using the ROUT method, where Q = 0.1%, and significance was determined by unpaired t test (*, $P < 0.05$). (G) Fluorescent images of HIO sections microinjected with PBS (left) and STM WT (right) exposed to EdU for 24 h. (H) High-magnification image of STM-injected HIO assessed for EdU-positive cells at 24 hpi

2.5 Discussion

Initial human intestinal responses to Salmonella enterica serovar Typhimurium are still incompletely understood despite the prominent contribution of this species to human disease burden. Here, we used the human intestinal organoid model to analyze transcriptional profiles defining early host responses to STM infection, including the contribution of two major virulence determinants, T3SS-1 and -2. We found that HIOs responded rapidly and robustly to all 3 infections by upregulating proinflammatory pathways early and transiently, whereas downregulation of host pathways, including cell cycle and DNA repair, occurred later and only in WT STM-infected HIOs.

Salmonella infection strongly induces inflammatory responses and exploits the inflammatory environment created during infection to outcompete the resident microbiota and replicate within the lumen of the intestine (28). Accordingly, our transcriptomics analysis found that the dominant response occurring in the HIOs was inflammatory. While this was largely expected for WT STM infection, based on studies in other model systems, we had predicted that infection with T3SS-1^{mut} would result in reduced activation of these pathways. Prior studies showed that T3SS-1 strongly contributes to the inflammatory response, with significantly reduced levels of inflammation and colitis in mouse models and little to no upregulation of proinflammatory cytokines in tissue culture models of STM infection (14–16). However, we observed largely similar patterns of induction of several proinflammatory mediators in HIOs infected with T3SS-1^{mut}. This included IL-8, which in HeLa cells was dependent on T3SS-1 effectors for upregulation (29). This finding highlights the advantage of using model systems that more closely reflect physiologic

infection conditions. Mice do not naturally present with the same disease as humans following Salmonella infection, suggesting that there are differences in infection progression, and although immortalized cell lines can more easily be manipulated than mouse models, the inoculum is removed after the initial infection; therefore, longer-term interactions between the luminal surface of the epithelium and the bacteria cannot be easily studied. The enclosed lumen of the HIOs naturally limits the extent of extracellular bacterial replication and allows the study of longer-term interactions, revealing a strong contribution of luminal bacteria in inducing upregulation of proinflammatory mediators, as shown by host response to T3SS-1^{mut}, which exhibits a >2-log defect in invasion. Prior evidence suggests that gut luminal bacteria can act as a reservoir to continually seed sites of systemic infection (30), and the HIO model may serve to explore the dynamic contribution of luminal bacteria to continued invasion, immune modulation, and remodeling of the luminal environment.

Among our upregulated gene sets, key targets reflected known modulators of STM infection. The strongest responder in all 3 infection conditions, CSF3 (encoding G-CSF), was previously implicated in regulating a supershedder phenotype of Salmonella to enhance the spread of the bacteria to other hosts, and injection of G-CSF in moderate-shedder animals recapitulated the supershedder phenotype (29). Additionally, IL17C and DEFB4 contribute to epithelial intrinsic defenses against bacterial pathogens by regulating intestinal barrier integrity and bacterial killing, respectively (17–19). Overall, the transcriptional responses across the 3 infection conditions were similar, with only a slight decrease in upregulation in the T3SS-1^{mut}-infected HIOs. Notably, transcriptional

upregulation of IL-6 appeared to be dependent on T3SS-1. Interestingly, while IL-6 transcript upregulation was dependent on T3SS-1, neither T3SS-1^{mut} nor T3SS-2^{mut} infection stimulated significant IL-6 protein production compared to that of PBS-injected HIOs. These observations suggest a novel function for T3SS-2 in posttranscriptional regulation of IL-6 production. Together, these findings highlight several avenues for future study, including IL-6 posttranscriptional regulation by T3SS-2 and how CSF3 regulation and function in the early stages of STM infection may contribute to a supershedder phenotype, using an HIO system reconstituted with immune cells, like neutrophils.

Downregulation of host gene expression was dependent on T3SS-1 and -2 and notably consisted primarily of cell cycle-related genes. Cell cycle regulation in the intestine affects the rate of cell turnover to shed infected or damaged cells and, therefore, is commonly targeted by bacteria (30, 31). A previous study from our consortium group showed that HIO colonization with a commensal strain of E. coli enhanced cell proliferation and, therefore, could be protective against invasive infections (6). In contrast, Pinchuk and colleagues recently reported that STM can block cell cycle progression in mouse intestinal cells and proposed that this enhances intestinal colonization of STM (32). This study showed that T3SS-2 effectors regulated cell proliferation through targeting proteins important for cleavage furrow formation rather than exerting regulation at the transcriptional level. Here, we found that both T3SS-1 and T3SS-2 contribute to downregulating cell cycle-related transcripts leading to a reduction in cellular proliferation, suggesting that STM can also regulate the cell cycle at the transcriptional level. Consistent with this observation, Maudet et al. reported that transcriptional regulation of

cyclin D1 during STM infection promoted cell cycle arrest in G2/M phase and identified the miR-15 family as key regulators (20). Expression of miRNAs is increasingly appreciated as a mechanism regulating gene expression during bacterial infections, and our results highlight miR-192-5p and miR-215-5p as likely contributors to STM-associated suppression of cell proliferation (31). Although our bioinformatics prediction showed significant association of all three miRNAs with our downregulated gene set, we only measured upregulation of miR-192-5p and miR-215-5p. There is known overlap in cell cycle genes that are regulated by each of these three miRNAs (31); thus, increased expression of any one or more of these miRNAs leading to downregulation of common target genes would likely be sufficient to predict associations for all three regulatory miRNAs. Notably, the Maudet et al. study identified miR-16, which we determined to be unchanged in the HIOs in this study, as one of the miRNA species that was downregulated during STM infection to regulate cell cycle progression (20). For further validation, we tested miRNA expression in HeLa cells (the primary cell line used in the Maudet et al. study), and although miR-16-5p expression was detected in our HeLa cell experiment, neither miR-192-5p nor miR-215-5p was detected (data not shown). These observations suggest that baseline miRNA expression is different in each model system, underscoring the need to more closely recapitulate physiologic conditions when studying host responses to Salmonella.

Finally, our observation that STM infection reduced proliferation in supporting mesenchymal cells builds on a previous study demonstrating that commensal E. coli strain ECOR2 stimulates epithelial cell proliferation (6), highlighting the complex

interactions that can be revealed in the HIO model. Mesenchymal cells serve many roles in the intestine, including sensing and responding to inflammation, both during initial pathogen recognition and during resolution, as well as modulating cellular proliferation through Wnt signaling (32). The mesenchymal cells also serve as a second-line defense against invading pathogens in the intestine (33). Mesenchymal cells engage in cross talk with nearby cells to limit tissue damage and can also reduce inflammation by secreting antagonizing receptors for IL-1 or TNF-α or through production of anti-inflammatory proteins, such as stanniocalcin-1 (34). Our findings hint at the cross talk between epithelial and mesenchymal cells, implicating epithelial signaling to the mesenchyme to reduce cellular proliferation during STM infection. This engagement may further enhance inflammation during STM infection due to potential depletion of immunoregulatory cells (32). Future work, including utilizing single-cell RNA-seq technology, will further elucidate the specific interactions between epithelial and mesenchymal cells during Salmonella infection.

Collectively, the complex and dynamic transcriptional response in the STM-infected HIOs demonstrates the utility of using this nontransformed epithelial cell model to examine what aspects are specific and physiologically relevant to human intestinal disease. HIOs supported both luminal and intracellular bacterial replication while still maintaining overall structural integrity, better mimicking the interaction of both these bacterial populations with the epithelium *in vivo*. This model system allows for the observation of infected cells as well as bystander cells that can be studied using single-cell RNA-seq, and because of the enclosed environment, the entire HIO can be visualized in sections or by live-cell

imaging. Additionally, with the enclosed lumen, it is possible to study sustained responses induced by the bacteria from the extracellular environment, an important aspect of STM infection biology that has been difficult to study in traditional cell culture models. As further evidence to strengthen this model for future studies, our upregulated gene set for the WT infection was highly concordant with data from an earlier study that looked at the iPSC-derived HIO transcriptional responses to WT STM infection (5); 90% of the top 30 genes regulated by STM were also significantly changed in our data set. This concordance opens areas for future work, including studying posttranscriptional regulation of cytokine production by T3SS-2 and epithelial-mesenchymal interactions modulating cell cycle processes during STM infection. Additionally, the HIO model is well suited to characterize host responses to other Salmonella enterica serovars to elucidate how individual serovars interact uniquely with the host, as well as layering in components such as a simplified microbiome or immune cells to study more complex interactions between Salmonella and the human intestine.

2.6 Materials and Methods

Table 2.1 Strains used in this study

Name	Strain	Genotype
Salmonella enterica serovar Typhimurium (STM)	SL1344	
STM T3SS-1^{mut}	SL1344	*orgA*::Tn5lacZY
STM T3SS-2^{mut}	SL1344	*ssaV*::*mudJ*
STM-DsRed	SL1344	pGEN plasmid expressing Ds-Red

2.6.1 HIO differentiation and culture

HIOs were generated by the In Vivo Animal and Human Studies Core at the University of Michigan Center for Gastrointestinal Research, as previously described (35). Human ES cell line WA09 (H9) was obtained from Wicell International Stem Cell Bank and cultured on Matrigel (BD Biosciences) coated 6-well plates in mTeSR1 media (Stem Cell Technologies) at 37°C in 5% CO2. Cells were seeded onto Matrigel-coated 24-well plates in fresh mTeSR1 media and grown until 85-90% confluence. Definitive endoderm differentiation was induced by washing the cells with PBS and culturing in endoderm differentiation media (RPMI 1640, 2%FBS, 2 mM L-glutamine, 100 ng/ml Activin A and 100 Units/ml Pen/Strep) for three days where media were exchanged each day. Cells were then washed with endoderm differentiation media without Activin A and cultured in mid/hindgut differentiation media (RPMI 1640, 2%FBS, 2 mM L-glutamine, 500 ng/ml FGF4, 500 ng/ml WNT3A and 100 Units/ml Pen/Strep) for 4 days until spheroids were present. Spheroids were collected, mixed with ice cold Matrigel (50µl of Matrigel + 25µl of media + 50 spheroids), placed in the center of each well of a 24-well plate, and incubated at 37°C for 10 minutes to allow Matrigel to solidify. Matrigel embedded spheroids were grown in ENR media (DMEM:F12, 1X B27 supplement, 2 mM L-glutamine, 100 ng/ml EGF, 100 ng/ml Noggin, 500 ng/mL Rspondin1, and 15 mM HEPES) for 14 days where medium was replaced every 4 days. Spheroids growing into organoids (HIOs) were dissociated from Matrigel by pipetting using a cut wide-tip (2-3 mm). HIOs were mixed with Matrigel (6 HIOs + 25µL of media + 50µL of Matrigel) and placed in the center of each well of 24-well plates and incubated at 37°C for 10 minutes. HIOs were further grown for 14 days in ENR media with medium exchanged every 4 days. Before use in experiments, HIOs were carved out of Matrigel, washed with DMEM:F12

media, and re-plated with 5 HIO/well in 50μL of Matrigel in ENR media with medium exchanged every 2-3 days for 7 days prior to microinjection.

2.6.2 Bacterial growth conditions and HIO microinjection

STM strains used in this study are listed in Table S5. Strains were stored at −80°C in LB medium containing 20% glycerol and cultured on Luria-Bertani (LB, Fisher) agar plates. Selected colonies were grown overnight at 37ºC under static conditions in LB liquid broth. Bacteria were pelleted, washed and re-suspended in PBS. Bacterial inoculum was estimated based on OD600 and verified by plating serial dilutions on agar plates to CFU. HIOs were cultured in groups of 5/well using 4-well plates (ThermoFisher). Individual HIO lumens were microinjected using a glass caliber needle with 1μl of PBS control or different STM mutants (10^5CFU/HIO for 8h infections or 10^3CFU/HIO for 24h infections). HIOs were washed with PBS and incubated for 2h at 37°C in ENR media to allow for re-sealing of the epithelial layer. HIOs were then treated with gentamicin (100 μg/ml) for 15 min to kill bacteria outside the HIOs, then incubated in fresh medium with gentamicin (10 μg/ml).

2.6.3 Quantitative measurement of HIO-associated bacteria and cytokine secretion

Quantitation of viable bacteria was assessed per HIO. Individual HIOs were removed from Matrigel, washed with PBS and homogenized in PBS. Total CFU/HIO were enumerated by serial dilution and plating on LB agar. To assess intracellular bacterial burden, HIOs were sliced in half, treated with gentamicin (100 μg/ml) for 10 min to kill luminal bacteria, washed with PBS, homogenized and bacterial CFU were enumerated on LB-agar. Medium from each well (5 HIOs/well) was collected at indicated time points after

microinjection and cytokines, chemokines and defensins were quantified by ELISA assay at the UM ELISA core.

2.6.4 Immunohistochemistry and immunofluorescence staining

HIOs were fixed with 10% neutral buffered formalin or Carnoy's solution for 2 days and embedded in paraffin. HIOs were sectioned (5 μm thickness) by the UM Histology Core and stained with hematoxylin and eosin (H&E). Carnoy's-fixed HIO sections were stained with periodic acid-Schiff (PAS) staining reagents according to manufacturer's instructions (Newcomersupply). H&E- and PAS-stained slides were imaged on an Olympus BX60 upright microscope. For immunofluorescence staining, formalin-fixed HIO sections were deparaffinized and subjected to antigen retrieval in sodium citrate buffer (10 mM Sodium citrate, 0.05% Tween 20, pH 6.0). Sections were permeabilized with PBS+ 0.2% Triton X-100 for 30 min, then incubated in blocking buffer (PBS, 5% BSA, and 10% normal goat serum) for 1h. Human Occludin was stained using rabbit anti-Occludin polyclonal antibody (ThermoFisher) in blocking buffer overnight at 4°C. Goat anti-mouse secondary antibody conjugated to Alexa-594 was used according to manufacturer's instructions (ThermoFisher) for 1h RT in blocking buffer. *Salmonella* were stained using FITC-conjugated Anti-*Salmonella* Typhimurium antibody (Santa Cruz, 1E6) in blocking buffer for 1h RT. DAPI was used to stain DNA. Sections were mounted using coverslips (#1.5) and Prolong Diamond Antifade Mountant (ThermoFisher). Images were taken on the Nikon A1 confocal microscope and processed using ImageJ.

2.6.5 Cell proliferation analysis

After microinjection, 25 μM EdU was added to the HIO culture medium and incubated at 37°C for 24 h to allow incorporation into dividing cells. HIOs were then fixed with 10% neutral buffered formalin for 2 days and embedded in paraffin. HIOs were sectioned (5-μm thickness) by the UM Histology Core, and samples were stained using the Click-iT EdU cellular proliferation kit (ThermoFisher) according to the manufacturer's protocol. HIOs were counterstained using the anti-Salmonella Typhimurium antibody and Hoechst to detect bacteria and DNA, respectively, before mounting in Prolong glass antifade mountant (ThermoFisher). Images were taken on an Olympus BX60 upright microscope and processed and analyzed using ImageJ and CellProfiler.

2.6.6 RNA sequencing

Total RNA was isolated from groups of 5 HIOs per replicate with a total of 4 replicates per condition using the mirVana miRNA isolation kit (ThermoFisher). Cytosolic and mitochondrial rRNA was removed from samples using the Ribo-Zero gold kit according to the manufacturer's instructions (Illumina). The quality of RNA was confirmed (RNA integrity number, >8.5) using a Bioanalyzer and used to prepare cDNA libraries by the UM DNA Sequencing Core. Libraries were sequenced on Illumina HiSeq 2500 platforms (single-end, 50-bp read length).

2.6.7 RT-qPCR analysis

Total RNA was isolated with 5 HIOs per replicate with a total of 4 biological replicates per condition using the mirVana miRNA isolation kit (ThermoFisher). cDNA was synthesized using random hexamers (Invitrogen), and gene expression was tested using PowerUp

SYBR green master mix (Invitrogen). The change in threshold cycle was calculated relative to glyceraldehyde-3-phosphate dehydrogenase (GAPDH) expression. The following primer sequences were used: for GAPDH, F, 5′-CTCTGCTCCTCCTGTTCGAC-3′; R, 5′-TTAAAAGCAGCCCTGGTGAC-3′; for CDK1, F, 5′-CACATGAGGTAGTAACACTCTG-3′; R, 5′-CAAATGTCAACTGGAGTTGAG-3′; for CDC23, F, 5′-CACTGCCTTTCGCTATCTG-3′; R, 5′-TTCCCGGGTATCATTAAATGC-3′; for CDC25, F, 5′-CTGGAGGTGAAGAACAACAG-3′; R, 5′-AGGAGAATCTAGACAGAAACCTG-3′. To quantify changes in miRNA expression, cDNA was synthesized using the miRCURY LNA RT kit (Qiagen) according to the manufacturer's protocol and detected using the miRCURY LNA SYBR green PCR kit (Qiagen) with the following primers: YP00205702, YP00204099, YP00204598, and YP00203902. SNORD44 was used as a housekeeping control to calculate the change in threshold cycle for each miRNA.

2.6.8 Statistical methods

Data were analyzed using GraphPad Prism 7 and R software. Statistical tests for all analyses are outlined in the figure legends. The means from at least 3 independent experiments are presented, with error bars showing standard deviations (SD). P values of less than 0.05 were considered significant: *, $P < 0.05$; **, $P < 0.01$; ***, $P < 0.001$; ****, $P < 0.0001$. All statistically significant comparisons within experimental groups are marked.

2.6.9 Data and software availability

Data were deposited into ArrayExpress (E-MTAB-10451). Source code for analyses can be found at https://github.com/rberger997/HIO_dualseq2 and https://github.com/aelawren/HIO_RNAseq.

2.6.10 RNA-seq analysis protocol

(i) Sequence alignment.

Sequencing generated FASTQ files of transcript reads were pseudoaligned to the human genome (GRCh38.p12) using kallisto software (36). Transcripts were converted to estimated gene counts using the tximport (37) package with gene annotation from Ensembl (38).

(ii) Differential gene expression.

Differential expression analysis was performed using the DESeq2 package (39), with P values calculated by the Wald test and adjusted P values calculated using the Benjamini & Hochberg method (40).

(iii) Pathway enrichment analysis.

Pathway analysis was performed using the Reactome pathway database and pathway enrichment analysis in R using the ReactomePA software package (41). miRNA analysis was performed using Gprofiler2 package (25).

Statistical analysis.

Analysis was done using RStudio version 1.1.453. Plots were generated using ggplot2 (42) with data manipulation done using dplyr (43). Euler diagrams of gene changes were generated using the Eulerr package (44). Cluster heatmaps were generated using the pheatmap package (45).

Acknowledgments

This work was supported by NIAID U19AI116482-01. A.-L.L. was supported by the Molecular Mechanisms of Microbial Pathogenesis training grant (NIH T32 AI007528). We thank the Host-Microbiome Initiative, the Center for Live Cell Imaging (CLCI), Microscopy and Image Analysis Laboratory (MIL), the Bioinformatics Core, the Comprehensive Cancer Center Immunology, and Histology Cores, supported by the University of Michigan Cancer Center Support Grant (P30CA46592), and the DNA Sequencing Core at the University of Michigan Medical School. We gratefully acknowledge members of the O'Riordan laboratory as well as members of the Wobus, Young, Takayama, and Spence laboratories for many helpful discussions.

References

1. CDC. 2020. Salmonella homepage. CDC, Atlanta, GA. https://www.cdc.gov/salmonella/index.html. Accessed November 2020.

2. Valdez Y, Grassl GA, Guttman JA, Coburn B, Gros P, Vallance BA, Finlay BB. 2009. Nramp1 drives an accelerated inflammatory response during Salmonella-induced colitis in mice. Cell Microbiol 11:351–362. 10.1111/j.1462-5822.2008.01258.x. PubMed.

3. Monack DM, Bouley DM, Falkow S. 2004. Salmonella typhimurium persists within macrophages in the mesenteric lymph nodes of chronically infected Nramp1+/+ mice and can be reactivated by IFNgamma neutralization. J Exp Med 199:231–241. 10.1084/jem.20031319. PubMed.

4. Spence JR, Mayhew CN, Rankin SA, Kuhar MF, Vallance JE, Tolle K, Hoskins EE, Kalinichenko VV, Wells SI, Zorn AM, Shroyer NF, Wells JM. 2011. Directed differentiation of human pluripotent stem cells into intestinal tissue in vitro. Nature 470:105–109. 10.1038/nature09691. PubMed.

5. Forbester JL, Goulding D, Vallier L, Hannan N, Hale C, Pickard D, Mukhopadhyay S, Dougan G. 2015. Interaction of Salmonella enterica serovar Typhimurium with intestinal organoids derived from human induced pluripotent stem cells. Infect Immun 83:2926–2934. 10.1128/IAI.00161-15. PubMed.

6. Hill DR, Huang S, Nagy MS, Yadagiri VK, Fields C, Mukherjee D, Bons B, Dedhia PH, Chin AM, Tsai YH, Thodla S, Schmidt TM, Walk S, Young VB, Spence JR. 2017. Bacterial colonization stimulates a complex physiological response in the immature human intestinal epithelium. Elife 6:e29132. 10.7554/eLife.29132. PubMed.

7. Leslie JL, Huang S, Opp JS, Nagy MS, Kobayashi M, Young VB, Spence JR. 2015. Persistence and toxin production by Clostridium difficile within human intestinal organoids result in disruption of epithelial paracellular barrier function. Infect Immun 83:138–145. 10.1128/IAI.02561-14. PubMed.

8. Lou L, Zhang P, Piao R, Wang Y. 2019. Salmonella pathogenicity island 1 (SPI-1) and its complex regulatory network. Front Cell Infect Microbiol 9:270. 10.3389/fcimb.2019.00270. PubMed.

9. Jennings E, Thurston TLM, Holden DW. 2017. Salmonella SPI-2 type III secretion system effectors: molecular mechanisms and physiological consequences. Cell Host Microbe 22:217–231. 10.1016/j.chom.2017.07.009. PubMed.

10. Alteri CJ, Himpsl SD, Pickens SR, Lindner JR, Zora JS, Miller JE, Arno PD, Straight SW, Mobley HL. 2013. Multicellular bacteria deploy the type VI secretion system to preemptively strike neighboring cells. PLoS Pathog 9:e1003608. 10.1371/journal.ppat.1003608. PubMed.

11. Galan JE, Curtiss R, III. 1989. Cloning and molecular characterization of genes whose products allow Salmonella typhimurium to penetrate tissue culture cells. Proc Natl Acad Sci U S A 86:6383–6387. 10.1073/pnas.86.16.6383. PubMed.

12. Pfeifer CG, Marcus SL, Steele-Mortimer O, Knodler LA, Finlay BB. 1999. Salmonella typhimurium virulence genes are induced upon bacterial invasion into phagocytic and nonphagocytic cells. Infect Immun 67:5690–5698. 10.1128/IAI.67.11.5690-5698.1999. PubMed.

13. Laughlin RC, Knodler LA, Barhoumi R, Payne HR, Wu J, Gomez G, Pugh R, Lawhon SD, Baumler AJ, Steele-Mortimer O, Adams LG. 2014. Spatial segregation of virulence gene expression during acute enteric infection with Salmonella enterica serovar Typhimurium. mBio 5:e00946-13. 10.1128/mBio.00946-13. PubMed.

14. Bruno VM, Hannemann S, Lara-Tejero M, Flavell RA, Kleinstein SH, Galan JE. 2009. Salmonella Typhimurium type III secretion effectors stimulate innate immune responses in cultured epithelial cells. PLoS Pathog 5:e1000538. 10.1371/journal.ppat.1000538. PubMed.

15. Barthel M, Hapfelmeier S, Quintanilla-Martinez L, Kremer M, Rohde M, Hogardt M, Pfeffer K, Russmann H, Hardt WD. 2003. Pretreatment of mice with streptomycin provides a Salmonella enterica serovar Typhimurium colitis model that allows analysis of both pathogen and host. Infect Immun 71:2839–2858. 10.1128/iai.71.5.2839-2858.2003. PubMed.

16. Hapfelmeier S, Stecher B, Barthel M, Kremer M, Muller AJ, Heikenwalder M, Stallmach T, Hensel M, Pfeffer K, Akira S, Hardt WD. 2005. The Salmonella pathogenicity island (SPI)-2 and SPI-1 type III secretion systems allow Salmonella serovar typhimurium to trigger colitis via MyD88-dependent and MyD88-independent mechanisms. J Immunol 174:1675–1685. 10.4049/jimmunol.174.3.1675. PubMed.

17. Cobo ER, Chadee K. 2013. Antimicrobial human beta-defensins in the colon and their role in infectious and non-infectious diseases. Pathogens 2:177–192. 10.3390/pathogens2010177. PubMed.

18. Reynolds JM, Martinez GJ, Nallaparaju KC, Chang SH, Wang YH, Dong C. 2012. Cutting edge: regulation of intestinal inflammation and barrier function by IL-17C. J Immunol 189:4226–4230. 10.4049/jimmunol.1103014. PubMed.

19. Gong H, Ma S, Liu S, Liu Y, Jin Z, Zhu Y, Song Y, Lei L, Hu B, Mei Y, Liu H, Liu Y, Wu Y, Dong C, Xu Y, Wu D, Liu H. 2018. IL-17C mitigates murine acute graft-vs.-host disease by promoting intestinal barrier functions and Treg differentiation. Front Immunol 9:2724. 10.3389/fimmu.2018.02724. PubMed.

20. Maudet C, Mano M, Sunkavalli U, Sharan M, Giacca M, Forstner KU, Eulalio A. 2014. Functional high-throughput screening identifies the miR-15 microRNA family as cellular restriction factors for Salmonella infection. Nat Commun 5:4718. 10.1038/ncomms5718. PubMed.

21. Aguilar C, Cruz AR, Rodrigues Lopes I, Maudet C, Sunkavalli U, Silva RJ, Sharan M, Lisowski C, Zaldivar-Lopez S, Garrido JJ, Giacca M, Mano M, Eulalio A. 2020. Functional screenings reveal different requirements for host microRNAs in Salmonella and Shigella infection. Nat Microbiol 5:192–205. 10.1038/s41564-019-0614-3. PubMed.

22. Herrera-Uribe J, Zaldivar-Lopez S, Aguilar C, Luque C, Bautista R, Carvajal A, Claros MG, Garrido JJ. 2018. Regulatory role of microRNA in mesenteric lymph nodes after Salmonella Typhimurium infection. Vet Res 49:9. 10.1186/s13567-018-0506-1. PubMed.

23. Schulte LN, Eulalio A, Mollenkopf HJ, Reinhardt R, Vogel J. 2011. Analysis of the host microRNA response to Salmonella uncovers the control of major cytokines by the let-7 family. EMBO J 30:1977–1989. 10.1038/emboj.2011.94. PubMed.

24. Huang T, Huang X, Chen W, Yin J, Shi B, Wang F, Feng W, Yao M. 2019. MicroRNA responses associated with Salmonella enterica serovar typhimurium challenge in peripheral blood: effects of miR-146a and IFN-gamma in regulation of fecal bacteria shedding counts in pig. BMC Vet Res 15:195. 10.1186/s12917-019-1951-4. PubMed.

25. Raudvere U, Kolberg L, Kuzmin I, Arak T, Adler P, Peterson H, Vilo J. 2019. g:Profiler: a web server for functional enrichment analysis and conversions of gene lists (2019 update). Nucleic Acids Res 47:W191–W198. 10.1093/nar/gkz369. PubMed.

26. Yan-Chun L, Hong-Mei Y, Zhi-Hong C, Qing H, Yan-Hong Z, Ji-Fang W. 2017. MicroRNA-192-5p promote the proliferation and metastasis of hepatocellular carcinoma cell by targeting SEMA3A. Appl Immunohistochem Mol Morphol 25:251–260. 10.1097/PAI.0000000000000296. PubMed.

27. Qu YL, Wang HF, Sun ZQ, Tang Y, Han XN, Yu XB, Liu K. 2015. Up-regulated miR-155-5p promotes cell proliferation, invasion and metastasis in colorectal carcinoma. Int J Clin Exp Pathol 8:6988–6994. PubMed.

28. Winter SE, Thiennimitr P, Winter MG, Butler BP, Huseby DL, Crawford RW, Russell JM, Bevins CL, Adams LG, Tsolis RM, Roth JR, Baumler AJ. 2010. Gut inflammation provides a respiratory electron acceptor for Salmonella. Nature 467:426–429. 10.1038/nature09415. PubMed.

29. Figueiredo JF, Barhoumi R, Raffatellu M, Lawhon SD, Rousseau B, Burghardt RC, Tsolis RM, Baumler AJ, Adams LG. 2009. Salmonella enterica serovar Typhimurium-induced internalization and IL-8 expression in HeLa cells does not have a direct relationship with intracellular Ca(2+) levels. Microbes Infect 11:850–858. 10.1016/j.micinf.2009.05.003. PubMed.

30. Barnes PD, Bergman MA, Mecsas J, Isberg RR. 2006. Yersinia pseudotuberculosis disseminates directly from a replicating bacterial pool in the intestine. J Exp Med 203:1591–1601. 10.1084/jem.20060905. PubMed.

31. Kehl T, Kern F, Backes C, Fehlmann T, Stockel D, Meese E, Lenhof HP, Keller A. 2020. miRPathDB 2.0: a novel release of the miRNA Pathway Dictionary Database. Nucleic Acids Res 48:D142–D147. 10.1093/nar/gkz1022. PubMed.

32. Pinchuk IV, Mifflin RC, Saada JI, Powell DW. 2010. Intestinal mesenchymal cells. Curr Gastroenterol Rep 12:310–318. 10.1007/s11894-010-0135-y. PubMed.

33. Nowarski R, Jackson R, Flavell RA. 2017. The stromal intervention: regulation of immunity and inflammation at the epithelial-mesenchymal barrier. Cell 168:362–375. 10.1016/j.cell.2016.11.040. PubMed.

34. Prockop DJ, Oh JY. 2012. Mesenchymal stem/stromal cells (MSCs): role as guardians of inflammation. Mol Ther 20:14–20. 10.1038/mt.2011.211. PubMed.

35. McCracken KW, Howell JC, Wells JM, Spence JR. 2011. Generating human intestinal tissue from pluripotent stem cells in vitro. Nat Protoc 6:1920–1928. 10.1038/nprot.2011.410. PubMed.

36. Bray NL, Pimentel H, Melsted P, Pachter L. 2016. Near-optimal probabilistic RNA-seq quantification. Nat Biotechnol 34:525–527. 10.1038/nbt.3519. PubMed.

37. Soneson C, Love MI, Robinson MD. 2015. Differential analyses for RNA-seq: transcript-level estimates improve gene-level inferences. F1000Res 4:1521. 10.12688/f1000research.7563.2. PubMed.

38. Rainer J. 2017. EnsDb.Hsapiens.v75: Ensembl based annotation package. R package version 2.99.0.

39. Love MI, Huber W, Anders S. 2014. Moderated estimation of fold change and dispersion for RNA-seq data with DESeq2. Genome Biol 15:550. 10.1186/s13059-014-0550-8. PubMed.

40. Benjamini YHY. 1995. Controlling the false discovery rate: a practical and powerful approach to multiple testing. J R Stat Soc Ser B 57:289–300.

41. Yu G, He QY. 2016. ReactomePA: an R/Bioconductor package for reactome pathway analysis and visualization. Mol Biosyst 12:477–479. 10.1039/c5mb00663e. PubMed.

42. Wickham H. 2016. ggplot2: elegant graphics for data analysis. Springer-Verlag, New York, NY. Crossref.

43. Wickham HFR, Henry L, Müller K, et al. 2015. dplyr: a grammar of data manipulation. R package version 0.4.3.

44. Larsson J. 2020. eulerr: area-proportional Euler and Venn diagrams with ellipses. R package version 6.1.0.

45. Kolde R. 2018. pheatmap: pretty heatmaps.

46. Jones BD, Falkow S. 1994. Identification and characterization of a Salmonella typhimurium oxygen-regulated gene required for bacterial internalization. Infect Immun 62:3745–3752. 10.1128/IAI.62.9.3745-3752.1994. PubMed.

47. Guy RL, Gonias LA, Stein MA. 2000. Aggregation of host endosomes by Salmonella requires SPI2 translocation of SseFG and involves SpvR and the fms-aroE intragenic region. Mol Microbiol 37:1417–1435. 10.1046/j.1365-2958.2000.02092.x. PubMed.

Chapter 3

Comparative Transcriptional Profiling of the Early Host Response to Infection by Typhoidal and Non-typhoidal *Salmonella* Serovars in Human Intestinal Organoids

3.1 Abstract

Salmonella enterica represents over 2500 serovars associated with a wide-ranging spectrum of disease; from self-limiting gastroenteritis to invasive infections caused by non-typhoidal serovars (NTS) and typhoidal serovars, respectively. Host factors strongly influence infection outcome as malnourished or immunocompromised individuals can develop invasive infections from NTS, however, comparative analyses of serovar-specific host responses have been constrained by reliance on limited model systems. Here we used human intestinal organoids (HIOs), a three-dimensional "gut-like" *in vitro* system derived from human embryonic stem cells, to elucidate similarities and differences in host responses to NTS and typhoidal serovars. HIOs discriminated between the two most prevalent NTS, *Salmonella enterica* serovar Typhimurium (STM) and *Salmonella enterica*

This chapter represents a published article: Abuaita BH*, Lawrence A-LE*, Berger RP, Hill DR, Huang S, Yadagiri VK, et al. (2021) Comparative transcriptional profiling of the early host response to infection by typhoidal and non-typhoidal Salmonella serovars in human intestinal organoids. PLoS Pathog 17(10): e1009987. https://doi.org/10.1371/journal.ppat.1009987

*Basel H. Abuaita and Anna-Lisa E. Lawrence contributed equally to this work. Order was determined alphabetically by last name.

serovar Enteritidis (SE), and typhoidal serovar *Salmonella enterica* serovar Typhi (ST) in epithelial cell invasion, replication and transcriptional responses. Pro-inflammatory

signaling and cytokine output was reduced in ST-infected HIOs compared to NTS infections, consistent with early stages of NTS and typhoidal diseases. While we predicted that ST would induce a distinct transcriptional profile from the NTS strains, more nuanced expression profiles emerged. Notably, pathways involved in cell cycle, metabolism and mitochondrial functions were downregulated in STM-infected HIOs and upregulated in SE-infected HIOs. These results correlated with suppression of cellular proliferation and induction of host cell death in STM-infected HIOs and in contrast, elevated levels of reactive oxygen species production in SE-infected HIOs. Collectively, these results suggest that the HIO model is well suited to reveal host transcriptional programming specific to infection by individual *Salmonella* serovars, and that individual NTS may provoke unique host epithelial responses during intestinal stages of infection.

3.2 Author Summary

Salmonella enterica is the major causative agent of bacterial infections associated with contaminated food and water. *Salmonella enterica* consists of over 2500 serovars of which Typhimurium (STM), Enteritidis (SE) and Typhi (ST) are the three major serovars with medical relevance to humans. These serovars elicit distinctive immune responses and cause different diseases in humans, including self-limiting diarrhea, gastroenteritis and typhoid fever. Differences in the human host response to these serovars are likely to be a major contributing factor to distinct disease outcomes but are not well characterized, possibly due to the limitations of human-derived physiological infection models. Distinct

from immortalized epithelial cell culture models, human intestinal organoids (HIOs) are three-dimensional structures derived from embryonic stem cells that differentiate into intestinal mesenchymal and epithelial cells, mirroring key organizational aspects of the intestine. In this study, we used HIOs to monitor transcriptional changes during early stages of STM, SE and ST infection. Our comparative analysis showed that HIO inflammatory responses are the dominant response in all infections, but ST infection induces the weakest upregulation of inflammatory mediators relative to the other serovars. In addition, we identified several cellular processes, including cell cycle and mitochondrial functions, that were inversely regulated between STM and SE infection despite these serovars causing similar localized intestinal infection in humans. Our findings reinforce HIOs as an emerging model system to study *Salmonella* serovar infection, and define global host transcriptional response profiles as a foundation for understanding human infection outcomes.

3.3 Introduction

Salmonella enterica greatly impacts human health causing an estimated 115 million infections worldwide every year and are one of the four leading causes of diarrheal diseases (*72*, *79*). *Salmonella enterica* consists of over 2500 serovars and infects the intestinal epithelial layer, causing a wide spectrum of phenotypes ranging from asymptomatic carriage to more severe systemic disease. *Salmonella* serovars are classified based on host specificity and disease outcomes. Host generalist serovars including *Salmonella enterica* serovar Typhimurium (STM) and Enteritidis (SE) infect a broad range of hosts and cause localized inflammation and self-limiting diarrhea in

healthy individuals or more severe gastroenteritis in children and the elderly. In contrast, host-restricted serovars including Typhi and Abortusovis infect only one host species and cause more serious clinical manifestations including typhoid fever in humans and abortions in mares respectively (*74*).

Although *Salmonella enterica* serovars share a conserved core genome, determinants of host specificity and varying clinical manifestations are poorly understood. The molecular basis for distinct host adaptation and disease outcome is likely to be multifactorial, mediated by bacteria and host-dependent mechanisms (*81*). Initial comparative genomic analyses identified specific signatures that may be indicative of some of these differences (*78*, *81*, *82*). However, comparison of host signatures across different serovars is still limited by host specificity and poorly representative model systems. Using human epithelial cell lines addresses host-specificity, but immortalized cell lines do not represent the multiple subsets of intestinal epithelial cells found in the gut and harbor mutations that likely alter cellular responses to bacterial infection.

Human intestinal organoids (HIOs) have emerged as an alternative *in vitro* model to study intestinal epithelial host responses to commensal microbiota and enteric pathogens (*83*). HIOs are differentiated from pluripotent stem cells into three-dimensional spheroids composed of a defined luminal space bound by a polarized epithelial barrier surrounded by mesenchyme. This is an improvement over existing models because the untransformed HIO epithelium is polarized, and contains multiple epithelial cell lineages

found in the intestine (*19*). Hill *et al.* showed that HIOs supported luminal growth of *Escherichia coli* following microinjection, and that physiological changes in the HIO occurred during colonization, such as an increase in mucus production, mirroring what happens *in vivo* during initial colonization (*21*). Our work and Forbester *et al.* also showed that STM invades HIO epithelial cells and induces inflammatory responses, suggesting that the HIO is an effective model to define intestinal host responses to enteric pathogens (*35*, *36*). Here, we used HIOs to compare the transcriptional profiles of intestinal epithelial responses to host-restricted *Salmonella enterica* serovar Typhi and two host unrestricted serovars Typhimurium and Enteritidis. We found that *Salmonella* infection induced a variation in magnitude of immune responses that was dependent on the infecting serovar. ST infection induced the weakest response, consistent with the idea that ST infection induces a weak host immune response to establish a systemic infection (*86*). Notably, we found that both STM and ST infection similarly decreased expression of pathways involved in cell cycle, DNA repair and DNA replication while SE infection increased these responses.

3.4 Results

3.4.1 *Salmonella* serovars invade HIO epithelial cells and induce distinct patterns of mucus production

To study initial host responses to *Salmonella*, we microinjected bacteria into the luminal space of the HIO to allow luminal replication throughout the course of infection **(Fig 3.1A)**. This HIO infection model allows for longer-term interactions between bacteria and the host both in the extracellular luminal space and intracellularly within epithelial cells and

therefore, it better resembles the continuous interaction between bacteria and intestinal cells during the natural course of infection. We first determined whether different *Salmonella* serovars could colonize and replicate within the HIOs and invade HIO

epithelial cells. We chose the most prevalent serovars that cause gastroenteritis, STM and SE, and a typhoidal serovar, ST. HIOs were microinjected with 10^3 CFU of STM, SE or ST, a relatively low inoculum, as previous work demonstrated that growth rate was negatively correlated with the number of CFU injected (*21*). Total bacterial burden per HIO was enumerated at 2.5 hours post-infection (hpi) to establish initial levels of colonization, and 24 hpi **(Fig 3.1B)**. All serovars showed at least a 1.5 log increase in bacterial burden at 24hpi, relative to 2.5hpi. Intracellular bacterial burden was quantified by gentamicin protection assay, as we previously showed the utility of this assay in the HIOs by comparing invasion between WT STM and a *Salmonella* pathogenicity island-1 (SPI-1) deficient isogenic mutant (*35*). Briefly, HIOs were cut open to expose luminal bacteria to gentamicin before lysing epithelial cells for enumeration of gentamicin-protected bacteria **(Fig 3.1C)**. Intracellular bacteria numbers increased over time with all three serovars, suggesting that intracellular replication or continued invasion contributes to increased bacterial load at 24hpi. At this low inoculum, STM consistently invaded HIO epithelial cells more efficiently than SE and ST.

To determine whether continued invasion or intracellular replication explained the increase in intracellular burden over time, infected HIOs were sectioned and stained with DAPI and anti-E-Cadherin antibody to visualize DNA and epithelial cells respectively,

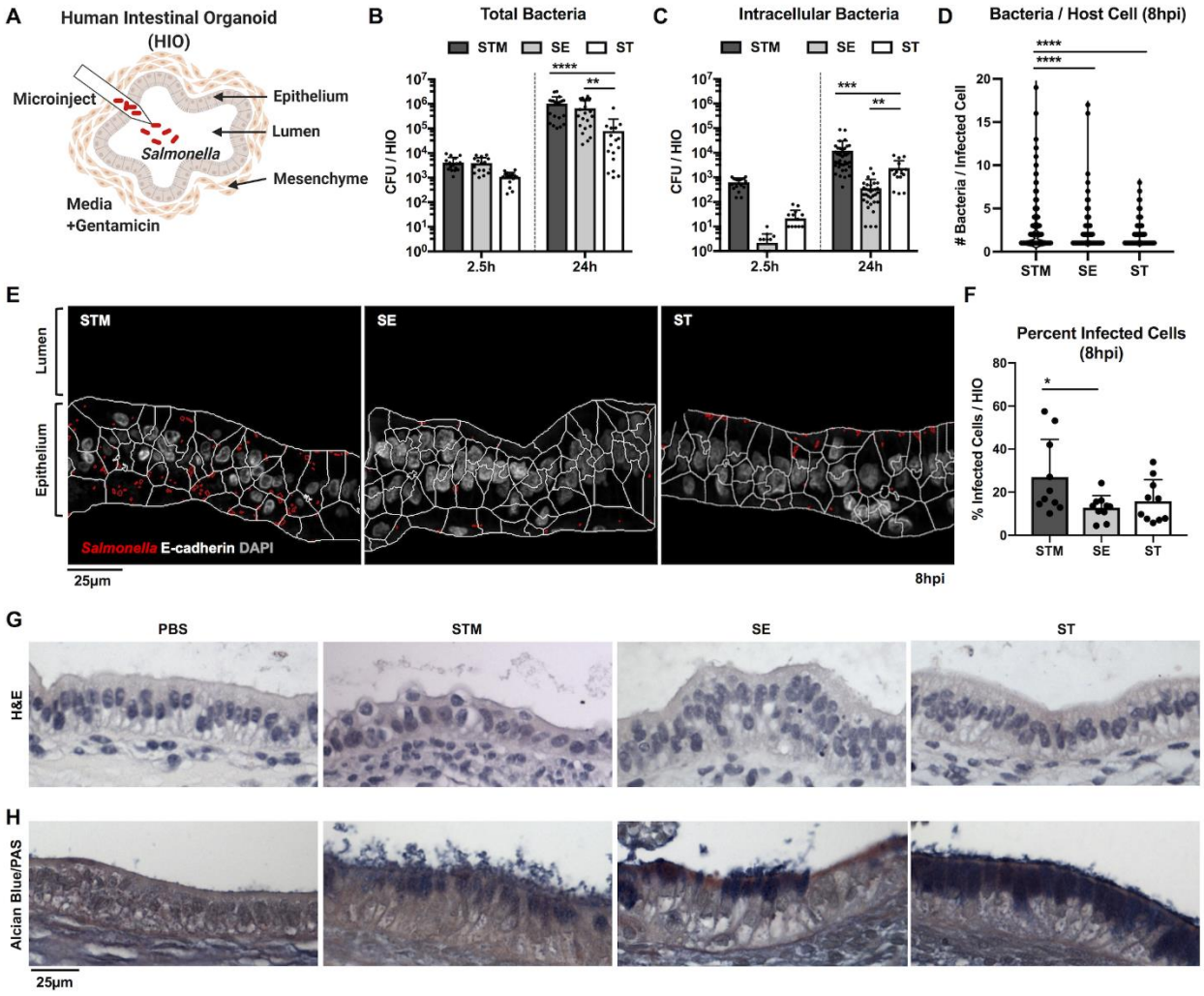

Figure 3.1 Salmonella enterica serovars invade HIO epithelial cells and stimulate mucin production. (A) Model depicting experimental set-up with the HIOs. HIOs are comprised of an epithelium lining surrounded by mesenchymal cells that self-organize into 3-dimensional structures. Bacteria (10^3 CFU) were microinjected into the HIO lumen and gentamicin was added to the medium after 2h to kill any bacteria introduced into the medium during microinjection. (B) Total bacterial burden was enumerated per HIO at 2.5h and 24h post infection. (C) Intracellular bacterial burden was enumerated after exposing luminal bacteria to gentamicin at 2.5h and 24h post infection. Graphs represent the mean of n>16 HIOs from three independent experiments. Statistical significance within the group was determined by two-way ANOVA and followed up by Tukey's multiple comparisons test. (D) Number of bacteria per cell was quantified using DAPI staining. (E) Representative confocal microscopy images of histology sections obtained from STM, SE, or ST infected HIOs for 8h. Sections were stained for E-cadherin and DAPI. Cell outlines based on the E-cadherin staining (white) and bacterial outlines detected using DAPI staining (red) were generated using CellProfiler. (F) Percent of infected cells were determined by quantifying 3 fields of view per HIO at 60x magnification with n=10 HIOs analyzed per group. (G and H) Histology sections of HIOs at 8hpi using hematoxylin and eosin (H&E) staining (G) and Alcian Blue/Periodic Acid-Schiff (PAS) staining (H). Statistical significance for (D) and (F) was determined by one-way ANOVA with Tukey's multiple comparisons test. P values < 0.05 were considered significant and designated by: *<0.05, **<0.01, ***<0.001 and ****<0.0001.

allowing quantification of the number of bacteria per cell **(Fig 3.1D-F)**. There were more bacteria per cell **(Fig 3.1D)** and a higher percentage of infected cells **(Fig 3.1F)** in STM-infected HIOs compared to SE- or ST-infected HIOs, supporting the conclusion that STM invades more efficiently than the other two serovars when initial bacterial numbers are

low. Most infected cells contained 1-2 bacteria, which might reflect continued invasion over time. However, particularly in STM-infected HIOs, where we measured a marked increase in CFU, we observed some cells that contained >10 bacteria per cell consistent with intracellular replication of *Salmonella*. Because there were differences in intracellular bacterial burden between serovars, we compared the expression of SPI-1 and SPI-2 genes during infection as differences in virulence gene expression may contribute to differences in invasion and intracellular replication. Transcriptional analysis of *Salmonella* genes from infected HIOs revealed that expression of SPI-1 genes was highest in STM at 2.5hpi, suggesting that enhanced expression of effectors mediating invasion, such as SopB or SopE may allow STM to enter HIO cells more efficiently than the other two serovars **(Fig 3.2)**.

Expression of SPI-1 effector genes decreased in all serovars over time while SPI-2 effector expression increased, indicating that the HIO environment reprograms bacterial gene expression. In order to determine the impact of maintaining live bacteria in the HIO lumen throughout the course of infection on HIO integrity and morphology, we performed hematoxylin and eosin (H&E) histology staining **(Fig 3.1G).** HIOs remained intact during infection with all serovars for the duration of the experiment. However, stressed regions of the HIO epithelial lining could sometimes be observed, especially during STM infection, where epithelial cells appeared to be extruded into the lumen. In addition, Alcian Blue and

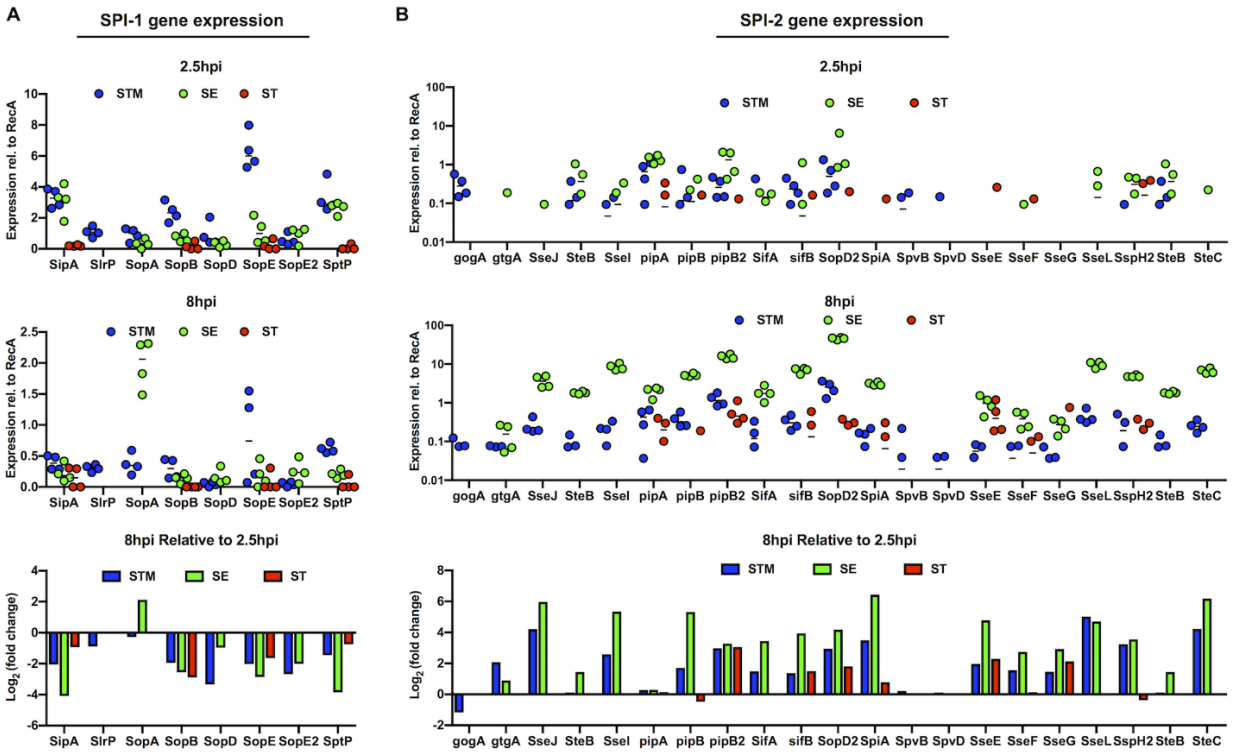

Figure 3.2 Temporal regulation of SPI-1 and SPI-2 gene expression in the HIOs by different Salmonella serovars. (A and B) SPI-1 and SPI-2 gene expression normalized to RecA expression at each time point in the HIOs. Log_2(fold change) at 8h relative to 2.5hpi was calculated and shown in the bottom row.

Periodic acid-Schiff reagent (PAS) staining was also performed to detect mucus, as a recent study showed that HIOs increase mucin production during bacterial colonization (*21*). In agreement with these findings, Alcian Blue and PAS staining showed an increase in mucus production in response to infection **(Fig 3.1H, quantified in 3.3)**. Of note, we observed unique staining patterns during infection with the different serovars. While STM infection resulted in luminal mucus accumulation, in ST-infected HIOs, mucus accumulated within epithelial cells, indicating that serovars can differentially modulate mucus production or secretion. Taken together, our data show that over a 24h period, all three *Salmonella* serovars colonize HIOs, and invade HIOs, inducing distinct patterns of mucus production without causing major destruction to the HIO epithelial layer.

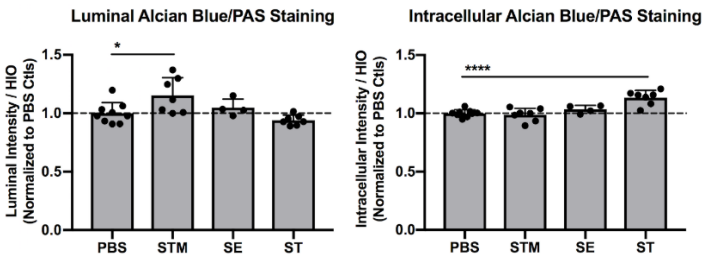

Figure 3.3 Quantification of Alcian blue and periodic acid-Schiff (PAS) staining. (A) Luminal and intracellular staining intensity from n>4 HIOs based on images shown in Fig 1G. Significance was determined by one-way ANOVA where P value: *<0.05 and ****<0.0001.

3.4.2 Host transcriptional dynamics differ between *Salmonella* serovars

To define the global HIO transcriptional response to the three *Salmonella* serovars, we performed RNA sequencing (RNA-seq) at 2.5h and 8hpi. HIOs were infected with 10^5 CFU of STM, SE or ST. A higher inoculum was used in order to establish comparable bacterial loads in the HIOs at 8h, and transcriptional changes were compared relative to control PBS-injected HIOs **(Fig 3.4)**.

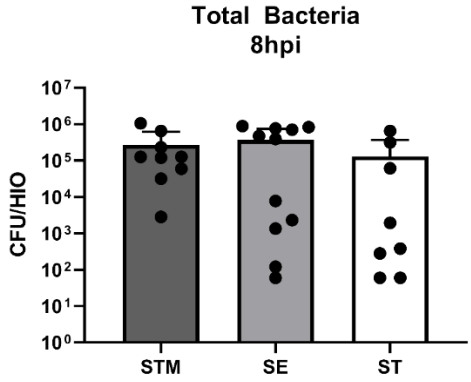

Figure 3.4 Similar bacterial loads are present in Salmonella serovar-infected HIOs. HIOs were infected with 10^5 CFU of STM, SE or SE and total bacterial burden per HIO was enumerated at 8hpi. Graph represents the mean of n>8 HIOs.

Principal component analysis (PCA) was performed on normalized gene counts to identify clustering patterns between conditions **(Fig 3.5A-C)**. PCA plots showed clear segregation

and clustering of samples based on both infection and time. Infected HIOs at 2.5h had the most variation relative to PBS where they were separated by the first (the greatest variance) principal component and further clustered based on infection with each serovar.

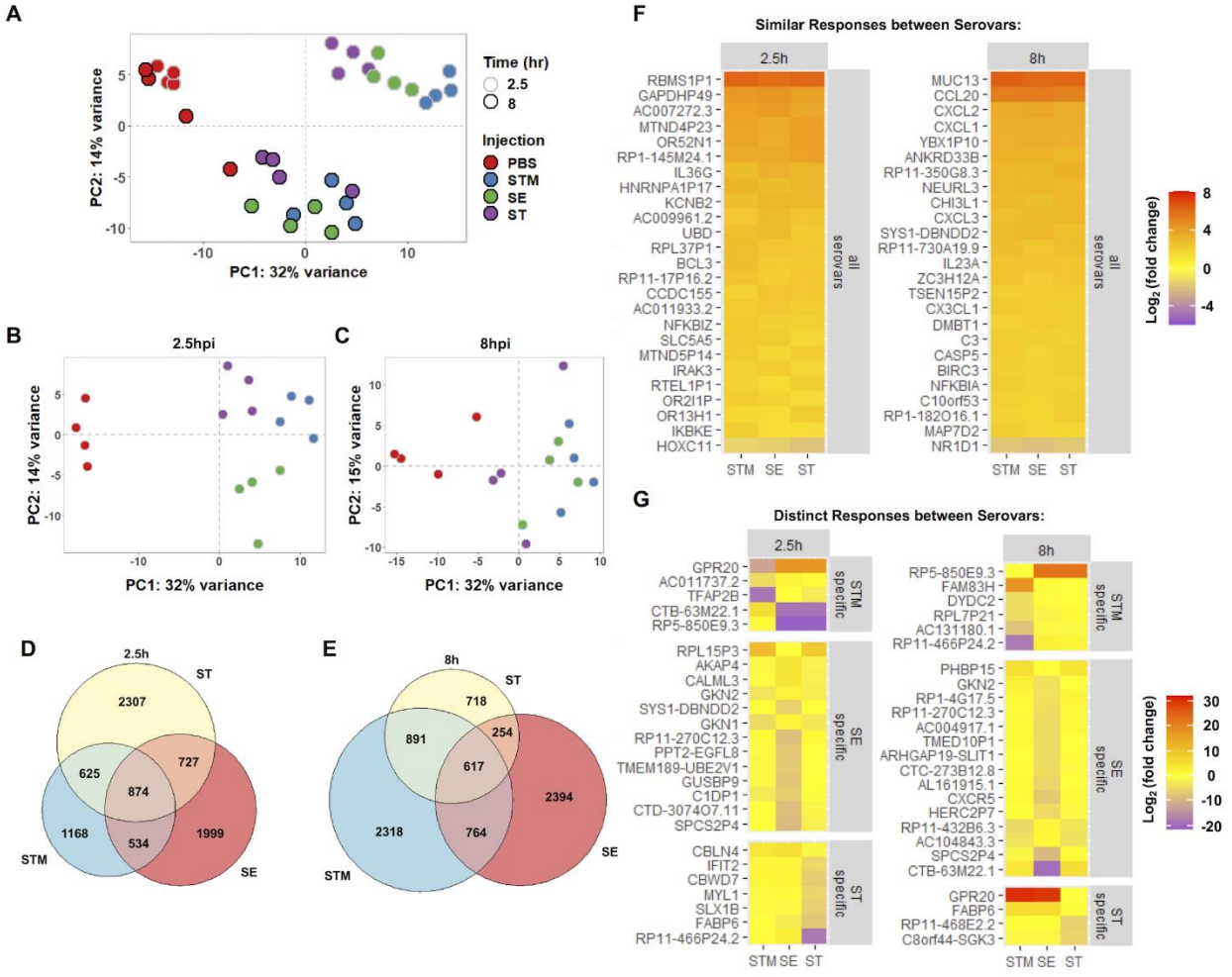

Figure 3.5 Changes in HIO gene expression are driven by both serovar and time post infection. (A) Principal component analysis of HIOs micro-injected with 10^5 CFU of the indicated *Salmonella* serovars. Each circle represents a biological replicate of a pool of five HIOs. (B and C) Principal component analysis of each time point 2.5h (B) and 8h (C). (D and E) Euler diagram comparison of gene expression changes in each HIO condition relative to PBS at 2.5h (D) and 8h (E) post infection. Genes were filtered by P value < 0.05. (F and G) Heatmaps depicting conserved responses between serovars (F) and distinct responses between serovars (G) based on significant genes sorted by greatest standard deviation between conditions of $\log_2$(fold change) compared to PBS controls.

STM-infected HIOs showed the greatest separation from the control, while SE-infected HIOs showed an intermediate and ST-infected HIOs showed the least separation. Infected HIOs at 8h were further separated by both the first and second (the second greatest variance) principal components. By 8hpi, the variation observed through the first component was decreased relative to 2.5h, suggesting that some early responses were transient **(Fig 3.5B, C)**. At 8h, there was less segregation between infected HIOs and PBS, with no clear clustering of serovars at this later time point.

To further define HIO responses during *Salmonella* infection, we identified differentially expressed genes (DEGs) between PBS controls and HIOs infected with STM, SE or ST. We found comparable numbers of DEGs during infection with all serovars at 2.5hpi **(Fig 3.5D)**. Some of the DEGs were shared between all infected HIOs, which likely represents a core host response to *Salmonella* infection. However, infection with each serovar also resulted in induction and suppression of a unique set of DEGs. We compared the DEGs from the HIOs with previously published *Salmonella* infection transcriptomics studies (*36*, *84*, *85*) and found that correlation between our dataset and the top responses to either STM or ST reported in each publication varied depending on the model system used **(Fig 3.6)**. There were high similarities in significant genes between our dataset and the dataset from the Forbester *et al*. study (*36*), in which a similar HIO model and wildtype STM strain was used. Notably, transcriptional dynamics from our analysis showed an increase in the number of DEGs at 8hpi in response to infection with the non-typhoidal serovars (NTS), STM and SE, while the number of DEGs during infection with ST decreased **(Fig 3.5E)**. To better understand the conserved and unique responses between serovars in the HIOs,

significant DEGs were sorted by the standard deviation of the log_2(fold change) for each serovar and top 25 conserved genes between serovars and top 25 variable genes at each time point were plotted **(Fig 3.5F, G)**. Included in the core response to all three serovars were proinflammatory mediators including upregulation of cytokine and chemokines (CCL20, CXCL2, CXCL1, CXCL3, IL23A, and IL36G), upregulation of components of the NF-κB signaling pathway (NFKBIZ, IKBKE, and NFKBIA) and one mucin (MUC13), among others. In contrast, the genes that comprised distinct responses to each serovar were involved in more diverse roles in the cell, including strong upregulation of the constitutively active G protein-coupled receptor (GPR20) in NTS (*87*) at 8 hpi, but not in ST-infected HIOs, and suppression of the intestinal fatty acid binding protein (FABP6) in ST-infected HIOs. Collectively, the HIO responses represent two patterns; core transcriptional responses that are changed during infection with all three *Salmonella* serovars and serovar-specific responses.

3.4.3 *Salmonella* serovars differentially alter inflammatory, stress response, vesicular trafficking, metabolism and cell cycle pathways

To identify biological pathways associated with DEGs from each infection condition, gene sets were separated into upregulated (increased) and downregulated (decreased) categories based on fold change relative to PBS and imported separately into the Reactome pathway analysis tool. In the upregulated datasets, the majority of significant pathways in all three infection conditions at both 2.5h and 8h belonged to the immune system category with over 80 pathways significantly enriched in STM and SE-infected HIOs at 8hpi accounting for almost 5% of all annotated immune system pathways in the Reactome database **(Fig 3.7A)**. We found that infection induced a complex response in both innate immune and cytokine signaling pathways including, but not limited to, Toll-

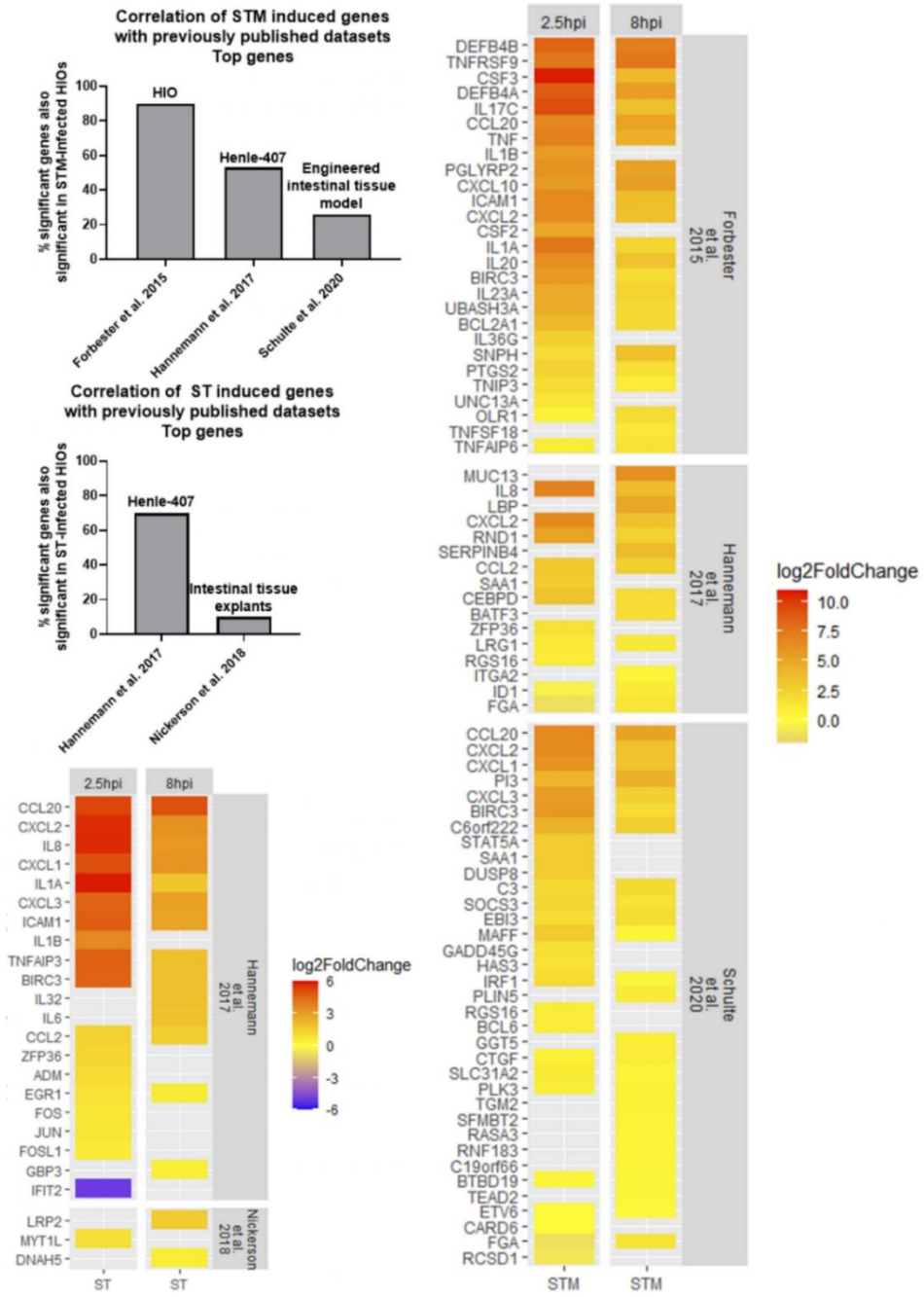

Figure 3.6 Comparison of HIO responses with previously published transcriptomics studies investigating host cell responses to Salmonella infection Top 30-50 genes reported in publications listed above were compared to our significant gene sets. The percentage of those genes that were also significant in either STM or ST-infected HIOs was plotted in the bar graphs with the model system used in each study listed at the top of each bar. Conserved gene changes were plotted in heatmaps to compare fold change across the different model systems.

like receptors, Interleukin mediators and Type I interferons **(Fig 3.7B)**. Notably, only in ST-infected HIOs were some immune system pathways associated with downregulated DEGs, such as non-canonical NF-κB and Interleukin-1 signaling. These results revealed that inflammatory pathways were the primary responses during *Salmonella* infection and are consistent with the hypothesis that typhoidal serovar infection is relatively "silent", producing less inflammatory mediators compared to NTS infection.

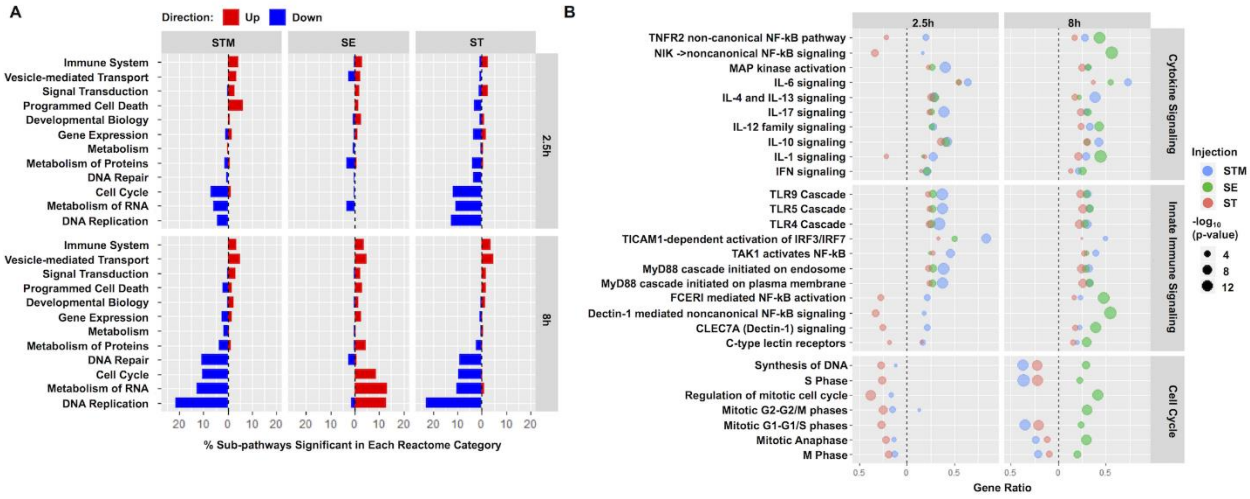

Figure 3.7 Immune system and cell cycle pathways encompass the predominant increases and decreases in gene expression during infection. (A) Fraction of sub-pathways clustering into the major Reactome cellular processes. Significantly upregulated (red) or downregulated (blue) genes were analyzed using ReactomePA and pathways were clustered into major cellular processes from the Reactome database. Major cellular processes with at least 12 significant sub-pathways in at least one infection condition were included with the proportion of significant pathways out of the entire group plotted on the x-axis. (B) Dot plot showing top pathways enriched from the Reactome database. Pathway coverage shown as gene ratio with significantly upregulated pathways shown on the right of the dotted line and downregulated pathways on the left. Dot size represents $-\log_{10}$(p-value) of enriched pathway during HIOs infection with STM in blue, SE in green and ST in red. Significant pathways were determined based on P value < 0.05.

Apart from the predominant inflammatory pathways, we also identified several differentially upregulated pathways in response to *Salmonella* serovars that have been linked to intestinal infection. These pathways included vesicular mediated transport,

antigen presentation, extracellular matrix organization (ECM), lipid and amino acid metabolism and cellular stress responses including IRE1α-mediated unfolded protein

response (UPR), mitophagy and the inflammasome **(Fig 3.8)**. Although there were genes in these pathways that were significantly upregulated in response to all three serovars, some were enriched only in response to a specific serovar. For example, we found that pathways belonging to ECM, UPR and tryptophan catabolism were significantly upregulated at 8hpi during STM infection but not during SE and ST infection. In contrast, we found that cholesterol metabolism pathways were highly enriched in ST infection while amino acid metabolism, cellular responses to hypoxia, the inflammasome and antigen presentation pathways were significantly induced only in SE-infected HIOs. Although vesicular trafficking has been shown to play a critical role during *Salmonella* infection (*88*), only HIOs infected with STM and ST serovars significantly upregulated many of these pathways.

Next, we turned our attention to the downregulated DEG datasets. Consistent with our previous study (*35*), most of the significantly downregulated pathways during STM and ST infections belonged to cell cycle, DNA replication and repair, metabolism of protein and metabolism of RNA **(Fig 3.7A)**, which point to potential reduction in cellular proliferation. Interestingly, in SE-infected HIOs, some of these categories including cell cycle and metabolism of proteins were instead associated with upregulated DEGs at 8hpi **(Fig 3.7A, B)**. Taken together, we find that while most inflammatory responses are upregulated, other responses, including ECM, cellular stress, lipid and amino acid

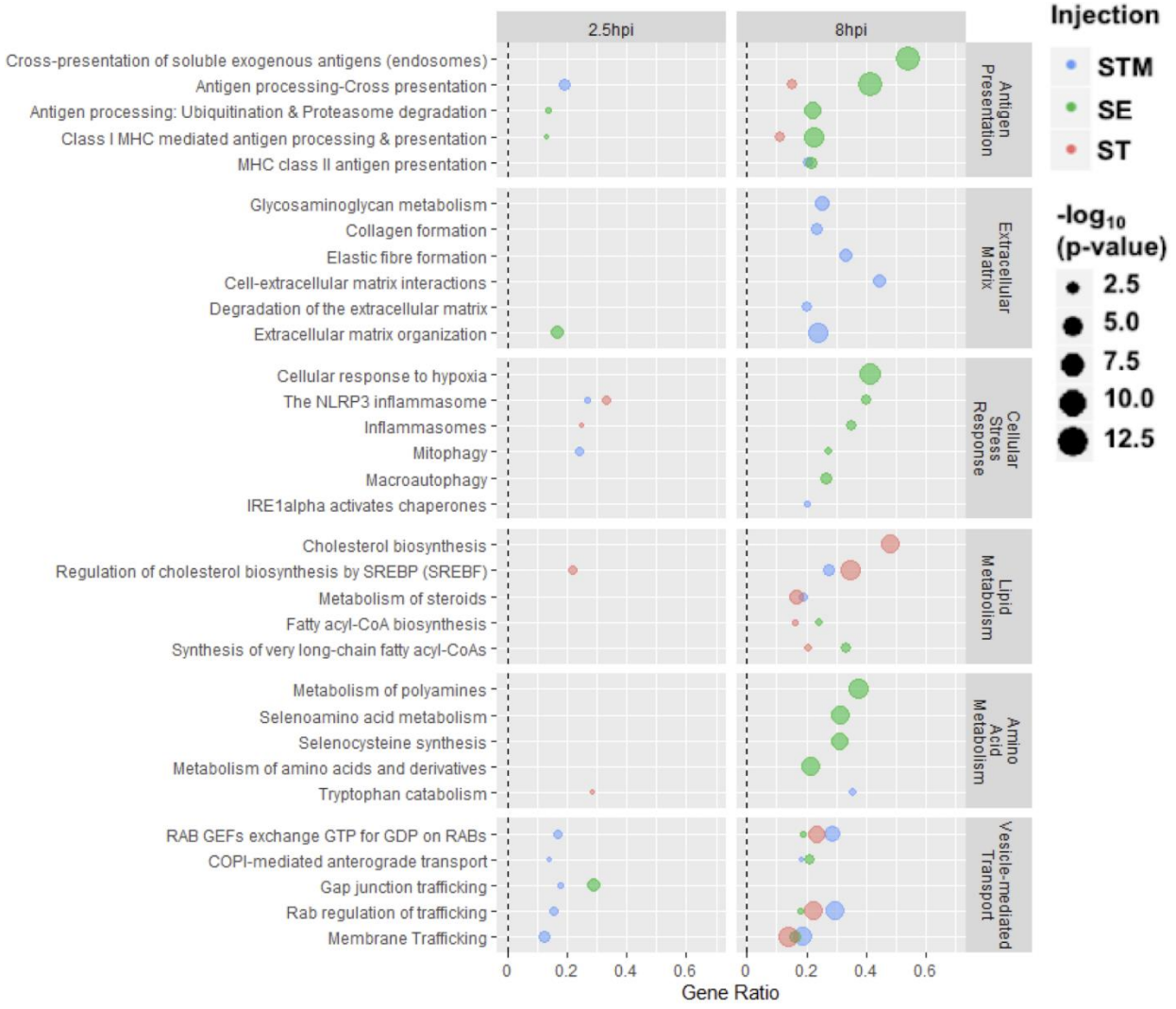

Figure 3.8 Select Reactome pathways that are differentially upregulated during HIO infection with different Salmonella serovars are related to antigen presentation, extracellular matrix, cellular stress responses, vesicular trafficking, lipid metabolism, and amino acid metabolism. Dotplot shows select Reactome pathways that are significantly enriched (P value < 0.05) from upregulated gene sets of HIOs infected with different *Salmonella* serovars relative to PBS control.

metabolism and cell cycle are differentially regulated upon infection with these three *Salmonella* serovars.

3.4.4 *Salmonella* serovars induce distinct HIO proinflammatory response profiles

Intestinal epithelial cells initiate inflammatory responses via production of proinflammatory mediators. Because the most dramatic transcriptional responses we observed were related to immune signaling, we sought to identify the HIO signature of inflammatory mediators including chemokines, cytokines and antimicrobial peptides (AMP) in response to each *Salmonella* serovar **(Fig 3.9A-C)**. We found that all these mediators were induced early during infection although with different magnitudes. For example, Colony Stimulating Factor 3 (CSF3), Interleukin 17C (IL17C), Interleukin 19 (IL19), C-C Motif Chemokine Ligand 20 (CCL20), C-X-C Motif Chemokine Ligand 1 (CXCL1), Defensin beta 4A (DEF4A) and Peptidase Inhibitor 3 (PI3) were highly induced during STM infection, moderately induced during SE infection and only weakly induced during ST infection. ST is thought to evade detection from the immune system through expression of the Vi capsule (*90*–*92*). Indeed, Vi capsule is induced in the static culture conditions prior to microinjection and was observed in HIOs during infection **(Fig 3.10)**. Of interest, IL17C signaling regulates epithelial host defense against mouse enteric pathogens (*93*). HIO production of IL17C and its known downstream proinflammatory mediators, including CSF3 and DEF4A, also suggest that IL17C signaling modulates

human intestinal host defense against *Salmonella* infection. To validate these transcriptional results, we measured production of specific inflammatory mediators (cytokine, chemokine and AMP) in the HIO culture medium by ELISA. All three serovars induced production of these inflammatory proteins **(Fig 3.9D and 3.11)**. In general, changes in protein level correlated with transcriptional changes observed in our RNA-seq

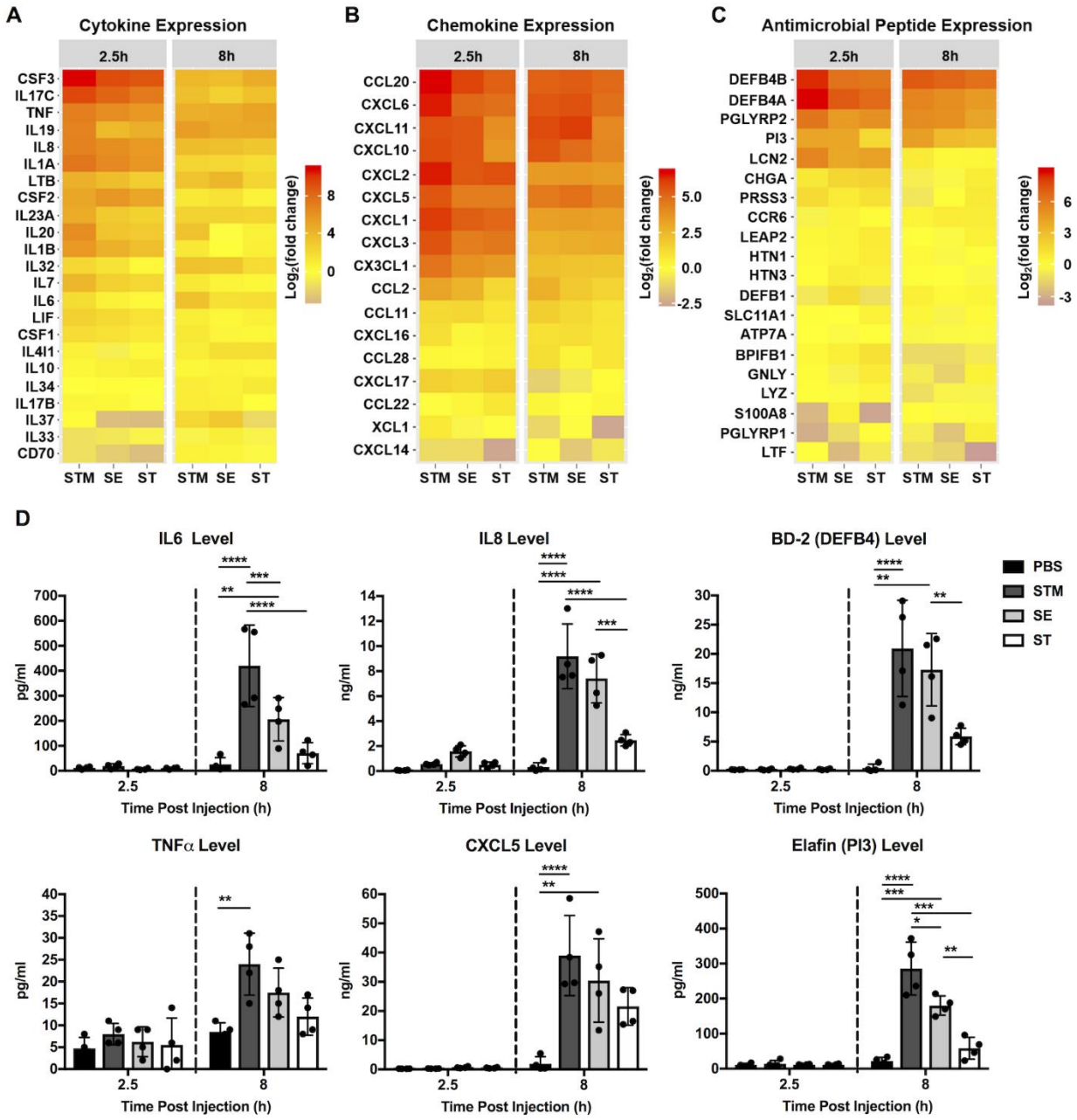

Figure 3.9 Differential gene expression and secretion of immune modulators by HIOs in response to infection. (A-C) Gene expression of Cytokine (A), Chemokine (B) and Antimicrobial peptide (C) are presented as $\log_2$ fold change relative to PBS at 2.5h and 8h post infection. (D) Cytokine, chemokine, and antimicrobial peptide levels measured from HIO supernatant at 2.5h and 8h post infection via ELISA. n=4 biological replicates. Error bars represent +/-SD. Significance calculated by two-way ANOVA. P values < 0.05 were considered significant and designated by: *<0.05, **<0.01, ***<0.001 and ****<0.0001.

dataset, where STM-infection resulted in the highest levels of cytokine production, SE-infection resulted in an intermediate phenotype and ST-infection induced the lowest

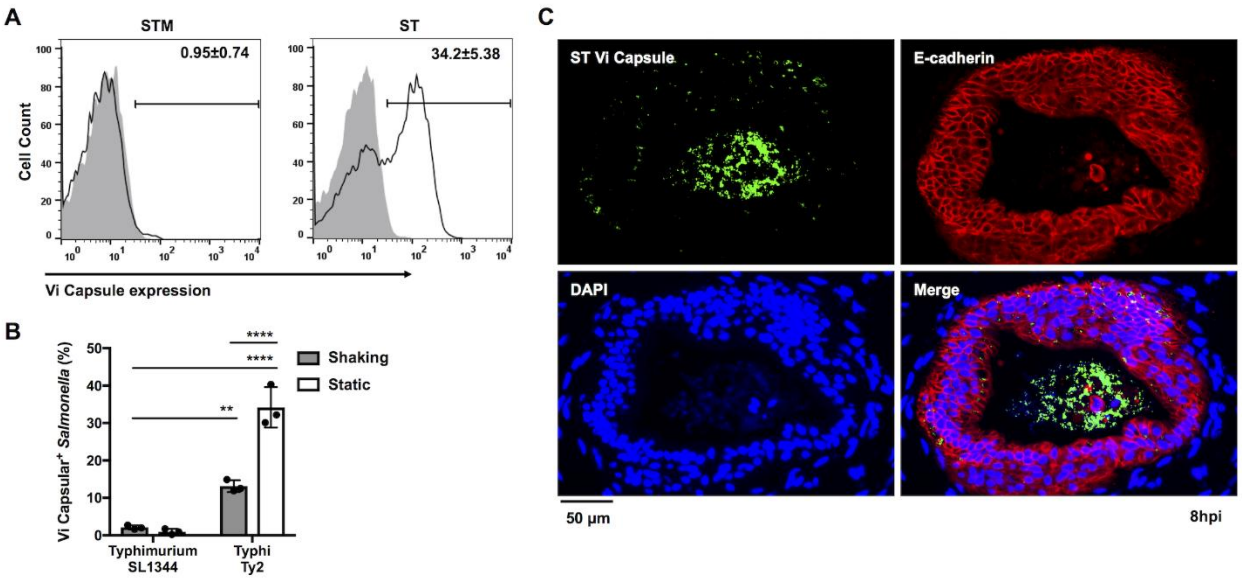

Figure 3.10 Salmonella typhi strain Ty2 expresses the Vi polysaccharide capsule when cultured in vitro under static conditions and in the HIO. (A) Representative flow cytometry histograms of Vi polysaccharide capsule expression by STM and ST. (B) Vi polysaccharide capsule expression was quantified by flow cytometry using rabbit Vi antisera. STM strain SL1344 and ST strain Ty2 were cultured overnight at 37°C under static or shaking conditions. Bacteria were washed, stained with rabbit Vi antisera and analyzed by flow cytometry. Percent capsule$^+$ cells was determined by gating against unstained cells. Graph indicates means +/- SD of n≥3 experiments. (C) Representative fluorescence microscopy images of ST-infected HIOs at 8hpi. Sections were stained with Rabbit antisera (green), anti-E Cadherin antibody (red) and DAPI (blue). P-value was calculated using two-way ANOVA with Sidek's post-test for multiple comparisons. P value: **<0.01 and ****<0.0001.

levels. Collectively, the data indicate that each serovar, even the two non-typhoidal serovars, interacts distinctly with the host to tune production of inflammatory mediators during infection.

3.4.5 Host cell cycle and cell death pathways are regulated during STM infection, but not during SE or ST infection

Our previous study and several others showed that STM infection decreases host cell proliferation during STM infection (*35*, *90*, *91*). To further investigate how cell cycle genes change in response to each serovar, we filtered the significant gene sets to examine

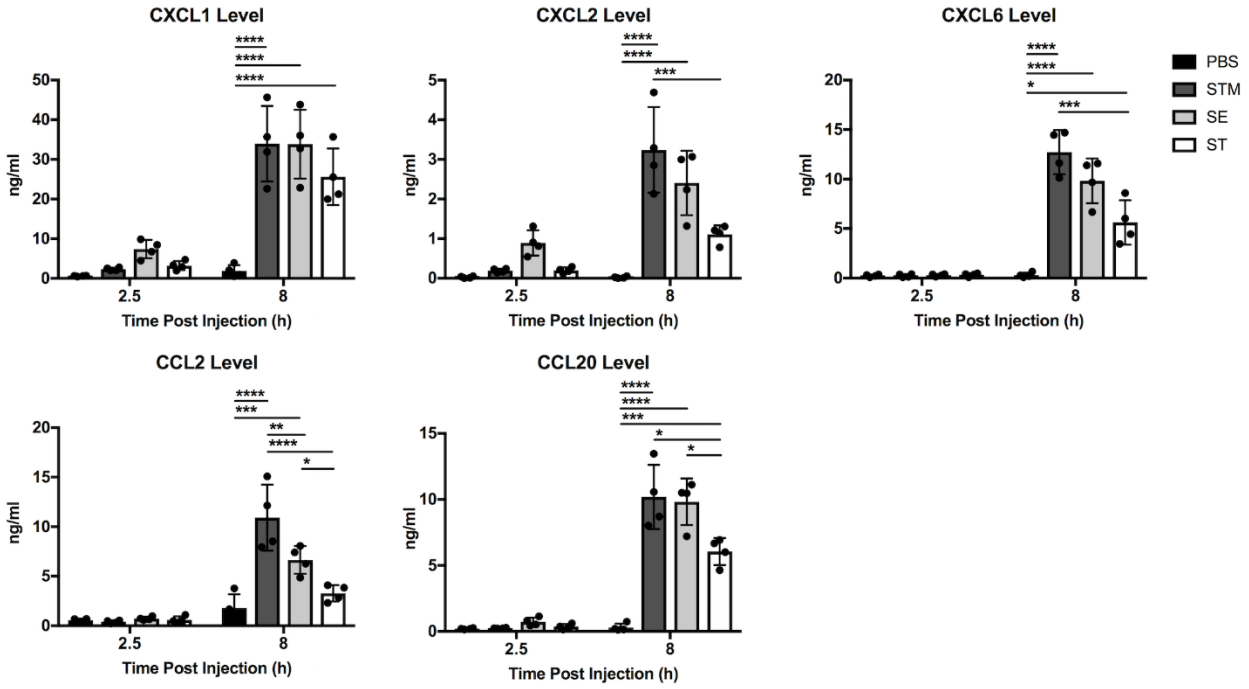

Figure 3.11 Chemokine secretion levels at 2.5h and 8hpi for HIOs microinjected with PBS, STM, SE, and ST. Graphs are presented as mean of n=4 biological replicates with standard deviation (SD) error bars. P value was calculated using two-way ANOVA with Tukey's post-test for multiple comparisons. P value: *<0.05; **<0.01, ***<0.001 and ****<0.0001.

expression patterns of cell cycle genes **(Fig 3.12A)**. Although some downregulation occurred early during infection, a stronger effect was measured at 8hpi where most cell cycle-regulated genes were suppressed at 8h in response to both STM and ST infection, although notably there were fewer significant DEGs associated with ST infection. In contrast, during SE infection, most of the cell cycle DEGs were upregulated, suggesting that STM and ST may reduce HIO cell proliferation while SE infection may uniquely increase it. To better understand which genes were responding and how gene level expression patterns differed between serovars, a heatmap showing the genes most variable between infection conditions was generated **(Fig 3.12B)**. Several genes critical for regulation of cell cycle progression were significantly downregulated during STM

infection, including PCNA and VRK1 which normally increase in expression in dividing cells and PRIM1/2 encoding the two subunits of DNA primase important for initiating DNA replication during cell division (*92–94*). These genes were observed to be downregulated, although weakly, during ST infection, and either weakly downregulated or upregulated during SE infection. To determine whether changes in cell cycle-related transcripts affected cell cycle progression, HIOs microinjected with PBS, STM, SE or ST were labeled with EdU to monitor proliferating cells for a period of 24h **(Fig 3.12C, D)**. Consistent with the observation that STM suppressed expression of critical cell cycle genes, there was a significant reduction in the number of cells that incorporated EdU in STM-infected HIOs compared to PBS controls. In contrast, there was no significant change in the number of EdU+ cells in either ST or SE-infected HIOs suggesting that changes in gene expression that occurred during these infections were not sufficient to functionally alter cell cycle progression in the HIOs.

Cell cycle and cell death pathways are both involved in maintaining intestinal homeostasis during infection. Since cell death is known to play a strong role during *Salmonella* infection and was highly represented in our Reactome pathway analysis in STM-infected HIOs **(Fig 3.7A)**, we measured cell death in the HIOs in response to all three serovars by performing Terminal deoxynucleotidyl transferase dUTP nick end labeling (TUNEL) **(Fig 3.12E, F**). Consistent with our pathway analysis, we found that STM infection resulted in a greater number of TUNEL-positive cells per HIO compared to PBS control. Surprisingly, the other NTS, SE, did not induce cell death at greater frequency compared to controls suggesting that the two NTS interact quite differently with the host. In contrast, ST induced an

intermediate response with some HIOs exhibiting increased host cell death compared to the PBS control. Together these results from the HIO model show that STM disrupts intestinal epithelial homeostasis to a greater degree than SE or ST, at least in part by suppressing host cell division and inducing host cell death.

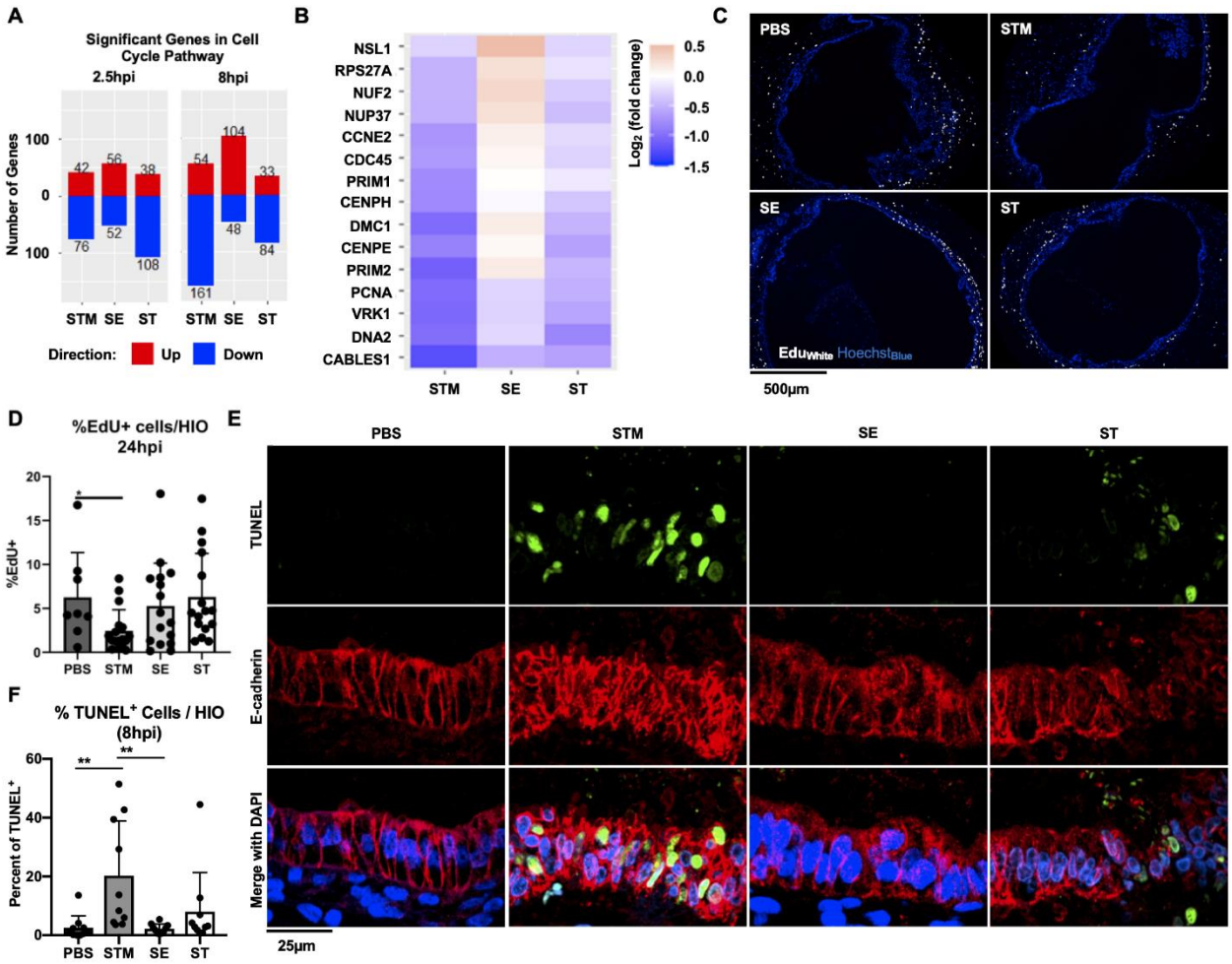

Figure 3.12 STM suppresses host cell cycle and induces cell death (A) The number of significant genes in the cell cycle pathway upregulated (red) or downregulated (blue) in each condition. (B) Top differentially expressed cell cycle genes sorted by greatest standard deviation between STM and SE conditions. (C) EdU staining in HIOs at 24hpi. EdU (white), Hoechst (blue). (D) Quantitation of EdU staining with n>8 HIOs. (E) TUNEL staining in HIOs at 8hpi. TUNEL (green) E-cadherin (red) DAPI (blue). (F) Quantitation of TUNEL staining with n=10 HIOs. Significance was determined by unpaired t-test where P value: *<0.05 and **<0.01.

3.4.6 Mitochondrial processes are differentially regulated during NTS infections

Although NTS cause similar disease manifestations in humans, they may interact with the intestinal epithelium by varied mechanisms as their genomes contain different accessory genes (*95*). Our data indicated that one of the most differentially regulated cellular processes between NTS was related to metabolism of proteins **(Fig 3.7A)**. To further identify major pathways within this category that were differentially regulated during infection with NTS, we sorted significant pathways that belonged to the metabolism of proteins category in the Reactome database to identify these pathways. We found pathways belonging to three major categories; translation, protein folding, and post-transcriptional regulation were increased in SE-infected HIOs but decreased during STM infection **(Fig 3.13A)**. Within the translation umbrella category, we found many mitochondrial-related processes, including mitochondrial translation, mitochondrial protein import and oxidative phosphorylation, were increased during SE infection but decreased during STM infection **(Fig 3.13B)**, suggesting that mitochondrial functions may differentiate between the host response to NTS during early stages of infection. Because mitochondria produce reactive oxygen species (ROS) during metabolism, we monitored generation of ROS in HIOs during infection **(Fig 3.13C-E)**. Consistent with an increase in mitochondrial gene expression, SE infection led to an accumulation of ROS in the HIOs when compared to PBS control. ROS induction was specific to SE, as neither STM nor ST infection triggered ROS generation when monitored at 24hpi. Together, our results suggest that SE infection induces specific HIO responses, including induction of mitochondria-related processes and ROS generation that distinguish this serovar from the more well-studied STM serovar.

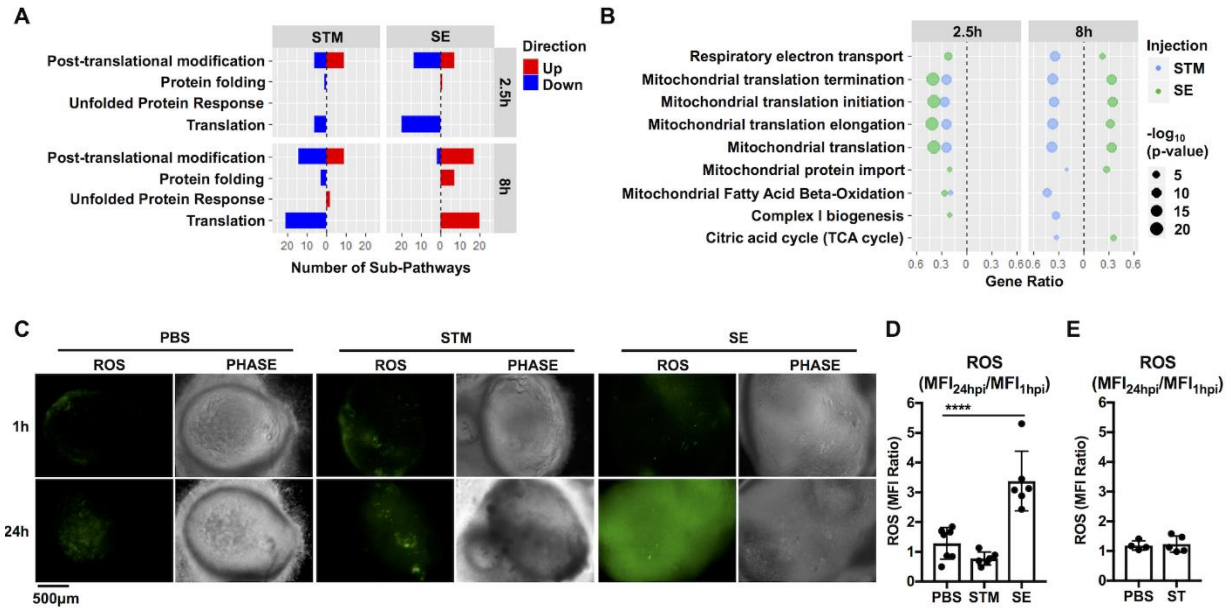

Figure 3.13 NTS infections inversely regulate changes in mitochondrial-related cellular processes at 8hpi and trigger differential ROS production. (A) Number of significant sub-pathways from the Reactome metabolism of proteins category during NTS infection. Upregulated (red) or downregulated (blue) pathways were identified using ReactomePA. Significant pathways were determined based on P value < 0.05. (B) Dot plot showing significantly enriched mitochondrial metabolism-related pathways in NTS-infected HIOs. Filtered by P value < 0.05. (C) Representative fluorescence images measuring reactive oxygen species (ROS) levels in HIOs by general oxidative stress dye, CM-H_2DCFDA. (D) Quantitation reactive oxygen species levels of (C) with n≥6 HIOs measuring the ratio of the mean fluorescence intensity (MFI Ratio) at 24h relative to 1hpi. (E) Quantification of reactive oxygen species levels in PBS or ST-infected HIOs at 24h relative to 1h. Error bars represent +/-SD. Statistical significance was determined by one-way ANOVA followed up by Tukey's multiple comparisons test. ****<0.0001.

3.5 Discussion

Despite sharing high genome identity, some *Salmonella* serovars cause infections that remain localized in the intestine while others cause more severe systemic infections. Differential host responses, especially the initial interactions with the human intestinal epithelium, are likely a contributing factor in determining infection outcome, something that has been difficult to study with other established infection models. Here we describe the first comprehensive transcriptomic analysis using human intestinal organoids infected with *Salmonella* serovars Typhimurium, Enteritidis and Typhi. We compared HIO transcriptional profiles at different time points during infection and identified responses

that were similar and unique to each serovar. As expected, inflammatory responses were a dominant early response during infection with all three serovars. However, at later times post infection, we observed distinct responses to each serovar including differences in expression of genes in cell cycle and mitochondrial function-related pathways. Direct comparison of HIO responses to these serovars revealed that many pathways decreased during STM infection were, in contrast, increased during SE infection even though these serovars cause similar diseases in humans. Thus, our data highlight the utility of the HIO model to define signatures of host responses to closely related enteric pathogens to understand how these responses may shape disease manifestations.

ST is a human-specific pathogen and other serovars exhibit different infection patterns in different organisms (*96*, *97*), therefore it is physiologically relevant to use human-derived cells to define human mechanisms of pathogenesis and host response. Many previous studies investigating host epithelial responses employed transformed cell lines (*84*, *98*–*101*), and although they have provided valuable insight into the specific mechanisms of *Salmonella* pathogenesis, particular aspects of epithelial function may not fully reflect what happens in an untransformed model system (*102*). More in-depth comparisons of host epithelial responses using different culture models revealed that approximately 50% of the top significantly regulated genes reported in a study published by Hannemann *et al.* (*84*) investigating responses to STM in a Henle-407 cell culture model were significant in our study while a study using a stem cell derived intestinal organoid culture model, published by Forbester *et al*. (*36*), showed a much higher correlation of epithelial gene expression to our dataset with about 90% of the reported top significant genes also being

significant in our study. In a more complex model system (an engineered organotypic model) (*85*), the correlation between datasets was relatively low with only about 30% similarity suggesting that addition of other components such as immune cells strongly contributes to the host response to infection. Additionally, studies looking at host responses to ST showed largely the same pattern (*84*, *98*, *99*, *103*). Across the various studies, the conserved responses largely belonged to immune-related processes suggesting that other types of responses may be more dependent on the specific model system. Our study aimed to compare and contrast three major *Salmonella enterica* serovars that are human pathogens, and we chose commonly used laboratory strains to represent each serovar. It is important to note that there may be meaningful differences in the epithelial host response even between strains within the same serovar. Although these findings merit a more detailed analysis to better understand how different model systems respond to each serovar or to different strains within serovars, we reason that the HIOs, composed of untransformed human intestinal epithelial and mesenchymal cells, might reveal specific responses that more closely mirror *in vivo* epithelial responses to infection.

Comparing different parameters of HIO infections revealed marked differences between the three serovars. Of particular interest was the efficiency with which STM infected the epithelium when the HIOs were injected with a relatively low inoculum (10^3), compared to SE and ST despite similar overall bacterial numbers within the HIO. This phenomenon could be explained by the earlier expression of genes encoding some SPI-1-dependent effectors in STM, especially SopE. In contrast, of the three serovars, SE expressed SPI-

2 related genes most robustly at 8hpi, which correlated with a substantial increase in intracellular bacteria. These variations between serovars in early interactions with the host may direct the timing and magnitude of some aspects of the innate immune response, based on relative proportions of luminal to intracellular bacteria. Additionally, intracellular STM can be found in either the vacuole or the cytosol, and a recent study identified specific bacterial adaptations required for these two different intracellular lifestyles (*104*). In the HIOs, we observed that some inflammatory pathways were decreased early during ST infection when compared to NTS. However, this effect was abrogated by 8hpi, emphasizing that ST may specifically modulate intestinal epithelial responses early and transiently during infection. Infection with each serovar stimulated distinct transcriptional profiles of numerous inflammatory mediators, potentially contributing to the difference in serovar-specific pathogenicity. We demonstrated that ST infection produced less secreted IL-6, IL-8, BD-2 and ELAFIN (PI3) compared to STM and SE infection, despite comparable increases in transcript levels. These findings lead us to speculate that ST may impair the ability of intestinal epithelial cells to release immune mediators through secretion blockade or post-transcriptional modification. Consistent with the hypothesis that ST disrupts secretion pathways in epithelial cells, we also observed accumulation of mucus within epithelial cells of ST-infected HIOs in contrast to STM-infected HIOs where mucus was expelled into the luminal space. Post-transcriptional control of cytokine production has also been previously established, but not in the context of *Salmonella* infection (*105–107*). Whether these mechanisms control ST pathogenesis and intestinal inflammatory responses are unknown, but could be elucidated in the HIO model.

Our finding that the three *Salmonella* serovars showed differential regulation of cell cycle pathways was intriguing. Intestinal epithelial cells undergo self-renewal to maintain barrier integrity, and infection with enteric pathogens can accelerate or inhibit cell proliferation to gain a survival advantage in the gut (*108*). For example, *Citrobacter rodentium* stimulates the proliferation of undifferentiated epithelial cells, which increases oxygenation of the mucosal surface in the colon to create a replicative niche (*109*). By contrast, some enteric pathogens, including STM, *Helicobacter pylori* and *Shigella* species are equipped with virulence factors to counteract intestinal cell proliferation and rapid epithelial turnover to enhance virulence (*108*). In our experiments, both STM and ST infections resulted in downregulation of many genes in the cell cycle pathway while SE infection resulted in upregulation of several of these genes. Follow-up studies measuring cellular proliferation revealed that STM infection resulted in a reduction of proliferating cells in the HIO, but no change was observed in SE or ST-infected HIOs. Of note, it was previously reported that STM blocks epithelial cell proliferation via Type 3 Secretion System-2 effectors SseF and SseG (*113*, *114*). These effectors are also encoded in the ST and SE genomes and were expressed in the HIOs at higher levels than in STM infection, suggesting that there may be alternative mechanisms leading to cell cycle suppression that remain to be uncovered.

Although STM and SE cause similar diseases in humans, we were surprised to observe that these two serovars exhibited the most variation in HIO responses relative to each other, including regulation of mitochondrial function-related genes. We previously showed that mitochondrial ROS plays a key role in shaping innate immune responses to bacterial

infection and contributes to bacterial killing by macrophages (*110*). Interestingly, we observed that many pathways involved in mitochondrial metabolism are upregulated during SE infection and downregulated during STM infection. Accordingly, we found that SE infection increased generation of antimicrobial ROS in the HIOs, suggesting that an increase in mitochondrial metabolism may be important in intestinal host defense. Indeed, mitochondrial integrity and function is required for the maintenance of healthy intestinal barriers to prevent bacterial translocation across the epithelial lining (*111*, *112*). In addition, recent studies demonstrated that metabolites produced by microbes in the gut can influence mitochondrial biogenesis and inflammation (*113*). Given that both STM and SE are present in the HIO lumen through the course of infection, it remains unclear whether SE uniquely increases expression of mitochondrial genes, or luminal bacteria generally increase expression of mitochondrial genes but STM uniquely decreases their expression, or both. SE encodes more than 200 genes that are absent in either the STM or ST genome, which are clustered in unique islands designated as “regions of difference” (ROD) (*78*). Some of these additional genes have been linked to SE pathogenesis using a mouse model of *Salmonella* infection (*116*). Therefore, we speculate that genes expressed only by SE might account for SE-specific induction of mitochondrial ROS and further work is required to elucidate mechanisms by which SE induces these specific responses.

Altogether, our findings show that HIOs are a productive model to study early interactions of *Salmonella* serovars with the intestinal epithelium. HIOs have been previously used to probe for transcriptional responses during STM infection (*35*, *36*), but to our knowledge

this is the first study to directly compare non-transformed human intestinal epithelial responses between non-typhoidal and typhoidal serovars. Looking beyond the pro-inflammatory pathways induced during infection by all three serovars, we identified unique host responses that are individually associated with these closely related serovars. Patterns emerging from our HIO experiments open up avenues for future studies to elucidate mechanisms by which different serovars fine-tune inflammatory output and modulate cell cycle and mitochondrial functions.

3.6 Materials and Methods

3.6.1 HIO Differentiation and Culture

HIO were generated by the I*n Vivo* Animal and Human Studies Core at the University of Michigan Center for Gastrointestinal Research as previously described (*20*). Briefly, human ES cell line WA09 was obtained from Wicell International Stem Cell Bank and cultured on Matrigel-coated (BD Biosciences) 6-well plates in mTeSR1 media (Stem Cell Technologies) at 37°C in 5% CO_2. Cells were seeded onto Matrigel-coated 24-well plates in fresh mTeSR1 media and grown until 85-90% confluence. Definitive endoderm differentiation was induced by washing the cells with PBS and culturing in endoderm differentiation media (RPMI 1640, 2% FBS, 2mM L-glutamine, 100ng/ml Activin A, 100U/ml of Penicillin and 100µg/ml of Streptomycin) for three days where fresh medium was added each day. Cells were then washed with endoderm differentiation media without Activin A and cultured in mid/hindgut differentiation media (RPMI 1640, 2% FBS, 2mM L-glutamine, 500ng/ml FGF4, 500ng/ml WNT3A, 100U/ml of Penicillin and 100µg/ml of Streptomycin) for 4days until spheroids were present. Spheroids were collected, mixed

with ice cold Matrigel (50 spheroids + 50µl of Matrigel + 25µl of media), placed in the center of each well of a 24-well plate, and incubated at 37°C for 10min to allow Matrigel to solidify. Matrigel embedded spheroids were grown in ENR media (DMEM:F12, 1X B27 supplement, 2mM L-glutamine, 100ng/ml EGF, 100ng/ml Noggin, 500ng/ml Rspondin1, and 15mM HEPES) for 14 days where media were replaced every 4days. Spheroids growing into organoids (HIOs) were dissociated from the Matrigel by pipetting using a cut wide-tip (2-3mm). HIOs were mixed with Matrigel (6 HIOs + 25µl of media + 50µl of Matrigel) and placed in the center of each well of 24-well plates and incubated at 37°C for 10min. HIOs were further grown for 14days in ENR media with fresh media every 4days. Prior to experiments, HIOs were carved out of the Matrigel, washed with DMEM:F12 media, and re-plated with 5 HIO/well in 50µl of Matrigel in ENR media with media exchanged every 2-3 days for 7days prior to microinjection.

3.6.2 Bacterial Growth Conditions and HIO Microinjection

Salmonella strains used in this study are *Salmonella* enterica serovar Typhimurium strain SL1344, *Salmonella* enterica serovar Enteritidis strain P125109 and *Salmonella* enterica serovar Typhi strain Ty2. Strains were stored at -70°C in LB medium containing 20% glycerol and cultured on Luria-Bertani (LB, Fisher) agar plates. Selected colonies were grown overnight at 37ºC under static conditions in LB liquid broth. Bacteria were pelleted, washed and re-suspended in PBS. The bacterial inoculum was estimated based on OD_{600} and verified by plating serial dilutions on agar plates to determine colony forming units (CFU). HIOs were cultured in group of 5 per well using 4-well plates (Thermo Fisher). Lumens of individual HIOs were microinjected with glass caliber needles with 1µl of PBS

or different strains of *Salmonella* (10^5 CFU/HIO for 2.5h or 8h for RNA-seq experiments or 10^3 CFU/HIO for 2.5h or 24h for bacterial burden experiments). HIOs were then washed with PBS and incubated for 2h at 37°C in ENR media. After 2h, HIOs were treated with 100µg/ml gentamicin for 15 min to kill any bacteria outside the HIOs, then incubated in a fresh medium containing 10µg/ml gentamicin.

3.6.3 ELISA and Bacterial Burden Analyses

Media from each well (5 HIOs/well) were collected at indicated time points after microinjection. Cytokines, chemokines and defensins were quantified by ELISA at the University of Michigan Cancer Center Immunology Core. Bacterial burden was assessed per HIO. Individual HIOs were removed from the Matrigel, washed with PBS and homogenized in PBS. Total CFU/HIO were enumerated by serial dilution and plating on LB agar. To assess intracellular bacterial burden, HIOs were cut open, treated with 100µg/ml gentamicin for 10min to kill luminal bacteria, washed with PBS, homogenized and plated on agar plates for 24h.

3.6.4 Immunohistochemistry and Immunofluorescence Staining

HIOs were fixed with either 10% neutral formalin or Carnoy's solution for 2 days and embedded in paraffin. Histology sections (5µm) were collected by the University of Michigan Cancer Center Histology Core and stained with hematoxylin and eosin (H&E). Carnoy's-fixed HIO sections were stained with Alcian Blue and Periodic Acid-Schiff (PAS) staining kit according to the manufacturer's instructions (Newcomersupply). H&E and Alcian Blue/PAS-stained slides were imaged on Olympus BX60 upright microscope. All

images were further processed using ImageJ. For immunofluorescence staining, formalin-fixed HIO sections were deparaffinized prior to performing antigen retrieval in sodium citrate buffer (10mM Sodium citrate, 0.05% Tween 20, pH 6.0). Sections were permeabilized with PBS + 0.2% Triton X-100 for 30min, then incubated in a blocking buffer (PBS, 5% BSA) for 1h. E-cadherin was stained using mouse anti-E-cadherin polyclonal antibody (clone 36, BD Biosciences) in a blocking buffer overnight at 4°C. Goat anti-mouse secondary antibody conjugated to Alexa-594 was used according to manufacturer's instructions (Thermo Fisher) for 1h RT in blocking buffer. To measure cell death, HIOs were stained using the *In situ* Cell Death Detection kit (Roche) following the manufacturer's instructions for paraffin fixed tissue. DAPI was used to stain DNA. Sections were mounted using coverslips (#1.5) and Prolong Glass Antifade Mountant (Thermo Fisher). Images were taken on the Nikon X1 Yokogawa spinning disc confocal microscope and processed using ImageJ and CellProfiler.

3.6.5 Vi Capsule Detection

Vi expression was monitored by flow cytometry. Bacteria grown under static and aerated conditions were washed with PBS and stained with *Salmonella* Vi Rabbit Antiserum (BD Biosciences) using 1:100 dilution followed by staining with goat anti-rabbit secondary antibody conjugated to PE. Bacteria were analyzed on FACSCanto Cell Analyzer (BD Biosciences). Data were further analyzed with FlowJo software and percent of Vi-positive bacteria was determined by gating against unstained cells. For histology staining, immunofluorescence was performed on 5µm histology sections of ST-infected HIOs using *Salmonella* Vi Rabbit Antiserum (1:250 dilution, BD Biosciences) followed by a secondary

goat anti-rabbit antibody conjugated to Alexa 488 (Thermo Fisher). DAPI was used to stain DNA. Images were taken on the Olympus BX60 upright microscope. All fluorescence images were processed and analyzed using ImageJ.

3.6.6 Cell Proliferation Analysis

After microinjection, 25μM EdU was added to the HIO culture medium and incubated at 37°C for 24h to allow incorporation into dividing cells. HIOs were fixed and sectioned as outlined above and stained using the Click-iT EdU Cellular Proliferation kit (Thermo Fisher) according to the manufacturer's protocol. HIOs were counterstained with Hoechst to detect DNA before mounting in Prolong Glass Antifade Mountant (Thermo Fisher). Images were taken on an Olympus BX60 upright microscope and processed and analyzed using ImageJ and CellProfiler.

3.6.7 RNA Sequencing and Analysis

Total RNA was isolated from groups of 5 HIOs per replicate with a total of 4 replicates per infection condition using the mirVana miRNA Isolation Kit (Thermo Fisher). The data shown here are part of a larger sample set that were analyzed for multiple studies. Thus, RNA-seq data from the PBS and STM samples are included in a previously published study (*35*), however, the SE and ST sample data and the associated analyses are unique to this study. The quality of RNA was confirmed, RNA integrity number (RIN)>8.5, using the Agilent TapeStation system. cDNA libraries were prepared by the University of Michigan DNA Sequencing Core after cytosolic and mitochondrial ribosomal RNAs depletion from samples using the TruSeq Stranded Total RNA with Ribo-Zero Gold Kit

according to manufacturer's protocol (Illumina). Libraries were sequenced on Illumina HiSeq 2500 platforms (single-end, 50bp read length). All samples were sequenced at a depth of 12 million reads per sample or greater.

3.6.8 Bioinformatics Comparison with Previously Published Transcriptomics Studies

Gene lists of the top 30-50 genes from indicated publications were used to filter against significant gene changes in infected HIOs with the corresponding serovar at either 2.5h or 8hpi. The fraction of genes from each list that were significant in the HIO dataset was then calculated. Log_2(fold change) of these significant genes was also determined and plotted using ggplot2 in R (*116*).

3.6.9 Data and Software Availability

All sequences are deposited in the EMBL-EBI Arrayexpress database (E-MTAB-10451). Source code for analyses can be found at: https://github.com/rberger997/HIO_dualseq2 and https://github.com/aelawren/Salmonella-serovars-RNA-seq.

3.6.10 RNA-seq Analysis Protocol

Sequence Alignment

Sequencing generated FASTQ files of transcript reads were pseudoaligned to the human genome (GRCh38.p12) using kallisto software (*117*). Transcripts were converted to

estimated gene counts using the tximport package with gene annotation from Ensembl (*118*, *119*).

Differential Gene Expression

Differential expression analysis was performed relative to PBS samples at each time point using the *DESeq2* package with P values calculated by the Wald test and adjusted P values calculated using the Benjamani & Hochberg method (*120*, *121*).

Pathway Enrichment Analysis

Pathway analysis was performed using the Reactome pathway database and pathway enrichment analysis in R using the ReactomePA software package (*122*).

Statistical Analysis

Analysis was done using RStudio version 1.1.453. Plots were generated using ggplot2 with data manipulation done using dplyr (*116*, *123*). Euler diagrams of gene changes were generated using the Eulerr package (*124*).

3.6.11 Reactive Oxygen Species (ROS) Measurement

HIOs were re-plated onto glass-bottom petri dishes (MatTek) and microinjected with 1µl of PBS/bacteria containing 50ng of CM-H_2DCFDA per HIO (Thermo Fisher). HIOs were

imaged using inverted widefield live fluorescent microscopy at indicated time points. Images were analyzed by ImageJ.

3.6.12 Quantification and Statistical Methods

Data were analyzed using Graphpad Prism 7 and R software. Statistical differences were determined using one-way ANOVA or two-way ANOVA (for grouped analyses) and followed-up by Tukey's multiple comparisons test. The mean of at least 3 independent experiments were presented with error bars showing standard deviation (SD). P values of less than 0.05 were considered significant and designated by: *<0.05, **<0.01, ***<0.001 and ****<0.0001.

Acknowledgments

This work was supported by NIH NIAID U19AI116482 (JRS, VBY, CEW, MXO). The funders had no role in study design, data collection and analysis, decision to publish, or preparation of the manuscript. A-LL was supported by the Molecular Mechanisms of Microbial Pathogenesis training grant (NIH T32 AI007528). We thank the Host Microbiome Initiative, the Center for Live Cell Imaging (CLCI), Microscopy and Image Analysis Laboratory (MIL), the Comprehensive Cancer Center Immunology and Histology Cores and the DNA Sequencing Core at University of Michigan Medical School. We thank C. Detweiler (Univ. of CO, Boulder) and H. Andrews-Polymenis (Texas A&M) for the kind gift of bacterial strains. We gratefully acknowledge the O'Riordan lab members for helpful discussions.

References

1. S. E. Majowicz, J. Musto, E. Scallan, F. J. Angulo, M. Kirk, S. J. O'Brien, T. F. Jones, A. Fazil, R. M. Hoekstra, International Collaboration on Enteric Disease "Burden of Illness" Studies, The global burden of nontyphoidal Salmonella gastroenteritis. *Clin. Infect. Dis.* **50**, 882–889 (2010).

2. J. A. Crump, S. P. Luby, E. D. Mintz, The global burden of typhoid fever. *Bull. World Health Organ.* **82**, 346–353 (2004).

3. V. Singh, Salmonella serovars and their host specificity. *J. Vet. Sci. Anim. Husb.* **1** (2013), doi:10.15744/2348-9790.1.301.

4. O. Gal-Mor, E. C. Boyle, G. A. Grassl, Same species, different diseases: how and why typhoidal and non-typhoidal Salmonella enterica serovars differ. *Front. Microbiol.* **5**, 391 (2014).

5. N. R. Thomson, D. J. Clayton, D. Windhorst, G. Vernikos, S. Davidson, C. Churcher, M. A. Quail, M. Stevens, M. A. Jones, M. Watson, A. Barron, A. Layton, D. Pickard, R. A. Kingsley, A. Bignell, L. Clark, B. Harris, D. Ormond, Z. Abdellah, K. Brooks, I. Cherevach, T. Chillingworth, J. Woodward, H. Norberczak, A. Lord, C. Arrowsmith, K. Jagels, S. Moule, K. Mungall, M. Sanders, S. Whitehead, J. A. Chabalgoity, D. Maskell, T. Humphrey, M. Roberts, P. A. Barrow, G. Dougan, J. Parkhill, Comparative genome analysis of Salmonella Enteritidis PT4 and Salmonella Gallinarum 287/91 provides insights into evolutionary and host adaptation pathways. *Genome Res.* **18**, 1624–1637 (2008).

6. S.-P. Nuccio, A. J. Bäumler, Comparative analysis of Salmonella genomes identifies a metabolic network for escalating growth in the inflamed gut. *MBio*. **5**, e00929-14 (2014).

7. Q.-H. Zou, R.-Q. Li, G.-R. Liu, S.-L. Liu, Comparative genomic analysis between typhoidal and non-typhoidal Salmonella serovars reveals typhoid-specific protein families. *Infect. Genet. Evol.* **26**, 295–302 (2014).

8. Y. E. Bar-Ephraim, K. Kretzschmar, H. Clevers, Organoids in immunological research. *Nat. Rev. Immunol.* **20**, 279–293 (2020).

9. J. R. Spence, C. N. Mayhew, S. A. Rankin, M. F. Kuhar, J. E. Vallance, K. Tolle, E. E. Hoskins, V. V. Kalinichenko, S. I. Wells, A. M. Zorn, N. F. Shroyer, J. M. Wells, Directed differentiation of human pluripotent stem cells into intestinal tissue in vitro. *Nature*. **470**, 105–109 (2011).

10. D. R. Hill, S. Huang, M. S. Nagy, V. K. Yadagiri, C. Fields, D. Mukherjee, B. Bons, P. H. Dedhia, A. M. Chin, Y.-H. Tsai, S. Thodla, T. M. Schmidt, S. Walk, V. B. Young, J. R. Spence, Bacterial colonization stimulates a complex physiological response in the immature human intestinal epithelium. *Elife*. **6** (2017), doi:10.7554/eLife.29132.

11. J. L. Forbester, D. Goulding, L. Vallier, N. Hannan, C. Hale, D. Pickard, S. Mukhopadhyay, G. Dougan, Interaction of Salmonella enterica Serovar Typhimurium with Intestinal Organoids Derived from Human Induced Pluripotent Stem Cells. *Infect. Immun.* **83**, 2926–2934 (2015).

12. A.-L. E. Lawrence, B. H. Abuaita, R. P. Berger, D. R. Hill, S. Huang, V. K. Yadagiri, B. Bons, C. Fields, C. E. Wobus, J. R. Spence, V. B. Young, M. X. O'Riordan, Salmonella enterica serovar Typhimurium SPI-1 and SPI-2 shape the global transcriptional landscape in a human intestinal organoid model system. *MBio*. **12** (2021), doi:10.1128/mBio.00399-21.

13. K. W. McCracken, J. C. Howell, J. M. Wells, J. R. Spence, Generating human intestinal tissue from pluripotent stem cells in vitro. *Nat. Protoc.* **6**, 1920–1928 (2011).

14. H. Wickham, *ggplot2: Elegant Graphics for Data Analysis* (Springer, 2016).

15. N. L. Bray, H. Pimentel, P. Melsted, L. Pachter, Near-optimal probabilistic RNA-seq quantification. *Nat. Biotechnol.* **34**, 525–527 (2016).

16. J. Rainer, EnsDb.Hsapiens.v75: Ensembl based annotation package. R package version 2.99.0 (2017).

17. C. Soneson, M. I. Love, M. D. Robinson, Differential analyses for RNA-seq: transcript-level estimates improve gene-level inferences. *F1000Res.* **4**, 1521 (2015).

18. Y. Benjamini, Y. Hochberg, Controlling the False Discovery Rate: A Practical and Powerful Approach to Multiple Testing. *Journal of the Royal Statistical Society: Series B (Methodological)*. **57** (1995), pp. 289–300.

19. M. I. Love, W. Huber, S. Anders, Moderated estimation of fold change and dispersion for RNA-seq data with DESeq2. *Genome Biol.* **15**, 550 (2014).

20. G. Yu, Q.-Y. He, ReactomePA: an R/Bioconductor package for reactome pathway analysis and visualization. *Mol. Biosyst.* **12**, 477–479 (2016).

21. H. Wickham, R. Francois, L. Henry, K. Müller, Others, dplyr: A grammar of data manipulation. *R package version 0. 4*. **3** (2015).

22. J. Larsson, eulerr: Area-Proportional Euler and Venn Diagrams with Ellipses (2019), (available at https://cran.r-project.org/package=eulerr).

23. S. Hannemann, J. E. Galán, Salmonella enterica serovar-specific transcriptional reprogramming of infected cells. *PLoS Pathog.* **13**, e1006532 (2017).

24. L. N. Schulte, M. Schweinlin, A. J. Westermann, H. Janga, S. C. Santos, S. Appenzeller, H. Walles, J. Vogel, M. Metzger, An Advanced Human Intestinal Coculture Model Reveals Compartmentalized Host and Pathogen Strategies during Salmonella Infection. *MBio*. **11** (2020), doi:10.1128/mBio.03348-19.

25. M. Hase, T. Yokomizo, T. Shimizu, M. Nakamura, Characterization of an orphan G protein-coupled receptor, GPR20, that constitutively activates Gi proteins. *J. Biol. Chem.* **283**, 12747–12755 (2008).

26. M. M. Weber, R. Faris, Subversion of the Endocytic and Secretory Pathways by Bacterial Effector Proteins. *Front Cell Dev Biol*. **6**, 1 (2018).

27. M. Raffatellu, D. Chessa, R. P. Wilson, R. Dusold, S. Rubino, A. J. Bäumler, The Vi capsular antigen of Salmonella enterica serotype Typhi reduces Toll-like receptor-dependent interleukin-8 expression in the intestinal mucosa. *Infect. Immun.* **73**, 3367–3374 (2005).

28. X. Song, S. Zhu, P. Shi, Y. Liu, Y. Shi, S. D. Levin, Y. Qian, IL-17RE is the functional receptor for IL-17C and mediates mucosal immunity to infection with intestinal pathogens. *Nat. Immunol.* **12**, 1151–1158 (2011).

29. A. J. M. Santos, C. H. Durkin, S. Helaine, E. Boucrot, D. W. Holden, Clustered Intracellular Salmonella enterica Serovar Typhimurium Blocks Host Cell Cytokinesis. *Infect. Immun.* **84**, 2149–2158 (2016).

30. C. Maudet, M. Mano, U. Sunkavalli, M. Sharan, M. Giacca, K. U. Förstner, A. Eulalio, Functional high-throughput screening identifies the miR-15 microRNA family as cellular restriction factors for Salmonella infection. *Nat. Commun.* **5**, 4718 (2014).

31. F. Schönenberger, A. Deutzmann, E. Ferrando-May, D. Merhof, Discrimination of cell cycle phases in PCNA-immunolabeled cells. *BMC Bioinformatics*. **16**, 180 (2015).

32. A. Valbuena, I. López-Sánchez, P. A. Lazo, Human VRK1 is an early response gene and its loss causes a block in cell cycle progression. *PLoS One*. **3**, e1642 (2008).

33. B. Giotti, S.-H. Chen, M. W. Barnett, T. Regan, T. Ly, S. Wiemann, D. A. Hume, T. C. Freeman, Assembly of a parts list of the human mitotic cell cycle machinery. *J. Mol. Cell Biol.* **11**, 703–718 (2019).

34. R. A. Edwards, G. J. Olsen, S. R. Maloy, Comparative genomics of closely related salmonellae. *Trends Microbiol.* **10**, 94–99 (2002).

35. P. Wigley, Salmonella enterica in the Chicken: How it has Helped Our Understanding of Immunology in a Non-Biomedical Model Species. *Front. Immunol.* **5**, 482 (2014).

36. A. D. Palmer, J. M. Slauch, Mechanisms of Salmonella pathogenesis in animal models. *Hum. Ecol. Risk Assess.* **23**, 1877–1892 (2017).

37. R. Salerno-Gonçalves, J. E. Galen, M. M. Levine, A. Fasano, M. B. Sztein, Manipulation of Salmonella Typhi Gene Expression Impacts Innate Cell Responses in the Human Intestinal Mucosa. *Front. Immunol.* **9**, 2543 (2018).

38. D. L. Weinstein, B. L. O'Neill, E. S. Metcalf, Salmonella typhi stimulation of human intestinal epithelial cells induces secretion of epithelial cell-derived interleukin-6. *Infect. Immun.* **65**, 395–404 (1997).

39. V. M. Bruno, S. Hannemann, M. Lara-Tejero, R. A. Flavell, S. H. Kleinstein, J. E. Galán, Salmonella Typhimurium type III secretion effectors stimulate innate immune responses in cultured epithelial cells. *PLoS Pathog.* **5**, e1000538 (2009).

40. S. Hannemann, B. Gao, J. E. Galán, Salmonella modulation of host cell gene expression promotes its intracellular growth. *PLoS Pathog.* **9**, e1003668 (2013).

41. A. Hausmann, G. Russo, J. Grossmann, M. Zünd, G. Schwank, R. Aebersold, Y. Liu, M. E. Sellin, W.-D. Hardt, Germ-free and microbiota-associated mice yield small intestinal epithelial organoids with equivalent and robust transcriptome/proteome expression phenotypes. *Cell. Microbiol.* **22**, e13191 (2020).

42. K. P. Nickerson, S. Senger, Y. Zhang, R. Lima, S. Patel, L. Ingano, W. A. Flavahan, D. K. V. Kumar, C. M. Fraser, C. S. Faherty, M. B. Sztein, M. Fiorentino, A. Fasano, Salmonella Typhi Colonization Provokes Extensive Transcriptional Changes Aimed at Evading Host Mucosal Immune Defense During Early Infection of Human Intestinal Tissue. *EBioMedicine*. **31**, 92–109 (2018).

43. T. R. Powers, A. L. Haeberle, A. V. Predeus, D. L. Hammarlöf, J. A. Cundiff, Z. Saldaña-Ahuactzi, K. Hokamp, J. C. D. Hinton, L. A. Knodler, Intracellular niche-specific profiling reveals transcriptional adaptations required for the cytosolic lifestyle of Salmonella enterica. *PLoS Pathog.* **17**, e1009280 (2021).

44. P. Anderson, Post-transcriptional control of cytokine production. *Nat. Immunol.* **9**, 353–359 (2008).

45. K. S. A. Khabar, Post-Transcriptional Control of Cytokine Gene Expression in Health and Disease. *Journal of Interferon & Cytokine Research*. **34** (2014), pp. 215–219.

46. J. Fan, N. M. Heller, M. Gorospe, U. Atasoy, C. Stellato, The role of post-transcriptional regulation in chemokine gene expression in inflammation and allergy. *Eur. Respir. J.* **26**, 933–947 (2005).

47. H. Ashida, M. Ogawa, M. Kim, H. Mimuro, C. Sasakawa, Bacteria and host interactions in the gut epithelial barrier. *Nat. Chem. Biol.* **8**, 36–45 (2011).

48. C. A. Lopez, B. M. Miller, F. Rivera-Chávez, E. M. Velazquez, M. X. Byndloss, A. Chávez-Arroyo, K. L. Lokken, R. M. Tsolis, S. E. Winter, A. J. Bäumler, Virulence factors enhance Citrobacter rodentium expansion through aerobic respiration. *Science*. **353**, 1249–1253 (2016).

49. B. H. Abuaita, T. L. Schultz, M. X. O'Riordan, Mitochondria-Derived Vesicles Deliver Antimicrobial Reactive Oxygen Species to Control Phagosome-Localized Staphylococcus aureus. *Cell Host Microbe*. **24**, 625-636.e5 (2018).

50. K. E. Cunningham, G. Vincent, C. P. Sodhi, E. A. Novak, S. Ranganathan, C. E. Egan, D. B. Stolz, M. B. Rogers, B. Firek, M. J. Morowitz, G. K. Gittes, B. S. Zuckerbraun, D. J. Hackam, K. P. Mollen, Peroxisome Proliferator-activated Receptor-γ Coactivator 1-α (PGC1α) Protects against Experimental Murine Colitis. *J. Biol. Chem.* **291**, 10184–10200 (2016).

51. F. Bär, W. Bochmann, A. Widok, K. von Medem, R. Pagel, M. Hirose, X. Yu, K. Kalies, P. König, R. Böhm, T. Herdegen, A. T. Reinicke, J. Büning, H. Lehnert, K. Fellermann, S. Ibrahim, C. Sina, Mitochondrial gene polymorphisms that protect mice from colitis. *Gastroenterology*. **145**, 1055-1063.e3 (2013).

52. A. Clark, N. Mach, The Crosstalk between the Gut Microbiota and Mitochondria during Exercise. *Front. Physiol.* **8**, 319 (2017).

53. C. A. Silva, C. J. Blondel, C. P. Quezada, S. Porwollik, H. L. Andrews-Polymenis, C. S. Toro, M. Zaldívar, I. Contreras, M. McClelland, C. A. Santiviago, Infection of mice by Salmonella enterica serovar Enteritidis involves additional genes that are absent in the genome of serovar Typhimurium. *Infect. Immun.* **80**, 839–849 (2012).

54. S. Ray, S. Das, P. K. Panda, M. Suar, Identification of a new alanine racemase in Salmonella Enteritidis and its contribution to pathogenesis. *Gut Pathog.* **10**, 30 (2018).

Chapter 4

Human Neutrophils Direct Epithelial Cell Extrusion and Enhance Intestinal Epithelial Host Defense During *Salmonella* Infection

4.1 Abstract

Pathological disease caused by enteric pathogens like *Salmonella enterica* is shaped by complex interactions between invading bacteria, intestinal cells, and immune cells. To explore the interplay between pathogen and host, we established a multi-component model of human intestinal organoids (HIOs) infected with *Salmonella enterica* serovar Typhimurium (STM), seeded with human polymorphonuclear leukocytes (PMNs). While PMNs did not affect luminal colonization of *Salmonella,* their presence reduced intracellular bacteria within the epithelium. Adding PMNs to infected HIOs resulted in substantial accumulation of apoptotic intestinal epithelial cells that was blocked by Caspase-1 or Caspase-3 inhibition. Cleaved-Caspase-3 was detected in epithelial cells, but inflammasome activation was only detected when PMNs were present. Caspase inhibition also increased bacterial burden in the epithelium, consistent with a protective role for induction of cell death in intestinal responses to infection. These data support a critical function for PMNs in promoting shedding of cells from the *Salmonella*-infected intestinal monolayer.

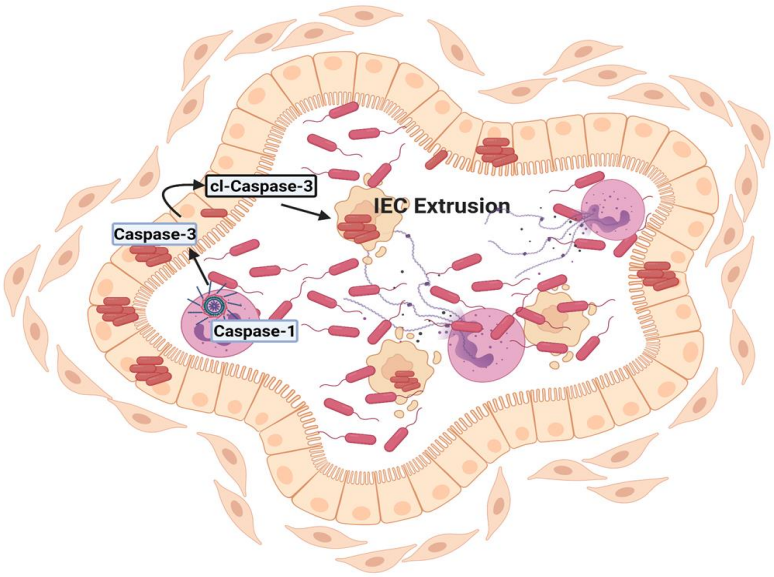

4.2 Graphical abstract

During *Salmonella* infection, PMNs transmigrate into the lumen of the HIO. PMNs undergo inflammasome activation and secrete mature IL-1 family mediators. Epithelial cells are shed into the lumen of the HIO during infection in the presence of PMNs and undergo apoptosis. PMN-mediated caspase activation enhances epithelial cell extrusion to reduce bacterial burden in the HIO.

4.3 Introduction

Foodborne illnesses account for an estimated 48 million infections in the United States every year with 128,000 individuals needing to be hospitalized (*125*). One of the most common causes of foodborne disease is *Salmonella enterica,* which is responsible for an estimated 1.35 million infections in the United States each year (*126*). *Salmonella enterica* infects via the fecal-oral route and once it reaches the intestinal tract it stimulates a strong inflammatory response from the host leading to gastroenteritis and diarrheal disease

(*127*). Although these symptoms are usually self-resolving, individuals with compromised immune systems or malnutrition can experience severe systemic illness, sometimes leading to death (*128*).

Salmonella pathogenesis is commonly studied *in vivo* using mouse infection models. Unfortunately, disease progression caused by *Salmonella* is often different in mice compared to humans, including the fact that mice rarely develop diarrhea during these infections (*10*). To better understand human infection, human-derived cells including human intestinal organoids (HIOs) have been used to define human-specific host responses to *Salmonella* (*35*, *36*, *129*). HIOs are derived from human pluripotent stem cells and self-organize to form a 3-dimensional polarized epithelium with differentiated epithelial cells and an underlying mesenchyme (*19*). Bacteria, including *Salmonella,* are able to replicate and stimulate robust inflammatory responses in the HIOs (*21*, *35*, *36*, *51*, *129*, *130*). Although the HIO model and other tissue culture models have been invaluable in revealing human-specific epithelial responses to *Salmonella* infection (*35*, *36*, *84*, *85*, *101*, *129*), key features missing from these models include immune cells known to shape the outcome of infection.

Several immune cell types contribute to control and resolution of *Salmonella* infections, however one of the earliest responders and the most abundant cell type found in *Salmonella*-infected individuals are polymorphonuclear leukocytes (PMNs), specifically neutrophils (*75*, *131*). Generally, PMNs defend against bacterial infections through

multiple mechanisms: antimicrobial effectors like degradative proteases and iron chelators, production of reactive oxygen species and formation of sticky antimicrobial neutrophil extracellular traps (NETs) (*132*). Although PMNs are potent killers of many bacterial pathogens (*133*), PMNs can serve several other functions such as affecting behavior of neighboring cells, including the intestinal epithelium by changing the microenvironment via molecular oxygen depletion, regulating nutrient availability, and through production of inflammatory mediators (*134*, *135*). How the interaction between epithelial cells and PMNs affect the outcome of bacterial infections is still poorly understood. To address this gap in knowledge, we generated a PMN-HIO model by co-culturing primary human PMNs with HIOs that were infected with *Salmonella enterica* serovar Typhimurium (STM) by microinjection of bacteria into the lumen. Using this PMN-HIO model, we characterized how PMNs modulate intestinal epithelial host defenses during infection, compared to HIOs alone. We show here that the presence of PMNs elevates intestinal epithelial proinflammatory signaling, including production of cytokines, chemokines and antimicrobial effectors. PMNs also induce apoptosis and extrusion of epithelial cells, thereby reducing *Salmonella* infectivity of the intestinal epithelial layer.

4.4 Results

4.4.1 Human PMNs transmigrate into the HIO lumen and reduce *Salmonella* intracellular burden in epithelial cells

PMNs are known to transmigrate across intestinal epithelial layers during early stages of inflammation (*136*, *137*), therefore we asked whether PMNs would transmigrate into the HIO lumen during infection. 10^5 *Salmonella enterica* Typhimurium (STM) were

microinjected into the HIO lumen and either cultured alone or with PMNs from healthy human volunteers

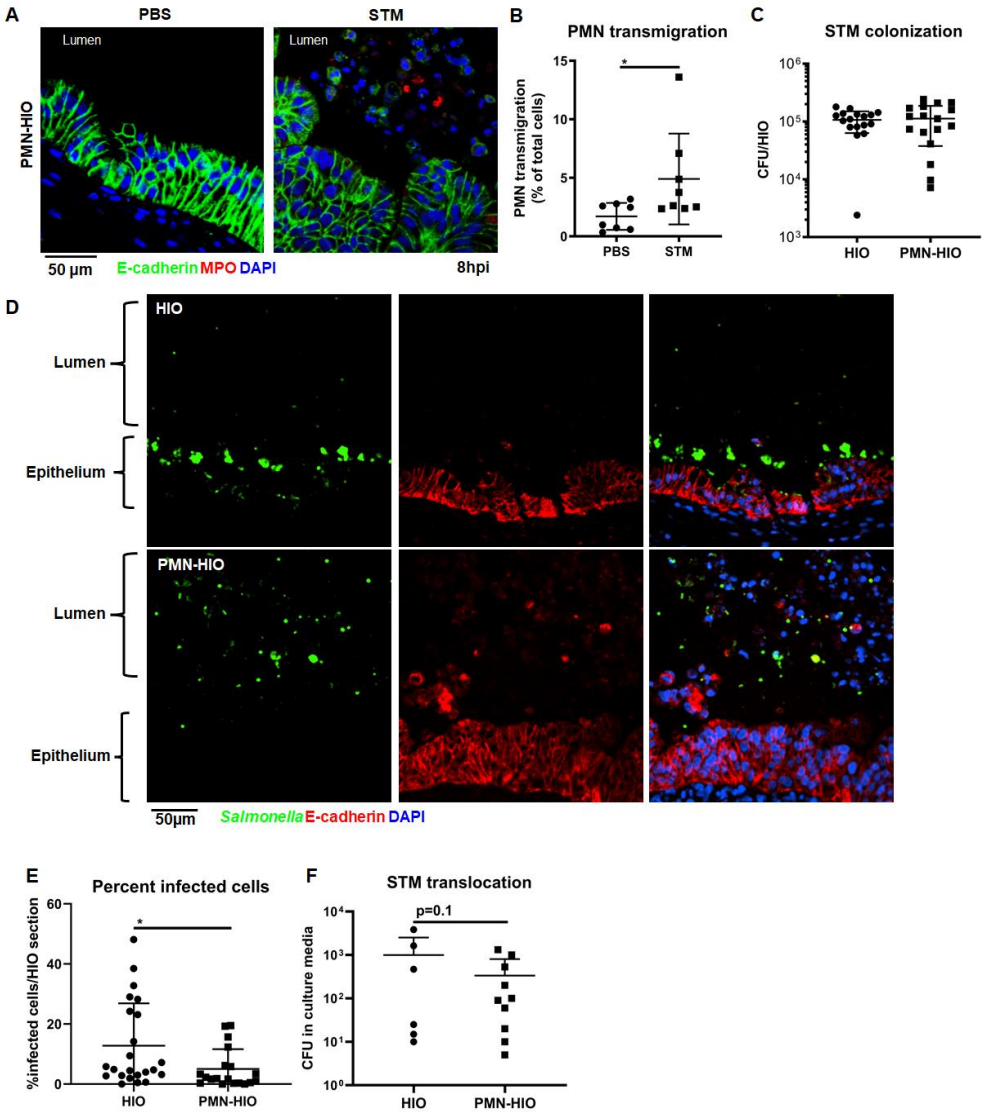

Figure 4.1 PMNs migrate into the lumen of the HIOs in response to infection and decrease infected epithelial cell numbers (A) Immunofluorescent staining of HIOs microinjected with PBS or STM and co-cultured with PMNs. E-cadherin (green) marks the epithelial lining, MPO (red) is specific to PMNs and DNA is stained with DAPI. (B) Transmigration of PMNs into the lumen of HIOs was quantified using flow cytometry. HIOs were microinjected with STM or PBS and co-cultured with CFSE-labeled PMNs for 8h. PMNs-HIOs were washed to remove any unassociated PMNs, dissociated into a single cell suspension and subjected to flow cytometry. Percentage of PMNs relative to total cells acquired per PMN-HIO was determined by FlowJo software. (C) Total bacterial burden per HIO or PMN-HIO was enumerated at 8hpi. (D) Representative immunofluorescent staining of HIOs and PMN-HIOs infected with STM. *Salmonella* is stained in green, E-cadherin to mark epithelial cells is shown in red, with DNA stained with DAPI in blue. (E) Quantitation of percent infected cells/HIO or PMN-HIO based on 3 fields per view per HIO. (F) Quantitation of disseminated *Salmonella* across the HIO epithelial lining was assessed by enumerating bacterial burden in culture media at 8hpi. Significance was determined using one-tailed t-test with p=0.1.

Graphs show the mean of n≥ 10 HIOs represented by dots from at least two independent experiments. Outliers were removed using the ROUT method with Q=0.1%. Unless otherwise stated, significance was determined by Mann-Whitney test with *p<0.05.

for 8h (PMN-HIOs). Immuno-fluorescent staining for neutrophil-specific myeloperoxidase (MPO) was performed on paraffin sections to monitor localization of PMNs within PMN-HIOs. In contrast to PBS-injected controls, MPO-positive cells were observed in the lumen of STM-infected HIOs, suggesting that PMNs were recruited to the site of infection **(Fig 4.1A)**. To quantify PMN recruitment to infected HIOs, PMNs were pre-labeled with Carboxyfluorescein succinimidyl ester (CFSE) prior to co-culture with HIOs. PMN-HIOs were collected at 8h post-infection (hpi), washed to remove unassociated neutrophils, dissociated into a single cell suspension and the percentage of CFSE-positive cells was enumerated by flow cytometry. Consistent with the immuno-fluorescent staining, we observed a significant increase in the number of PMNs associated with infected HIOs compared to PBS controls, with approximately 5% of total cells present in the PMN-HIOs staining positive for CFSE **(Fig 4.1B)**. Next, to determine whether PMNs could control *Salmonella* within the HIO, bacterial burden in HIOs and PMN-HIOs was enumerated. Although PMNs were able to kill STM in pure PMN cultures, with ~30% of STM being killed by 4hpi **(Fig 4.2)**, PMNs did not alter STM colonization in the HIOs **(Fig 4.1C)**.

We also tested whether neutrophils were able to deploy NETs in the STM-infected HIOs. NETs were detected in the HIO lumen of STM-infected PMN-HIOs **(Fig 4.3)**. In addition, culture supernatants were analyzed for production of antimicrobial effectors via ELISA **(Fig 4.4)**. Some antimicrobial effectors such as Elafin (PI3), a small cationic peptide secreted at mucosal surfaces (*138*), and Calprotectin (S100A8 and S100A9) were produced at higher levels in PMN-HIOs, compared to HIOs alone, indicating that PMNs augment epithelial host defenses. However, *Salmonella* has evolved mechanisms to

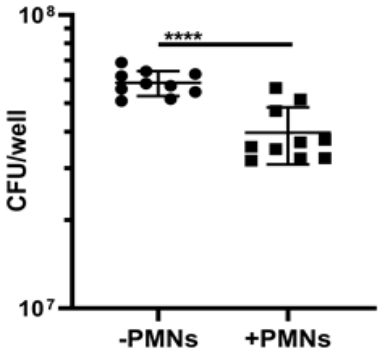

Figure 4.2 PMNs kill STM PMN bactericidal activity against *Salmonella* was quantified by enumerating CFU at 4h in the presence of PMNs relative to bacteria cultured alone. Results are from n=4 independent experiments with PMNs isolated from blood of different donors.

overcome Calprotectin-mediated immunity and thrive under these conditions; upregulation of these antimicrobial effectors is likely insufficient to reduce *Salmonella* colonization in the PMN-HIOs (*139*, *140*).

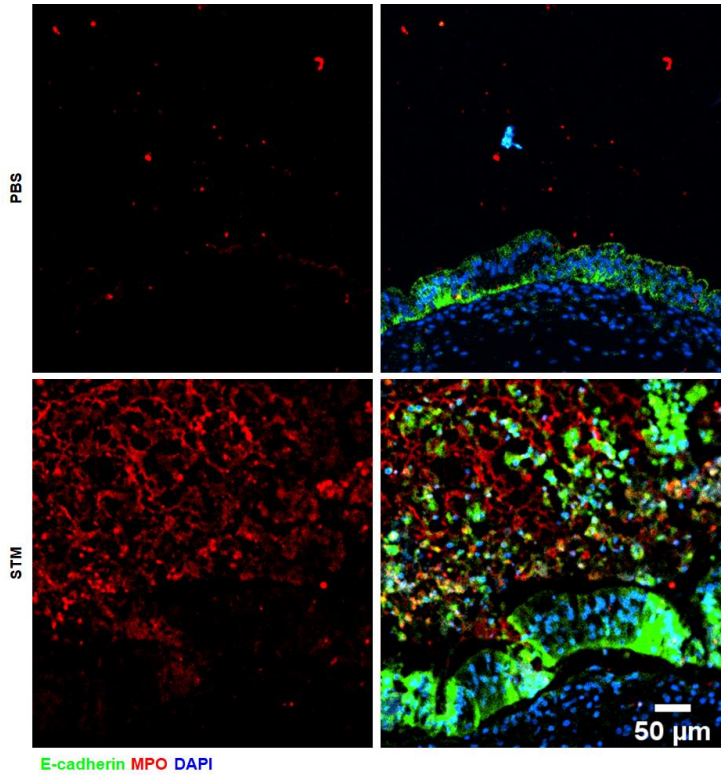

Figure 4.3 PMNs form NETs in PMN-HIOs during Salmonella infection Immunofluorescent staining of PMN-HIOs microinjected with PBS or STM and stained for epithelial cells marked with E-cadherin (green), PMNs marked by MPO (red) and DNA with DAPI (blue).

To further assess what impact PMNs might have on *Salmonella*-infected HIOs, intracellular bacterial burden in epithelial cells was quantified by fluorescence microscopy **(Fig 4.1D, 4.1E)**. This analysis revealed that there were significantly fewer intracellular bacteria in the epithelial lining of PMN-HIOs compared to HIOs alone. Notably, we also observed a reduction in epithelial-surface associated bacteria indicating that PMNs reduce STM attachment and intracellular bacterial burden within the epithelium. A previous report using a murine systemic Salmonellosis model also demonstrated that PMNs kill *Salmonella* that translocate across the intestinal epithelial layer (*141*). To test if PMNs contributed to extra-intestinal killing of *Salmonella* in the PMN-HIO model, STM-infected HIOs were cultured without antibiotics in the presence or absence of PMNs to quantify bacterial burden after STM translocation across the epithelial layer at 8hpi. While there was considerable variation in these results, likely corresponding to asynchronous bacterial translocation across the epithelial lining of the HIOs, there was a trend towards reduced bacterial burden in the PMN-HIO culture media **(Fig 4.1F)**, suggesting that PMNs may also control *Salmonella* replication after dissemination across the epithelial barrier. Together, these results show that PMNs transmigrate into the HIO lumen and reduce bacterial burden within the epithelial layer.

4.4.2 PMNs enhance HIO immune activation and programmed cell death pathways in response to *Salmonella* infection

We reasoned that PMNs would likely modulate the intestinal host response to *Salmonella* infection. HIOs and PMN-HIOs were microinjected with STM or PBS and harvested at 8hpi for global RNA-sequencing (RNA-seq). Principal component analysis (PCA) was

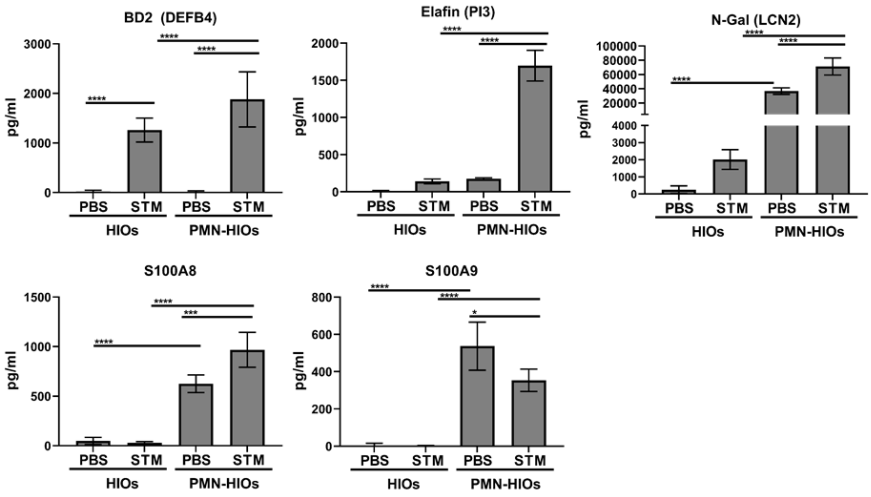

Figure 4.4 The antimicrobial response is intact in PMN-HIOs Quantification of antimicrobial protein levels in culture media of HIOs and PMN-HIOs microinjected with PBS or STM for 8h measured by ELISA. Graphs indicate the mean of n=4 replicates +/- standard deviation. Significance was determined by 2-way ANOVA where *p<0.05, **p<0.01, ***p<0.001, ****p<0.0001.

performed on normalized gene counts to determine whether there was clustering between HIOs and PMN-HIOs **(Fig 4.5A)**. While there was clear segregation between STM-infected HIOs and PMN-HIOs, there was no clear clustering between PBS control HIOs and PMN-HIOs, suggesting that PMNs change the transcriptional profile of the HIOs only during infection. Consistent with this analysis, there was greater variation between infected HIOs and PMN-HIOs compared to the variation between PBS control HIOs and PMN-HIOs as determined by Pearson correlation clustering, with even greater separation between uninfected and infected samples **(Fig 4.5B)**. To assess how PMNs changed the

HIO response during infection, significant gene changes were calculated relative to PBS control HIOs and filtered for adjusted p-value <0.05. Venn diagrams were generated to compare gene changes during STM infection +/- PMNs **(Fig 4.5C)**. Although a substantial number of genes were changed during STM infection in both HIOs and PMN-HIOs, over 1900 additional genes were induced in STM-infected PMN-HIOs relative to HIOs alone. Importantly, there were very few genes induced in PBS control PMN-HIOs, confirming that adding PMNs to the HIOs alone does not trigger dramatic changes in transcriptional programming, but the complex interaction between PMNs, HIOs and *Salmonella* drove a robust transcriptional response.

To identify biological processes induced in the PMN-HIOs, we performed pathway enrichment analysis using the Reactome pathway database **(Fig 4.5D, 4.5E)**. Each pathway was analyzed for gene ratio (fraction of genes in a pathway that were significantly changed relative to total genes in that pathway) plotted on the x-axis, and the statistical significance, depicted as dot size, based on $-\log_{10}$(p-value). As anticipated, immune system-related pathways were among the most significantly enriched pathways in response to infection **(Fig 4.5D)**. These included pathways belonging to various immune processes like signaling by interleukins, Toll-like receptor and NF-kB pathways, as well as PMN-specific pathways like reactive oxygen species production in phagocytes and neutrophil degranulation. Next, we identified the top non-immune processes that were enhanced by PMNs **(Fig 4.5E)**, which identified pathways related to extracellular matrix (ECM) organization, cell death, and signal transduction among others. ECM pathways such as integrin cell surface interactions and syndecan interactions were only enriched in

infected PMN-HIOs **(Fig 4.5E Top Panel)**. In contrast, cell death pathways, including caspase activation and programmed cell death, were induced weakly in STM-infected HIOs but were enriched more significantly in STM-infected PMN-HIOs **(Fig 4.5E Middle Panel)**. These results demonstrate that PMN migration into the HIO induces novel responses to infection that are initiated by epithelial cells, including several immune-related pathways, ECM production, and regulation of host cell death.

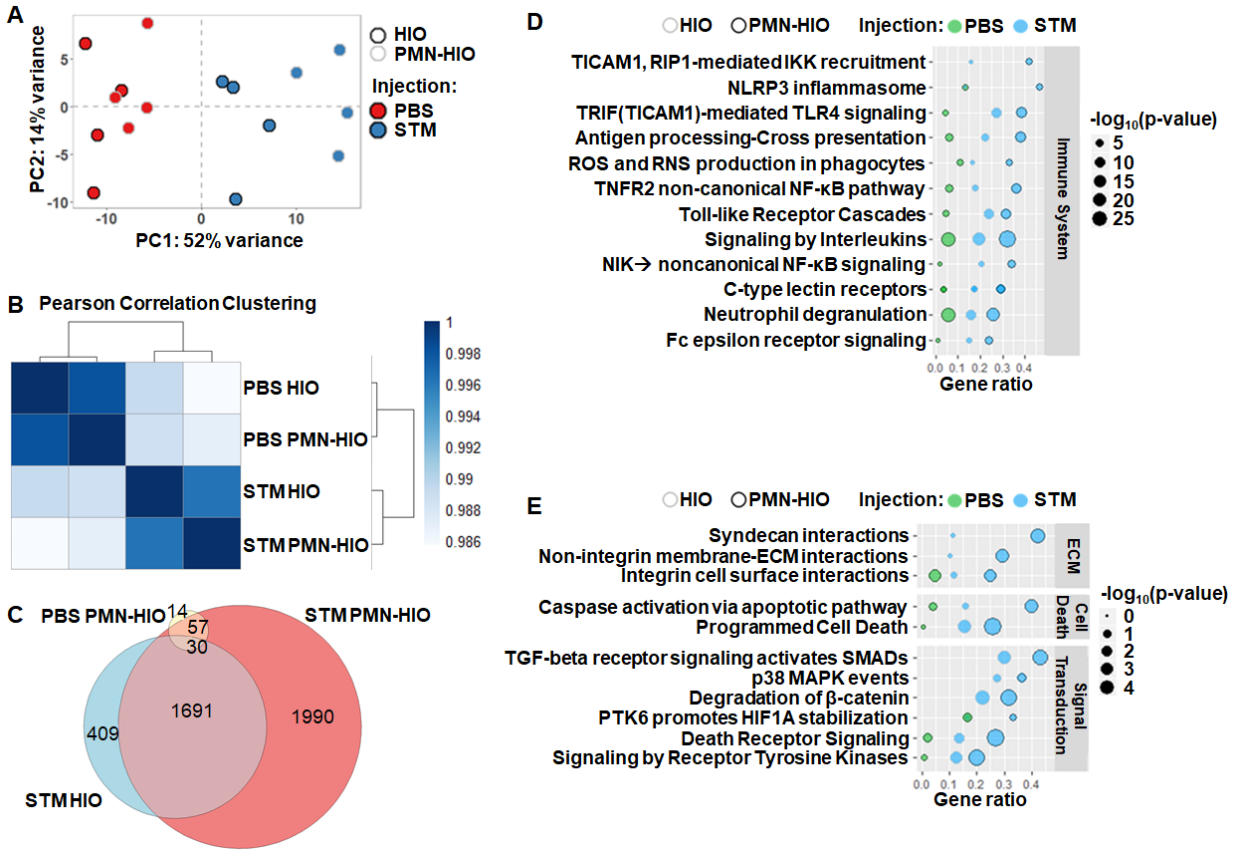

Figure 4.5 PMNs enhance infected HIO transcriptional responses including immune signaling, extracellular matrix interactions and programmed cell death (A) PCA plot of HIOs and PMN-HIOs infected with STM or PBS as the mock control for 8h. (B) Pearson correlation clustering of all RNA-seq experimental conditions. (C) Venn diagram comparing differentially regulated genes with p-adjusted value <0.05 from STM-injected HIOs, PBS-injected PMN-HIOs, and STM-injected PMN-HIOs relative to PBS-injected HIOs. (D) Reactome pathway enrichment results of selected immune pathways that were significantly upregulated in STM-injected PMN-HIOs. Gene ratio is shown on the x-axis and the dot size corresponds to the -$\log_{10}$(p-value). HIO samples are outlined in gray while PMN-HIOs are outlined in black. PBS-injection (green) and STM-injection (blue). (E) Reactome pathway enrichment results of pathways belonging to extracellular matrix organization (ECM), cell death, and signal transduction categories were performed as in (D).

4.4.3 PMNs elevate production of cytokines, chemokines and cell adhesion molecules in the PMN-HIOs

We recently reported that STM induces robust pro-inflammatory signaling in the HIO through transcriptional upregulation of cytokine and chemokine genes and downstream secretion of these effectors (*35*). Because we observed a further increase in pathway enrichment of several pro-inflammatory pathways in the infected PMN-HIOs compared to infected HIOs, we examined the contribution of PMNs in changing expression and production of some of these pro-inflammatory mediators including cytokines, chemokines and cell adhesion molecules. Consistent with our pathway enrichment results, PMN-HIOs increased expression of almost every cytokine, chemokine and cell adhesion molecule that was significantly changed during STM infection in the HIOs alone **(Fig 4.6A-C)**. This elevated response caused by PMNs was largely dependent on infection as there was very little upregulation of these genes in PBS control PMN-HIOs. Of interest in the infected PMN-HIOs, we observed increased transcript levels of cytokines CSF-3, IL-6, IL-8 **(Fig 4.6A)**, chemokines CXCL-10 and CCL-2 **(Fig 4.6B)**, and cell adhesion molecules SELE and ICAM1 **(Fig 4.6C)**, all of which are essential for progression and resolution of intestinal inflammation (*145*, *146*). To assess whether these transcriptional changes carried through to protein level changes, supernatants from HIOs and PMN-HIOs were collected for ELISA to measure cytokine and chemokine output **(Fig 4.6D)**, and paraffin sections were used to perform immunofluorescent staining to measure expression of cell adhesion molecule ICAM-1 **(Fig 4.6E)**. Protein level analyses revealed similar patterns to the transcriptional results. Overall, production of most cytokines and chemokines in infected PMN-HIOs was increased compared to infected HIOs or uninfected PMN-HIO

controls. This included significant increases in IL-6, IL-8, CXCL-10, and CCL-2 production in

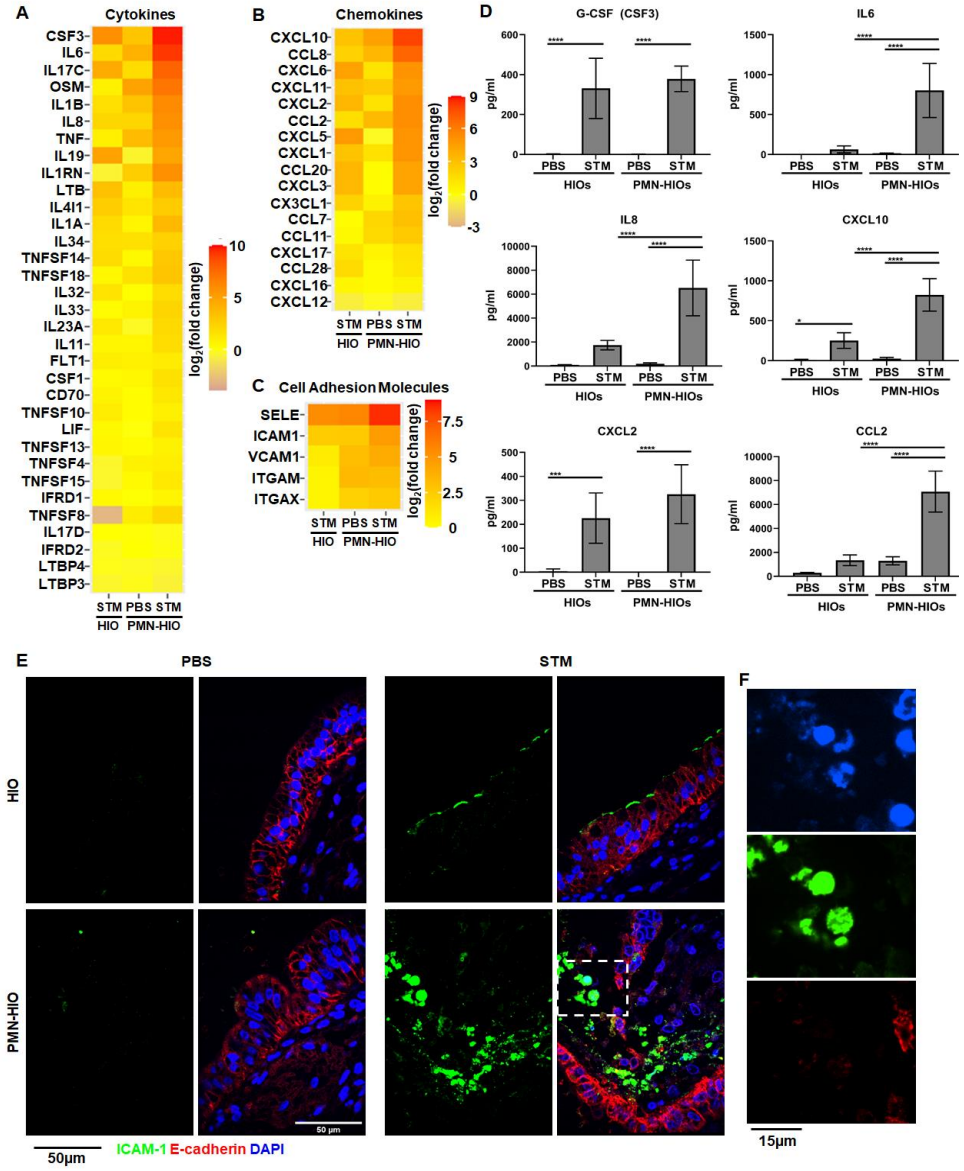

Figure 4.6 PMN association with HIOs amplifies production of cytokines, chemokines and cell adhesion molecules in infected HIOs (A-C) Gene expression data presented as log_2(fold change) relative to PBS-injected HIOs for (A) Cytokines, (B) chemokines, and (C) cell adhesion molecules. All genes that were significantly changed from PBS-injected HIOs in at least one condition with p-adjusted <0.05 are included. (D) ELISA data from HIO media sampled at 8hpi with 5 HIOs per well with n=4 replicates. (E) Representative fluorescence microscopy images of histology sections obtained from HIOs and PMN-HIOs injected with PBS or STM for 8h. ICAM-1 expression is shown in green. Sections were counterstained to show epithelial cell outlines stained using E-cadherin antibody in red, and DNA using DAPI in blue. (F) Zoom of boxed region of panel (E). Significance was determined by 2-way ANOVA where *p<0.05, **p<0.01, ***p<0.001, ****p<0.0001.

infected PMN-HIOs compared to infected HIOs. However, some targets such as G-CSF (encoded by *CSF3*) or CXCL-2 did not significantly change with the addition of PMNs. While other mediators correlated with the transcript data, *CSF3* transcript was dramatically upregulated in infected PMN-HIOs compared to infected HIOs even though there was no difference in secreted protein levels. It is possible that transcriptional upregulation occurred late during infection and so this change would not be observed until later for G-CSF secretion in the supernatant. Immunofluorescent staining of histology sections revealed an increase in apical ICAM-1 in infected HIOs, consistent with previous reports characterizing infection and LPS-dependent induction of ICAM-1 expression (*147*), and staining intensity further increased in infected PMN-HIOs **(Fig 4.6E)**. ICAM-1 staining was not only localized to epithelial cells, but was also expressed at high levels by PMNs as observed by the characteristic multi-lobed nuclei **(Fig 4.6F)**. This finding suggests that both PMNs and epithelial cells upregulate ICAM-1 expression in PMN-HIOs in response to infection. All together, we found that inflammatory signaling was enhanced by the addition of PMNs to the HIOs during infection, including upregulation of pro-inflammatory markers on both HIO cells and PMNs.

4.4.4 Inflammasome activation and IL1 production is mediated by PMNs during infection

The NLRP3 inflammasome is a key regulator of intestinal inflammation (*148*). Our RNA-seq pathway analysis also showed upregulation of genes encoding NLRP3 inflammasome components during infection in the PMN-HIOs, but not in infected HIOs alone **(Fig 4.5D)**. To assess how PMNs shape Inflammasome activation in the PMN-HIOs model, first we examined gene level expression data from our RNA-seq dataset of the inflammasome signaling pathway to identify under which conditions inflammasome

signaling was activated. While there was weak upregulation of IL-1β and IL-1α in STM-infected HIOs, we did not observe significant changes in expression of any other mediators or machinery required for inflammasome assembly **(Fig 4.7A)**. In contrast, when PMNs were added to infected HIOs, we observed stronger upregulation of *IL-1* genes and effectors involved in inflammasome activation including the upregulation of *NLRP3* and *Caspase-1* (*CASP1*). To further characterize this phenotype, we collected culture supernatants from HIOs and PMN-HIO and quantified levels of IL-1 family cytokines during infection **(Fig 4.7B)**. IL-1β or IL-1α in infected HIOs was undetectable; release of these cytokines required the presence of PMNs as IL-1β or IL-1α levels significantly increased in STM-infected PMN-HIOs. We also observed production of IL-1RA, the antagonist of the IL-1 receptor, in infected PMN-HIOs suggesting that PMNs may induce signaling processes that tune the magnitude of immune activation. In contrast, IL-33, another important alarmin in mucosal immunity (*149*), was produced in all conditions independent of the presence of PMNs. A recent study suggested that IL-33 is released constitutively by epithelial cells where it is then processed extracellularly by serine proteases including elastase which is released by PMNs (*150*). This processed form is then thought to enhance inflammatory signaling. Interestingly, we observed significantly lower levels of IL-33 in STM-infected PMN-HIOs, which may be caused by PMN processing. If true, this would correlate with the enhanced inflammatory environment that is created by PMNs. To further define which cells within the PMN-HIOs contribute to inflammasome activation and IL-1 processing, paraffin sections of STM-infected PMN-HIOs were stained for ASC, an adaptor protein required for inflammasome assembly **(Fig 4.7C, 4.7D)** (*133*). ASC-positive signal was not observed in HIO epithelial

cells, but instead was associated with cells positive for vimentin, a protein expressed by PMNs and mesenchymal cells within the PMN-HIOs. ASC and Vimentin double positive cells were primarily located within the lumen of PMN-HIOs, suggesting that these cells are PMNs. Closer examination of nuclear morphology of the ASC-positive cells by DAPI staining revealed multi-lobed nuclei, further supporting that inflammasome activation and IL-1 processing occur in PMNs. Together, these findings suggest that PMNs are the primary site of inflammasome activation and production of IL-1 family cytokines during infection in the PMN-HIO model.

4.4.5 PMNs induce shedding of apoptotic epithelial cells.

In addition to the vimentin-positive cells in the PMN-HIO lumen, we also observed robust accumulation of E-cadherin-positive cells **(Fig 4.1A, 4.1D, and 4.3)**. Activation of programmed cell death was enriched in infected PMN-HIOs compared to infected HIOs, including specifically caspase activation via apoptotic pathway **(Fig 4.5E Middle Panel)**. To determine whether enrichment of these pathways resulted in functional changes in host cell death, we performed Terminal deoxynucleotidyl transferase dUTP nick end labeling (TUNEL) on HIOs and PMN-HIOs microinjected with either PBS or STM. While we observed a substantial number of TUNEL-positive cells in the mesenchyme, this was detected under all conditions including in PBS-injected HIOs, so we specifically quantified TUNEL signal in the luminal space. The presence of PMNs induced robust accumulation of TUNEL-positive cells in the lumen of infected HIOs **(Fig 4.8A, 4.8B)**. Accumulation of

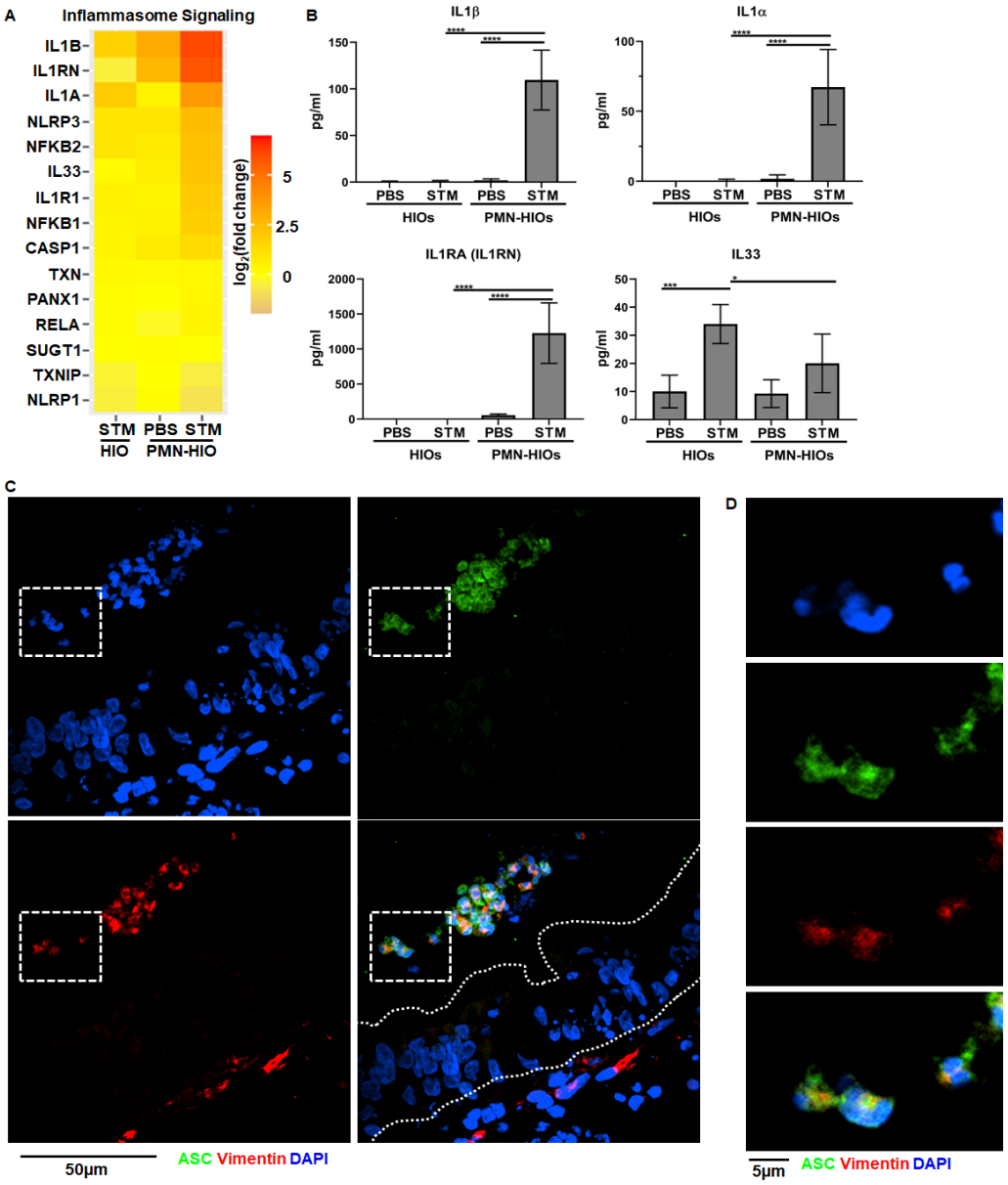

Figure 4.7 Inflammasome activation and IL-1 production is mediated by PMNs during infection (A) Gene expression data presented as log_2(fold change) relative to PBS-injected HIOs for members of the IL-1 signaling pathway. All genes are significantly changed from PBS-injected HIOs in at least one condition with p-adjusted value <0.05. (B) Cytokine levels in culture media of HIOs and PMN-HIOs were quantified using ELISA. Graphs indicate the mean of n=4 biological replicates +/- SD from media sampled at 8hpi with 5 HIOs or PMN-HIOs per well. (C) Immunofluorescent staining of histology sections of PMN-HIOs. Sections were stained for ASC expression (green), Vimentin (red) to mark PMNs and mesenchymal cells and DNA (blue) was labeled with DAPI. (D) Zoom of (C) showing luminal ASC-positive cells (green) with multilobed PMN nuclei. Statistical significance was determined by 2-way ANOVA where *p<0.05, **p<0.01, ***p<0.001, ****p<0.0001.

luminal apoptotic cells was selectively induced by PMNs during infection, as neither infected HIOs or uninfected PMN-HIOs showed this phenotype. To confirm that these

cells were epithelial cells and not PMNs, we stained for the epithelial marker E-cadherin, and found that the vast majority of TUNEL-positive cells in PMN-HIOs were epithelial cells **(Fig 4.8C, 4.8D)**. To better characterize what form of cell death these luminal epithelial cells were undergoing, we stained for cleaved Caspase-3 as a marker of apoptosis and found that luminal epithelial cells were positive for cleaved Caspase-3 **(Fig 4.8E)**. PMN-induced cell shedding was not restricted to infected cells, as we could observe both infected and uninfected cells in the PMN-HIO lumen **(Fig 4.9)**. Together these results suggest that PMNs promote epithelial cell apoptosis and cell shedding during infection.

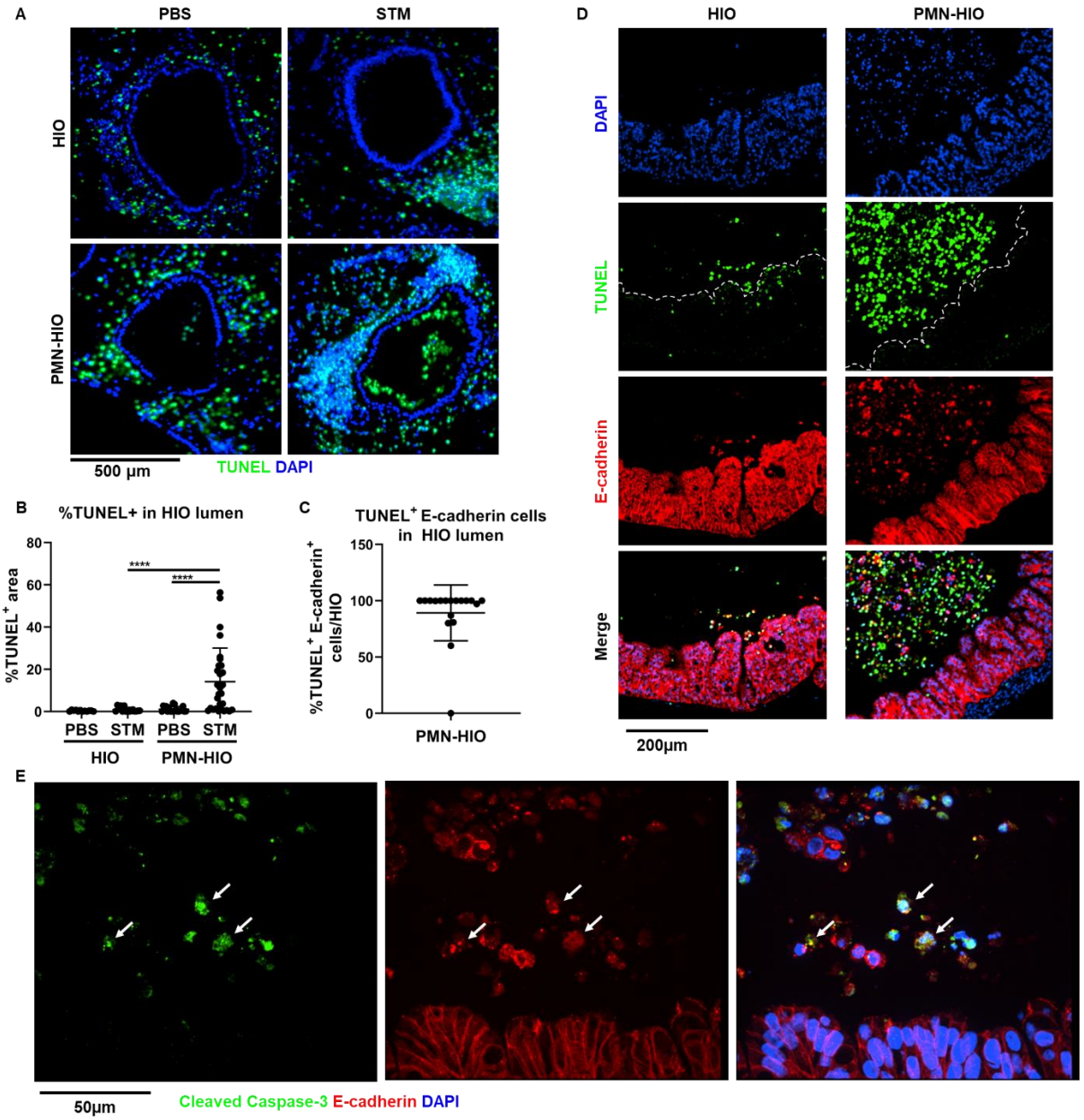

Figure 4.8 PMNs induce apoptosis and shedding of epithelial cells during STM infection. (A) Immunofluorescent images of TUNEL staining of histology sections of HIOs and PMN-HIOs injected with PBS or STM at 8hpi. (B) Quantitation of TUNEL positive cells in the lumen of HIOs and PMN-HIOs from (A). Graphs represent HIOs from 2 independent experiments with >12 HIOs per group. (C) Quantitation of percent of apoptotic epithelial cells in HIO lumen. Double-positive cells in HIO lumen staining for both TUNEL and E-cadherin were considered apoptotic epithelial cells. (D) Representative confocal microscopy images of histology sections from STM-injected HIOs or PMN-HIOs at 8h. Sections were co-stained with TUNEL (green), epithelial cell marker E-cadherin (red), PMN marker MPO (white), and DNA marker DAPI (blue). (E) Confocal microscopy images of histology sections of HIOs and PMN-HIOs that were stained for E-cadherin (red), cleaved caspase-3 (green), and DNA (blue). Arrowheads point to cleaved caspase-3 positive epithelial cells. Outliers were removed using the ROUT method with Q=0.1%. Significance was determined via one-way ANOVA with post-Tukey's test for multiple comparisons where ***p<0.001 and ****p<0.0001.

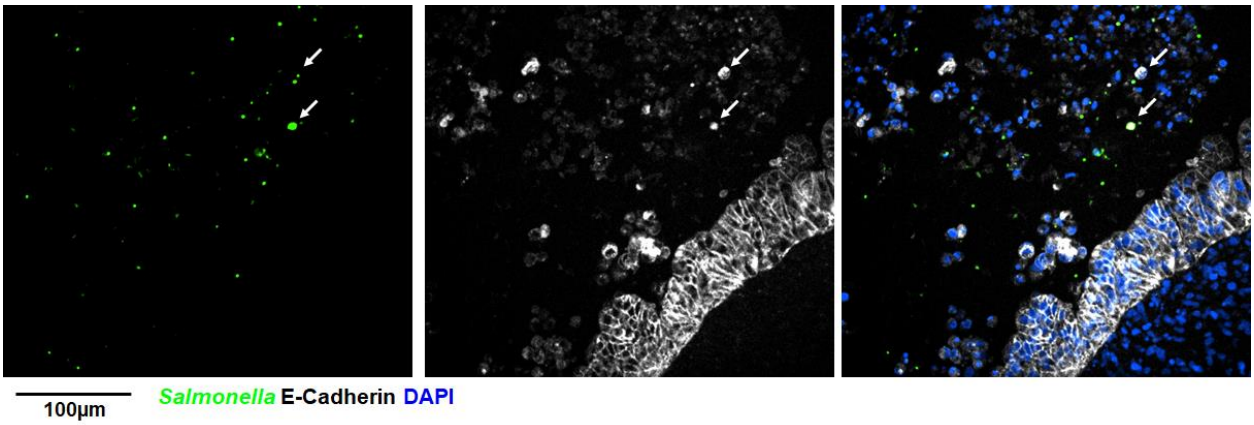

Figure 4.9 Some but not all extruded cells are infected with Salmonella Immunofluorescent staining of STM-infected PMN-HIO stained for *Salmonella* (green), E-cadherin (white) and DAPI (blue). Arrowheads point to infected extruded cells.

4.4.6 Caspase-1 and Caspase-3 inhibition reduces shedding of epithelial cells and increases intracellular bacterial burden in PMN-HIOs

Epithelial apoptosis and shedding may serve to reduce bacterial burden in the intestinal epithelium. To define the functional consequences of PMN-induced epithelial cell death on host defense, we treated PMN-HIOs with various caspase inhibitors. Accumulation of TUNEL-positive epithelial cells was monitored in infected PMN-HIOs in the presence or absence of Caspase-1 (z-YVAD-FMK), Caspase-3 (z-DEVD-FMK), or pan-Caspase (z-VAD-FMK) inhibitors. We performed TUNEL analysis on paraffin sections from infected PMN-HIOs at 8hpi **(Fig 4.10A, 4.10B)**. Caspase-1 or Caspase-3 inhibition, as well as the pan-Caspase inhibitor, significantly reduced accumulation of TUNEL-positive cells in the lumen of infected PMN-HIOs, indicating that PMN-dependent Caspase-1 and -3 activation is required for efficient shedding of epithelial cells. To test how caspase inhibition and therefore reduced shedding affected STM infection, PMN-HIOs were stained with an anti-*Salmonella* antibody to characterize the localization of bacteria in the

HIO by quantifying the percentage of infected cells and number of bacteria per cell **(Fig 4.10C, 4.10E)**. Consistent with our hypothesis that PMNs enhance shedding of epithelial

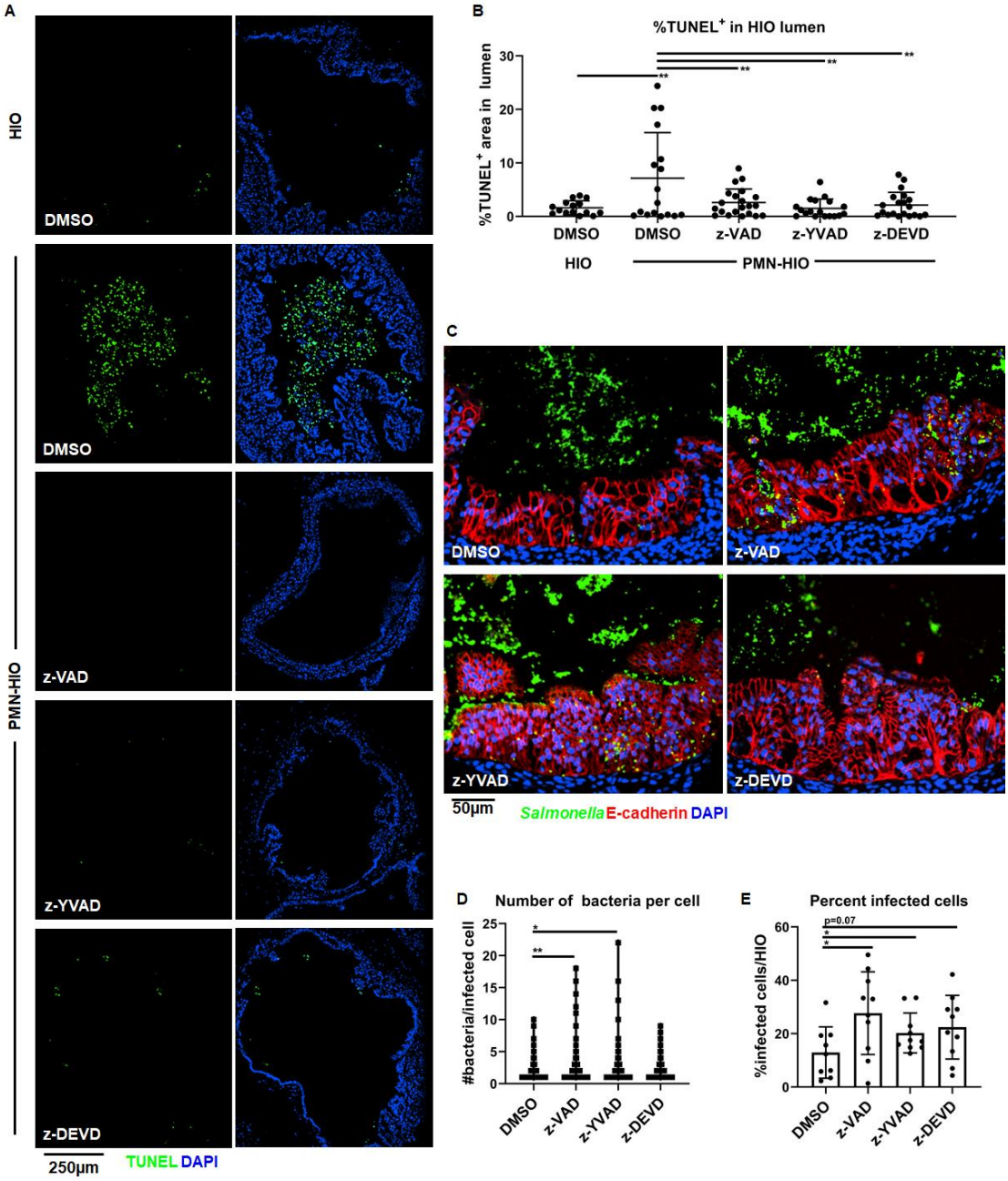

Figure 4.10 Caspase-1 and Caspase-3 inhibition reduces shedding of infected epithelial cells in the lumen of PMN-HIOs (A) Representative fluorescence microscopy images of TUNEL staining of HIO and PMN-HIO histology sections. HIOs were microinjected with STM and either cultured alone or co-cultured with PMNs in the presence of inhibitors for Caspase-1 (z-YVAD), Caspase-3 (z-DEVD), pan-Caspase (z-VAD), or DMSO control. (B) Quantitation of the percent of lumen filled with TUNEL-positive cells of STM-infected HIOs or PMN-HIOs with indicated treatments. (C) Fluorescent microscopy images of STM infected HIO and PMN-HIO histology sections. Samples were stained for *Salmonella* (green), E-cadherin (red), and

DAPI (blue). (D) Quantitation of the number of bacteria per cell based on images shown in (C) (E) Quantitation of the percent infected cells/HIO using 3 fields of view per HIO section. Unless otherwise stated, graphs show the mean of n≥ 10 HIOs represented by dots from at least two independent experiments. Outliers were removed using the ROUT method with Q=0.1%. Significance was determined by one-way ANOVA with post-Tukey's test for multiple comparisons where *p<0.05, **p<0.01.

cells through caspase activation, there were greater numbers of bacteria per cell in Caspase-1 or pan-Caspase inhibitor-treated PMN-HIOs, but surprisingly not in Caspase-3 inhibitor-treated PMN-HIOs **(Figure 4.10D)**. Additionally, the percentage of infected cells increased with Caspase-1 or pan-Caspase inhibition, while there was a trend toward an increased number of infected cells during Caspase-3 inhibition **(Fig 4.10E)**. These data suggest that either Caspase-1 or Caspase-3 inhibition reduces accumulation of dead cells in the PMN-HIO lumen, but Caspase-1 activity is additionally important for regulating epithelial bacterial burden. Taken together, our data support a model where inflammasome activation in PMNs induces Caspase-3-mediated apoptosis and shedding of infected epithelial cells into the intestinal lumen to control *Salmonella* infection.

4.5 Discussion

Despite a handful of studies showing that neutrophils (PMNs) respond to *Salmonella* infection in the gut (*75*, *141*, *151*, *152*), the specific contributions of PMNs in regulating intestinal epithelial cell host defense and infection outcome are not well understood. Here we used a co-culture model of human intestinal organoids (HIOs) with primary human PMNs, termed PMN-HIOs, to elucidate these roles. We found that while there was no difference in luminal colonization of *Salmonella* in the HIOs, PMNs did reduce intracellular bacterial burden in the epithelium and caused a trend of decreased extracellular dissemination across the epithelial layer. By performing RNA-seq, we observed that PMNs enhanced the HIO response to infection. PMN-dependent transcriptional programming included upregulation of proinflammatory mediators like activation of the

inflammasome as well as increased transcription of programmed cell death pathways. Upregulation of cell death pathways correlated with a significant increase in apoptotic epithelial cells in the lumen of infected PMN-HIOs. We found that inflammasome-mediated Caspase-1 activation in PMNs was required for epithelial shedding and that inhibition of Caspase-1 activity increased intracellular bacterial burden in HIO epithelial cells. Thus, we propose a model where PMNs enhance shedding of infected epithelial cells from the intestinal barrier to reduce intracellular bacterial loads, potentially tilting infection outcome favorably toward the host.

Our observation that PMNs did not affect total bacterial colonization in the HIO lumen was rather unexpected, both because the antimicrobial response was intact in the PMN-HIO cultures and our findings and that of others that PMNs kill *Salmonella* in the absence of HIOs via the formation of bactericidal NETs (*152*). We also observed transmigration and NET formation by PMNs in the HIO lumen, so the lack of *Salmonella* killing in the HIO lumen was not due to PMNs not being present at the site of infection. These observations suggest the possibility that *Salmonella* may employ specific mechanisms to overcome PMN effector functions in the HIO luminal environment. Interestingly, we observed robust production of Elafin, which is annotated as an antimicrobial peptide in REACTOME, but also functions as a neutrophil elastase inhibitor (*153*). While PMNs are potent killers of invading pathogens, mechanisms used by PMNs to kill pathogens are not highly selective and therefore PMN activation can cause tissue damage if not tightly controlled (*154*). In fact, Elafin has been shown to inhibit neutrophil elastase to reduce tissue damage caused by neutrophil overactivation (*155*, *156*). Neutrophil elastase strongly contributes to the

antimicrobial function of PMNs for both intracellular killing via phagocytosis and decorating NETs (*133*, *157*, *158*). These findings would suggest that enhanced expression of Elafin by the HIOs in the presence of PMNs may protect the HIO from additional damage and may explain in part the inability of PMNs to directly kill *Salmonella* within the HIO lumen.

Instead of killing *Salmonella* in the lumen of the HIO, PMNs reduced the intracellular bacterial burden in epithelial cells. We hypothesized that this resulted from elevated levels of cell extrusion from the epithelial lining, a process mediated by caspase activation. Previous reports have highlighted the importance of epithelial cell extrusion in preventing dissemination of *Salmonella* beyond the intestine and that there are epithelial cell intrinsic mechanisms to rid the epithelial lining of *Salmonella* (*53*, *159–163*). While we can detect low levels of shed epithelial cells in STM-infected HIOs alone consistent with prior studies, this phenotype was dramatically enhanced in the presence of PMNs. Our data implicates a previously unappreciated role for PMNs in enhancing rates of epithelial cell apoptosis and extrusion during *Salmonella* infection to help control infection outcome. There are numerous mechanisms by which PMNs can drive epithelial cell death like production of oxidants by activated PMNs which was shown to activate apoptotic pathways in the epithelium (*164*, *165*). Consistent with these reports, we identified enrichment of reactive oxygen species formation in the pathway analysis from our RNA-seq dataset. Alternatively, another mechanism that could enhance epithelial cell apoptosis in the PMN-HIOs comes from a study showing that NET formation can induce cell death in both epithelial and endothelial cells (*166*). This process was largely dependent on the

extracellular presence of histones released when PMNs spit out their DNA during NET formation. We did observe NET formation during *Salmonella* infection, and *Salmonella*-induced NET formation in PMN-HIOs may contribute to the accumulation of apoptotic epithelial cells. These reports are consistent with our findings that both infected and uninfected epithelial cells are being shed from the intestinal monolayer in the PMN-HIOs. By enhancing overall levels of epithelial cell shedding, this process contributes to reducing bacterial burden in the epithelium.

Our findings suggested that Caspase-1 activity was required for accumulation of apoptotic epithelial cells in the HIO lumen, but markers of inflammasome activation were only observed when PMNs were present. Although the importance of Caspase-1 in PMN activation and antimicrobial functions are not fully understood, there is some evidence that Caspase-1 may contribute to NET formation. One study showed that Caspase-11 (a caspase which is activated similarly to Caspase-1 via the inflammasome) dependent processing of Gasdermin D was required for NET formation in mice (*167*). While there may be additional signaling roles of Caspase-1 in PMN activation, we propose a model whereby PMNs transmigrate into the inflamed intestine, undergo Caspase-1 mediated NET formation to trigger epithelial cell death and shedding of infected cells to reduce bacterial burden. Future studies will further probe the role of Caspase-1 activation in PMNs in the HIO model during *Salmonella* infection.

4.6 Methods:

4.6.1 Contact for reagent and resource sharing

All RNA sequences are deposited in the EMBL-EBI Arrayexpress database (E-MTAB-11089). Source code for RNA-seq analyses can be found at aelawren/PMN-HIO-RNA-seq: R scripts for PMN-HIO RNA-seq analysis (github.com). Other reagents and resources can be obtained by directing requests to the Lead Contacts, Basel Abuaita (babuaita@umich.edu) and Mary O'Riordan (oriordan@umich.edu).

4.6.2 Human Intestinal Organoids (HIOs)

HIOs were generated by the *In Vivo* Animal and Human Studies Core at the University of Michigan Center for Gastrointestinal Research as previously described (*19*). Prior to experiments, HIOs were removed from the Matrigel, washed with DMEM:F12 media, and re-plated with 5 HIOs/well in 50 µL of Matrigel (Corning) in ENR media ((DMEM:F12, 1X B27 supplement, 2 mM L-glutamine, 100 ng/ml EGF, 100 ng/ml Noggin, 500 ng/ml Rspondin1, and 15 mM HEPES). Media was exchanged every 2-3 days for 7 days.

4.6.3 Human Polymorphonuclear Leukocytes (PMNs)

PMNs were isolated from blood of healthy human volunteers as previously described (*167*). The purity of PMNs was assessed by flow cytometry using APC anti-CD16 and FITC anti-CD15 antibodies (Miltenyi Biotec); markers characteristic of human neutrophils.

4.6.4 Bacterial Growth and HIO Microinjection

Salmonella enterica serovar Typhimurium SL1344 (STM) was used throughout the manuscript. Bacteria were stored at −80°C in Luria-Bertani (LB, Fisher) medium

containing 20% glycerol and cultured on LB agar plates. Individual colonies were grown overnight at 37ºC under static conditions in LB liquid broth. Bacteria were pelleted, washed and re-suspended in PBS. Bacterial inoculum was estimated based on OD_{600} and verified by plating serial dilutions on agar plates to determine colony forming units (CFU). Lumens of individual HIOs were microinjected with glass caliber needles with 1 µl of PBS or STM (10^5 CFU/HIO) as previously described (*22*, *35*, *129*). HIOs were then washed with PBS and incubated for 2h at 37°C in ENR media. HIOs were treated with 100 µg/ml gentamicin for 15 min to kill any bacteria outside the HIOs, then incubated in fresh medium +/- PMNs (5 X 10^5 PMNs/5HIOs/well in a 24-well plate).

4.6.5 Bacterial Burden and Cytokine Analyses

Bacterial burden was assessed per HIO. Individual HIOs were removed from Matrigel, washed with PBS and homogenized in PBS. Total CFU/HIO were enumerated by serial dilution and plating on LB agar. To assess bacterial translocation across the epithelial layer, infected HIOs were washed with PBS, treated with with 100 µg/ml gentamicin for 15 min and re-seeded without antibiotics individually into a 96 well plate alone or with PMNs (10^5 PMNs/HIOs/well). Bacterial burden in the culture media was enumerated at 8hpi by serial dilution and plating on LB agar. For cytokine analysis, media from each well containing 5 HIOs/well were collected at 8hpi. Cytokines, chemokines and antimicrobial proteins were quantified by ELISA at the University of Michigan Cancer Center Immunology Core.

4.6.6 Immunofluorescence Staining and Microscopy

HIOs were fixed with 10% neutral formalin for 2 days and embedded in paraffin. Histology sections (5 μm) were collected by the University of Michigan Cancer Center Histology Core. Sections were deparaffinized and antigen retrieval was performed in sodium citrate buffer (10 mM sodium citrate, 0.05% Tween 20, pH 6.0). Sections were permeabilized with PBS+ 0.2% Triton X-100 for 30 min, then incubated in blocking buffer (PBS, 5% BSA, and 10% normal goat serum) for 1h. Primary antibodies; anti-E-Cadherin (BD Biosciences, clone 36), anti-MPO (Agilent, clone A0398), anti-ICAM1 (Sigma-Aldrich, Cat# HPA002126), anti-Vimentin (DSHB, Cat# AMF-17b), anti-ASC (Cell Signaling, Cat#13833) and anti-cleaved Caspase-3 (Cells Signaling, Cat# 9661) were added to the histology sections in blocking buffer overnight at 4°C. Goat anti-mouse and anti-rabbit secondary antibodies conjugated to Alexa-488, Alexa-594 or Alexa-647 were used according to manufacturer's instructions (Thermo Fisher) for 1h RT in blocking buffer. DAPI (Thermo Fisher) was used to stain DNA. Bacteria were stained using anti-*Salmonella* Typhimurium FITC-conjugated antibody (Santa Cruz, Cat# sc-52223). Sections were mounted using coverslips (#1.5) and Prolong Diamond or Prolong Glass Antifade Mountant (Thermo Fisher). Images were taken on Olympus BX60 upright compound microscope, Nikon A1 confocal microscope or Nikon X1 Yokogawa spinning disc confocal microscope and processed using ImageJ and quantitation was performed in ImageJ or CellProfiler.

4.6.7 TUNEL Assay

Apoptosis was analyzed by fluorescence microscopy using *In Situ Cell Death Detection Kit* (Roche) or Biotium CF594 TUNEL Assay Apoptosis Detection Kit (Thermofisher) according to the manufacturers' protocols. Histology sections were permeabilized using Proteinase K (20 µg/ml) or 0.2% Triton X-100 in PBS and blocked using PBS+ 5%BSA. Sections were stained with primary antibodies overnight at 4°C in blocking buffer and then were incubated in the terminal deoxynucleotidyl transferase end labeling (TUNEL) buffer for 1h at 37°C. Slides were washed with PBS and incubated with fluorescent conjugated secondary antibodies. Sections were then counterstained with DAPI to label the DNA. For quantification of TUNEL positive cells, the percent of the HIO lumen filled with TUNEL+ cells was quantified using ImageJ software.

4.6.8 RNA Sequencing and Analysis

Total RNA was isolated from 5 HIOs per group with a total of 4 replicates per condition using the mirVana miRNA Isolation Kit (Thermo Fisher). The quality of RNA was confirmed, ensuring the RNA integrity number (RIN)> 8.5, using the Agilent TapeStation system. cDNA libraries were prepared by the University of Michigan DNA Sequencing Core using the TruSeq Stranded mRNA Kit (Illumina) according to the manufacturer's protocol. Libraries were sequenced on Illumina HiSeq 2500 platforms (single-end, 50 bp read length). All samples were sequenced at a depth of 10.5million reads per sample or greater. Sequencing generated FASTQ files of transcript reads that were pseudoaligned to the human genome (GRCh38.p12) using kallisto software (*117*). Transcripts were

converted to estimated gene counts using the tximport package (*119*) with gene annotation from Ensembl (*118*).

4.6.9 Gene Expression and Pathway Enrichment Analysis

Differential expression analysis was performed using the DESeq2 package (*121*) with *P* values calculated by the Wald test and adjusted *P* values calculated using the Benjamani & Hochberg method (*120*). Pathway analysis was performed using the Reactome pathway database and pathway enrichment analysis in R using the ReactomePA software package (*122*).

4.6.10 Quantification and Statistical Methods

RNA-seq data analysis was done using RStudio version 1.1.453. Plots were generated using ggplot2 (*116*) with data manipulation done using dplyr (*123*). Euler diagrams of gene changes were generated using the Eulerr package (*124*). Other data were analyzed using Graphpad Prism 9. Statistical differences were determined using statistical tests indicated in the figure legends. The mean of at least 2 independent experiments were presented with error bars showing standard deviation (SD). *P* values of less than 0.05 were considered significant and designated by: $*P < 0.05$, $**P < 0.01$, $***P < 0.001$ and **** $P < 0.0001$.

Acknowledgements

This work was supported by the NIH awards U19AI116482-01 (V.B.Y, J.R.S, C.E.W, and M.X.O) and R21AI13540 (M.X.O). A-L.E.L was supported by NIH T32 AI007528. We thank the Host Microbiome Initiative, Microscopy and Image Analysis Laboratory (MIL),

the Comprehensive Cancer Center Immunology (supported by the NCI and NIH award P30CA046592) and Histology Cores and the DNA Sequencing Core at University of Michigan Medical School. We gratefully acknowledge the O'Riordan lab members for helpful discussions, and Roberto Cieza for assistance with data management.

References

1. CDC, Foodborne Germs and Illnesses (2020), (available at https://www.cdc.gov/foodsafety/foodborne-germs.html).

2. Salmonella Homepage (2021), (available at https://www.cdc.gov/salmonella/).

3. A. C. Baird-Parker, Foodborne salmonellosis. *Lancet*. **336**, 1231–1235 (1990).

4. J. J. Gilchrist, C. A. MacLennan, Invasive Nontyphoidal Salmonella Disease in Africa. *EcoSal Plus*. **8** (2019), doi:10.1128/ecosalplus.ESP-0007-2018.

5. S. Hapfelmeier, W.-D. Hardt, A mouse model for S. typhimurium-induced enterocolitis. *Trends Microbiol.* **13**, 497–503 (2005).

6. A.-L. E. Lawrence, B. H. Abuaita, R. P. Berger, D. R. Hill, S. Huang, V. K. Yadagiri, B. Bons, C. Fields, C. E. Wobus, J. R. Spence, V. B. Young, M. X. O'Riordan, Salmonella enterica Serovar Typhimurium SPI-1 and SPI-2 Shape the Global Transcriptional Landscape in a Human Intestinal Organoid Model System. *MBio*. **12** (2021), doi:10.1128/mBio.00399-21.

7. J. L. Forbester, D. Goulding, L. Vallier, N. Hannan, C. Hale, D. Pickard, S. Mukhopadhyay, G. Dougan, Interaction of Salmonella enterica Serovar Typhimurium with Intestinal Organoids Derived from Human Induced Pluripotent Stem Cells. *Infect. Immun.* **83**, 2926–2934 (2015).

8. B. H. Abuaita, A.-L. E. Lawrence, R. P. Berger, D. R. Hill, S. Huang, V. K. Yadagiri, B. Bons, C. Fields, C. E. Wobus, J. R. Spence, V. B. Young, M. X. O'Riordan, Comparative transcriptional profiling of the early host response to infection by typhoidal and non-typhoidal Salmonella serovars in human intestinal organoids. *bioRxiv* (2020), p. 2020.11.25.397620, , doi:10.1101/2020.11.25.397620.

9. J. R. Spence, C. N. Mayhew, S. A. Rankin, M. F. Kuhar, J. E. Vallance, K. Tolle, E. E. Hoskins, V. V. Kalinichenko, S. I. Wells, A. M. Zorn, N. F. Shroyer, J. M. Wells, Directed differentiation of human pluripotent stem cells into intestinal tissue in vitro. *Nature*. **470**, 105–109 (2011).

10. D. R. Hill, S. Huang, M. S. Nagy, V. K. Yadagiri, C. Fields, D. Mukherjee, B. Bons, P. H. Dedhia, A. M. Chin, Y.-H. Tsai, S. Thodla, T. M. Schmidt, S. Walk, V. B. Young, J. R. Spence, Bacterial colonization stimulates a complex physiological response in the immature human intestinal epithelium. *Elife*. **6** (2017), doi:10.7554/eLife.29132.

11. S. S. Karve, S. Pradhan, D. V. Ward, A. A. Weiss, Intestinal organoids model human responses to infection by commensal and Shiga toxin producing Escherichia coli. *PLoS One*. **12**, e0178966 (2017).

12. S. Pradhan, A. A. Weiss, Probiotic Properties of Escherichia coli Nissle in Human Intestinal Organoids. *MBio*. **11** (2020), doi:10.1128/mBio.01470-20.

13. L. N. Schulte, M. Schweinlin, A. J. Westermann, H. Janga, S. C. Santos, S. Appenzeller, H. Walles, J. Vogel, M. Metzger, An Advanced Human Intestinal Coculture Model Reveals Compartmentalized Host and Pathogen Strategies during Salmonella Infection. *MBio*. **11** (2020), doi:10.1128/mBio.03348-19.

14. S. Hannemann, J. E. Galán, Salmonella enterica serovar-specific transcriptional reprogramming of infected cells. *PLoS Pathog.* **13**, e1006532 (2017).

15. S. Hannemann, B. Gao, J. E. Galán, Salmonella modulation of host cell gene expression promotes its intracellular growth. *PLoS Pathog.* **9**, e1003668 (2013).

16. A. Rydström, M. J. Wick, Monocyte recruitment, activation, and function in the gut-associated lymphoid tissue during oral Salmonella infection. *J. Immunol.* **178**, 5789–5801 (2007).

17. C. Tükel, M. Raffatellu, D. Chessa, R. P. Wilson, M. Akçelik, A. J. Bäumler, Neutrophil influx during non-typhoidal salmonellosis: who is in the driver's seat? *FEMS Immunol. Med. Microbiol.* **46**, 320–329 (2006).

18. B. Amulic, C. Cazalet, G. L. Hayes, K. D. Metzler, A. Zychlinsky, Neutrophil function: from mechanisms to disease. *Annu. Rev. Immunol.* **30**, 459–489 (2012).

19. V. Brinkmann, U. Reichard, C. Goosmann, B. Fauler, Y. Uhlemann, D. S. Weiss, Y. Weinrauch, A. Zychlinsky, Neutrophil extracellular traps kill bacteria. *Science*. **303**, 1532–1535 (2004).

20. E. L. Campbell, W. J. Bruyninckx, C. J. Kelly, L. E. Glover, E. N. McNamee, B. E. Bowers, A. J. Bayless, M. Scully, B. J. Saeedi, L. Golden-Mason, S. F. Ehrentraut, V. F. Curtis, A. Burgess, J. F. Garvey, A. Sorensen, R. Nemenoff, P. Jedlicka, C. T. Taylor, D. J. Kominsky, S. P. Colgan, Transmigrating neutrophils shape the mucosal microenvironment through localized oxygen depletion to influence resolution of inflammation. *Immunity*. **40**, 66–77 (2014).

21. B. M. Fournier, C. A. Parkos, The role of neutrophils during intestinal inflammation. *Mucosal Immunol.* **5**, 354–366 (2012).

22. A. C. Chin, C. A. Parkos, Pathobiology of neutrophil transepithelial migration: implications in mediating epithelial injury. *Annu. Rev. Pathol.* **2**, 111–143 (2007).

23. K. L. Mumy, B. A. McCormick, The role of neutrophils in the event of intestinal inflammation. *Curr. Opin. Pharmacol.* **9**, 697–701 (2009).

24. A. J. Simpson, A. I. Maxwell, J. R. Govan, C. Haslett, J. M. Sallenave, Elafin (elastase-specific inhibitor) has anti-microbial activity against gram-positive and gram-negative respiratory pathogens. *FEBS Lett.* **452**, 309–313 (1999).

25. V. E. Diaz-Ochoa, D. Lam, C. S. Lee, S. Klaus, J. Behnsen, J. Z. Liu, N. Chim, S.-P. Nuccio, S. G. Rathi, J. R. Mastroianni, R. A. Edwards, C. M. Jacobo, M. Cerasi, A. Battistoni, A. J. Ouellette, C. W. Goulding, W. J. Chazin, E. P. Skaar, M. Raffatellu,

Salmonella Mitigates Oxidative Stress and Thrives in the Inflamed Gut by Evading Calprotectin-Mediated Manganese Sequestration. *Cell Host Microbe*. **19**, 814–825 (2016).

26. J. Z. Liu, S. Jellbauer, A. J. Poe, V. Ton, M. Pesciaroli, T. E. Kehl-Fie, N. A. Restrepo, M. P. Hosking, R. A. Edwards, A. Battistoni, P. Pasquali, T. E. Lane, W. J. Chazin, T. Vogl, J. Roth, E. P. Skaar, M. Raffatellu, Zinc Sequestration by the Neutrophil Protein Calprotectin Enhances Salmonella Growth in the Inflamed Gut. *Cell Host Microbe*. **11**, 227–239 (2012).

27. C. Cheminay, D. Chakravortty, M. Hensel, Role of neutrophils in murine salmonellosis. *Infect. Immun.* **72**, 468–477 (2004).

28. R. Sumagin, C. A. Parkos, Epithelial adhesion molecules and the regulation of intestinal homeostasis during neutrophil transepithelial migration. *Tissue Barriers*. **3**, e969100 (2015).

29. C. Andrews, M. H. McLean, S. K. Durum, Cytokine Tuning of Intestinal Epithelial Function. *Front. Immunol.* **9**, 1270 (2018).

30. D. Wang, R. N. Dubois, A. Richmond, The role of chemokines in intestinal inflammation and cancer. *Curr. Opin. Pharmacol.* **9**, 688–696 (2009).

31. X. C. Li, A. M. Jevnikar, D. R. Grant, Expression of functional ICAM-1 and VCAM-1 adhesion molecules by an immortalized epithelial cell clone derived from the small intestine. *Cell. Immunol.* **175**, 58–66 (1997).

32. G. T. Huang, L. Eckmann, T. C. Savidge, M. F. Kagnoff, Infection of human intestinal epithelial cells with invasive bacteria upregulates apical intercellular adhesion molecule-1 (ICAM)-1) expression and neutrophil adhesion. *J. Clin. Invest.* **98**, 572–583 (1996).

33. S. A. Hirota, J. Ng, A. Lueng, M. Khajah, K. Parhar, Y. Li, V. Lam, M. S. Potentier, K. Ng, M. Bawa, D.-M. McCafferty, K. P. Rioux, S. Ghosh, R. J. Xavier, S. P. Colgan, J. Tschopp, D. Muruve, J. A. MacDonald, P. L. Beck, NLRP3 inflammasome plays a key role in the regulation of intestinal homeostasis. *Inflamm. Bowel Dis.* **17**, 1359–1372 (2011).

34. Z. Hodzic, E. M. Schill, A. M. Bolock, M. Good, IL-33 and the intestine: The good, the bad, and the inflammatory. *Cytokine*. **100**, 1–10 (2017).

35. E. Lefrançais, S. Roga, V. Gautier, A. Gonzalez-de-Peredo, B. Monsarrat, J.-P. Girard, C. Cayrol, IL-33 is processed into mature bioactive forms by neutrophil elastase and cathepsin G. *Proc. Natl. Acad. Sci. U. S. A.* **109**, 1673–1678 (2012).

36. F. Martinon, K. Burns, J. Tschopp, The inflammasome: a molecular platform triggering activation of inflammatory caspases and processing of proIL-beta. *Mol. Cell*. **10**, 417–426 (2002).

37. J. R. Kurtz, J. A. Goggins, J. B. McLachlan, Salmonella infection: Interplay between the bacteria and host immune system. *Immunol. Lett.* **190**, 42–50 (2017).

38. C. A. Lee, M. Silva, A. M. Siber, A. J. Kelly, E. Galyov, B. A. McCormick, A secreted Salmonella protein induces a proinflammatory response in epithelial cells, which promotes neutrophil migration. *Proc. Natl. Acad. Sci. U. S. A.* **97**, 12283–12288 (2000).

39. Q. L. Ying, S. R. Simon, Kinetics of the inhibition of human leukocyte elastase by elafin, a 6-kilodalton elastase-specific inhibitor from human skin. *Biochemistry*. **32**, 1866–1874 (1993).

40. C. A. Parkos, Neutrophil-Epithelial Interactions: A Double-Edged Sword. *Am. J. Pathol.* **186**, 1404–1416 (2016).

41. J.-P. Motta, L. G. Bermúdez-Humarán, C. Deraison, L. Martin, C. Rolland, P. Rousset, J. Boue, G. Dietrich, K. Chapman, P. Kharrat, J.-P. Vinel, L. Alric, E. Mas, J.-M. Sallenave, P. Langella, N. Vergnolle, Food-grade bacteria expressing elafin protect against inflammation and restore colon homeostasis. *Sci. Transl. Med.* **4**, 158ra144 (2012).

42. J.-P. Motta, L. Magne, D. Descamps, C. Rolland, C. Squarzoni-Dale, P. Rousset, L. Martin, N. Cenac, V. Balloy, M. Huerre, L. F. Fröhlich, D. Jenne, J. Wartelle, A. Belaaouaj, E. Mas, J.-P. Vinel, L. Alric, M. Chignard, N. Vergnolle, J.-M. Sallenave, Modifying the protease, antiprotease pattern by elafin overexpression protects mice from colitis. *Gastroenterology*. **140**, 1272–1282 (2011).

43. C. T. N. Pham, Neutrophil serine proteases: specific regulators of inflammation. *Nat. Rev. Immunol.* **6**, 541–550 (2006).

44. E. P. Reeves, H. Lu, H. L. Jacobs, C. G. M. Messina, S. Bolsover, G. Gabella, E. O. Potma, A. Warley, J. Roes, A. W. Segal, Killing activity of neutrophils is mediated through activation of proteases by K+ flux. *Nature*. **416**, 291–297 (2002).

45. I. Rauch, K. A. Deets, D. X. Ji, J. von Moltke, J. L. Tenthorey, A. Y. Lee, N. H. Philip, J. S. Ayres, I. E. Brodsky, K. Gronert, R. E. Vance, NAIP-NLRC4 Inflammasomes Coordinate Intestinal Epithelial Cell Expulsion with Eicosanoid and IL-18 Release via Activation of Caspase-1 and -8. *Immunity*. **46**, 649–659 (2017).

46. S. M. Crowley, X. Han, J. M. Allaire, M. Stahl, I. Rauch, L. A. Knodler, B. A. Vallance, Intestinal restriction of Salmonella Typhimurium requires caspase-1 and caspase-11 epithelial intrinsic inflammasomes. *PLoS Pathog.* **16**, e1008498 (2020).

47. A. Hausmann, D. Böck, P. Geiser, D. L. Berthold, S. A. Fattinger, M. Furter, J. A. Bouman, M. Barthel-Scherrer, C. M. Lang, E. Bakkeren, I. Kolinko, M. Diard, D. Bumann, E. Slack, R. R. Regoes, M. Pilhofer, M. E. Sellin, W.-D. Hardt, Intestinal epithelial NAIP/NLRC4 restricts systemic dissemination of the adapted pathogen

Salmonella Typhimurium due to site-specific bacterial PAMP expression. *Mucosal Immunol.* **13**, 530–544 (2020).

48. L. A. Knodler, S. M. Crowley, H. P. Sham, H. Yang, M. Wrande, C. Ma, R. K. Ernst, O. Steele-Mortimer, J. Celli, B. A. Vallance, Noncanonical inflammasome activation of caspase-4/caspase-11 mediates epithelial defenses against enteric bacterial pathogens. *Cell Host Microbe*. **16**, 249–256 (2014).

49. M. K. Holly, X. Han, E. J. Zhao, S. M. Crowley, J. M. Allaire, L. A. Knodler, B. A. Vallance, J. G. Smith, Salmonella enterica Infection of Murine and Human Enteroid-Derived Monolayers Elicits Differential Activation of Epithelium-Intrinsic Inflammasomes. *Infect. Immun.* **88** (2020), doi:10.1128/IAI.00017-20.

50. M. E. Sellin, A. A. Müller, B. Felmy, T. Dolowschiak, M. Diard, A. Tardivel, K. M. Maslowski, W.-D. Hardt, Epithelium-intrinsic NAIP/NLRC4 inflammasome drives infected enterocyte expulsion to restrict Salmonella replication in the intestinal mucosa. *Cell Host Microbe*. **16**, 237–248 (2014).

51. S. H. Jia, J. Parodo, E. Charbonney, J. L. Y. Tsang, S. Y. Jia, O. D. Rotstein, A. Kapus, J. C. Marshall, Activated neutrophils induce epithelial cell apoptosis through oxidant-dependent tyrosine dephosphorylation of caspase-8. *Am. J. Pathol.* **184**, 1030–1040 (2014).

52. S. A. Gudipaty, J. Rosenblatt, Epithelial cell extrusion: Pathways and pathologies. *Semin. Cell Dev. Biol.* **67**, 132–140 (2017).

53. M. Saffarzadeh, C. Juenemann, M. A. Queisser, G. Lochnit, G. Barreto, S. P. Galuska, J. Lohmeyer, K. T. Preissner, Neutrophil extracellular traps directly induce epithelial and endothelial cell death: a predominant role of histones. *PLoS One*. **7**, e32366 (2012).

54. K. W. Chen, M. Monteleone, D. Boucher, G. Sollberger, D. Ramnath, N. D. Condon, J. B. von Pein, P. Broz, M. J. Sweet, K. Schroder, Noncanonical inflammasome signaling elicits gasdermin D-dependent neutrophil extracellular traps. *Sci. Immunol.* **3**, eaar6676 (2018).

55. B. H. Abuaita, G. J. Sule, T. L. Schultz, F. Gao, J. S. Knight, M. X. O'Riordan, The IRE1α Stress Signaling Axis Is a Key Regulator of Neutrophil Antimicrobial Effector Function. *J. Immunol.* (2021), doi:10.4049/jimmunol.2001321.

56. D. R. Hill, S. Huang, Y.-H. Tsai, J. R. Spence, V. B. Young, Real-time Measurement of Epithelial Barrier Permeability in Human Intestinal Organoids. *J. Vis. Exp.* (2017), doi:10.3791/56960.

57. N. L. Bray, H. Pimentel, P. Melsted, L. Pachter, Near-optimal probabilistic RNA-seq quantification. *Nat. Biotechnol.* **34**, 525–527 (2016).

58. C. Soneson, M. I. Love, M. D. Robinson, Differential analyses for RNA-seq: transcript-level estimates improve gene-level inferences. *F1000Res.* **4**, 1521 (2015).

59. J. Rainer, EnsDb.Hsapiens.v75: Ensembl based annotation package. R package version 2.99.0 (2017).

60. M. I. Love, W. Huber, S. Anders, Moderated estimation of fold change and dispersion for RNA-seq data with DESeq2. *Genome Biol.* **15**, 550 (2014).

61. Y. Benjamini, Y. Hochberg, Controlling the False Discovery Rate: A Practical and Powerful Approach to Multiple Testing. *Journal of the Royal Statistical Society: Series B (Methodological)*. **57** (1995), pp. 289–300.

62. G. Yu, Q.-Y. He, ReactomePA: an R/Bioconductor package for reactome pathway analysis and visualization. *Mol. Biosyst.* **12**, 477–479 (2016).

63. H. Wickham, *ggplot2: Elegant Graphics for Data Analysis* (Springer, 2016).

64. H. Wickham, R. Francois, L. Henry, K. Müller, Others, dplyr: A grammar of data manipulation. *R package version 0. 4*. **3** (2015).

65. J. Larsson, eulerr: Area-Proportional Euler and Venn Diagrams with Ellipses (2019), (available at https://cran.r-project.org/package=eulerr).

Chapter 5

Discussion

5.1 Summary and major conclusions

In this dissertation, I have presented studies on the use of human intestinal organoids (HIOs) to probe interactions between *Salmonella enterica* and the human intestinal epithelium. Each chapter focused on a different aspect of infection. We first used a transcriptomics approach to determine the contribution of type three secretion systems (T3SS) to infection by *S. enterica* serovar Typhimurium (STM). We found that T3SS-1 contributed to invasion into epithelial cells in the HIO, but bacteria without a functional T3SS-1 still induced a robust inflammatory response by signaling through the luminal compartment. We found that both T3SS-1 and T3SS-2 were important for cell cycle suppression and proposed this was mediated by *Salmonella* induced changes in miRNA expression. By using these T3SS mutants we are now better able to understand the contribution of luminal bacteria in signaling to the intestinal epithelium.

Next, we exploited the HIO model to investigate host responses to three serovars of *S. enterica.* We chose the 3 dominant serovars relevant to human health: STM, *S. enterica* serovar Enteritidis (SE), and Typhi (ST). Using RNA-sequencing to monitor both host and bacteria transcriptomes as well as quantitative microscopy approaches, we found that all

three serovars induced distinct HIO responses. We measured differences in host cell stress including changes in cellular proliferation, cell death, mucus production, and reactive oxygen species (ROS) production. We detected differing rates of bacterial invasion and replication within HIO epithelial cells and observed unique expression patterns of T3SS-1 and -2 effectors in each of the three serovars. Together these results revealed unappreciated differences in infection patterns between three closely related serovars.

	Non-typhoidal serovars		Typhoidal serovar
	STM	SE	ST
Replication in HIOs	Yes	Yes	Yes
Invasion	High	Low	Intermediate
SPI-1 expression	High	Intermediate	Low
Intracellular replication	Intermediate	High	High
SPI-2 expression	Intermediate	High	Intermediate
Epithelial cell death	Yes	No	Mixed
HIO ROS production	No	Yes	No
HIO Cell Cycle regulation	Decreases	No effect	No effect

Figure 5.1 Comparison of *S. enterica* serovars in HIOs

Finally, in the last data chapter, we co-cultured HIOs with polymorphonuclear lymphocytes (PMNs), to investigate the role of innate immune cells in affecting the host epithelial response to STM infection. We detected no changes in total bacteria in the presence of PMNs but did measure a significant decrease in the intracellular bacterial burden. We found that PMNs enhanced production of pro-inflammatory mediators and antimicrobials in PMN-HIOs, and increased rates of epithelial cell death in infected HIOs. These findings suggested that PMNs contribute to gut immunity during *S. enterica* infection by shedding infected cells from the epithelial lining.

5.2 Primary questions arising from this dissertation

How do NTS interact so differently with the epithelium yet cause similar diseases?

The most unexpected finding in this dissertation was that the two nontyphoidal serovars (NTS), STM and SE, which cannot be distinguished in the clinic without serotyping, interact differently with the host. Both serovars cause gastroenteritis in healthy individuals and therefore we predicted that they would behave similarly in the HIO. Instead, in almost every experimental readout, the results for STM and SE were distinct. STM invaded and replicated better in the epithelium, induced more cytokine production, suppressed cell division, induced cell death, and was susceptible to PMN killing. On the other hand, SE invaded very poorly in comparison, stimulated reduced levels of cytokines, did not significantly enhance cell death, did induce ROS, and evaded killing by PMNs. It is possible that there is natural variation in the host response to individual strains so testing additional NTS strains including other STM and SE isolates would show the range of host responses that are induced by NTS. However, another possibility is that since the majority of infected individuals recover at home without seeking medical treatment, we do not truly know the range of host responses or clinical symptoms that occur between infections. While these differences can be explained in part by host genetics, a more detailed characterization of symptoms and gut pathology would provide insight into what is expected from infection with each serovar. Throughout the previous chapters, host genetics were kept constant. Therefore, any differences in behavior between the two serovars would be caused by the infecting pathogen. Since the majority of published *Salmonella* work has been performed on STM, we lack a clear understanding of how

infections vary between serovars, and thus we need to study these other serovars to understand if they cause similar diseases using different mechanisms.

What causes ST to act more “silently” during initial stages of infection?

Infections with typhoidal and nontyphoidal serovars present differently in the human host. One question that has been the focus of *Salmonella* researchers over the years is how typhoidal serovars remain relatively silent in the gut prior to spreading systemically. It has been proposed that Vi capsule expression by ST helps mask ST from detection by the host. Although we detect capsule expression by ST in our experiments, only 30-40% of bacteria express capsule prior to microinjection into the HIO. Due to challenges in the experimental set-up, we do not have quantitative results for the number of bacteria expressing Vi capsule once inside the HIO, however our finding that less than half of the bacteria express capsule prior to infection suggests that capsule may not fully explain the difference between NTS and typhoidal serovars. Consistent with known disease progression, we measured reduced cytokine output by ST compared to the NTS, however, we also found that ST induced upregulation of fewer HIO genes compared to the NTS. In fact, some genes were suppressed during infection, including genes belonging to inflammatory signaling pathways such as the non-canonical NF-κB signaling pathway. Additionally, we found that there was disrupted secretion of mucus from ST-infected HIOs suggesting that ST may also target secretory pathways during infection. Overall, our findings raise the question of how ST suppresses immune responses during initial stages of infection. Our data provide hints that ST may be blocking host recognition

through several mechanisms and future work may provide better insight into how ST evades host recognition in the gut.

5.3 Future directions

There are numerous directions that can be pursued based on the data presented in this dissertation. Based on the questions we addressed in the previous section, a priority should be to infect HIOs with different strains of NTS to understand the range of host responses. Multiple experimental readouts can be done with one HIO infection including characterizing invasion and intracellular replication and monitoring host stress responses via quantitative microscopy techniques. In chapter 3, we measured different patterns of expression of SPI-1 and SPI-2 effectors by STM and SE and therefore studying the regulation of these genes under various growth conditions may provide better insight into differences in infectivity between these two NTS.

In the appendix, I outlined data revealing dramatic differences in STM and SE interactions with human PMNs in culture. Since PMNs are one of the most dominant responders to NTS, additional infection experiments with PMNs in the absence of HIOs will enhance our understanding of the range of disease that occurs with various NTS. Performing random transposon mutagenesis and killing assays with PMNs will aid in identification of SE genes that contribute to survival in the presence of PMNs. Future work on how *Salmonella* serovars regulate formation of neutrophil extracellular traps (NETs) during infection will also be valuable to determine how SE prevents killing by PMNs. As presented in the appendix, we generated transposon mutants that appear to have altered interactions with

macrophages. These mutants can be screened during PMN infection to determine if these genes are also critical for regulating SE interactions with PMNs.

Another question that arose from this dissertation was how ST infection results in reduced inflammatory responses in the HIOs. Future work can focus on studying the interaction of ST with the host secretory machinery by staining for cytokines and performing flow cytometry to determine if secretion is blocked. If ST blocks secretion during infection, mutants of known virulence factors can be tested for their contribution to this phenotype, alternatively, transposon mutagenesis screening approaches could be performed. We also gained some insight into ST-specific host responses in the HIOs from our RNA-seq study. We identified genes that responded differently to ST compared to the NTS including FABP6 and GPR20. These, as well as other ST-specific genes can be studied to determine their contribution to infection outcome.

To determine the contribution of Vi capsule in driving early responses to ST in the gut, two alternative approaches could be considered. HIOs can be microinjected with ST mutants constitutively expressing Vi Capsule or mutants lacking capsule. Culture supernatants would be probed for pro-inflammatory cytokine levels to determine if capsule significantly inhibits recognition and immune responses in the HIO. Alternatively, using existing chimeric strains of STM expressing Vi capsule could be microinjected and HIOs assayed for cytokine production to determine if capsule is able to silence recognition of STM. While it is likely that ST suppresses inflammation through multiple routes, these experiments will illuminate the contribution of capsule in infection outcome.

Looking more broadly, I have also tested the feasibility of using human intestinal enteroids (HIEs) in *Salmonella* infection studies (data not shown). Although the HIE model is still quite complex, it avoids some of the complications that arise from using HIOs. Intestinal segment-specific host-pathogen responses can be examined in the HIEs, and single-cell based approaches can be utilized. Several groups are using single-cell RNA-seq to study how individual cells respond to infection, and this approach can easily be applied to the HIE model.

Lastly, a more thorough analysis comparing various *Salmonella* infection models should be performed. I started this analysis in chapter 3 by comparing the top differentially expressed genes across model systems, however a more detailed analysis would be valuable. The HIO model system is difficult to work with and so it would be beneficial to the field to understand which model systems faithfully reflect which aspects of infection. Should HIOs be the predominant model system moving forward, or do transformed cell lines or the murine intestinal epithelium provide similar results? Or is there a reason for performing studies with different model systems in parallel? Although more challenging, performing a direct comparison between biopsies of patients infected with *Salmonella* to the infections with commonly used model systems would provide invaluable knowledge into the accuracy of modelling *Salmonella* infection in the lab.

Appendix 1:

Salmonella enterica Serovar Enteritidis in PMN-HIOs

A1.1 Introduction

Neutrophils are the dominant immune cell type that respond to nontyphoidal *Salmonella enterica* serovars in the gut (*75*, *131*). In chapter 4 I outlined data using a co-culture model of neutrophils, or polymorphonuclear leukocytes (PMNs), with human intestinal organoids (HIOs) to uncover the role of PMNs in the intestinal response to *S. enterica* infection. As described in that chapter, we found that PMNs enhanced epithelial intrinsic defenses instead of killing *Salmonella* directly. This was observed through enhanced proinflammatory signaling, increased production of antimicrobial effectors, and through enhanced levels of programmed cell death. Enhancement of programmed cell death pathways led to an accumulation of shed epithelial cells in the lumen of PMN-HIOs as well as a reduction in intracellular bacteria contained in the epithelial lining of the HIO. Induction of cell death required both presence of PMNs and STM as neither condition alone resulted in accumulation of apoptotic epithelial cells.

We found that Caspase-1-mediated signaling in PMNs contributed to this cell death phenotype suggesting that programmed cell death in PMNs signals to epithelial cells to undergo cell death and cell shedding. Consistent with these findings, formation of neutrophil extracellular traps (NETs) by PMNs has been shown to require Caspase

activation (*3*). It has also been reported that NET formation in the gut can lead to epithelial cell death (*4*). Using the PMN-HIO model we found that NETs are formed in the lumen during infection and so specific interactions between the bacteria and PMNs leading to NET formation may be the mechanism by which PMNs reduce intracellular bacterial burden and epithelial cell shedding during *Salmonella* infection.

The work presented in Chapter 4 investigated the role of PMNs during infection of *Salmonella enterica* serovar Typhimurium (STM), however we now know, based on the work presented in Chapter 3, that different nontyphoidal serovars behave quite differently (*5*). Since these serovars interact with the epithelium in varying ways, it is likely that PMNs would also differentially influence infection outcome to these serovars. In this appendix, I present findings using the PMN-HIO co-culture model to uncover the role of PMNs during infection with another nontyphoidal serovar, *S. enterica* serovar Enteritidis (SE).

A1.2 Results

To better understand how PMN-HIOs respond to different nontyphoidal serovars, we performed RNA-sequencing at 8h post infection (hpi) on PMN-HIOs infected with either STM, SE or mock infected with PBS. As presented in Chapter 4 of this dissertation, PMNs enhanced epithelial responses to STM by increasing both the number of genes that responded to infection as well as the magnitude of fold change of these genes. To better understand how PMN-HIOs responded to different serovars, a Venn diagram was generated to identify the number of genes that were significantly changed during infection **(Fig A1.1A)**. Consistent with our observations in infected HIOs from Chapter 3, some

genes were induced in response to both serovars, however the vast majority of genes were induced uniquely by only one serovar. Over 2000 genes were uniquely changed in STM-infected PMN-HIOs while over 1000 genes were changed only in SE-infected PMN-HIOs. These results strongly suggest that PMNs respond uniquely to different nontyphoidal serovars of *S. enterica* even if humans present with similar diseases during infection. Next to determine how this affected sample clustering we performed Pearson correlation clustering on PBS, STM, and SE-injected HIOs and PMN-HIOs **(Fig A1.1B)**. As expected, the uninfected samples clustered away from the remaining infected samples, however what was rather unexpected was that the remaining infected samples clustered based on the infecting serovar and not whether PMNs were present. This clustering pattern suggests that there is more variation in host responses caused by the infecting serovar than from adding PMNs to HIOs. To better understand how these differences in clustering patterns carried through to changes in biological processes, we performed pathway enrichment analysis using the Reactome database **(Fig A1.1C, D)**. The dominant process that was induced during infection in HIOs and PMN-HIOs related to the immune system in Reactome **(Fig A1.1C)**. This involved processes such as toll-like receptor signaling, signaling by interleukins and NF-kb signaling. These processes were all more enriched in PMN-HIOs compared to HIOs suggesting that PMNs help amplify the immune response to *Salmonella* infection; consistent with our findings outlined in Chapter 4. However, these pathways were not as highly enriched in SE-infected PMN-HIOs compared to STM-infected PMN-HIOs as there was a lower gene ratio for all these pathways in SE-infected PMN-HIOs. This could possibly be explained by the lower levels of invasion by SE compared to STM as shown in Chapter 3 **(Fig 3.1)**, although it is more

likely that STM and SE are recognized differently by pattern recognition receptors in the HIOs since an invasion-defective mutant of STM was still able to induce a robust inflammatory response as presented in Chapter 2 **(Fig 2.3)** (*35*). After observing differences in pro-inflammatory signaling in SE-infected PMN-HIOs compared to STM-infected PMN-HIOs, we wanted to identify which other pathways were differentially regulated by the two serovars. To do this, the top pathways that were identified in Chapter 4 were re-analyzed for enrichment during SE-infection **(Fig A1.1D)**. While some pathways were similarly regulated during infection with the two serovars in PMN-HIOs such as extracellular matrix associated pathways, other pathways such as HIF1A stabilization was more highly enriched in SE-infected PMN-HIOs. In Reactome, the HIF1A stabilization pathway is a small pathway and only 4 genes were significantly changed during infection in SE-infected PMN-HIOs while 3 were changed in STM-infected PMN-HIOs (data not shown). Between the two infection conditions the EGFR gene was the only gene that was uniquely upregulated during SE-infection. While there is some data implicating a role in EGFR signaling in innate immune signaling (*7*), we chose to focus on pathways that we previously showed were important during STM infection in the PMN-HIOs since the purpose of this study was to directly compare how PMNs differentially regulate infection outcome between the two serovars. Along these lines, we observed an increase in programmed cell death pathways in STM-infected PMN-HIOs. After analyzing the SE-infection dataset, we detected a lower degree of enrichment of the programmed cell death pathway in PMN-HIOs compared to the STM-infection and a slight reduction in enrichment in the apoptotic signaling pathway **(Fig A1.1D)**. These results suggest that SE may be modulating cell death pathways differently than STM in the PMN-HIOs.

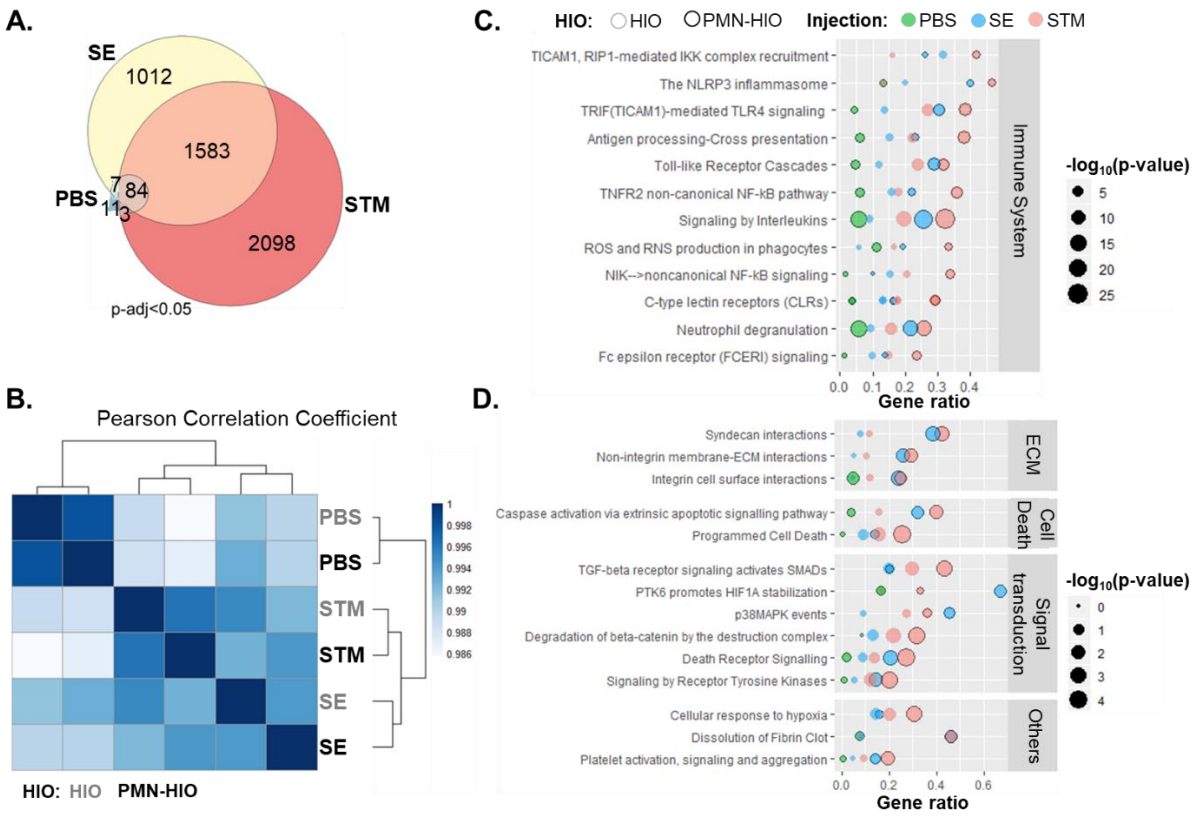

Figure A1.1 SE induces different responses in PMN-HIOs compared to STM (A) Venn diagram comparing differentially regulated genes with p-adjusted value <0.05 from PBS, STM or SE-injected PMN-HIOs. Significance was calculated relative to PBS-injected HIOs. (B) Pearson correlation clustering of all RNA-seq experimental conditions. (C) Reactome pathway enrichment results of select immune pathways that were significantly upregulated in PMN-HIOs. Gene ratio is shown on the x-axis and the dot size corresponds to the -log10(p-value). HIO samples are outlined in gray while PMN-HIOs are outlined in black. PBS-injection (green), STM-injection (red), and SE-injection (blue). (D) Reactome pathway enrichment results of pathways belonging to extracellular matrix organization (ECM), cell death, signal transduction, or miscellaneous categories were plotted as in (D).

To follow-up on our pathway analysis data showing a reduced enrichment of cell death pathways in SE-infected PMN-HIOs compared to STM, we analyzed the RNA-seq dataset for the Inflammasome signaling pathway, since this was determined to be critical in driving cell death in STM-infected PMN-HIOs. To do this, the same gene set that was used in Chapter 4 **(Fig 4.7A)** was used to filter against the SE-infected HIOs and PMN-HIOs **(Fig A1.2A)**. Inflammasome signaling members were upregulated in SE-infected PMN-HIOs. Some genes were more highly upregulated during SE infection such as IL-1B and IL-1A, however effectors needed to process IL-1β into its active form such as Caspase-1 and

NLRP3 were not as highly upregulated in SE-infected PMN-HIOs. To determine what effect these transcriptional changes had on inflammasome activation, we measured secretion of these effectors by ELISA **(Fig A1.2B)**. Consistent with our observation that Capsase-1 and NLRP3 were not as highly upregulated during SE-infection, we measured significantly less secretion of IL-1 family members in the supernatants of SE-infected PMN-HIOs. These results suggest that inflammasome activation, which was detected in PMNs in the PMN-HIO model **(Fig 4.7C, D)** was not as highly induced during SE infection.

Since we observed that Caspase-1 activity was required for accumulation of epithelial cells in the lumen of PMN-HIOs during STM infection, we decided to test whether SE also induced this elevated cell death phenotype in PMN-HIOs. To do this, we performed Terminal deoxynucleotidyl transferase dUTP nick end labeling (TUNEL) on HIOs and PMN-HIOs microinjected with either PBS, STM or SE **(Fig A1.2C, D)**. Consistent with the reduced enrichment of programmed cell death pathways in SE-infected PMN-HIOs, and reduced levels of inflammasome signaling mediators, there was no significant increase in TUNEL-positive cells in SE-infected PMN-HIOs. This further points towards the differences in interaction between the host and individual nontyphoidal serovars.

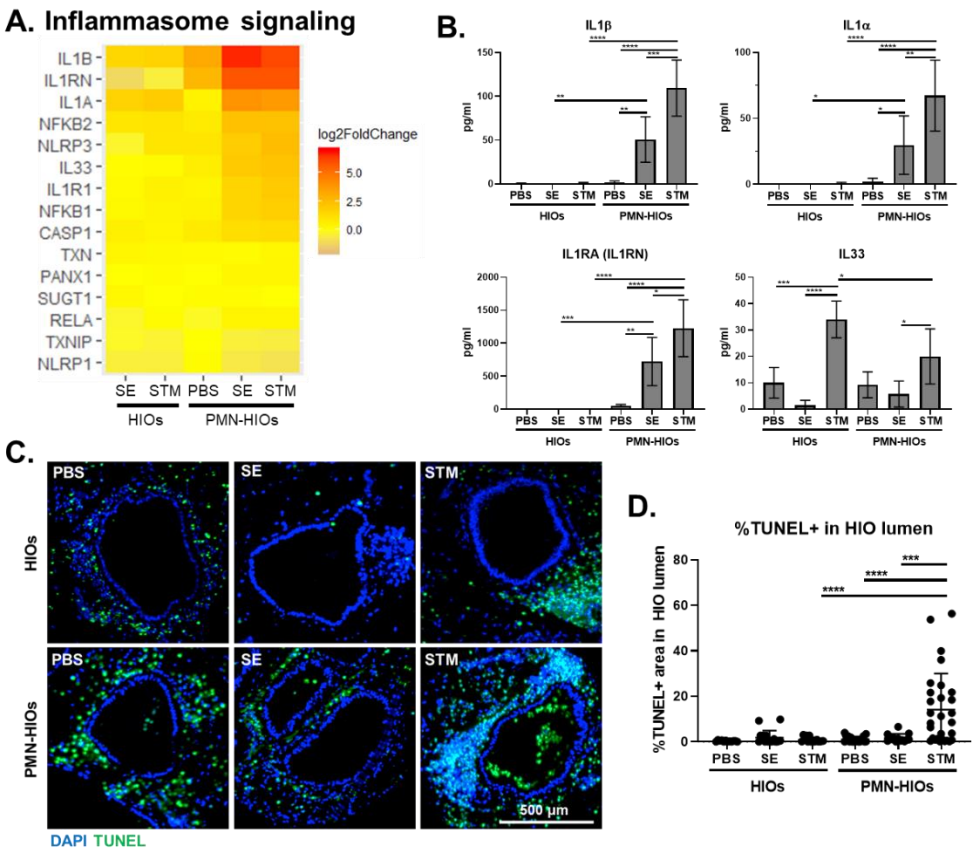

Figure A1.2 SE differentially regulates Inflammasome signaling and cell death in PMN-HIOs (A) Gene expression data presented as log2(fold change) relative to PBS-injected HIOs for members of the Inflammasome signaling pathway. All genes were significantly different from PBS-injected HIOs in at least one condition with p-adjusted value <0.05. (B) Cytokine levels in culture media of HIOs and PMN-HIOs were quantified using ELISA. Graphs indicate the mean of n=4 biological replicates +/- SD from media sampled at 8hpi with 5 HIOs or PMN-HIOs per well. (C) Immunofluorescent images of TUNEL staining of histology sections of HIOs and PMN-HIOs injected with PBS, STM, or SE at 8hpi. (D) Quantitation of TUNEL positive cells in the lumen of HIOs and PMN-HIOs from (C). Graphs represent HIOs from 2 independent experiments with >12 HIOs per group.

Since Inflammasome signaling was different in STM and SE-infected PMN-HIOs and since we observed that Caspase-1 dependent signaling in PMNs was required for the accumulation of apoptotic cells in the lumen of STM-infected HIOs, we wanted to test whether there was any difference in PMN morphology in PMN-HIOs infected with the two serovars. We previously detected NETs forming in the lumen during STM infection and proposed that this may be a contributing factor to the enhanced cell death phenotype. To

test whether NETs were also formed in SE-infected PMN-HIOs, PMN-HIOs were stained for Myeloperoxidase (MPO), a PMN specific marker, as well as E-cadherin, a marker for epithelial cells and imaged them using spinning disk confocal microscopy **(Fig. A1.3)**. Although we did observe recruitment of PMNs into the lumen during SE infection, as indicated by the MPO-positive staining, the morphology of the staining was quite distinct from the STM-infected PMN-HIOs. During STM infection, we observed a networked pattern of MPO staining suggesting the formation of NETs, while during SE infection the staining pattern was much more punctate, where individual PMNs could be resolved. We also note that the E-cadherin staining pattern varied between conditions. While we do observe E-cadherin staining intensity increasing in damaged cells, the epithelial thickness naturally varies between HIOs and does not correlate with infection. These findings further suggest that the nontyphoidal serovars have unique interactions with PMNs leading to different responses in the HIOs.

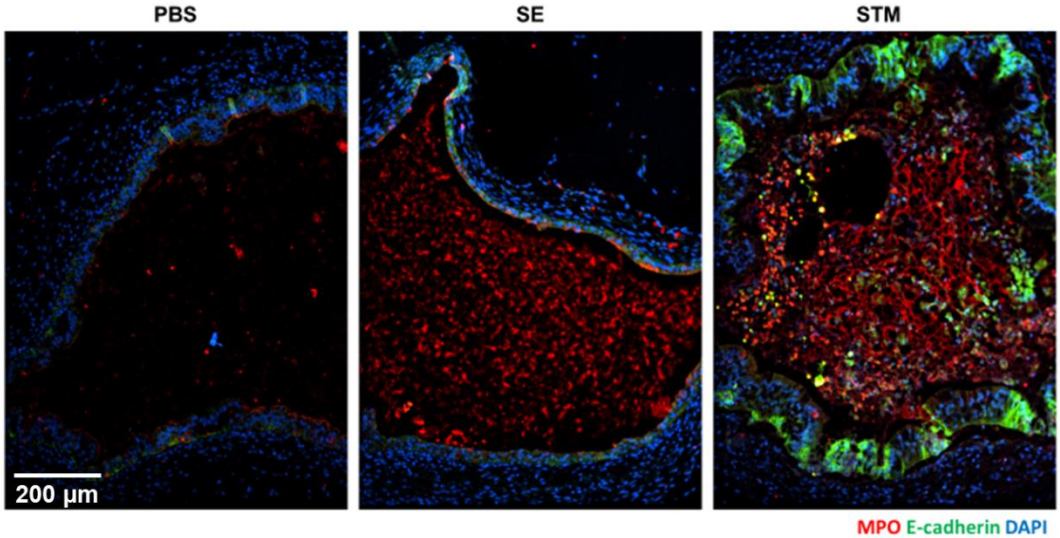

Figure A1.3 Both STM and SE recruit PMNs during infection, but STM and not SE induce NET formation in PMN-HIOs Immunofluorescent staining of PMN-HIOs microinjected with PBS or STM and stained for epithelial cells marked with E-cadherin (green), PMNs marked by MPO (red) and DNA with DAPI (blue).

Next to test whether these differences in MPO morphology in the PMN-HIOs were caused by differences in STM and SE interaction with PMNs, we purified PMNs and infected them with either STM or SE in the absence of HIOs and assayed for their ability to kill SE or STM and their ability to form NETs; a sign of PMN activation and one of the key antimicrobial effectors of PMNs. In mock infected PMNs, the cells remained round with multi-lobed nuclei as seen by the DAPI stain **(Fig A1.4A)**. In infected PMNs, the nuclei condense, and neutrophil elastase intensity increased within the cells. Although SE-infected PMNs still had morphological changes associated with activation, they did not form NETs, or projections of DNA and neutrophil elastase, as seen during STM infection. NETs are an important antimicrobial tool used by PMNs to catch and kill bacteria (*8*), as seen by STM clustered on neutrophil elastase projections. Since NETs are not formed during SE infection, we wanted to test whether this led to a change in killing ability by the PMNs. To do this, bacteria were cultured with and without PMNs and at 4hpi, cells were collected, and serial dilutions were plated to enumerate colony forming units (CFU). While we measured approximately 30% killing of STM by 4hpi, there was no change in survival of SE in the presence of PMNs across experiments from 4 different donors **(Fig A1.4B)**. Together these results suggest that nontyphoidal serovars interact distinctly with PMNs and SE evades killing by PMNs which may lead to differences in interactions in the PMN-HIO co-culture model and therefore in the human intestine.

A1.3 Discussion

Since nontyphoidal *S. enterica* serovars interact in unique ways with the HIOs, we wanted to test how PMNs impacted infection by using the PMN-HIO co-culture model. In chapter

4 of this dissertation, we performed extensive characterization of STM infection in PMN-HIOs and found that PMNs enhanced epithelial intrinsic defenses against STM to reduce infectivity of *Salmonella*. To test how PMNs affect SE infection, we performed RNA-seq on SE-infected PMN-HIOs and compared those responses to those observed in STM-infected PMN-HIOs. We also performed additional follow-up experiments which focused on some of the phenotypes we observed in STM-infected PMN-HIOs; particularly the elevated cell death phenotype, Caspase-1 mediated signaling, and direct interactions with PMNs.

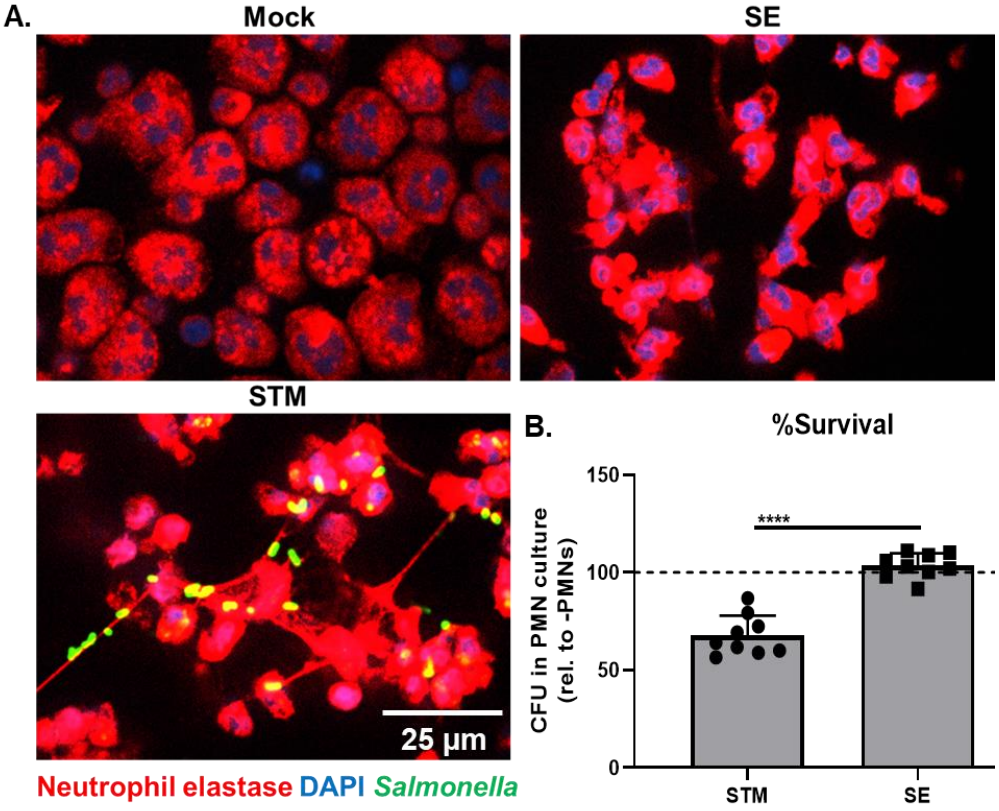

Figure A1.4 SE does not induce NET formation and evades PMN killing in pure PMN cultures
(A) Immunofluorescent staining of PMNs infected with SE or STM, or control PBS and stained for Neutrophil Elastase (red) and DNA with DAPI (blue), STM infected samples were stained with an anti-*Salmonella* Typhimurium antibody. (B) PMN bactericidal activity against Salmonella was quantified by enumerating CFU at 4h in the presence of PMNs relative to bacteria cultured alone. Results are from n=4 independent experiments with PMNs isolated from blood of different donors.

Consistent with our data in Chapter 3 where STM and SE elicited unique responses in infected HIOs, we found that these differences were further elevated when PMNs were added to the culture. We found that our RNA-seq samples clustered based on the infecting serovar and not based on the absence or presence of PMNs. We also found that Caspase-1 mediated processes were not as highly activated during SE infection which correlated with a reduction in epithelial cell death and accumulation of TUNEL-positive cells in the lumen.

Since there is a connection between Caspase activation and NET formation (*3*), we decided to test whether this difference in interaction within the PMN-HIOs could be explained by differences in interactions with PMNs directly. Surprisingly, we found that SE interacted very differently with PMNs compared to STM; we did not observe NET formation and we did not observe killing of SE by PMNs. Additional follow-up work should be performed to better understand these differences. Several potential explanations could be the focus for follow-up analysis, including differences in cell surface molecules and pathogen associated molecular patterns (PAMPs); colony morphology between STM and SE are very different where SE forms wrinkled colonies and STM forms smooth colonies (data not shown). It is possible that SE forms a capsule-like structure to protect it from recognition or killing by PMNs. Using random transposon mutagenesis, we have generated ‘smooth colonies’ of SE which can be used in follow-up experiments to test this possibility.

Alternatively, flagella, another PAMP which is important in activating innate immune signaling pathways, may also be a contributing factor in these differences in interactions. STM and SE express different flagellin proteins (*9*, *10*) and have a difference in motility; SE is much less motile than STM (data not shown) so it is also possible that reduced or expression of different flagellin proteins may lead to differences in immune activation leading to these different infection-associated phenotypes.

The main question rising from all these experiments, however, is how does this impact overall infection outcome. With all these differences in interactions with intestinal epithelial cells and PMNs which form the first and second lines of defense, it is very surprising that these two serovars present clinically with very similar symptoms. In the clinic it is impossible to distinguish between infection with these two serovars without doing serotyping and so how is it possible that these differences in interactions with two very important cell types lead to the same infection outcome? It is possible this area is understudied due to fact that the majority of infected individuals are able to recover from the infection without any medical treatment and so there may be nuances in the host response to these two serovars that are not well appreciated. In the past these questions have been difficult to address due to lack of appropriate model systems, but now that we have shown that PMN-HIOs can be used to study *Salmonella* infection, some of these questions can begin to be addressed.

A1.4 Materials and Methods

A1.4.1 Contact for reagent and resource sharing

All RNA sequences are deposited in the EMBL-EBI Arrayexpress database (E-MTAB-11089). Source code for RNA-seq analyses can be found at aelawren/PMN-HIO-RNA-seq: R scripts for PMN-HIO RNA-seq analysis (github.com). Other reagents and resources can be obtained by directing requests to the Lead Contacts, Basel Abuaita (babuaita@umich.edu) and Mary O'Riordan (oriordan@umich.edu).

A1.4.2 Human Intestinal Organoids (HIOs)

HIOs were generated by the *In Vivo* Animal and Human Studies Core at the University of Michigan Center for Gastrointestinal Research as previously described (*19*). Prior to experiments, HIOs were removed from the Matrigel, washed with DMEM:F12 media, and re-plated with 5 HIOs/well in 50 µL of Matrigel (Corning) in ENR media ((DMEM:F12, 1X B27 supplement, 2 mM L-glutamine, 100 ng/ml EGF, 100 ng/ml Noggin, 500 ng/ml Rspondin1, and 15 mM HEPES). Media was exchanged every 2-3 days for 7 days.

A1.4.3 Human Polymorphonuclear Leukocytes (PMNs)

PMNs were isolated from blood of healthy human volunteers as previously described (*12*). The purity of PMNs was assessed by flow cytometry using APC anti-CD16 and FITC anti-CD15 antibodies (Miltenyi Biotec); markers characteristic of human neutrophils.

A1.4.4 Bacterial Growth and HIO Microinjection

Salmonella enterica serovar Typhimurium SL1344 (STM) or *Salmonella enterica* serovar Enteritidis P125109 (SE) was used throughout the manuscript. Bacteria were stored at

−80°C in Luria-Bertani (LB, Fisher) medium containing 20% glycerol and cultured on LB agar plates. Individual colonies were grown overnight at 37ºC under static conditions in LB liquid broth. Bacteria were pelleted, washed, and re-suspended in PBS. Bacterial inoculum was estimated based on OD_{600} and verified by plating serial dilutions on agar plates to determine colony forming units (CFU). Lumens of individual HIOs were microinjected with glass caliber needles with 1 µl of PBS or STM (10^5 CFU/HIO) as previously described (*22*, *35*, *129*). HIOs were then washed with PBS and incubated for 2h at 37°C in ENR media. HIOs were treated with 100 µg/ml gentamicin for 15 min to kill any bacteria outside the HIOs, then incubated in fresh medium +/- PMNs (5 X 10^5 PMNs/5HIOs/well in a 24-well plate).

A1.4.5 Bacterial Burden and Cytokine Analyses

To assess killing by PMNs, 10^5 CFU bacteria were added to a 6 well plate +/-10^5 PMNs. At 4hpi, media was collected, and serial dilutions were plated on LB agar to enumerate CFU. For cytokine analysis, media from each well containing 5 HIOs/well were collected at 8hpi. Cytokines, chemokines, and antimicrobial proteins were quantified by ELISA at the University of Michigan Cancer Center Immunology Core.

A1.4.6 Immunofluorescence Staining and Microscopy

HIOs were fixed with 10% neutral formalin for 2 days and embedded in paraffin. Histology sections (5 µm) were collected by the University of Michigan Cancer Center Histology Core. Sections were deparaffinized and antigen retrieval was performed in sodium citrate buffer (10 mM sodium citrate, 0.05% Tween 20, pH 6.0). Sections were permeabilized

with PBS+ 0.2% Triton X-100 for 30 min, then incubated in blocking buffer (PBS, 5% BSA, and 10% normal goat serum) for 1h. Primary antibodies; anti-E-Cadherin (BD Biosciences, clone 36), anti-MPO (Agilent, clone A0398), anti-Neutrophil Elastase (ab21595) were added to the histology sections in blocking buffer overnight at 4°C. Goat anti-mouse and anti-rabbit secondary antibodies conjugated to Alexa-488, Alexa-594 or Alexa-647 were used according to manufacturer's instructions (Thermo Fisher) for 1h RT in blocking buffer. DAPI (Thermo Fisher) was used to stain DNA. Bacteria were stained using anti-*Salmonella* Typhimurium FITC-conjugated antibody (Santa Cruz, Cat# sc-52223). Sections were mounted using coverslips (#1.5) and Prolong Diamond or Prolong Glass Antifade Mountant (Thermo Fisher). Images were taken on Olympus BX60 upright compound microscope or Nikon X1 Yokogawa spinning disc confocal microscope and processed using ImageJ and quantitation was performed in ImageJ or CellProfiler.

A1.4.7 TUNEL Assay

Apoptosis was analyzed by fluorescence microscopy using *In Situ Cell Death Detection Kit* (Roche) according to the manufacturers' protocols. Histology sections were permeabilized using Proteinase K (20 µg/ml) or 0.2% Triton X-100 in PBS and blocked using PBS+ 5%BSA. Sections were stained with primary antibodies overnight at 4°C in blocking buffer and then were incubated in the terminal deoxynucleotidyl transferase end labeling (TUNEL) buffer for 1h at 37°C. Slides were washed with PBS and incubated with fluorescent conjugated secondary antibodies. Sections were then counterstained with DAPI to label the DNA. For quantification of TUNEL positive cells, the percent of the HIO lumen filled with TUNEL+ cells was quantified using ImageJ software.

A1.4.8 RNA Sequencing and Analysis

Total RNA was isolated from 5 HIOs per group with a total of 4 replicates per condition using the mirVana miRNA Isolation Kit (Thermo Fisher). The quality of RNA was confirmed, ensuring the RNA integrity number (RIN)> 8.5, using the Agilent TapeStation system. cDNA libraries were prepared by the University of Michigan DNA Sequencing Core using the TruSeq Stranded mRNA Kit (Illumina) according to the manufacturer's protocol. Libraries were sequenced on Illumina HiSeq 2500 platforms (single-end, 50 bp read length). All samples were sequenced at a depth of 10.5million reads per sample or greater. Sequencing generated FASTQ files of transcript reads that were pseudoaligned to the human genome (GRCh38.p12) using kallisto software (*117*). Transcripts were converted to estimated gene counts using the tximport package (*119*) with gene annotation from Ensembl (*118*).

A1.4.9 Gene Expression and Pathway Enrichment Analysis

Differential expression analysis was performed using the DESeq2 package (*121*) with *P* values calculated by the Wald test and adjusted *P* values calculated using the Benjamani & Hochberg method (*120*). Pathway analysis was performed using the Reactome pathway database and pathway enrichment analysis in R using the ReactomePA software package (*122*).

A1.4.10 Quantification and Statistical Methods

RNA-seq data analysis was done using RStudio version 1.1.453. Plots were generated using ggplot2 (*116*) with data manipulation done using dplyr (*123*). Euler diagrams of gene changes were generated using the Eulerr package (*124*). Other data were analyzed using Graphpad Prism 9. Statistical differences were determined using statistical tests indicated in the figure legends. The mean of at least 2 independent experiments were presented with error bars showing standard deviation (SD). *P* values of less than 0.05 were considered significant and designated by: *$P < 0.05$, **$P < 0.01$, ***$P < 0.001$ and **** $P < 0.0001$.

References

1. L. W. Peterson, D. Artis, Intestinal epithelial cells: regulators of barrier function and immune homeostasis. *Nat. Rev. Immunol.* **14**, 141–153 (2014).

2. C. Chelakkot, J. Ghim, S. H. Ryu, Mechanisms regulating intestinal barrier integrity and its pathological implications. *Exp. Mol. Med.* **50**, 103 (2018).

3. A. M. Mowat, W. W. Agace, Regional specialization within the intestinal immune system. *Nat. Rev. Immunol.* **14**, 667–685 (2014).

4. F. Hugenholtz, W. M. de Vos, Mouse models for human intestinal microbiota research: a critical evaluation. *Cell. Mol. Life Sci.* **75**, 149–160 (2018).

5. M. Barthel, S. Hapfelmeier, L. Quintanilla-Martínez, M. Kremer, M. Rohde, M. Hogardt, K. Pfeffer, H. Rüssmann, W.-D. Hardt, Pretreatment of mice with streptomycin provides a Salmonella enterica serovar Typhimurium colitis model that allows analysis of both pathogen and host. *Infect. Immun.* **71**, 2839–2858 (2003).

6. J. W. Collins, K. M. Keeney, V. F. Crepin, V. A. K. Rathinam, K. A. Fitzgerald, B. B. Finlay, G. Frankel, Citrobacter rodentium: infection, inflammation and the microbiota. *Nat. Rev. Microbiol.* **12**, 612–623 (2014).

7. M. Lecuit, S. Dramsi, C. Gottardi, M. Fedor-Chaiken, B. Gumbiner, P. Cossart, A single amino acid in E-cadherin responsible for host specificity towards the human pathogen Listeria monocytogenes. *EMBO J.* **18**, 3956–3963 (1999).

8. Y. Valdez, G. A. Grassl, J. A. Guttman, B. Coburn, P. Gros, B. A. Vallance, B. B. Finlay, Nramp1 drives an accelerated inflammatory response during Salmonella-induced colitis in mice. *Cell. Microbiol.* **11**, 351–362 (2009).

9. D. M. Monack, D. M. Bouley, S. Falkow, Salmonella typhimurium persists within macrophages in the mesenteric lymph nodes of chronically infected Nramp1+/+ mice and can be reactivated by IFNgamma neutralization. *J. Exp. Med.* **199**, 231–241 (2004).

10. S. Hapfelmeier, W.-D. Hardt, A mouse model for S. typhimurium-induced enterocolitis. *Trends Microbiol.* **13**, 497–503 (2005).

11. R. L. Santos, R. M. Tsolis, S. Zhang, T. A. Ficht, A. J. Bäumler, L. G. Adams, Salmonella-induced cell death is not required for enteritis in calves. *Infect. Immun.* **69**, 4610–4617 (2001).

12. Elfenbein Johanna R., Endicott-Yazdani Tiana, Porwollik Steffen, Bogomolnaya Lydia M., Cheng Pui, Guo Jinbai, Zheng Yi, Yang Hee-Jeong, Talamantes Marissa, Shields Christine, Maple Aimee, Ragoza Yury, DeAtley Kimberly, Tatsch Tyler, Cui Ping, Andrews Katharine D., McClelland Michael, Lawhon Sara D., Andrews-Polymenis Helene, Fang F. C., Novel Determinants of Intestinal Colonization of

Salmonella enterica Serotype Typhimurium Identified in Bovine Enteric Infection. *Infect. Immun.* **81**, 4311–4320 (2013).

13. I. Vlisidou, M. Lyte, P. M. van Diemen, P. Hawes, P. Monaghan, T. S. Wallis, M. P. Stevens, The neuroendocrine stress hormone norepinephrine augments Escherichia coli O157:H7-induced enteritis and adherence in a bovine ligated ileal loop model of infection. *Infect. Immun.* **72**, 5446–5451 (2004).

14. C. Menge, I. Stamm, P. M. van Diemen, P. Sopp, G. Baljer, T. S. Wallis, M. P. Stevens, Phenotypic and functional characterization of intraepithelial lymphocytes in a bovine ligated intestinal loop model of enterohaemorrhagic Escherichia coli infection. *J. Med. Microbiol.* **53**, 573–579 (2004).

15. K. P. Keenan, D. D. Sharpnack, H. Collins, S. B. Formal, A. D. O'Brien, Morphologic evaluation of the effects of Shiga toxin and E coli Shiga-like toxin on the rabbit intestine. *Am. J. Pathol.* **125**, 69–80 (1986).

16. G. J. Leitch, M. E. Iwert, W. Burrows, Experimental cholera in the rabbit ligated ileal loop: toxin-induced water and ion movement. *J. Infect. Dis.* **116**, 303–312 (1966).

17. T. Lea, in *The Impact of Food Bioactives on Health: in vitro and ex vivo models*, K. Verhoeckx, P. Cotter, I. López-Expósito, C. Kleiveland, T. Lea, A. Mackie, T. Requena, D. Swiatecka, H. Wichers, Eds. (Springer International Publishing, Cham, 2015), pp. 103–111.

18. N. V. Guseva, S. Dessus-Babus, C. G. Moore, J. D. Whittimore, P. B. Wyrick, Differences in Chlamydia trachomatis serovar E growth rate in polarized endometrial and endocervical epithelial cells grown in three-dimensional culture. *Infect. Immun.* **75**, 553–564 (2007).

19. J. R. Spence, C. N. Mayhew, S. A. Rankin, M. F. Kuhar, J. E. Vallance, K. Tolle, E. E. Hoskins, V. V. Kalinichenko, S. I. Wells, A. M. Zorn, N. F. Shroyer, J. M. Wells, Directed differentiation of human pluripotent stem cells into intestinal tissue in vitro. *Nature*. **470**, 105–109 (2011).

20. K. W. McCracken, J. C. Howell, J. M. Wells, J. R. Spence, Generating human intestinal tissue from pluripotent stem cells in vitro. *Nat. Protoc.* **6**, 1920–1928 (2011).

21. D. R. Hill, S. Huang, M. S. Nagy, V. K. Yadagiri, C. Fields, D. Mukherjee, B. Bons, P. H. Dedhia, A. M. Chin, Y.-H. Tsai, S. Thodla, T. M. Schmidt, S. Walk, V. B. Young, J. R. Spence, Bacterial colonization stimulates a complex physiological response in the immature human intestinal epithelium. *Elife*. **6** (2017), doi:10.7554/eLife.29132.

22. D. R. Hill, S. Huang, Y.-H. Tsai, J. R. Spence, V. B. Young, Real-time Measurement of Epithelial Barrier Permeability in Human Intestinal Organoids. *J. Vis. Exp.* (2017), doi:10.3791/56960.

23. D. D. Zomer-van Ommen, A. V. Pukin, O. Fu, L. H. C. Quarles van Ufford, H. M. Janssens, J. M. Beekman, R. J. Pieters, Functional Characterization of Cholera Toxin Inhibitors Using Human Intestinal Organoids. *J. Med. Chem.* **59**, 6968–6972 (2016).

24. T. Sato, D. E. Stange, M. Ferrante, R. G. J. Vries, J. H. Van Es, S. Van den Brink, W. J. Van Houdt, A. Pronk, J. Van Gorp, P. D. Siersema, H. Clevers, Long-term expansion of epithelial organoids from human colon, adenoma, adenocarcinoma, and Barrett's epithelium. *Gastroenterology*. **141**, 1762–1772 (2011).

25. M. M. Mahe, N. Sundaram, C. L. Watson, N. F. Shroyer, M. A. Helmrath, Establishment of human epithelial enteroids and colonoids from whole tissue and biopsy. *J. Vis. Exp.* (2015), doi:10.3791/52483.

26. P. Jung, T. Sato, A. Merlos-Suárez, F. M. Barriga, M. Iglesias, D. Rossell, H. Auer, M. Gallardo, M. A. Blasco, E. Sancho, H. Clevers, E. Batlle, Isolation and in vitro expansion of human colonic stem cells. *Nat. Med.* **17**, 1225–1227 (2011).

27. W. Y. Zou, S. E. Blutt, S. E. Crawford, K. Ettayebi, X.-L. Zeng, K. Saxena, S. Ramani, U. C. Karandikar, N. C. Zachos, M. K. Estes, (Humana Press, 2017), pp. 1–19.

28. I. Schoultz, Å. V. Keita, The Intestinal Barrier and Current Techniques for the Assessment of Gut Permeability. *Cells*. **9** (2020), doi:10.3390/cells9081909.

29. J. D. Rouch, A. Scott, N. Y. Lei, R. S. Solorzano-Vargas, J. Wang, E. M. Hanson, M. Kobayashi, M. Lewis, M. G. Stelzner, J. C. Y. Dunn, L. Eckmann, M. G. Martín, Development of Functional Microfold (M) Cells from Intestinal Stem Cells in Primary Human Enteroids. *PLoS One*. **11**, e0148216 (2016).

30. S. Middendorp, K. Schneeberger, C. L. Wiegerinck, M. Mokry, R. D. L. Akkerman, S. van Wijngaarden, H. Clevers, E. E. S. Nieuwenhuis, Adult stem cells in the small intestine are intrinsically programmed with their location-specific function. *Stem Cells*. **32**, 1083–1091 (2014).

31. M. M. Lamers, J. Beumer, J. van der Vaart, K. Knoops, J. Puschhof, T. I. Breugem, R. B. G. Ravelli, J. Paul van Schayck, A. Z. Mykytyn, H. Q. Duimel, E. van Donselaar, S. Riesebosch, H. J. H. Kuijpers, D. Schipper, W. J. van de Wetering, M. de Graaf, M. Koopmans, E. Cuppen, P. J. Peters, B. L. Haagmans, H. Clevers, SARS-CoV-2 productively infects human gut enterocytes. *Science*. **369**, 50–54 (2020).

32. S.-C. Lin, L. Qu, K. Ettayebi, S. E. Crawford, S. E. Blutt, M. J. Robertson, X.-L. Zeng, V. R. Tenge, B. V. Ayyar, U. C. Karandikar, X. Yu, C. Coarfa, R. L. Atmar, S. Ramani, M. K. Estes, Human norovirus exhibits strain-specific sensitivity to host interferon pathways in human intestinal enteroids. *Proc. Natl. Acad. Sci. U. S. A.* **117**, 23782–23793 (2020).

33. K. Ettayebi, S. E. Crawford, K. Murakami, J. R. Broughman, U. Karandikar, V. R. Tenge, F. H. Neill, S. E. Blutt, X.-L. Zeng, L. Qu, B. Kou, A. R. Opekun, D. Burrin, D.

Y. Graham, S. Ramani, R. L. Atmar, M. K. Estes, Replication of human noroviruses in stem cell-derived human enteroids. *Science*. **353**, 1387–1393 (2016).

34. B. H. Abuaita, A.-L. E. Lawrence, R. P. Berger, D. R. Hill, S. Huang, V. K. Yadagiri, B. Bons, C. Fields, C. E. Wobus, J. R. Spence, V. B. Young, M. X. O'Riordan, Comparative transcriptional profiling of the early host response to infection by typhoidal and non-typhoidal Salmonella serovars in human intestinal organoids. *PLoS Pathog.* **17**, e1009987 (2021).

35. A.-L. E. Lawrence, B. H. Abuaita, R. P. Berger, D. R. Hill, S. Huang, V. K. Yadagiri, B. Bons, C. Fields, C. E. Wobus, J. R. Spence, V. B. Young, M. X. O'Riordan, Salmonella enterica Serovar Typhimurium SPI-1 and SPI-2 Shape the Global Transcriptional Landscape in a Human Intestinal Organoid Model System. *MBio*. **12** (2021), doi:10.1128/mBio.00399-21.

36. J. L. Forbester, D. Goulding, L. Vallier, N. Hannan, C. Hale, D. Pickard, S. Mukhopadhyay, G. Dougan, Interaction of salmonella enterica serovar Typhimurium with intestinal organoids derived from human induced pluripotent stem cells. *Infect. Immun.* **83**, 2926–2934 (2015).

37. J. L. Forbester, E. A. Lees, D. Goulding, S. Forrest, A. Yeung, A. Speak, S. Clare, E. L. Coomber, S. Mukhopadhyay, J. Kraiczy, F. Schreiber, T. D. Lawley, R. E. W. Hancock, H. H. Uhlig, M. Zilbauer, F. Powrie, G. Dougan, Interleukin-22 promotes phagolysosomal fusion to induce protection against Salmonella enterica Typhimurium in human epithelial cells. *Proc. Natl. Acad. Sci. U. S. A.* **115**, 10118–10123 (2018).

38. P. Geiser, M. L. Di Martino, P. Samperio Ventayol, J. Eriksson, E. Sima, A. K. Al-Saffar, D. Ahl, M. Phillipson, D.-L. Webb, M. Sundbom, P. M. Hellström, M. E. Sellin, Salmonella enterica Serovar Typhimurium Exploits Cycling through Epithelial Cells To Colonize Human and Murine Enteroids. *MBio*. **12** (2021), doi:10.1128/mBio.02684-20.

39. J. L. Leslie, S. Huang, J. S. Opp, M. S. Nagy, M. Kobayashi, V. B. Young, J. R. Spence, Persistence and toxin production by Clostridium difficile within human intestinal organoids result in disruption of epithelial paracellular barrier function. *Infect. Immun.* **83**, 138–145 (2015).

40. M. A. Engevik, H. A. Danhof, A. L. Chang-Graham, J. K. Spinler, K. A. Engevik, B. Herrmann, B. T. Endres, K. W. Garey, J. M. Hyser, R. A. Britton, J. Versalovic, Human intestinal enteroids as a model of Clostridioides difficile-induced enteritis. *Am. J. Physiol. Gastrointest. Liver Physiol.* **318**, G870–G888 (2020).

41. M. A. Engevik, M. B. Yacyshyn, K. A. Engevik, J. Wang, B. Darien, D. J. Hassett, B. R. Yacyshyn, R. T. Worrell, Human Clostridium difficile infection: altered mucus production and composition. *Am. J. Physiol. Gastrointest. Liver Physiol.* **308**, G510-24 (2015).

42. M. A. Engevik, K. A. Engevik, M. B. Yacyshyn, J. Wang, D. J. Hassett, B. Darien, B. R. Yacyshyn, R. T. Worrell, Human Clostridium difficile infection: inhibition of NHE3 and microbiota profile. *Am. J. Physiol. Gastrointest. Liver Physiol.* **308**, G497-509 (2015).

43. D. Holthaus, E. Delgado-Betancourt, T. Aebischer, F. Seeber, C. Klotz, Harmonization of Protocols for Multi-Species Organoid Platforms to Study the Intestinal Biology of Toxoplasma gondii and Other Protozoan Infections. *Front. Cell. Infect. Microbiol.* **10**, 610368 (2020).

44. K. L. Mohawk, A. D. O'Brien, Mouse models of Escherichia coli O157:H7 infection and shiga toxin injection. *J. Biomed. Biotechnol.* **2011**, 258185 (2011).

45. M. R. Barron, R. J. Cieza, D. R. Hill, S. Huang, V. K. Yadagiri, J. R. Spence, V. B. Young, The lumen of human intestinal organoids poses greater stress to bacteria compared to the germ-free mouse intestine: Escherichia coli deficient in RpoS as a colonization probe. *mSphere*. **5** (2020), doi:10.1128/mSphere.00777-20.

46. A. Rajan, M. J. Robertson, H. E. Carter, N. M. Poole, J. R. Clark, S. I. Green, Z. K. Criss, B. Zhao, U. Karandikar, Y. Xing, M. Margalef-Català, N. Jain, R. L. Wilson, F. Bai, J. M. Hyser, J. Petrosino, N. F. Shroyer, S. E. Blutt, C. Coarfa, X. Song, B. V. Prasad, M. R. Amieva, J. Grande-Allen, M. K. Estes, P. C. Okhuysen, A. W. Maresso, Enteroaggregative E. coli Adherence to Human Heparan Sulfate Proteoglycans Drives Segment and Host Specific Responses to Infection. *PLoS Pathog.* **16**, e1008851 (2020).

47. G. Swaminathan, N. Kamyabi, H. E. Carter, A. Rajan, U. Karandikar, Z. K. Criss, N. F. Shroyer, M. J. Robertson, C. Coarfa, C. Huang, T. E. Shannon, M. Tadros, M. K. Estes, A. W. Maresso, K. J. Grande-Allen, Effect of substrate stiffness on human intestinal enteroids' infectivity by enteroaggregative Escherichia coli. *Acta Biomater.* **132**, 245–259 (2021).

48. A. Rajan, L. Vela, X.-L. Zeng, X. Yu, N. Shroyer, S. E. Blutt, N. M. Poole, L. G. Carlin, J. P. Nataro, M. K. Estes, P. C. Okhuysen, A. W. Maresso, Novel Segment- and Host-Specific Patterns of Enteroaggregative Escherichia coli Adherence to Human Intestinal Enteroids. *MBio*. **9** (2018), doi:10.1128/mBio.02419-17.

49. J. In, J. Foulke-Abel, N. C. Zachos, A.-M. Hansen, J. B. Kaper, H. D. Bernstein, M. Halushka, S. Blutt, M. K. Estes, M. Donowitz, O. Kovbasnjuk, Enterohemorrhagic Escherichia coli reduce mucus and intermicrovillar bridges in human stem cell-derived colonoids. *Cell Mol Gastroenterol Hepatol*. **2**, 48-62.e3 (2016).

50. T. Secher, C. Brehin, E. Oswald, Early settlers: which E. coli strains do you not want at birth? *Am. J. Physiol. Gastrointest. Liver Physiol.* **311**, G123-9 (2016).

51. S. S. Karve, S. Pradhan, D. V. Ward, A. A. Weiss, Intestinal organoids model human responses to infection by commensal and Shiga toxin producing Escherichia coli, 1–20 (2017).

52. Y. Yin, D. Zhou, Organoid and Enteroid Modeling of Salmonella Infection. *Front. Cell. Infect. Microbiol.* **8**, 102 (2018).

53. M. K. Holly, X. Han, E. J. Zhao, S. M. Crowley, J. M. Allaire, L. A. Knodler, B. A. Vallance, J. G. Smith, Salmonella enterica Infection of Murine and Human Enteroid-Derived Monolayers Elicits Differential Activation of Epithelium-Intrinsic Inflammasomes. *Infect. Immun.* **88** (2020), doi:10.1128/IAI.00017-20.

54. B. J. Koestler, C. M. Ward, C. R. Fisher, A. Rajan, A. W. Maresso, S. M. Payne, Human Intestinal Enteroids as a Model System of Shigella Pathogenesis. *Infect. Immun.* **87** (2019), doi:10.1128/IAI.00733-18.

55. S. Ranganathan, M. Doucet, C. L. Grassel, B. Delaine-Elias, N. C. Zachos, E. M. Barry, Evaluating Shigella flexneri Pathogenesis in the Human Enteroid Model. *Infect. Immun.* **87** (2019), doi:10.1128/IAI.00740-18.

56. A. Llanos-Chea, R. J. Citorik, K. P. Nickerson, L. Ingano, G. Serena, S. Senger, T. K. Lu, A. Fasano, C. S. Faherty, Bacteriophage Therapy Testing Against Shigella flexneri in a Novel Human Intestinal Organoid-Derived Infection Model. *J. Pediatr. Gastroenterol. Nutr.* **68**, 509–516 (2019).

57. T. L. Hale, G. T. Keusch, in *Medical Microbiology*, S. Baron, Ed. (University of Texas Medical Branch at Galveston, Galveston (TX), 2011).

58. A. Haage, What's it all about? Organoids (2017), (available at https://www.ascb.org/science-news/whats-it-all-about-organoids/).

59. S. S. Wilson, M. Mayo, T. Melim, H. Knight, L. Patnaude, X. Wu, L. Phillips, S. Westmoreland, R. Dunstan, E. Fiebiger, S. Terrillon, Optimized Culture Conditions for Improved Growth and Functional Differentiation of Mouse and Human Colon Organoids. *Front. Immunol.* **11**, 547102 (2020).

60. U. Lakshmipathy, B. Pelacho, K. Sudo, J. L. Linehan, E. Coucouvanis, D. S. Kaufman, C. M. Verfaillie, Efficient transfection of embryonic and adult stem cells. *Stem Cells*. **22**, 531–543 (2004).

61. C. Rajendra, T. Wald, K. Barber, J. R. Spence, F. Fattahi, O. D. Klein, Generation of Knockout Gene-Edited Human Intestinal Organoids. *Methods Mol. Biol.* **2171**, 215–230 (2020).

62. B.-K. Koo, D. E. Stange, T. Sato, W. Karthaus, H. F. Farin, M. Huch, J. H. van Es, H. Clevers, Controlled gene expression in primary Lgr5 organoid cultures. *Nat. Methods*. **9**, 81–83 (2011).

63. J. Y. Co, M. Margalef-Català, X. Li, A. T. Mah, C. J. Kuo, D. M. Monack, M. R. Amieva, Controlling Epithelial Polarity: A Human Enteroid Model for Host-Pathogen Interactions. *Cell Rep.* **26**, 2509-2520.e4 (2019).

64. L. Dolat, R. H. Valdivia, An endometrial organoid model of interactions between Chlamydia and epithelial and immune cells. *J. Cell Sci.* **134** (2021), doi:10.1242/jcs.252403.

65. J. M. Lemme-Dumit, M. Doucet, N. C. Zachos, M. F. Pasetti, Epithelial and neutrophil interactions and coordinated response to Shigella in a human intestinal enteroid-neutrophil co-culture model. *bioRxiv* (2021), p. 2020.09.03.281535, , doi:10.1101/2020.09.03.281535.

66. G. Noel, N. W. Baetz, J. F. Staab, M. Donowitz, O. Kovbasnjuk, M. F. Pasetti, N. C. Zachos, A primary human macrophage-enteroid co-culture model to investigate mucosal gut physiology and host-pathogen interactions. *Sci. Rep.* **7**, 45270 (2017).

67. J. F. Staab, J. M. Lemme-Dumit, R. Latanich, M. F. Pasetti, N. C. Zachos, Co-culture system of human enteroids/colonoids with innate immune cells. *Curr. Protoc. Immunol.* **131**, e113 (2020).

68. N. Sasaki, K. Miyamoto, K. M. Maslowski, H. Ohno, T. Kanai, T. Sato, Development of a Scalable Coculture System for Gut Anaerobes and Human Colon Epithelium. *Gastroenterology*. **159**, 388-390.e5 (2020).

69. T. Y. Fofanova, C. J. Stewart, J. M. Auchtung, R. L. Wilson, R. A. Britton, K. J. Grande-Allen, M. K. Estes, J. F. Petrosino, A novel human enteroid-anaerobe co-culture system to study microbial-host interaction under physiological hypoxia. *bioRxiv* (2019), p. 555755.

70. L. Sunuwar, J. Yin, M. Kasendra, K. Karalis, J. Kaper, J. Fleckenstein, M. Donowitz, Mechanical Stimuli Affect Escherichia coli Heat-Stable Enterotoxin-Cyclic GMP Signaling in a Human Enteroid Intestine-Chip Model. *Infect. Immun.* **88** (2020), doi:10.1128/IAI.00866-19.

71. X. Li, A. Ootani, C. Kuo, in *Gastrointestinal Physiology and Diseases: Methods and Protocols*, A. I. Ivanov, Ed. (Springer New York, New York, NY, 2016), pp. 33–40.

72. J. A. Crump, S. P. Luby, E. D. Mintz, The global burden of typhoid fever. *Bull. World Health Organ.* **82**, 346–353 (2004).

73. S. E. Majowicz, J. Musto, E. Scallan, F. J. Angulo, M. Kirk, S. J. O'Brien, T. F. Jones, A. Fazil, R. M. Hoekstra, The Global Burden of Nontyphoidal *Salmonella* Gastroenteritis. *Clin. Infect. Dis.* **50**, 882–889 (2010).

74. V. Singh, Salmonella serovars and their host specificity. *J. Vet. Sci. Anim. Husb.* **1** (2013), doi:10.15744/2348-9790.1.301.

75. C. Tükel, M. Raffatellu, D. Chessa, R. P. Wilson, M. Akçelik, A. J. Bäumler, Neutrophil influx during non-typhoidal salmonellosis: who is in the driver's seat? *FEMS Immunol. Med. Microbiol.* **46**, 320–329 (2006).

76. N. A. Feasey, G. Dougan, R. A. Kingsley, R. S. Heyderman, M. A. Gordon, Invasive non-typhoidal salmonella disease: an emerging and neglected tropical disease in Africa. *Lancet*. **379**, 2489–2499 (2012).

77. G. Arya, R. Holtslander, J. Robertson, C. Yoshida, J. Harris, J. Parmley, A. Nichani, R. Johnson, C. Poppe, Epidemiology, Pathogenesis, Genoserotyping, Antimicrobial Resistance, and Prevention and Control of Non-Typhoidal Salmonella Serovars. *Current Clinical Microbiology Reports*. **4**, 43–53 (2017).

78. N. R. Thomson, D. J. Clayton, D. Windhorst, G. Vernikos, S. Davidson, C. Churcher, M. A. Quail, M. Stevens, M. A. Jones, M. Watson, A. Barron, A. Layton, D. Pickard, R. A. Kingsley, A. Bignell, L. Clark, B. Harris, D. Ormond, Z. Abdellah, K. Brooks, I. Cherevach, T. Chillingworth, J. Woodward, H. Norberczak, A. Lord, C. Arrowsmith, K. Jagels, S. Moule, K. Mungall, M. Sanders, S. Whitehead, J. A. Chabalgoity, D. Maskell, T. Humphrey, M. Roberts, P. A. Barrow, G. Dougan, J. Parkhill, Comparative genome analysis of Salmonella Enteritidis PT4 and Salmonella Gallinarum 287/91 provides insights into evolutionary and host adaptation pathways. *Genome Res.* **18**, 1624–1637 (2008).

79. S. E. Majowicz, J. Musto, E. Scallan, F. J. Angulo, M. Kirk, S. J. O'Brien, T. F. Jones, A. Fazil, R. M. Hoekstra, International Collaboration on Enteric Disease "Burden of Illness" Studies, The global burden of nontyphoidal Salmonella gastroenteritis. *Clin. Infect. Dis.* **50**, 882–889 (2010).

80. O. Gal-Mor, E. C. Boyle, G. A. Grassl, Same species, different diseases: how and why typhoidal and non-typhoidal Salmonella enterica serovars differ. *Front. Microbiol.* **5**, 391 (2014).

81. S.-P. Nuccio, A. J. Bäumler, Comparative analysis of Salmonella genomes identifies a metabolic network for escalating growth in the inflamed gut. *MBio*. **5**, e00929-14 (2014).

82. Q.-H. Zou, R.-Q. Li, G.-R. Liu, S.-L. Liu, Comparative genomic analysis between typhoidal and non-typhoidal Salmonella serovars reveals typhoid-specific protein families. *Infect. Genet. Evol.* **26**, 295–302 (2014).

83. Y. E. Bar-Ephraim, K. Kretzschmar, H. Clevers, Organoids in immunological research. *Nat. Rev. Immunol.* **20**, 279–293 (2020).

84. S. Hannemann, J. E. Galán, Salmonella enterica serovar-specific transcriptional reprogramming of infected cells. *PLoS Pathog.* **13**, e1006532 (2017).

85. L. N. Schulte, M. Schweinlin, A. J. Westermann, H. Janga, S. C. Santos, S. Appenzeller, H. Walles, J. Vogel, M. Metzger, An Advanced Human Intestinal Coculture Model Reveals Compartmentalized Host and Pathogen Strategies during Salmonella Infection. *MBio*. **11** (2020), doi:10.1128/mBio.03348-19.

86. M. Hase, T. Yokomizo, T. Shimizu, M. Nakamura, Characterization of an orphan G protein-coupled receptor, GPR20, that constitutively activates Gi proteins. *J. Biol. Chem.* **283**, 12747–12755 (2008).

87. M. M. Weber, R. Faris, Subversion of the Endocytic and Secretory Pathways by Bacterial Effector Proteins. *Front Cell Dev Biol*. **6**, 1 (2018).

88. M. Raffatellu, D. Chessa, R. P. Wilson, R. Dusold, S. Rubino, A. J. Bäumler, The Vi capsular antigen of Salmonella enterica serotype Typhi reduces Toll-like receptor-dependent interleukin-8 expression in the intestinal mucosa. *Infect. Immun.* **73**, 3367–3374 (2005).

89. X. Song, S. Zhu, P. Shi, Y. Liu, Y. Shi, S. D. Levin, Y. Qian, IL-17RE is the functional receptor for IL-17C and mediates mucosal immunity to infection with intestinal pathogens. *Nat. Immunol.* **12**, 1151–1158 (2011).

90. A. J. M. Santos, C. H. Durkin, S. Helaine, E. Boucrot, D. W. Holden, Clustered Intracellular Salmonella enterica Serovar Typhimurium Blocks Host Cell Cytokinesis. *Infect. Immun.* **84**, 2149–2158 (2016).

91. C. Maudet, M. Mano, U. Sunkavalli, M. Sharan, M. Giacca, K. U. Förstner, A. Eulalio, Functional high-throughput screening identifies the miR-15 microRNA family as cellular restriction factors for Salmonella infection. *Nat. Commun.* **5**, 4718 (2014).

92. F. Schönenberger, A. Deutzmann, E. Ferrando-May, D. Merhof, Discrimination of cell cycle phases in PCNA-immunolabeled cells. *BMC Bioinformatics*. **16**, 180 (2015).

93. A. Valbuena, I. López-Sánchez, P. A. Lazo, Human VRK1 is an early response gene and its loss causes a block in cell cycle progression. *PLoS One*. **3**, e1642 (2008).

94. B. Giotti, S.-H. Chen, M. W. Barnett, T. Regan, T. Ly, S. Wiemann, D. A. Hume, T. C. Freeman, Assembly of a parts list of the human mitotic cell cycle machinery. *J. Mol. Cell Biol.* **11**, 703–718 (2019).

95. R. A. Edwards, G. J. Olsen, S. R. Maloy, Comparative genomics of closely related salmonellae. *Trends Microbiol.* **10**, 94–99 (2002).

96. P. Wigley, Salmonella enterica in the Chicken: How it has Helped Our Understanding of Immunology in a Non-Biomedical Model Species. *Front. Immunol.* **5**, 482 (2014).

97. A. D. Palmer, J. M. Slauch, Mechanisms of Salmonella pathogenesis in animal models. *Hum. Ecol. Risk Assess.* **23**, 1877–1892 (2017).

98. R. Salerno-Gonçalves, J. E. Galen, M. M. Levine, A. Fasano, M. B. Sztein, Manipulation of Salmonella Typhi Gene Expression Impacts Innate Cell Responses in the Human Intestinal Mucosa. *Front. Immunol.* **9**, 2543 (2018).

99. D. L. Weinstein, B. L. O'Neill, E. S. Metcalf, Salmonella typhi stimulation of human intestinal epithelial cells induces secretion of epithelial cell-derived interleukin-6. *Infect. Immun.* **65**, 395–404 (1997).

100. V. M. Bruno, S. Hannemann, M. Lara-Tejero, R. A. Flavell, S. H. Kleinstein, J. E. Galán, Salmonella Typhimurium type III secretion effectors stimulate innate immune responses in cultured epithelial cells. *PLoS Pathog.* **5**, e1000538 (2009).

101. S. Hannemann, B. Gao, J. E. Galán, Salmonella modulation of host cell gene expression promotes its intracellular growth. *PLoS Pathog.* **9**, e1003668 (2013).

102. A. Hausmann, G. Russo, J. Grossmann, M. Zünd, G. Schwank, R. Aebersold, Y. Liu, M. E. Sellin, W.-D. Hardt, Germ-free and microbiota-associated mice yield small intestinal epithelial organoids with equivalent and robust transcriptome/proteome expression phenotypes. *Cell. Microbiol.* **22**, e13191 (2020).

103. K. P. Nickerson, S. Senger, Y. Zhang, R. Lima, S. Patel, L. Ingano, W. A. Flavahan, D. K. V. Kumar, C. M. Fraser, C. S. Faherty, M. B. Sztein, M. Fiorentino, A. Fasano, Salmonella Typhi Colonization Provokes Extensive Transcriptional Changes Aimed at Evading Host Mucosal Immune Defense During Early Infection of Human Intestinal Tissue. *EBioMedicine*. **31**, 92–109 (2018).

104. T. R. Powers, A. L. Haeberle, A. V. Predeus, D. L. Hammarlöf, J. A. Cundiff, Z. Saldaña-Ahuactzi, K. Hokamp, J. C. D. Hinton, L. A. Knodler, Intracellular niche-specific profiling reveals transcriptional adaptations required for the cytosolic lifestyle of Salmonella enterica. *PLoS Pathog.* **17**, e1009280 (2021).

105. P. Anderson, Post-transcriptional control of cytokine production. *Nat. Immunol.* **9**, 353–359 (2008).

106. K. S. A. Khabar, Post-Transcriptional Control of Cytokine Gene Expression in Health and Disease. *Journal of Interferon & Cytokine Research*. **34** (2014), pp. 215–219.

107. J. Fan, N. M. Heller, M. Gorospe, U. Atasoy, C. Stellato, The role of post-transcriptional regulation in chemokine gene expression in inflammation and allergy. *Eur. Respir. J.* **26**, 933–947 (2005).

108. H. Ashida, M. Ogawa, M. Kim, H. Mimuro, C. Sasakawa, Bacteria and host interactions in the gut epithelial barrier. *Nat. Chem. Biol.* **8**, 36–45 (2011).

109. C. A. Lopez, B. M. Miller, F. Rivera-Chávez, E. M. Velazquez, M. X. Byndloss, A. Chávez-Arroyo, K. L. Lokken, R. M. Tsolis, S. E. Winter, A. J. Bäumler, Virulence factors enhance Citrobacter rodentium expansion through aerobic respiration. *Science*. **353**, 1249–1253 (2016).

110. B. H. Abuaita, T. L. Schultz, M. X. O'Riordan, Mitochondria-Derived Vesicles Deliver Antimicrobial Reactive Oxygen Species to Control Phagosome-Localized Staphylococcus aureus. *Cell Host Microbe*. **24**, 625-636.e5 (2018).

111. K. E. Cunningham, G. Vincent, C. P. Sodhi, E. A. Novak, S. Ranganathan, C. E. Egan, D. B. Stolz, M. B. Rogers, B. Firek, M. J. Morowitz, G. K. Gittes, B. S. Zuckerbraun, D. J. Hackam, K. P. Mollen, Peroxisome Proliferator-activated Receptor-γ Coactivator 1-α (PGC1α) Protects against Experimental Murine Colitis. *J. Biol. Chem.* **291**, 10184–10200 (2016).

112. F. Bär, W. Bochmann, A. Widok, K. von Medem, R. Pagel, M. Hirose, X. Yu, K. Kalies, P. König, R. Böhm, T. Herdegen, A. T. Reinicke, J. Büning, H. Lehnert, K. Fellermann, S. Ibrahim, C. Sina, Mitochondrial gene polymorphisms that protect mice from colitis. *Gastroenterology*. **145**, 1055-1063.e3 (2013).

113. A. Clark, N. Mach, The Crosstalk between the Gut Microbiota and Mitochondria during Exercise. *Front. Physiol.* **8**, 319 (2017).

114. C. A. Silva, C. J. Blondel, C. P. Quezada, S. Porwollik, H. L. Andrews-Polymenis, C. S. Toro, M. Zaldívar, I. Contreras, M. McClelland, C. A. Santiviago, Infection of mice by Salmonella enterica serovar Enteritidis involves additional genes that are absent in the genome of serovar Typhimurium. *Infect. Immun.* **80**, 839–849 (2012).

115. S. Ray, S. Das, P. K. Panda, M. Suar, Identification of a new alanine racemase in Salmonella Enteritidis and its contribution to pathogenesis. *Gut Pathog.* **10**, 30 (2018).

116. H. Wickham, *ggplot2: Elegant Graphics for Data Analysis* (Springer, 2016).

117. N. L. Bray, H. Pimentel, P. Melsted, L. Pachter, Near-optimal probabilistic RNA-seq quantification. *Nat. Biotechnol.* **34**, 525–527 (2016).

118. J. Rainer, EnsDb.Hsapiens.v75: Ensembl based annotation package. R package version 2.99.0 (2017).

119. C. Soneson, M. I. Love, M. D. Robinson, Differential analyses for RNA-seq: transcript-level estimates improve gene-level inferences. *F1000Res.* **4**, 1521 (2015).

120. Y. Benjamini, Y. Hochberg, Controlling the False Discovery Rate: A Practical and Powerful Approach to Multiple Testing. *Journal of the Royal Statistical Society: Series B (Methodological)*. **57** (1995), pp. 289–300.

121. M. I. Love, W. Huber, S. Anders, Moderated estimation of fold change and dispersion for RNA-seq data with DESeq2. *Genome Biol.* **15**, 550 (2014).

122. G. Yu, Q.-Y. He, ReactomePA: an R/Bioconductor package for reactome pathway analysis and visualization. *Mol. Biosyst.* **12**, 477–479 (2016).

123. H. Wickham, R. Francois, L. Henry, K. Müller, Others, dplyr: A grammar of data manipulation. *R package version 0. 4*. **3** (2015).

124. J. Larsson, eulerr: Area-Proportional Euler and Venn Diagrams with Ellipses (2019), (available at https://cran.r-project.org/package=eulerr).

125. CDC, Foodborne Germs and Illnesses (2020), (available at https://www.cdc.gov/foodsafety/foodborne-germs.html).

126. Salmonella Homepage (2021), (available at https://www.cdc.gov/salmonella/).

127. A. C. Baird-Parker, Foodborne salmonellosis. *Lancet*. **336**, 1231–1235 (1990).

128. J. J. Gilchrist, C. A. MacLennan, Invasive Nontyphoidal Salmonella Disease in Africa. *EcoSal Plus*. **8** (2019), doi:10.1128/ecosalplus.ESP-0007-2018.

129. B. H. Abuaita, A.-L. E. Lawrence, R. P. Berger, D. R. Hill, S. Huang, V. K. Yadagiri, B. Bons, C. Fields, C. E. Wobus, J. R. Spence, V. B. Young, M. X. O'Riordan, Comparative transcriptional profiling of the early host response to infection by typhoidal and non-typhoidal Salmonella serovars in human intestinal organoids. *bioRxiv* (2020), p. 2020.11.25.397620, , doi:10.1101/2020.11.25.397620.

130. S. Pradhan, A. A. Weiss, Probiotic Properties of Escherichia coli Nissle in Human Intestinal Organoids. *MBio*. **11** (2020), doi:10.1128/mBio.01470-20.

131. A. Rydström, M. J. Wick, Monocyte recruitment, activation, and function in the gut-associated lymphoid tissue during oral Salmonella infection. *J. Immunol.* **178**, 5789–5801 (2007).

132. B. Amulic, C. Cazalet, G. L. Hayes, K. D. Metzler, A. Zychlinsky, Neutrophil function: from mechanisms to disease. *Annu. Rev. Immunol.* **30**, 459–489 (2012).

133. V. Brinkmann, U. Reichard, C. Goosmann, B. Fauler, Y. Uhlemann, D. S. Weiss, Y. Weinrauch, A. Zychlinsky, Neutrophil extracellular traps kill bacteria. *Science*. **303**, 1532–1535 (2004).

134. E. L. Campbell, W. J. Bruyninckx, C. J. Kelly, L. E. Glover, E. N. McNamee, B. E. Bowers, A. J. Bayless, M. Scully, B. J. Saeedi, L. Golden-Mason, S. F. Ehrentraut, V. F. Curtis, A. Burgess, J. F. Garvey, A. Sorensen, R. Nemenoff, P. Jedlicka, C. T. Taylor, D. J. Kominsky, S. P. Colgan, Transmigrating neutrophils shape the mucosal microenvironment through localized oxygen depletion to influence resolution of inflammation. *Immunity*. **40**, 66–77 (2014).

135. B. M. Fournier, C. A. Parkos, The role of neutrophils during intestinal inflammation. *Mucosal Immunol.* **5**, 354–366 (2012).

136. A. C. Chin, C. A. Parkos, Pathobiology of neutrophil transepithelial migration: implications in mediating epithelial injury. *Annu. Rev. Pathol.* **2**, 111–143 (2007).

137. K. L. Mumy, B. A. McCormick, The role of neutrophils in the event of intestinal inflammation. *Curr. Opin. Pharmacol.* **9**, 697–701 (2009).

138. A. J. Simpson, A. I. Maxwell, J. R. Govan, C. Haslett, J. M. Sallenave, Elafin (elastase-specific inhibitor) has anti-microbial activity against gram-positive and gram-negative respiratory pathogens. *FEBS Lett.* **452**, 309–313 (1999).

139. V. E. Diaz-Ochoa, D. Lam, C. S. Lee, S. Klaus, J. Behnsen, J. Z. Liu, N. Chim, S.-P. Nuccio, S. G. Rathi, J. R. Mastroianni, R. A. Edwards, C. M. Jacobo, M. Cerasi, A. Battistoni, A. J. Ouellette, C. W. Goulding, W. J. Chazin, E. P. Skaar, M. Raffatellu, Salmonella Mitigates Oxidative Stress and Thrives in the Inflamed Gut by Evading Calprotectin-Mediated Manganese Sequestration. *Cell Host Microbe*. **19**, 814–825 (2016).

140. J. Z. Liu, S. Jellbauer, A. J. Poe, V. Ton, M. Pesciaroli, T. E. Kehl-Fie, N. A. Restrepo, M. P. Hosking, R. A. Edwards, A. Battistoni, P. Pasquali, T. E. Lane, W. J. Chazin, T. Vogl, J. Roth, E. P. Skaar, M. Raffatellu, Zinc Sequestration by the Neutrophil Protein Calprotectin Enhances Salmonella Growth in the Inflamed Gut. *Cell Host Microbe*. **11**, 227–239 (2012).

141. C. Cheminay, D. Chakravortty, M. Hensel, Role of neutrophils in murine salmonellosis. *Infect. Immun.* **72**, 468–477 (2004).

142. R. Sumagin, C. A. Parkos, Epithelial adhesion molecules and the regulation of intestinal homeostasis during neutrophil transepithelial migration. *Tissue Barriers*. **3**, e969100 (2015).

143. C. Andrews, M. H. McLean, S. K. Durum, Cytokine Tuning of Intestinal Epithelial Function. *Front. Immunol.* **9**, 1270 (2018).

144. D. Wang, R. N. Dubois, A. Richmond, The role of chemokines in intestinal inflammation and cancer. *Curr. Opin. Pharmacol.* **9**, 688–696 (2009).

145. X. C. Li, A. M. Jevnikar, D. R. Grant, Expression of functional ICAM-1 and VCAM-1 adhesion molecules by an immortalized epithelial cell clone derived from the small intestine. *Cell. Immunol.* **175**, 58–66 (1997).

146. G. T. Huang, L. Eckmann, T. C. Savidge, M. F. Kagnoff, Infection of human intestinal epithelial cells with invasive bacteria upregulates apical intercellular adhesion molecule-1 (ICAM)-1) expression and neutrophil adhesion. *J. Clin. Invest.* **98**, 572–583 (1996).

147. S. A. Hirota, J. Ng, A. Lueng, M. Khajah, K. Parhar, Y. Li, V. Lam, M. S. Potentier, K. Ng, M. Bawa, D.-M. McCafferty, K. P. Rioux, S. Ghosh, R. J. Xavier, S. P. Colgan, J. Tschopp, D. Muruve, J. A. MacDonald, P. L. Beck, NLRP3 inflammasome plays a key role in the regulation of intestinal homeostasis. *Inflamm. Bowel Dis.* **17**, 1359–1372 (2011).

148. Z. Hodzic, E. M. Schill, A. M. Bolock, M. Good, IL-33 and the intestine: The good, the bad, and the inflammatory. *Cytokine*. **100**, 1–10 (2017).

149. E. Lefrançais, S. Roga, V. Gautier, A. Gonzalez-de-Peredo, B. Monsarrat, J.-P. Girard, C. Cayrol, IL-33 is processed into mature bioactive forms by neutrophil elastase and cathepsin G. *Proc. Natl. Acad. Sci. U. S. A.* **109**, 1673–1678 (2012).

150. F. Martinon, K. Burns, J. Tschopp, The inflammasome: a molecular platform triggering activation of inflammatory caspases and processing of proIL-beta. *Mol. Cell*. **10**, 417–426 (2002).

151. J. R. Kurtz, J. A. Goggins, J. B. McLachlan, Salmonella infection: Interplay between the bacteria and host immune system. *Immunol. Lett.* **190**, 42–50 (2017).

152. C. A. Lee, M. Silva, A. M. Siber, A. J. Kelly, E. Galyov, B. A. McCormick, A secreted Salmonella protein induces a proinflammatory response in epithelial cells, which promotes neutrophil migration. *Proc. Natl. Acad. Sci. U. S. A.* **97**, 12283–12288 (2000).

153. Q. L. Ying, S. R. Simon, Kinetics of the inhibition of human leukocyte elastase by elafin, a 6-kilodalton elastase-specific inhibitor from human skin. *Biochemistry*. **32**, 1866–1874 (1993).

154. C. A. Parkos, Neutrophil-Epithelial Interactions: A Double-Edged Sword. *Am. J. Pathol.* **186**, 1404–1416 (2016).

155. J.-P. Motta, L. G. Bermúdez-Humarán, C. Deraison, L. Martin, C. Rolland, P. Rousset, J. Boue, G. Dietrich, K. Chapman, P. Kharrat, J.-P. Vinel, L. Alric, E. Mas, J.-M. Sallenave, P. Langella, N. Vergnolle, Food-grade bacteria expressing elafin protect against inflammation and restore colon homeostasis. *Sci. Transl. Med.* **4**, 158ra144 (2012).

156. J.-P. Motta, L. Magne, D. Descamps, C. Rolland, C. Squarzoni-Dale, P. Rousset, L. Martin, N. Cenac, V. Balloy, M. Huerre, L. F. Fröhlich, D. Jenne, J. Wartelle, A. Belaaouaj, E. Mas, J.-P. Vinel, L. Alric, M. Chignard, N. Vergnolle, J.-M. Sallenave, Modifying the protease, antiprotease pattern by elafin overexpression protects mice from colitis. *Gastroenterology*. **140**, 1272–1282 (2011).

157. C. T. N. Pham, Neutrophil serine proteases: specific regulators of inflammation. *Nat. Rev. Immunol.* **6**, 541–550 (2006).

158. E. P. Reeves, H. Lu, H. L. Jacobs, C. G. M. Messina, S. Bolsover, G. Gabella, E. O. Potma, A. Warley, J. Roes, A. W. Segal, Killing activity of neutrophils is mediated through activation of proteases by K+ flux. *Nature*. **416**, 291–297 (2002).

159. I. Rauch, K. A. Deets, D. X. Ji, J. von Moltke, J. L. Tenthorey, A. Y. Lee, N. H. Philip, J. S. Ayres, I. E. Brodsky, K. Gronert, R. E. Vance, NAIP-NLRC4 Inflammasomes Coordinate Intestinal Epithelial Cell Expulsion with Eicosanoid and IL-18 Release via Activation of Caspase-1 and -8. *Immunity*. **46**, 649–659 (2017).

160. S. M. Crowley, X. Han, J. M. Allaire, M. Stahl, I. Rauch, L. A. Knodler, B. A. Vallance, Intestinal restriction of Salmonella Typhimurium requires caspase-1 and caspase-11 epithelial intrinsic inflammasomes. *PLoS Pathog.* **16**, e1008498 (2020).

161. A. Hausmann, D. Böck, P. Geiser, D. L. Berthold, S. A. Fattinger, M. Furter, J. A. Bouman, M. Barthel-Scherrer, C. M. Lang, E. Bakkeren, I. Kolinko, M. Diard, D.

Bumann, E. Slack, R. R. Regoes, M. Pilhofer, M. E. Sellin, W.-D. Hardt, Intestinal epithelial NAIP/NLRC4 restricts systemic dissemination of the adapted pathogen Salmonella Typhimurium due to site-specific bacterial PAMP expression. *Mucosal Immunol.* **13**, 530–544 (2020).

162. L. A. Knodler, S. M. Crowley, H. P. Sham, H. Yang, M. Wrande, C. Ma, R. K. Ernst, O. Steele-Mortimer, J. Celli, B. A. Vallance, Noncanonical inflammasome activation of caspase-4/caspase-11 mediates epithelial defenses against enteric bacterial pathogens. *Cell Host Microbe*. **16**, 249–256 (2014).

163. M. E. Sellin, A. A. Müller, B. Felmy, T. Dolowschiak, M. Diard, A. Tardivel, K. M. Maslowski, W.-D. Hardt, Epithelium-intrinsic NAIP/NLRC4 inflammasome drives infected enterocyte expulsion to restrict Salmonella replication in the intestinal mucosa. *Cell Host Microbe*. **16**, 237–248 (2014).

164. S. H. Jia, J. Parodo, E. Charbonney, J. L. Y. Tsang, S. Y. Jia, O. D. Rotstein, A. Kapus, J. C. Marshall, Activated neutrophils induce epithelial cell apoptosis through oxidant-dependent tyrosine dephosphorylation of caspase-8. *Am. J. Pathol.* **184**, 1030–1040 (2014).

165. S. A. Gudipaty, J. Rosenblatt, Epithelial cell extrusion: Pathways and pathologies. *Semin. Cell Dev. Biol.* **67**, 132–140 (2017).

166. M. Saffarzadeh, C. Juenemann, M. A. Queisser, G. Lochnit, G. Barreto, S. P. Galuska, J. Lohmeyer, K. T. Preissner, Neutrophil extracellular traps directly induce epithelial and endothelial cell death: a predominant role of histones. *PLoS One*. **7**, e32366 (2012).

167. K. W. Chen, M. Monteleone, D. Boucher, G. Sollberger, D. Ramnath, N. D. Condon, J. B. von Pein, P. Broz, M. J. Sweet, K. Schroder, Noncanonical inflammasome signaling elicits gasdermin D-dependent neutrophil extracellular traps. *Sci. Immunol.* **3**, eaar6676 (2018).

168. B. H. Abuaita, G. J. Sule, T. L. Schultz, F. Gao, J. S. Knight, M. X. O'Riordan, The IRE1α Stress Signaling Axis Is a Key Regulator of Neutrophil Antimicrobial Effector Function. *J. Immunol.* (2021), doi:10.4049/jimmunol.2001321.

169. D. M. Hardbower, K. Singh, M. Asim, T. G. Verriere, D. Olivares-Villagómez, D. P. Barry, M. M. Allaman, M. K. Washington, R. M. P. Jr., M. B. Piazuelo, K. T. Wilson, EGFR regulates macrophage activation and function in bacterial infection. *J. Clin. Invest.* **126**, 3296–3312 (2016).

170. F. de O. Barbosa, O. C. de Freitas Neto, D. F. A. Batista, A. M. de Almeida, M. da S. Rubio, L. B. R. Alves, R. de O. Vasconcelos, P. A. Barrow, A. Berchieri Junior, Contribution of flagella and motility to gut colonisation and pathogenicity of Salmonella Enteritidis in the chicken. *Braz. J. Microbiol.* **48**, 754–759 (2017).

171. H. R. Bonifield, K. T. Hughes, Flagellar phase variation in Salmonella enterica is mediated by a posttranscriptional control mechanism. *J. Bacteriol.* **185**, 3567–3574 (2003).